Mtelela, Cassy (2016) ***Sedimentology and stratigraphy of the late Cenozoic lake beds succession, Rukwa Rift Basin, Tanzania: implications for hydrocarbon prospectivity.*** **PhD thesis, James Cook University.**

Sedimentology and stratigraphy of the late Cenozoic Lake Beds succession, Rukwa Rift Basin, Tanzania: Implications for hydrocarbon prospectivity

Thesis submitted by

Cassy MTELELA

B.Sc. (with Geology) (University of Dar es Salaam, Tanzania),

M.Sc. (University of Dar es Salaam, Tanzania)

in September, 2016

For the Degree of Doctor of Philosophy in the College of Science and Engineering,

James Cook University, Australia.

Statement of Access

I, the undersigned author of this thesis, understand that James Cook University will make this thesis available for use within the university library and allow access in other approved libraries after submission. All users consulting this thesis will have to sign the following statement:

> *In consulting this thesis I agree not to copy or closely paraphrase it in whole or in part without the written consent of the author; and to make proper public written acknowledgement for any assistance which I have obtained from it.*

Beyond this, I do not wish to place any restrictions on access to this thesis.

Cassy Mtelela
September, 2016

Declaration

I declare that this thesis is my own work and has not been submitted in any form for another degree or diploma at any university or other institution or tertiary education. Information derived from the published or unpublished work of others has been acknowledged in the text and a list of those references is given.

Cassy Mtelela

September, 2016

Statement of the Contribution of Others

Nature of the Assistance	Contribution	Names and Affiliation of Co-authors
Intellectual Support	Proposal Writing	Dr. Eric Roberts, JCU
	Data Analysis	Dr. Eric Roberts, JCU
	Editing	Dr. Eric Roberts, JCU Mr. Robert Downie, Heritage Oil Ltd. Dr. Marc Hendrix, UM Dr. Hannah Hilbert-Wolf, JCU Dr. Patrick O'Connor, OU Dr. Nancy Stevens, OU
Field-Analytical Support	Field Research	Dr. Eric Roberts, JCU Mr. Robert Downie, Heritage Oil Ltd. Dr. Marc Hendrix, UM Dr. Hannah Hilbert-Wolf, JCU Dr. Patrick O'Connor, OU Dr. Nancy Stevens, OU
	Data Analysis	Dr. Eric Roberts, JCU Mr. Robert Downie, Heritage Oil Ltd. Dr. Marc Hendrix, UM
Financial Support	Fieldwork and Analytical	TPDC Heritage Oil Rukwa Tanzania Ltd SEES & GRS
	Conference and Travels	TPDC Heritage Oil Rukwa Tanzania Ltd EGRU

Chapter or Appendix	Details of publication (s)	Nature and extent of input by thesis author
1	Mtelela, C., Roberts, E.M., Downie, R. and Hendrix, M.S., Interplay of structural, climatic and volcanic controls on late Quaternary lacustrine-deltaic sedimentation patterns in the Western Branch of the East African Rift System, Rukwa Rift Basin, Tanzania. Journal of Sedimentary Research (2016): v. 86, p. 1179-1207.	I wrote most of the paper, developed most of the concepts, and conducted all analyses, but benefited greatly from the advices of my supervisor and contributors
2	Mtelela, C., Roberts, E.M., Hilbert-Wolf, H.L., Downie, R., Hendrix, M.S., O'Connor, P.M. and Stevens, N.J., Sedimentology and paleoenvironments of a new fossiliferous late Miocene-Pliocene sedimentary succession in the Rukwa Rift Basin, Tanzania. Journal of African Earth Sciences (in press): Article ref. # AES2776.	I wrote most of the paper, developed majority of the concepts, and conducted all analyses, but I benefited greatly from the advices of my supervisor and contributors
3	Mtelela, C. and Roberts, E.M.	I wrote most of the chapter, and benefited greatly from the advices and edits by my supervisor
4	Mtelela, C. and Roberts, E.M.	I wrote most of the chapter, and benefited greatly from the advices and edits by my supervisor
Appendix	Eric M. Roberts, Christopher N. Todd, Duur K. Aanen, Tania	I contributed to the writing and development of

<table>
<tr><td></td><td>Nobre, Hannah L. Hilbert-Wolf, Patrick M. O’Connor, Leif Tapanila, Cassy Mtelela, Nancy J. Stevens . 2016. Oligocene Termite Nests with In Situ Fungus Garden from the Rukwa Rift Basin, Tanzania, Support a Paleogene African Origin for Insect Agriculture. PLOS ONE. DOI: 10.1371/journal.pone.0156847</td><td>concepts</td></tr>
<tr><td colspan="3">I confirm the candidate’s contribution to this paper and consent to the inclusion of the paper in this thesis.

Primary Advisor: Dr. Eric Roberts

Signature:

Date:</td></tr>
</table>

Acknowledgements

There are many people who were involved or contributed in some way to my thesis work over the last four years. Although not everyone can be thanked here individually, their help is greatly appreciated.

I owe the greatest debt of thanks to my supervisors, Eric Roberts and Paul Dirks, and to my Ph.D committee. Huge thanks to my primary supervisor and mentor Eric Roberts for all his support during the last 4 years and without whom I know this project and my arrival at James Cook University would have never happened. His wisdom, guidance through fieldwork to analysis of data and write ups, patience and generosity made this study a success, and are highly appreciated. Eric Roberts uplifted my expertise in sedimentology and stratigraphic analysis, and I am looking forward to continue working with him and adopt the passion, integrity, and drive that you devote to every project you set out to accomplish.

Many thanks to Tanzania Petroleum Development Corporation and Heritage Oil Rukwa Tanzania Ltd. for providing me a full PhD bursary that included fees, stipend, travels and funding to conduct three field seasons in the Rukwa Rift, as well as laboratory analytic expenses. Supplementary funds for research, conference fees and travels from the Economic Geological Research Unit (EGRU), Graduate Research School (GRS) and the then School of Earth and Environmental Sciences (SEES) are equally appreciated.

I would like to thank Robert Downie for intellectual support, and linking me with Heritage Oil Rukwa Tanzania. Thanks to the staff of Heritage Oil Rukwa Tanzania Ltd. in the Dar es Salaam office for support in the fieldwork logistics. Also thanks to Marc Hendrix, Hannah Hilbert-Wolf, Nelson Boniface, Josephat Edmund, Patrick O'Connor, Nancy Stevens, Zubeir Jinnah and the rest of the Rukwa Rift Basin Project team members for their field assistance and valuable discussions.

Thanks to all staff at CSTE, especially Bec, Melissa, Judy and Jo, for all your time and help.

Lastly but not least, thanks to my family, relatives and friends for understanding, encouragements, and support of variety of forms. And to my colleagues at the James Cook University, including Quaid Khan Jadoon, Prince Owusu, and the rest of the Gravel Monkeys (sedimentary geology research group) members.

Abstract

The late Cenozoic Lake Beds succession forms the most significant strata for economic and academic aspects in the Rukwa Rift Basin, yet represents the least studied and most poorly understood sedimentary package in the basin. Deposition of the Lake Beds succession resulted from the tectonic development of the modern East African Rift System, and thus represents an important archive of the associated environmental and climate changes in eastern Africa, as well as a record of floral and faunal evolution during this time. Economically, the Rukwa Rift Basin was subject to brief, but unsuccessful hydrocarbon exploration during the late 1980s. The results of these investigations were inconclusive, but indicated potential source and reservoir rocks for hydrocarbon in the different portion of the basin stratigraphy, underlying the Lake Beds succession. However, hydrocarbon exploration in the basin has been hampered by a poor understanding of the basin stratigraphy and sedimentology. For instance, the upper half of the rift stratigraphy (including the Lake Beds succession) was long considered to be too young for hydrocarbon generation and accumulation. However, recentl discoveries of significant hydrocarbon accumulations in the Neogene rift basin strata in Lake Albert (Uganda) and Turkana (Kenya) have prompted renewed hydrocarbon exploration in the Rukwa Rift Basin by Heritage Oil, but with a focus on the potentially correlative Late Cenozoic Lake Beds succession. This project was, therefore, developed to conduct the first detailed investigation on Lake Beds stratigraphic and sedimentology, via outcrop-based lithofacies mapping, sedimentary petrology, X-ray power diffraction mineralogy, provenance analysis, geochronology, sequence stratigraphy and re-examination of existing legacy exploration well-cuttings.

The results demonstrate a complex stratigraphy and depositional history for the Lake Beds, and are used to: establish a formal stratigraphic framework; reconstruct tectonic, paleoenvironmental and palaeoclimatic trends in the basin through time; and assess the hydrocarbon prospectivity of these strata. Two new formations, herein named the Malangali and Ilasilo formations, are defined. The Malangali Formation represents a previously unrecognized late Miocene to Pliocene unit in the RRB, which is subdivided into the lower Mpona and upper Hamposia members. The Mpona Member records a myriad of volcanically influenced alluvial, fluvial and lacustrine depositional environments recording the initiation of Neogene rifting and volcanism in the RRB. A major unconformity and provenance shift marks the transition between the two members. The Hamposia Member is characterised by well-developed paleosols and large sandy channel systems interpreted to record a semi-arid depositional environment and preserving a previously unknown fauna of this age dominated by fishes, turtles, crocodyliformes, hippopotami, and large ungulates. Overlying the Malangali Formation, is a thick succession of Late Quaternary volcanic-rich lacustrine dominated strata. Above this, the upper 100 m of the basin stratigraphy is widely exposed across the RRB and formally

defined in this study as the Ilasilo Formation. Detailed sedimentologic, geochronologic and sequence stratigraphic analysis of these strata reveal eight discrete depositional sequences that record significant tectonic and climate-driven lake cyclicity in the Rukwa Rift Basin during the Quaternary, including +/-70 m lake level fluctuations that occurred over the last 50 ka. Lake cyclicity and sedimentation were also strongly influenced by periodic, intense volcanism in the nearby Rungwe Volcanic Center, which lead to rapid transitions between overfilled and underfilled lake basins.

This sedimentologic and stratigraphic investigation indicates positive characteristic for hydrocarbon source, reservoir and seal rock capacity in the late Cenozoic Lake Beds Group. A synthesis of facies analysis, sandstone petrography and well-cuttings examination indicates that base level cyclicity of Lake Rukwa during late Cenozoic resulted in deposition of alternating profundal lacustrine deposits that are organic-rich (diatomaceous) and fluvial deltaic sandstone and conglomerate dominated deposits that are highly porous and permeable, respectively. Furthermore, lithologic, petrographic and mineralogy studies presented herein indicate that the uppermost portion of the strata (the Ilasilo Formation) is dominated by less porous and impermeable volcanic units that are identified as potential seal rocks. These preliminary findings encourages follow up exploration techniques across the basin, as well as sampling and analysis of the subsurface portion of the strata and underlying older units to fully appreciate the hydrocarbon prospectivity of the Rukwa Rift Basin, and in particular, the late Cenozoic Lake Beds Group as a complete "hydrocarbon kitchen".

Table of Contents

List of Tables

List of Figures

Chapter 1

Chapter 2

Chapter 3

Chapter 4

Preamble

It is intended that the entire contents of this thesis will be published in internationally-recognized Earth Science journals. At the time of submission, Chapter 1 was already published in the Journal of Sedimentary Research and Chapter 2 was accepted for publication (in press) in the Journal of African Earth Sciences. Chapter 3 and 4 are being prepared for submission after thesis examination and final thesis submission.

This thesis consists of four chapters, and each chapter represents an independent body of work that is presented in a format similar to the journal to which it has been (or will be) submitted to. Hence, minor repetition such as geologic setting maps is unavoidable. I have also included a discrete additional research product (see Appendix), a paper published in Plos ONE of which I contributed a significant component of the original research conducted during the course of my own research in the Rukwa Rift Basin.

Although each chapter represents a separate, stand-alone piece of work, all of the chapters are related to the central theme of this thesis: Sedimentology and stratigraphy of the Lake Cenozoic Lake Beds succession.

Subject of this Thesis

The Rukwa Rift, a segment of the Western Branch of East African Rift System in southwestern Tanzania, presents a highly prospective, frontier basin for new hydrocarbon exploration in Africa because of its high rates of sedimentation, rapid subsidence, and complex structural controls; all of which are conditions considered favorable for hydrocarbon generation and accumulation (cf. Rosendahl and Livingstone, 1983; Morley et al., 1990, 1999; Tiercelin et al., 2004, 2012). Furthermore, high geothermal gradients normally associated with rifting events are considered conducive for early maturation of source rocks (i.e., maturation of very young source rocks) even at relatively shallow depths (Morley et al., 1990; Mbede, 1991; Morley et al., 1999). Such basins have been termed "hydrocarbon kitchens" by Tiercelin et al. (2012), in which the hydrocarbon source, reservoir and seal can be found together in a single, typically young, stratigraphic succession. Prior to this project, very little about the youngest stratigraphic sequence in the Rukwa Rift Basin was known; however, Heritage Oil, identified this portion of the basin as having similarities with recent hydrocarbon kitchens discovered in the Albertine Rift of Uganda, and this observation formed the initial basis for this thesis project (B. Downey, pers. comm).

The hydrocarbon exploration history in the Rukwa Rift Basin (RRB) of Tanzania goes back to the 1980s. At this time, a gravity survey was conducted by Petro-Canada International Assistance Corporation as part of an assistance program for the Tanzania Petroleum Development Corporation (TPDC) (Pierce and Lipkov, 1988). This reconnaissance gravity survey provided the initial regional view of the geometry of the basin which established the presence of a deep (6-7 km) rift basin (Pierce and Lipkov, 1988; Morley et al., 1999). The RRB was subsequently investigated for hydrocarbons during widespread southern and central African seismic programs. These programs were driven by hydrocarbon discoveries reported in rift basins, such as Muglad, Melut and Blue Nile Basins of southern Sudan by Chevron Oil (Schull, 1984, 1988). As part of these programs, two hydrocarbon exploration wells (Galula-1 and Ivuna-1) were drilled by the Amoco Production Company within the RRB in 1987 (Wescott et al., 1991; Kilembe and Rosendahl, 1992; Wescott, 1993); the results of which were not conclusive and further exploration was halted. However, preliminary well-log analysis indicated that hot shale and liptinite rich coals of the K_2 unit of the Karoo Supergroup may serve as mature oil and gas prone source rocks (Wescott et al., 1991; Kilembe and Rosendahl, 1992). The overlying sandstone units in the Karoo Supergroup, Red Sandstone Group and Lake Beds succession were all identified as potential reservoir rocks (TPDC, 2011). These early findings and recent hydrocarbon discoveries in the Turkana Basin (Kenya) and Albertine Graben of Uganda (Logan et al., 2009; Thuo, 2009; PEDP, 2011; Cresswell, 2012; Tiercelin et al., 2012), are what led to renewed hydrocarbon exploration in the RRB by Heritage Oil starting in 2011, with special focus on the age-equivalent Miocene-Recent Lake Beds succession.

The Lake Beds strata constitute the uppermost succession of the RRB stratigraphy, which was deposited during the development of the late Cenozoic East African Rift System (Grantham et al., 1958; Wescott et al., 1991; Mliga, 1994). The Lake Beds unconformably overlie the Oligocene Nsungwe Formation, or the Cretaceous Galula Formation, or the late Paleozoic Karoo Supergroup, in different parts of the field area (Mliga, 1994; Mbede, 2000; Roberts et al., 2010; see also Figs. 1 and 2 in chapter 1). Despite the hydrocarbon potential of the Lake Beds succession, very little research has been done in these strata relating to their sedimentology, geochemistry or geochronology (e.g. Ebinger et al., 1989; Wescott et al., 1991; Mliga, 1994). Lack of detailed outcrop-based sedimentologic, stratigraphic and geochronologic studies limits understanding of the depositional age, provenance, litho- and chrono-stratigraphic correlations, as well as depositional environments and alluvial architecture. This knowledge gap is critical to understanding the geology of the Lake Beds strata, and study of this stratigraphic unit is vital in evaluating the hydrocarbon potential, as well as mineral and water resource in the basin, and to more fully understand the tectonic evolution of the Rukwa Rift Basin. This project, therefore, is aimed at providing the first comprehensive investigation of the Lake Beds succession, focusing on sedimentology, stratigraphy and hydrocarbon prospectivity of this important unit. The specific objectives include:

1. *To apply facies and alluvial architectural analysis of the lower, middle and upper Lake Beds Succession in the Rukwa Rift Basin to reconstruct the depositional environments through time and identify new fossil localities in this portion of the East African Rift System.*
2. *To study and formally define the lithostratigraphy of the Lake Beds, and where possible, provide additional chronostratigraphic (radiocarbon and/or radioisotopic) constraints of the lithostratigraphic units.*
3. *To use sedimentary petrology, clay mineralogy and alluvial architecture to evaluate source, reservoir and seal characteristics of Lake Beds succession as a potential hydrocarbon exploration target.*
4. *And finally, to understand regional tectonic, climatic and volcanic controls on sedimentation patterns and basin development during the Miocene to Recent in the Rukwa Rift Basin.*

To achieve the objectives set in this research, I conducted an extensive fieldwork in the Rukwa Rift Basin, and also worked alongside Hannah Hilbert-Wolf, at James Cook University. Hannah and I worked together in the field during this time on two parallel, but independent research projects in the rift basin between 2012 and 2016. My project, like Hannah's, was conducted as part of the Rukwa Rift Basin Project, which represents a collaboration between geologists and palaeontologists from James Cook University, Ohio University (USA), the University of Dar es Salaam (Tanzania) and many other universities focusing on the discovery and documentation of the 100 million year history of this little known segment of the East African Rift System. This project combines palaeontologic and geologic exploration in the rift, with a long term goal of understanding the tectonic, sedimentary, and evolutionary history of the basin. The Rukwa Rift Basin Project originally focused on understanding the early history of the rift, with a focus on strata and faunas from the Cretaceous and Oligocene time periods. However, in 2012 Heritage Oil (Heritage Rukwa Limited) agreed to support the expansion of the project to include an investigation of the uppermost Miocene-Recent stratigraphy of the basin, and in doing so, I was sponsored to conduct my PhD on this topic. My role in the Rukwa Rift Basin project was to undertake geologic and lithofacies mapping of the Lake Beds succession, as well as petrologic, geochemical and radiocarbon dating. Hence, I have had the pleasure of investigating the geologic context of the important stratigraphic unit, and helping to discover a wholly new faunal record from the East African Rift System. Details on research methodology are presented under methods sections of each chapter.

Structure of the Thesis

Findings of this research are presented in four chapters:

Chapter 1 presents the first detailed, outcrop based sedimentology of the Pleistocene-Holocene upper Lake Beds succession in the Rukwa Rift Basin. Here, a combination of facies analysis, petrologic investigations, dating and sequence stratigraphy is used to: 1) document the detailed sedimentology and stratigraphy of this important archive of Quaternary climate and environmental change; 2) reconstruct its depositional systems and paleoenvironments; and 3) decipher the role and influence of explosive volcanism, climate and tectonics on stratigraphy, alluvial architecture and basin evolution. The first sections describe the sedimentology of the upper Lake Beds succession, and provide interpretations regarding the depositional environments. This is followed by a study of the conglomerate and sandstone petrology; the results of which are used to characterize the Lake Beds deposits into volcaniclastic and siliciclastic petrofacies end members, supplement field observations, and constrain the sources of sediment which filled the basin during this time. Radiocarbon dating report and implication on Lake Beds chronology follows, which is used in combination with facies analysis to review and reinterpret previous informal subdivisions of the Lake Beds strata. This section is followed by a sequence stratigraphic analysis section on the upper Lake Beds succession. Here, six depositional sequences that constitute the upper Lake Beds are described in detail, and these results are ntegrated with previous data on regional and local paleoclimate, faulting and explosive volcanism from the Rungwe Volcanic Province to determine relative roles of climate, volcanism and tectonics on sedimentary processes and sequence development.

Chapter 2 presents a detailed sedimentologic investigation of a previously unknown, fossiliferous series of Miocene-Pliocene outcrop exposures in the Rukwa Rift Basin, which document, for the first time, the initiation of late Cenozoic rifting in the basin. This sedimentologic investigation also benefited from new radioisotopic age constraints on this unit conducted by a parallel research program by Hannah Hilbert-Wolf (see Hilbert-Wolf, Roberts, Downey and Mtelela, in press), which revealed late Miocene-Pliocene depositional ages for the strata. This unit (the lower part of the Lake Beds succession) is, therefore, a rare and significant new example of a fossiliferous succession of this age in the Western Branch of East Africa Rift System. This chapter focuses on detailed sedimentologic description of the strata and interpretation of depositional environments, sequence stratigraphy and basin evolution. Moreover, this paper announces the discovery of a new Mio-Pliocene fauna from this portion of the East African Rift System. Research methodology is similar to Chapter 1.

Chapter 3 presents the preliminary sedimentology and stratigraphy of the final portion of the Lake Beds succession identified in the Rukwa Rift Basin, the middle Lake Beds. Unlike the lower and upper Lake Beds, the complexity and lack of detailed age constraint for the middle Lake Beds make it difficult to fully assess its geologic history. However, based on sedimentologic analysis, this chapter subdivides the middle Lake Beds into five distinctive informal members (A-E), and attributes the deposition of this unit to tectonic movements (subsidence and uplift) and contemporaneous volcanism in the nearby Rungwe Volcanic Province interpreted to have occurred during the deposition of this unit.

Chapter 4 focuses on establishing a formal stratigraphic nomenclature for the Lake Beds Group, building upon lithostratigraphic descriptions of all three portions of the strata presented in chapters 1, 2, and 3. In addition, this chapter also seeks to preliminarily evaluate the entire sedimentary history and the hydrocarbon prospectivity of the Lake Beds Succession in the Rukwa Rift Basin. To do this, qualitative and quantitative clay and bulk rock X-ray diffraction (XRD) analysis of the Lake Beds Group deposits is presented. The clay mineralogy is used as proxy for paleoclimate, whereas quantitative bulk rock fraction (sand- to clay-sized) XRD analysis is used to supplement microscopic sandstone petrography presented in chapter 1 and 2 to further understand Lake Beds physical and mineralogical characteristics. A synthesis of facies analysis, sedimentary petrology and measured paleocurrent indicators (presented in chapter 1 and 2), enable reconstruction of a major four-fold depositional model for the development of the Lake Beds Group. The chapter ends with a discussion on hydrocarbon exploration potential of the Lake Beds Group, in terms of source, reservoir and seal rock potential of the strata, based on synthesis of a combination of facies analysis, petrology, and XRD analysis of the deposits across the stratigraphy. A short conclusions chapter (Chapter 5) at the end of the thesis summarizes the results and provides a prospectus on future research goals in the Rukwa Rift Basin.

Chapter 1

Interplay of structural, climatic, and volcanic controls on late Quaternary lacustrine - deltaic sedimentation patterns in the Western Branch of the East African Rift System, Rukwa Rift Basin, Tanzania

Keywords: Rukwa; Facies Analysis; Africa; Lake Beds; Quaternary.

ABSTRACT

This paper presents the first detailed, outcrop-based sedimentologic investigation of the Pleistocene - Holocene upper Lake Beds succession in the Rukwa Rift Basin, located in the Western Branch of the East African Rift System, southwestern Tanzania. The goal of this investigation is to examine the sedimentary facies and reconstruct the depositional environments of this important archive of Quaternary climate and environmental change. Eleven diagnostic facies associations comprising 24 facies were identified and provide the basis for recognition of three key deposystems: 1) alluvial-to-fluvial channel system; 2) lake delta system; and 3) profundal lacustrine system. Analysis of paleocurrent indicators and sandstone provenance indicate widely dispersed source regions and drainage patterns that were strongly influenced by major border-fault systems and episodic volcanism. Six stratigraphic sequences (A - F), ranging from ~2 to 17 m thick, were identified based on stratal stacking patterns and the development of sequence-bounding unconformities and lacustrine flooding surfaces. Sedimentation processes, facies architecture, and stratigraphic packaging record a complex interplay between Quaternary climate fluctuations and intense episodic volcanism in the nearby Rungwe Volcanic Province, set against large-scale tectonic controls associated with synchronous development of the East African Rift System.

Sequence stratigraphic analysis reveals that the Rukwa Rift Basin episodically shifted between a balanced-fill lake basin and an overfilled lake basin. Deep water, basin-wide lake expansion occurred at different times during the late Quaternary. The final depositional sequence preserved in the basin, a fluvial–underfilled lake basin, initiated ~7.9 ka and has persisted to the present day. High-frequency climate change played the key role in sequence development in the upper Lake Beds. However, voluminous, rift-related volcanism and erosion of abundant labile volcanic materials from the Rungwe Volcanic Province, as well as syntectonic evolution of the rift, led to high sedimentation rates and transformation of flash floods and debris flows in the hinterlands (rift margin) to hyperpycnal flows towards the basin depocenter.

INTRODUCTION

The late Cenozoic was an exceptionally dynamic period in the geologic and evolutionary history of East Africa. Large-scale rifting, volcanism, and uplift in this part of Africa record the development of the East African Rift System (EARS) during this time. Indeed, the Neogene-Quaternary is also marked by significant climate changes, including a Miocene to Pleistocene transition from warm to glacial, and the change from humid to arid conditions between the early and mid-Holocene (e.g., deMenocal 1995; Thevenon et al. 2002; Barker et al. 2003; Trauth et al. 2003, 2005).

High-resolution tectonic and climatic records, as well as abundant preservation of fossils in many portions of the EARS, are attributed to the rapid production and burial of large volumes of volcaniclastic sediments (Hay 1986; Stollhofen et al. 2008). Contemporaneously, active rifting led to the uplift and erosion of the basement rock along the rift flanks (WoldeGabriel et al. 2000). Pyroclastic flows and fallouts, and fluvially reworked volcaniclastics are typically more widespread across volcanogenic basins of the northern part of the EARS, mainly in the eastern branch (e.g., Smith 1991; Smith et al. 2002; Ashley and Hay 2012). In contrast, the southern part of the EARS is less volcanogenic, and sedimentation is more limited to detritus derived from weathering and erosion of the uplifted Precambrian through Mesozoic basement rocks. Although the effects of volcanism on fluvial and lacustrine sedimentation patterns have been documented in volcanic-arc settings (e.g., Smith 1987; Smith 1991; Palmer and Shawkey 1997; Manville 2001; Lepre 2014), less well understood is the role of volcanism in the evolution of continental rift basins. In particular, few studies have investigated how punctuated voluminous volcanism affects facies architecture, depositional environments, and sequence development in rift basins (e.g., Yuretich 1982; WoldeGabriel et al. 2000; Ashley and Hay 2012). A better understanding of the linkages among climate, tectonism, and especially volcanism and the architecture of sedimentary deposits in rifts is crucial to efforts aimed at evaluating the hydrocarbon, mineral, and water-resource potential of such basins.

The late Quaternary upper Lake Beds succession in the Rukwa Rift Basin (RRB), southwestern Tanzania (Fig. 1) is a well exposed, volcanically influenced rift basin in the Western Branch of the EARS. Despite the considerable interest in the paleontologic and paleoanthropologic potential of this extensive sedimentary succession (e.g., Clark et al. 1970), very little outcrop-based sedimentology or stratigraphy has been conducted. With the exception of recent work by Cohen et al. (2013) and several older contributions (e.g., Haberyan 1987; Delvaux et al. 1998; Thevenon et al. 2002), few detailed studies of the Lake Beds have been published since the colonial geologic survey studies in the mid-twentieth century (Quennell et al. 1956; Grantham et al. 1958). As a result, the Lake Beds succession in the Rukwa Rift remains poorly understood, particularly in term of its sedimentology and depositional environments, stratigraphy, age, and provenance.

A detailed investigation of the extensive outcrop exposures of the uppermost, exposed portion of the Lake Beds in the southern end of the Rukwa Rift Basin is presented here. The primary aims are: (1) to document the detailed sedimentology and stratigraphy of this very young Quaternary rift fill; (2) to reconstruct its depositional systems and paleoenvironments; and (3) to decipher the role and influence of explosive volcanism, climate, and tectonics on stratigraphy, architecture, and basin evolution.

GEOLOGIC SETTING AND BACKGROUND

The Rukwa Rift Basin (RRB) forms part of the Western Branch of East African Rift System, and is one of the thickest Phanerozoic sedimentary successions in East Africa. Regional seismic and gravity surveys conducted in the late 1980s reveal as much as 8 - 11 km of sedimentary fill in the basin (Kilembe and Rosendahl 1992; Morley at al. 1999). The basin is about 360 km long and 40 km wide, and is located in a structural relay zone between the Tanganyika and Malawi rifts (Fig. 1). The RRB is a down-to-northeast half-graben, bounded by the long-lived Lupa border fault and Tanzania Craton to the northeast, by the Ufipa fault and uplifted Ufipa block to the west, and by the Rungwe Volcanic Province and Mbozi block to the south and southwest (Ebinger et al. 1989; Kilembe and Rosendahl 1992). Archean granitoids and uplifted Proterozoic metamorphic rocks of the Ubendian shear belt flank the RRB (Quennell 1956; Daly et al. 1985).

Deposition in the RRB began in the late Carboniferous - Permian with the Karoo Supergroup, which ranges from 800 m to 3.5 km thick (Morley et al. 1999). Overlying this is the Red Sandstone Group, which has been subdivided into two formations, the Cretaceous Galula Formation and the Oligocene Nsungwe Formation (Roberts et al. 2004, 2010, 2012; Stevens et al. 2013). The uppermost depositional unit in the RRB is the Neogene to Recent Lake Beds succession, which forms the focus of this investigation.

The Lake Beds succession constitutes a widespread stratigraphic unit in the RRB (Kilembe and Rosendahl 1992; Morley et al. 1999). Seismic reflection data demonstrate a west to east increase in stratal thickness, reaching up to 4 km thick near the Lupa border fault (Fig. 1; Kilembe and Rosendahl 1992). The uppermost parts of the succession are well exposed throughout much of the southern RRB, particularly in the Ilasilo - Galula, Ikuha, and Ikumbi areas, as well as in the Songwe valley and along the Chambua, Hamposia, Namba, and Chizi river drainages (Fig. 2). Deeper levels are recorded in the Ivuna-1 and Galula-1 wells, drilled in 1987 in the central and western portions of the basin, respectively (Fig. 1).

The depositional age and stratigraphy of the Lake Beds is poorly constrained. Earlier regional geological mapping by Quennell et al. (1956) suggested a two-phase subdivision of the Lake Beds into a lower Pliocene - lower Pleistocene unit and an upper Pleistocene - Holocene unit. Based on structural and lithological features, a subsequent survey by Grantham et al. (1958) also suggested subdividing the Lake Beds into a lower unit consisting of gently NE-dipping sandstone and volcanic siltstone and an upper unit characterized by flat-lying conglomerate, pumice tuff, and limestone. Subsequent microfloral analysis of a limited suite of undifferentiated Lake Beds cuttings samples from the Ivuna and Galula wells yielded late Pliocene - Holocene ages (Wescott et al. 1991). Ebinger et al. (1989) suggested that the Lake Beds are probably late Miocene - Pleistocene based on K-Ar geochronology data on the Rungwe volcanics. Aside from these efforts to characterize the Lake Beds succession and estimate its age, there have been few stratigraphic investigations or facies descriptions since the regional geologic mapping of the 1950s. Although ”Lake Beds” succession has not been classified into formal lithostratigraphic terms, they represents a widely recognized rock unit in the Rukwa Rift Basin. Different nomenclatures have been informally adopted for the Lake Beds in the published works on the Rukwa Basin, such as Lake Beds Group, Lake Beds Sequence, Lake Beds Formation, etc. (e.g., Kilembe and Rosendahl 1992; Morley et al. 1999; Roberts et al. 2010; Hilbert-Wolf and Roberts 2015) in which capital letters are applied for Lake Beds, and some adopting the informal lithostratigraphic subdivision proposed by Grantham et al. (1958). As such, we consider the ”Lake Beds” as semi-formal terms for the uppermost mega-sequence in the Rukwa Rift Basin, and for the sake of consistency, we propose to adopt the capitalized style of nomenclature referring to this sedimentary strata.

Most of the published research on the Lake Beds in the RRB has focused on paleolimnology (e.g., Haberyan 1987; Talbot and Livingstone 1989; Barker et al. 2002) and tectonics (e.g., Delvaux et al. 1998) as a basis for interpreting climate change and lake-level fluctuation. For example, analysis of two sediment cores recovered from modern Lake Rukwa yielded an ~ 23 ka record of climate and lake-level fluctuations in the rift (Haberyan 1987; Talbot and Livingstone 1989; Barker et al. 2002; Thevenon et al. 2002). These studies suggest that Lake Rukwa, which is now shallow (< 15 m deep) and covers the central portion of the basin, occupied the whole basin during the early Holocene, but nearly dried out at times during the late Holocene (Kennerley 1962; Haberyan 1987). Barker et al. (2002) suggested that a lowstand characterized the RRB during the Last Glacial Maximum (~ 23 - 20 ka), and that overall lake expansion and development of pluvial conditions followed, with maximum water depth being reached ca. 13.5 ka. Between ~ 16 and 5 ka, lake highstands are attributed to a wetter climate (Haberyan 1987). More arid conditions followed around 4 ka, resulting in elevated lake salinity and an overall lake-level drop throughout the late Holocene (Haberyan 1987; Talbot and Livingstone 1989; Nicholson 1999).

Combining remote-sensing, structural, and sedimentologic data in the vicinity of the main basin-bounding faults, along with ^{14}C dating of paleo-lake terraces and fan deltas around the edge of the lake, Delvaux et al. (1998) provided further evidence of long-term variations in water level and paleo-shoreline positions. These workers suggested that lake high stands reached upwards of 170 m above the present-day lake level, at which point Lake Rukwa overflowed into Lake Tanganyika. The latter findings support the interpretation by Haberyan (1987) that a maximum lake highstand of approximately 200 m occurred during a more humid climatic phase. Besides a strong climatic control, Delvaux et al. (1998) concluded that the late Quaternary lake level and sedimentation in the RRB were also influenced by displacements along several of the basin-bounding faults.

Most recently, Cohen et al. (2013) investigated ostracodes and molluscs preserved in the upper Lake Beds in natural exposures south and north of Lake Rukwa. They reported a suite of radiocarbon ages ranging from ~ 11 ka to 6 ka from the 1 – 2-m-thick Lake Beds sections north of modern Lake Rukwa, along the Katavi trench and from highstand fan delta deposits near Muze. From Lake Beds exposures south of modern Lake Rukwa, the authors obtained ^{14}C ages between ~ 23 and 7 ka on ostracode and mollusc shells collected from the uppermost 20 m of a deep gully exposed along the Songwe River, a succession that we describe here as section IL6. They also summarized a similar range of published and unpublished radiocarbon ages from other nearby locations, including colluvial deposits on the foot wall of the Lupa Fault scarp along the bank of the Zira River (~ 23 ka) and a suite of samples from 3 - 8 km south of Galula town (11- 6 ka).

Published investigations of the RRB Lake Beds suggest that only the uppermost 50 - 60 m of the > 4-km-thick Lake Beds deposits are actually exposed throughout most of the Rukwa Rift. As such, these rocks are informally referred to herein as the upper Lake Beds (ULB). A lower stratigraphic boundary has not yet been defined for the ULB, and a more full treatment of the stratigraphy and nomenclature of the entire Lake Beds must await better dating and analysis of the stratigraphy of the Ivuna-1 and Galula-1 wells, as well as investigation of as yet undescribed strata identified by the authors between the Cretaceous Galula Formation and the ULB strata on the western margin of the rift system.

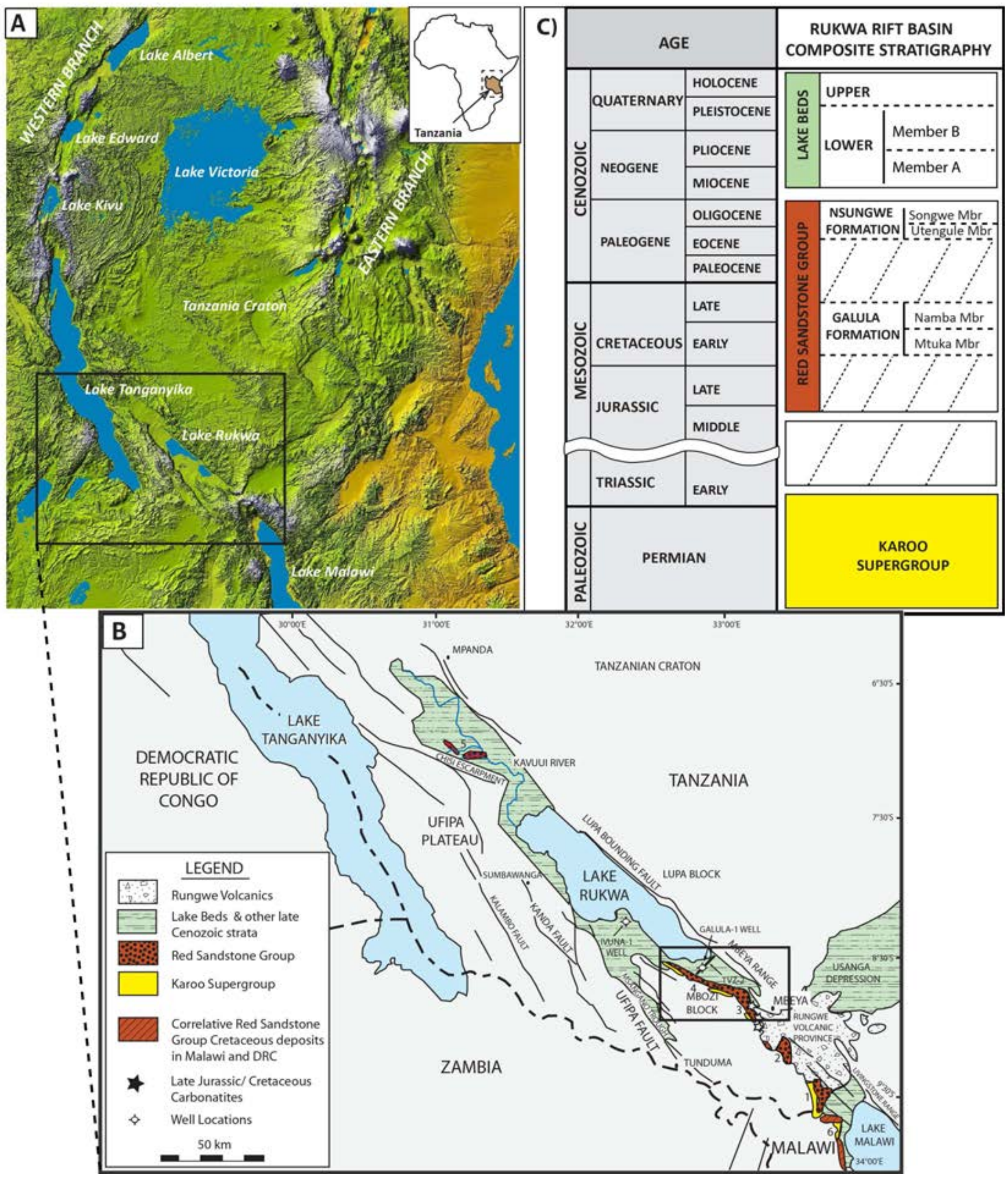

Fig. 1.—**A)** Map showing studies area (inset box) in southwestern Tanzania. **B)** Geological map of the Rukwa Rift Basin showing tectonic elements and distribution of rock units. Inset box is shown in Fig. 2. **C)** Composite stratigraphy of the Rukwa Rift Basin (modified from Roberts et al., 2010).

METHODS

This study involved geologic mapping and lithofacies analysis of the exposed Lake Beds strata across the southern end of the Rukwa Rift Basin (Fig. 2). A combination of Google Earth satellite imagery and topographic maps were used to identify key field localities. Topographic maps and the Mbeya 244 quarter-degree geological map (Grantham et al. 1958) were used as base maps. Stratigraphic sections were measured across the southern portion of the basin, particularly where well exposed cliffs are formed along incised stream drainages. Stratigraphic sections were measured using a Jacob's staff and Brunton compass in most cases. However for some cliff-face exposures, a laser range finder and tape measure were instead employed. Geographic locations of each section were taken using a GPS set to the Arc 1960 datum. Paleocurrent orientations were measured on three-dimensionally exposed ripple, planar and trough cross-stratified beds using a Brunton compass. Lithofacies were identified based on bedding style, sedimentary and biogenic structures, sediment textures, and lithology. Facies codes used in this paper mainly follow Miall (1977), with minor modifications added to highlight the distinctive characteristics of the Lake Beds. In the descriptions presented here, the first letter, capitalized, represents grain size (i.e., G = Gravel, S = Sand, F = Fine grained facies, including very fine sand, silt and mud). The second, lower case letter describes textural or structural attributes of the lithofacies (e.g., p = planar cross-bedding, c = clast supported). The third letter, in most cases, has been added for a reference to lithologic composition, particularly for the volcaniclastic dominated lithofacies (e.g., Spv = planar cross-bedded volcaniclastic sandstones). Lithofacies were grouped into distinctive assemblages (facies associations) and linked to inferred depositional processes and environments. The definition and identification of individual facies associations is based on specific lithofacies present, bedding thicknesses, nature of the bounding contacts, post-depositional features, and fossil type and abundance.

Measured stratigraphic sections were correlated by physically walking out exposures in the field and tracing marker horizons where possible, and by correlating key marker horizons and both new (presented herein) and previously reported radiocarbon ages. Representative sandstone samples were collected for petrographic analysis. Sandstone and siltstone composition and texture (e.g., grain size, shape, sorting, and porosity) were investigated via petrographic microscopy and scanning electron microscopy (SEM). The detrital-mineral composition of siliciclastic sandstones in thin section were statistically analyzed by point-counting techniques, following the modified Gazzi-Dickinson method (Ingersoll et al. 1984), to determine percentage proportions of quartz, feldspar, and rock fragments. Pebble counts were also performed in the field to further characterize the composition of conglomerate units through the Lake Beds stratigraphy and to supplement the sandstone petrology. Five organic-rich mudstone and siltstone samples containing abundant large fragments of carbonized plant material, along with one unionoid bivalve shell sample, were collected from different units across the stratigraphic sections for radiocarbon dating. The analysis was conducted using the accelerator mass spectrometry (AMS) technique at the Beta Analytic Laboratory of Miami, Florida, USA.

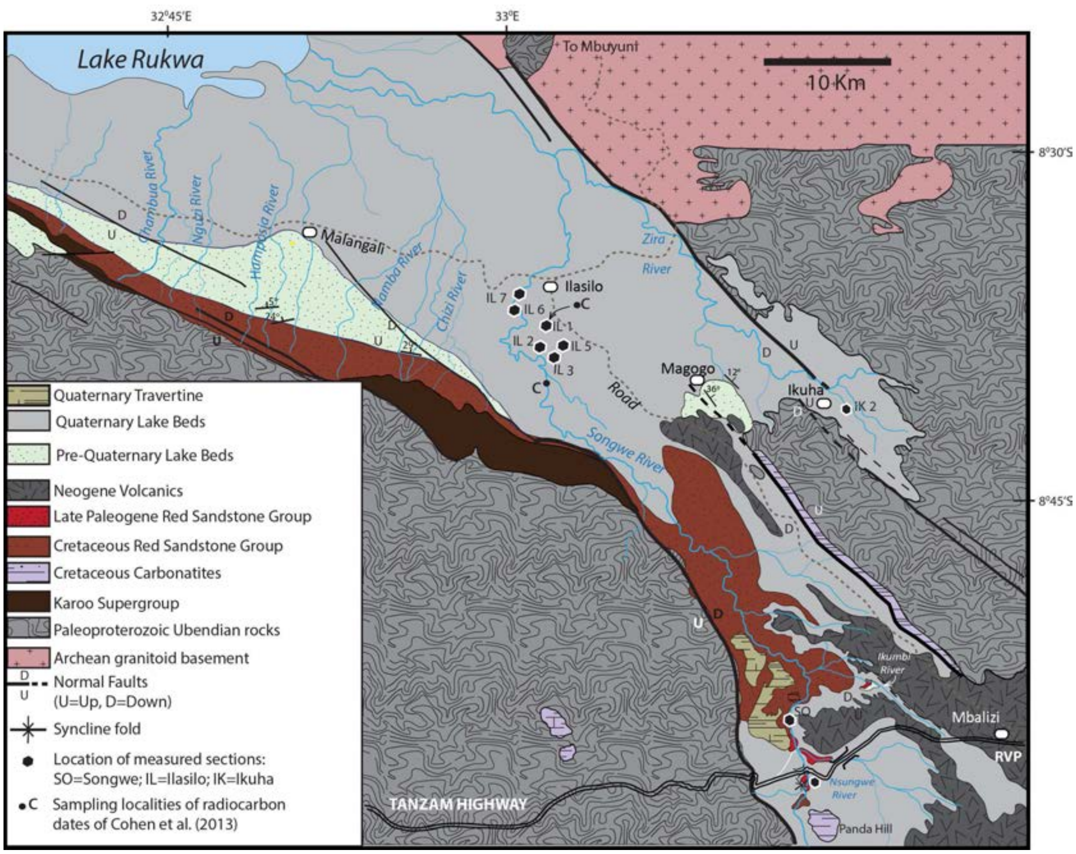

Fig. 2.—Geologic map of the southern Rukwa Rift Basin, highlighting the distribution of upper Lake Beds strata and location of the measured sections along the upper Songwe River (Songwe area), the lower Songwe River (Ilasilo area) and around the Ikuha area. Other lithologies and structures are adopted from Grantham et al. (1958) and Roberts et al. (2010).

FACIES ANALYSIS

A total of 24 lithofacies were recognized in the ULB, and are presented in Tables 1 and 2. Lithofacies observed in this study are entirely clastic and grouped by grain size and composition, ranging from dominantly volcaniclastic to dominantly siliciclastic. Lithofacies and the presence of diagnostic architectural elements were used to define eleven genetically related facies associations (FAs). Each of these FAs is described below, followed by an interpretation of associated depositional environments (Table 3). FAs are ordered by descending grain size.

Table 1. Coarse-grained lithofacies of the upper Lake Beds.

Code	Lithofacies	Texture and Composition	Structures and Features	Colour	Interpretation
Gcmi	Clast-supported Intraformati-onal conglomera-te	Clasts: pebble sized;moderate to poorly sorted; sub-round to rounded; dominated by intra formational siltstone rip-up clasts and rare pumice clasts Matrix: fine- to medium-grained sand	Massive to crudely-bedded weak normal grading in places	Grayish yellow-green (5GY 7/2)	Unidirectional high energy deposits
Gcme	Clast-supported extraformati onal conglomerat e	Clasts: pebble- to boulder-sized moderate- to poorly sorted; sub-angular to rounded, oblate to prolate clasts; dominantly vein quartz, metamorphic and volcanics, rare travertine clasts; poorly indurated ; poorly indurated to indurated Matrix: medium- to coarse-grained sand	Typically massive or moderately graded high-relief basal erosional surfaces	Medium gray (N5), medium light-gray(N6), to pale yellowish-brown (10YR 6/2)	Unidirectional high-energy deposits.
Smvp	Massive volcanic-clastic and tuffa- ceous pebbly sandstone	Medium sand- to pebble-sized; moderate-well sorted; pumice dominated; rare quartz grains.	Commonly massive, weakly graded; bivalves, fish and gastropods locally	Medium light gray (N6), grayish yellow green (5GY 7/2), pale red (5R 6/2), light olive-gray (5Y 6/1), to	Medium- to high-energy deposits

				yellowish-gray (5Y7/2).	
Spvp	Planar cross-bedded volcani-clastic pebbly sandstone.	Very coarse-grained sand to granules and pebbles; moderately sorted; pebbles are sub-round to rounded, dominantly pumice.	Planar cross-bedded	Medium gray (N5), medium light- gray (N6).	Unidirectional medium to low-energy flow deposits
Shvp	Horizontally stratified volcani-clastic pebbly sandstone.	Medium- to very coarse-grained sand with pebbles; moderate-poorly sorted, sub-round to rounded; dominated by pumice and mafic volcanic lithic fragments; minor quartz feldspars and muscovite; rare siltstone rip-up clasts.	Planar stratification and parting lineation.	Medium light-gray(N5), light olive-gray (5Y 6/1).	Medium- to high-energy upper plane-bed deposits
Sp	Planar cross-bedded sandstone	Medium- to coarse-grained sand; moderate-well sorted; composed of mainly quartz, feldspar, and mica; less pumice and mafic volcanic lithics	Tabular cross-bedded.	Yellowish gray (5Y7/2), pale red (10R6/6), pale brown (5Y5/2), to pale yellowish brown (10YR 6/2)	Unidirectional, low-and high-energy flow regime deposits.
Spv	Planar cross-bedded volcani-clastic sandstone	Fine- to medium-grained sand, locally coarse-grained; moderate-poorly sorted; with floating pumice granules and pebbles; less common rip-up siltstone less common rip-up siltstone pebbles and cobbles	Tabular cross-bedded; fining upward, coset thickness ranging from 0.06 to 3m	Light olive gray (5Y6/1), medium light gray (N6), to grayish yellow green (5GY7/2)	Unidirectional low flow regime deposits
St	Trough cross-bedded sandstone	Medium- to coarse-grained sand; moderate-well-sorted, locally poorly sorted; dominated by quartz, feldspars and mica; less mafic volcanic	Trough cross-bedded; coset thickness ranges from 0.05 to 2.7m; localized	Yellowish gray (5Y), pale red (10R 6/6), to pale yellowish-	Low and high (3-D dunes) low regime deposits.

		lithics and pumice; rare floating pumice and quartz pebbles	fish bones.	brown (10YR 6/2)	
Stv	Trough cross-bedded volcani-clastic sandstone	Fine- to medium-grained sand; moderately well sorted; dominated by pumice and mafic volcanic lithics, with subordinate silicate minerals; rare floating pumice granules and pebbles.	Trough cross-bedded; coset thicknesses range from 0.05 to 2.5m.	Medium light gray(N6), yellowish gray(5Y)	Low and high (3-D dunes) pyroclastic flow regime deposits.
Shv	Horizontally stratified volcaniclastic sandstone	Fine-, medium- to coarse-grained sand; dominantly volcaniclastic in composition; commonly with floating pumice granules and pebbles	Planar bedded	Medium light-gray(N6), to medium dark gray (N4)	Unidirectional medium-high flow regime deposits.
Sr	Ripple cross-laminated sandstone	Fine- to medium-grained sand; dominantly siliciclastic with proportionally less pumice grains.	Ripple cross-lamination, and climbing ripples	Pale red (10R 6/6)	Unidirectional, low flow regime migrating ripples.
Srv	Ripple cross-laminated volcani-clastic sandstone	Very fine- to fine grained sand, exclusively volcaniclastic in composition.	Ripple cross-lamination, and climbing ripples	Olive gray (5Y 4/1), grayish yellow-green(5GY 7/2)	Unidirectional, lower flow regime
Sm	Massive sandstone	Fine-, medium- to coarse-grained sand; dominantly quartzo-feldspatholithic in composition, with isolated floating quartz and pumice.	Typically massive, crudely bedded or crudely fining upward in places.	Pale red (10R 6/2), pale olive (10Y 6/2), to moderate reddish brown (10R 4/6)	Rapid (high energy) sediment-ation deposits
Smv	Massive volcanic Sandstone	Medium- to coarse-grained sand; tuffaceous or volcaniclastic-pumice rich; moderate-well-sorted.	Massive; fining upward bed form	Medium light gray (N6), yellowish-gray(5Y 7/2), to	Rapid (high-energy) pyroclastic flow deposits

				grayish yellow-green (5GY7/2)	

Table 2. Fine-grained lithofacies of the upper Lake Beds.

Code	Lithofacies	Texture amd Composition	Structures and Features	Color	Interpretation
Fcvs	Current-rippled volcanic siltstone	Ash and silt-sized grains; with rare floating pumice sands and granules	Current ripples	Medium dark-gray(N5), grayish yellow, green (5GY 7/2)	Water-reworked pyroclastic flow deposits
Fhvs	Horizontally stratified volcanic siltstone	Ash and silt-sized grains	Planar stratification	Moderate orange pink (5YR 8/4), light olive gray (5Y 6/1), yellowish gray (5Y 8/1), pinkish gray (5YR 8/1), to pale yellowish brown (10YR6/2).	Subaqueous pyroclastic flow/ fallout deposits
Fmvs	Massive volcanic siltstone	Ash and silt-sized grains	Typically massive; crudely bedded in places	Pale yellowish brown (10YR 6/2), light olive gray (5Y 5/2), pale red (10R 6/2), pale pink (5RP 8/2), to pinkish gray (5YR 8/1).	Rapid (low-high energy) subaqueous pyroclastic fallout deposits
Fvso	Organic-rich	Ash and silt-sized grains	Typically planar tabular bedded, laminated and rippled; massive in places	Medium gray (N5), dark yellowish-brown (10YR 4/2), yellowish-gray (5Y7/2)	Rapid subaqueous settle-out of volcanic detritus
Fvsd	Deformed volcanic	Clayey silt; in most cases organic-rich	Convoluted bedding	Medium dark gray (N5), grayish yellow-green	Subaqueous high energy pyroclastic

	siltstone			(5GYB7/2), olive gray (5Y 4/1).	flow deposits.
Fl	Finely laminated siltstone, mudstone and claystone	Clay- to silt-sized grains; with calcareous nodules and less common floating granules and pebbles	Fine laminated and cross-laminated in places; commonly organic rich; locally containing fish bones	Dark yellowish brown(10YR 4/2), olive gray (5Y 4/1), pale yellowish brown (10YR 6/2), dusky yellowish-brown (10YR 4/2), to grayish- orange (10YR 7/4)	Sheet flooding and/or suspension load deposits.
Fcf	Massive fines	Poorly sorted, sandy mud, silt and clay; typically organic rich; less common calcareous nodules, and calcified roots	Typically massive;	Yellowish-gray (5Y 7/2), light brown (5YR 6/4), brownish gray (5Y8/4), dark yellowish brown (10YR 4/2), to dusky yellow	Suspension or overbank flood deposits.
Fva	Vitric ash	Silty clay diatomaceous vitric ash	Planar tabular bedded and thinly laminated; partly mottled or rippled, each lamination shows normal grading/fining upwards.	Grayish yellow-green (5GY 7/2), very pale orange (10YR 8/2), to pale olive (10Y 6/2)	Low energy water-lain or airfall ash deposits
Fr	Rooted fines	Silt- to fine sand	Primary structures destroyed; calcified roots, sediment-filled rootlets, burrows calcareous nodules, and termite nests	Pale red (10R 6/2), yellowish-gray (5Y7/2), moderate reddish orange (10R 6/6)	Paleosol

Table 3. Facies associations (FAs), architectural-elements and depositional environments of the upper Lake Beds.

FA	**Facies**	**Diagnostic Features**	**Architectural Elements**	**Depositional Process**	**Macrofossil**	**Depositional Environment**
FA 1	Gcme, Sm, Smv	Moderate-poorly sorted	Moderate-poorly sorted	Pseudoplastic debris flows, sheet flooding	Unfossiliferous	Alluvial plain
FA 2	Gcmi, Gcme , St, Sm	Massive to crudely bedded, weakly graded, erosional basal and top surfaces.	SG, CH	Channel-fill, sediment, gravity fallout.	Unfossiliferous	Fluvial channel lags
FA 3	Gcme, Smvp, Shvp, St, Shv, Srv, Fhvs	Large scale, high angle (>30^{o}) dipping sandstone bed series	CH, LA	Turbidity currents or hyperpycnal distributary channel flows	Fish bones locally	Gilbert-type delta foresets
FA 4	Gcme, Smv, Stv	Lenticular beds, with trough and planar cross-bedding	GB, CH,	Debris flow, sheet flooding	Isolated fish bones locally	Interdistributary channels.
FA 5	Smvp, Shvp, Sh, St, Sr, Srv, Fmvs, Fhvs, Fva	Large scale, low angle cross-bedding, upper plane bedding moderate-well-sorted, commonly fining upward beds, with erosional or upper coset boundary	CH, LA, LS	Hyperconcentrated(hyperpycnal) distributary turbidite channel flows	Isolated bivalves, fish and gastropods locally	Delta front
FA 6	Sm, Smv, St, (Gcmi, Gcme)	High degree of sediment rounding, Upward fining and cut/fill	CH, SG , SB	Channel-fill, sediment gravity fallout	Isolated fish bones locally	Fluvial Channels
FA 7	Sr, St, Fhvs,	Tabular, alternating beds of horizontally	SE: SB, FF	Distributary channel flows, suspension	Locally fish bones and	Lower delta plain

	Fmvs	stratified siltstone and cross-laminated sandstone		load fallout.	termite nests	
FA 8	Sm, Fmvs, Fvso, FcF, Fr	Massive, bioturbated beds; with rootlets, burrows, calcareous nodules and termite nests.	SG, FF	Overbank deposition, abandoned channels.	Trace fossils	Floodplain
FA 9	Shv, Fhvs, Fvso, Fcf, Fl	Lenticular (concave upward), organic-rich fines (mud-, silt-, and claystone), massive or thinly bedded or laminated	FF(CH)	Overbank deposition or abandoned channel-fill of suspension/gravity fallout fines,	Isolated fish bones locally	Marsh
FA 10	Srv, Fcvs, Fva, Sr, Sh, Fl,	Overall fine-grained; sand-stone, siltstone and volcanic ash; climbing ripple cross-laminations, moderate- well sorted, fining upward	CH, DA, FF	Subaqueous turbidity currents,	Isolated fish bones	Prodelta
FA 11	Fvso, Fmvs, Fhvs, Fvsd,	Horizontally stratified, lateral extensive, organic-rich(diatomaceous) fine-grained deposits; mudstone, ash and thin very fine-grained siltstone and sandstone	SG, CH	Suspension fallout and underflow turbidity currents	Isolated fish bones, diatoms	Lake floor

Architectural elements; SG=Sediment-gravity flow, GB=Gravel Bars, SE=Sandy Sheet, LS=Laminated Sand sheet, CH=Channel fill, SB=Sand Bed form, LA=Lateral Accretion, DA=Downstream Accretion, FF=Floodplain Fines, including paleosol and overbank (after Miall, 1996).

FA1: Thick, Poorly Indurated Conglomerate

FA1 comprises gently (< 10°) inclined lenticular and tabular, clast-supported extraformational conglomerate (Gcme) that is intercalated and/ or interbedded with similarly inclined medium- to coarse-grained muddy or tuffaceous sandstone (Sm, Smv) (Tables 1 - 3; Fig. 3A). Individual lenticular and locally tabular beds range from 0.5 to 2 m thick, but combine to form depositional packages (FAs) that are 2 - 6 m thick with erosional upper and lower contacts. In places, bedsets of FA1 reach 13 m thick.

FA1 is well exposed throughout the Songwe Valley, the Ifisi area, and in particular, the Ikumbi area. Conglomerate and sandstone beds of this facies are typically moderately to poorly indurated. Conglomerate (Gcme) facies are typically massive or crudely stratified, with poorly preserved pebble imbrication and a crude upward fining. They are composed of angular, subangular, and subrounded pebbles, cobbles, and rare boulders in a matrix of poorly sorted medium- to coarse-grained muddy sandstone. Lithoclasts are polymictic and include vein quartz, metamorphic, metavolcanic, and rare volcanic and reworked sandstone clasts. Subordinate sandstone facies (Sm and Smv) are similarly massive or crudely bedded, muddy, and moderately to poorly sorted. Grain size ranges from medium- to coarse-grained sand, with abundant isolated pebbles. Calcareous concretions, commonly rhizocretions, and root traces are very common in some intervals of FA1, particularly in the Ifisi - Songwe areas, where they form discrete horizons.

Interpretation.—FA1 is interpreted to represent alluvial deposition based on the predominance of large grain sizes and angularity, poor overall sorting, crude upward fining, and clast composition. Massive and poorly sorted conglomerate and sandstone couplets commonly form thick inclined macroform architectural elements, which are interpreted to be high-energy debris-flow or sheet-flood deposits on proximal to medial alluvial surfaces (cf. Miall 1996). Tabular beds of this FA represent sheet-flood deposition, whereas lenticular beds represent channelized debris-flow deposits, respectively.

In many places, FA1 exposures do not preserve large-scale inclined macroform elements, yet the general sedimentological character of the deposits remains similar. In these areas the lack of large-scale inclined macroforms is more consistent with more gently sloping distal alluvial settings, where fluvial processes dominate. The alternating nature of conglomerate and sandstone beds in FA1, as well as presence of horizonated calcareous concretions, rhizocretions, and root traces, indicates episodic sedimentation and pedogenesis.

FA2: Thin, Indurated Conglomerate

FA2 is characterized by relatively indurated, clast-supported intraformational and extraformational conglomerate (Gcmi, Gcme) and thin, subordinate sandstones facies Sm and St (Tables 1 and 3). This FA is found predominantly on the eastern and southeastern margins of the basin, in the Songwe, Ikumbi, and Ifisi areas. Individual FA2 units range from 0.5 to 5 m thick, and are typically massive or crudely stratified with weak normal grading. The intraformational clasts are dominantly volcanic siltstone rip-up clasts and pumice, ranging from subangular to rounded pebble- and cobble-size particles. The extraformational conglomerate contains varying proportions of vein quartz, metamorphic, volcanic and metavolcanic clasts. Grain size ranges widely from sub-angular to subrounded pebbles, cobbles, and boulders. Matrix consists of a mixture of medium- to coarse-grained sandstone. FA2 units change character between the lower and upper parts of the exposed stratigraphic section, with coarser units lower in the section and finer units higher up in the section.

Interpretation.—FA2 is interpreted to represent basal lag deposits of braided fluvial channels, based on its massive, poorly sorted nature and basal erosional contact (cf. Miall 1996). The coarseness and angularity of clasts in FA2, as well as its occurrence near the uplifted rift flanks, suggests proximity to sediment source regions. The recurrence of this FA across the study area, where it is interbedded or intercalated with lenticular to subhorizontal beds of volcanic sandstone and siltstone of FA9, suggests a channel belt that underwent multi-stage filling or reactivation. In places, deposits of FA2 are interbedded with or capped by profundal deposits, indicating episodic, rapid fluctuations of base level.

FA3: Steeply Inclined Conglomerate and Sandstone

FA3 is developed in the Ikuha and Ilasilo areas, and is characterized by 4 – 7-m-thick, steeply dipping (30 to 40°) conglomerate or pebbly sandstone (Gcme, Smvp, Shvp) beds that grade down-dip into medium- to coarse-grained sandstone (St, Shv, Srv), and siltstone (Fhvs) facies (Tables 1 - 3). Bounding upper and lower contacts are typically sharp and locally erosional. Individual beds range from 10 to 25 cm thick and are characterized by erosional to gradational internal contacts. Conglomeratic beds (Gcme and Shvp facies) are moderately to well sorted. Clasts are subangular to rounded and of granule to pebble size. Lithologies include vein quartz, pumice, mafic volcanics, granitic gneiss, and metavolcanics. Matrix consists of fine- to medium-grained sandstone. Sandstone beds are well sorted, planar-stratified, and ripple or trough cross-laminated and commonly fine upward from medium- or coarse-grained sandstone into fine- to very fine-grained sandstone. Measurement of paleocurrent indicators on trough-cross bedding in the Ikuha area suggest southeast- to eastward-oriented flow, whereas at Ilasilo and near Hamposia, measurements of paleocurrent indicators indicate flow to the southeast and north (directions), respectively. Fossils recorded in FA3 are limited to isolated, locally pyritized fish bones.

Interpretation.—FA3 is interpreted to record accretion of sediments on a steep subaqueous delta slope, typical of fluvial Gilbert-type deltas. This interpretation is based on the similarity in facies and facies architecture with Gilbert-delta deposits described in the literature (cf. Gilbert 1885, 1890; Garcia-Garcia et al. 2006). The massive or crudely stratified conglomeratic and pebbly sandstone intervals of this FA are interpreted to represent gravity-flow deposits, whereas ripples and trough cross-stratified sandstones indicate deposition by traction processes. Thick bedsets consisting of alternating conglomerate and sandstone beds likely reflect the waxing and waning nature of a sustained hyperconcentrated flow that evolved from pseudoplastic debris flows or sheet floods in the hinterlands (e.g., Pierson and Scott 1985). Subangular to rounded, oblate to prolate pebble shapes (cf. Zingg 1935) in these delta foresets suggest long-distance sediment transportation.

FA4: Minor Lenticular to Subhorizontal Sandstone

FA4 is rare, and comprises 0.5 to 1 m thick, conglomeratic, trough cross-bedded, and planar cross-bedded volcaniclastic (epiclastic) sandstone (Gcme, Smv, Stv: Table 1, 2, 3). FA4 beds are tabular (sheet-like) or lenticular (tens of meters long) and are separated from each other by prominent erosional surfaces. Conglomeratic sandstone beds are massive and characterized by isolated polymict pebble- to boulder-size clasts (dominantly subangular to rounded pumice and calcareous nodules) in a framework of medium-grained, moderately sorted volcaniclastic sandstone.

Interpretation.—FA4 is interpreted to represent interdistributary-channel deposition, based mainly on the nature of the bounding surfaces, tabular to broadly lenticular bedding geometry, subangular to rounded pebble shapes, and cross-stratification. This interpretation is supported in the associated conglomeratic sandstone facies (Smv) by the dominance of volcanic siltstone rip-ups, which were likely reworked by erosion of underlying Lake Bed units or derived from reworking of primary epiclastic fine-grained volcanic deposits up-slope. Lenticular, coarse-grained and conglomeratic sandstone deposits in this FA are interpreted as high-energy fluvial deposits, whereas tabular massive vitric ash (tuff) units are interpreted as sheet-flood deposits. Thick, structureless (massive) beds of this facies association suggest rapid sediment deposition.

FA5: Gently Inclined Sandstone and Siltstone

FA5 is observed both in various parts of the study area and at various stratigraphic levels. This FA consists of thick (up to 8 m) successions, of large-scale, low-angle (less than 30°)-dipping sandstone and/or siltstone beds (clinoforms), which are composed of a combination of various facies, including: Shvp, Smvp, Sh, Sr, St, Srv, Fhvs, Fmvs, and Fva (Tables 1 - 3; Figs. 3B - D). FA5 units are commonly characterized by sharp to erosional basal contacts and erosional upper contacts. A distinctive volcanic pebbly sandstone facies (Shvp and Smvp) is most abundant, occurring as beds of 0.1 - 1.5 m thick dominated by subrounded to rounded coarse-grained sandstone. Granules and pebbles of pumice, quartz, and metamorphic lithics and rare siltstone rip-up clasts up to 6 cm in diameter (Fig. 3B) also occur. In most cases, FA5 is characterized by stacked beds composed of the facies Smvp or Shvp overlain by Sr and Srv and capped with Sh. Beds fine upward from pebbly conglomerate to very fine-grained sandstone. In other places and at different stratigraphic levels, FA5 is composed of repeated tripartite packages of sandstone – siltstone - volcanic ash. In the latter instances, individual sandstone beds (Shv, Srv, Sr and St) are ~0.05-1 m thick, and consist of fine- to medium-grained sandstone with rare granule- to pebble-size pumice clasts. Volcanic siltstone beds (Fhvs and Fmvs facies) are typically well sorted, and commonly fine upwards to nearly pure ash (Fva).

A range of sedimentary structures are preserved in FA5, from trough cross-stratification to planar stratification with parting lineations to current-ripple cross-lamination. The large-scale, low-angle clinoform sets dip variably towards the north, northwest, and west in different parts of the sections around Ilasilo. FA5 is fossiliferous, with gastropods, bivalves, and isolated pyritized fish bones being locally abundant.

Interpretation.—Based on the overall coarse-grained composition, sedimentary structures of individual beds, and large-scale, low-angle-dipping bedsets or clinoforms, FA5 is interpreted to represent delta-front deposits of a river-dominated delta. This interpretation is consistent with the presence of a wide array of freshwater gastropods, bivalves, and fish remains. Variations in grain size, from coarse- to fine-grained sandstone, siltstone, and ash beds in this FA are interpreted to reflect relative variations in flow velocity associated with proximal to distal sub-environments of a delta-front system (e.g., Smith 1991; Fielding 2010).

Upper-flow-regime planar bedding and lower-flow-regime unidirectional ripple cross-lamination in FA5 indicate the presence of subaqueous tractive currents. In contrast, relatively fine-grained, thinly laminated intervals reflect episodic waning subaqueous flow and sediment fallout (cf. Tanner 1967). The alternating traction and fallout sedimentary structures and the common fining-upward grain-size trends in FA5 are interpreted to reflect proximal turbidite deposits (cf. Lamb et al. 2008) or waning currents from hyperpycnal events associated with storm-generated flash flooding.

In the upper, medial to distal reaches of these delta-front deposits, the repeated facies stacking pattern is consistent with proximal Bouma cycles (Bouma, 1962). The basal parallel-laminated sandstone with parting lineations is interpreted as upper-plane bedding developed as part of the Bouma Tb interval. These are commonly overlain by highly aggradation current-ripple cross-laminated sandstone, interpreted to be Bouma Tc intervals. Overlying parallel-laminated very fine-grained sandstone or siltstone intervals are interpreted to reflect suspension settling during waning flow (Bouma Td intervals).

The recurrence of alternating, parallel-laminated pebbly sandstone beds with ripple cross-laminated fine- to medium-grained sandstone beds, commonly over 1 m thick, suggests fluctuating flow energy related to long-lived fluvial discharge in a delta-mouth environment in which hyperpycnal flows are typical (e.g. Plink-Björklund and Steel 2004; Zavala et al. 2006). In the study area, the fluctuating flow discharge is inferred to have originated from the dilution of debris flows upstream that were initiated by high-intensity precipitation events, as described from terrestrial volcanic environments elsewhere (e.g., Pierson and Scott 1985).

FA6: Massive to Cross-Stratified Sandstone

FA6 consists of 1.5 – 4-m-thick lenticular and tabular massive to cross-stratified sandstone (Sm, St, Smv) and subordinate conglomerate (Gcme, Gcmi) facies (Tables 1 - 3; Fig. 3E). FA6 is laterally extensive across the study area, particularly in the Songwe, Ikuha, and Ilasilo areas. In the Songwe area, the FA6 is dominated by multistory clast-supported cobble and boulder conglomerate bodies of FA2 that are interbedded with horizontally stratified sandstone, siltstone, and ash beds. In most occurrences around Ilasilo and Ikuha, this FA is dominated by thick, medium- to coarse-grained sandstone units that are locally interbedded with organic-rich mudstone (Fvso, Fcf). Mudstone beds in FA6 are typically 30 - 40 cm thick but are limited in lateral extent to about 20 m.

Locally, FA6 is characterized by beds with erosional lower contacts. The beds are up to 90 cm thick and fine upward from conglomerate to medium- or fine-grained sandstone. In many places, the uppermost sandstone beds are bioturbated, preserving carbonized rootlets and rare calcareous nodules. A distinctive feature of this FA is the presence of isolated ”floating” pumice and quartz pebbles, in otherwise moderately to well sorted Smv and St facies.

Channel-form architectural elements are commonly recognized in FA6. In places, channel-form conglomeratic sandstone units of this FA incise down into underlying, tabular organic-rich mudstone and volcanic siltstone deposits of FA11. The only large vertebrate fossils found in the upper Lake Beds occur in FA6 in the Ikuha Valley and consist of isolated and heavily abraded bones or bone fragments, typified by limb and vertebral skeletal elements of large ungulates. Outside of the Ikuha Valley, vertebrate fossils in FA6 are rare and limited to isolated fish bones.

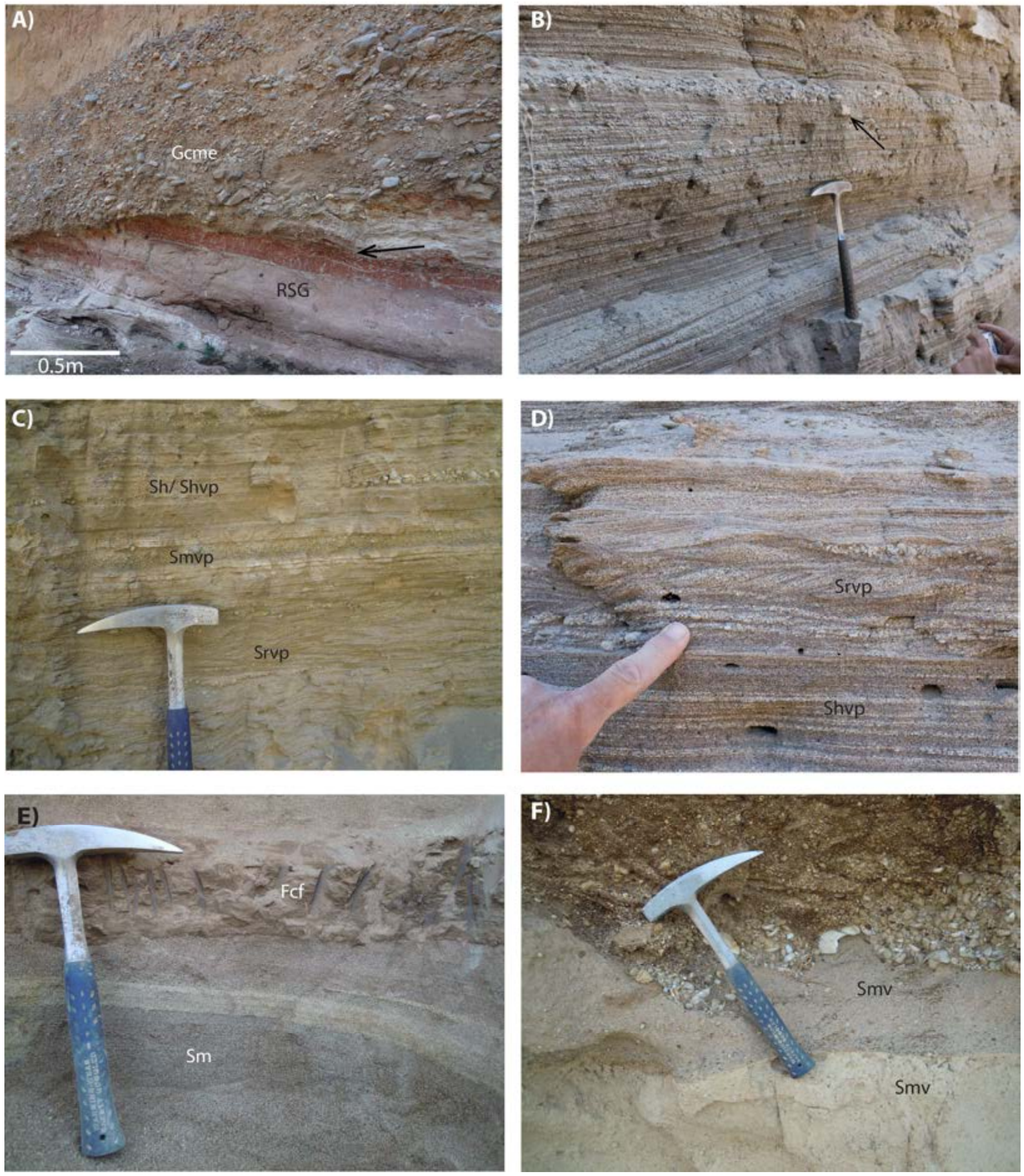

Fig. 3.—Upper Lake Beds coarse-grained facies. **A)** Clast-supported extraformational conglomerate (Gcme) within a matrix of fine- to medium-grained tuffaceous sandstone. Arrow shows angular unconformity with underlying Red Sandstone Group (RSG). **B-C)** Massive, ripple- and horizontally-stratified volcaniclastic sandstones; facies Smvp, Srvp, Shvp and Sh. Arrow in B points to volcanic siltstone rip-up. **D)** Close-up of asymmetric ripples. **E)** Crudely stratified to massive, interbedded mudstone and sandstone (Fcf, Sm facies). **F)** Basal channel lag containing bivalve shells, gastropod shells and fish bones near the top of the Ilasilo (IL) section 6.

Interpretation.—FA6 is interpreted to record dominantly fluvial processes on an upper (subaerial) lacustrine delta-plain setting. This interpretation is based mainly on: (1) unidirectional paleocurrent indicators in sandstone and abundant cut-and-fill structures; (2) textural maturity consistent with fluvial processes; and (3) the presence of channel-form architectural elements. The thick and generally massive nature of many beds of this FA is attributed to gravitational collapse of bedload sedimentation (cf. Miall 1996), as well as the destruction of primary sedimentary structures by bioturbation and soil formation. The latter is suggested by the abundance of rootlets and pedogenic calcareous nodules indicating phases of soil development following channel abandonment, subaerial exposure, and localized erosion. The presence of mudstone beds in the upper parts of FA5 is interpreted to reflect rapid floodplain deposition under hydromorphic conditions. This interpretation is consistent with dark gray (high organic content) coloration in the mudstone facies, suggestive of low oxygenation common to hydromorphic floodplain environments.

In the Songwe area, FA6 is interpreted as part of a braided-channel succession with multistory multilateral channel-fill geometry and close association with conglomerate beds of FA1 and FA2. These characteristics are similar to those described by Antia and Fielding (2011), and are comparable to alluvial deposition models of Miall (1992). In constrast, lenticular, conglomeratic sandstone deposits of FA6 incise profundal deposits in the Ilasilo area and are interpreted to represent fluvial channel deposits developed during a much later stage of the basin history, postdating a major drop in base level.

FA7: Interbedded Tabular Sandstone and Siltstone

FA7 is defined by ~1.0 - 1.5-m-thick tabular bodies of massive or horizontally stratified siltstone (Fmvs, Fhvs) interbedded with fine- to medium-grained, ripple and trough cross-laminated sandstone (Sr, St) facies (Tables 1 - 3: Fig. 4A). Current ripples (Sr) range from 2 to 8 cm thick and sets of St are up to 0.5 m thick. Erosional lower contacts and sharp to gradational upper contacts are typical. Individual beds exhibit sharp internal erosional surfaces, and channel macroform elements are common. Fossils are locally abundant in FA7, including moderately abundant but isolated pyritized fish bones, as well as simple horizontal to vertical trace fossils.

Interpretation.—Based on the fine-grained, well-sorted nature of the strata and the abundance of small-scale current-ripple lamination and trough cross-bedding, coupled with minor channelization, FA7 is interpreted to record sedimentation on a lower (subaqueous) delta plain. The repeated alternation of sandstone and siltstone facies in this FA indicates waxing and waning of traction currents associated with storm-generated flash floods. Trough or ripple cross-laminated sandstone is interpreted to have been deposited by traction currents, whereas massive and horizontally laminated siltstone intervals developed as rapid and gradual suspension fallout deposition from low-energy, waning-flow regimes. The tabular nature of the low-angle, ripple-laminated sandstone beds also suggest deposition by unconfined waning flows, and the asymmetric ripple-laminated intervals suggest influence by a unidirectional current.

FA8: Crudely Stratified to Massive Interbedded Mudstone and Sandstone

FA8 deposits are represented by 25 – 60-cm-thick, tabular very fine-grained, massive or crudely stratified sandstone and siltstone facies (Sm, Fmvs, Fvso), and massive and bioturbated mudstone facies (Fcf, Fr) (Tables 1 - 3). Sandstone portions of this FA are typically well sorted and fine upward. FA8 is common in the Ilasilo and Ikuha areas, and is often vertically and laterally adjacent to coarser-grained FA7 deposits. FA7 units are typically organic-rich and often marked by an erosional top surface. Locally, these deposits contain abundant rootlets, burrows, and isolated calcareous nodules, which are particularly common below internal erosional surfaces and near the uppermost bounding surface.

Interpretation.—The lateral and vertical association of FA8 with FA7, coupled with the abundance of features interpreted as pedogenic (rootlets, $CaCO_3$ nodules), suggest a floodplain environment in which low-energy suspension fallout and sediment-gravity-flow deposits developed in an upper-delta-plain environment. Fining-upward patterns and lateral facies transitions into coarser-grained strata of FA5 further supports this interpretation. The fine-grained nature and tabular to lenticular bed geometry indicates deposition in an overbank setting including small ephemeral ponds with subsequent subaerial exposure of small lakes or pond-like depressions across a wide delta plain.

FA9: Lenticular, Organic, Laminated Mudstone

FA9 is characterized by thin-bedded or laminated organic-rich mudstone and minor sandstone (Shv, Fhvs, Fvso, FcF, Fl: Table 2, 3) and occurs commonly in the Songwe area. These deposits forms lenticular bodies of 0.4 to 2 m thick that onlap onto buttress unconformities associated with significant predepositional topography (cf. Hilbert-Wolf and Roberts 2015) cut into conglomeratic packages of FA2. The sandstone facies are well sorted and, fine- to medium grained, whereas volcanic siltstone is generally massive or laminated. Both sandstone and siltstone beds display internal upward fining. FA9 is characterized by disseminated and fragmented carbonized plant material, mostly reeds.

Interpretation.—This facies association is interpreted to represent low-energy sediment accumulation into small ponded depressions, marshes in wetlands, or waterlogged floodplains. This interpretation is based on the fine-grained, lenticular nature of the sediment infill, high organic content, and the presence of abundant reedy plant debris, as well as seeds and leaves. Thin laminations and the upward-fining character of individual laminae and beds are attributed to gradual sediment accumulation mainly by suspension fallout. The buttress unconformities formed by onlap of FA9 (see Fig. 2D in Hilbert-Wolf and Roberts 2015) with thick, multistory conglomerate bodies of FA 2 are interpreted to reflect deposition in abandoned channel segments. The spatial association of fluvial channel deposits (FA2), found both lateral to, above, and below FA9 deposits supports this interpretation.

FA10: Tabular, Cross-Laminated Siltstone and Ash

FA10 consists of up to 4-m-thick, multistory tabular bodies of very fine-grained sandstone and siltstone (Srv, Stv, Fcvs) that are locally interbedded and/or intercalated with tabular to lenticular ash beds (Fva) (Tables 1 - 3; Figs. 4B - D, 5A). FA10 deposits are defined by a gradational or erosional basal contact, overlying tabular organic-rich mudstone and volcanic siltstone-ash beds series of FA11, and in most cases an erosional upper bounding surface. FA10 is well exposed in the study area, especially around the Ilasilo and Ihuka areas. Sandstone intervals are characterized by ripple or trough cross-lamination. They are typically moderately to well sorted and in places contain stacked pumice granules and pebbles that occur as floats or thin lenticular beds only a few grain diameters thick. Locally, for instance at the lower parts of Ilasilo section 6, FA10 is dominated by siliciclastic deposits consisting of very fine-grained sandstone facies (Sr, Sh), interbedded with siltstone and mudstone (Fl, Fcf) facies. In the latter occurrences, individual sandstone and siltstone beds are well graded and fine upward.

A wide variety of sedimentary structures occur in this FA10, including ripple cross-lamination, subcritically climbing ripples (Fig. 4C), convoluted bedding, and regionally extensive, meter-scale soft-sediment deformation features (intestiform folds) that are typically enclosed in horizontally stratified beds (Figs. 4B, 5A; Hilbert-Wolf and Roberts 2015).

Freshwater and lacustrine fossils, including fish scales and cranial remains, as well as trace fossils (e.g., termite galleries and nests), are locally abundant in this FA.

Interpretation.—FA10 is interpreted to record low-energy deposits in an area of transition from a delta front to prodelta environments. This interpretation is based mainly on the overall fine-grained nature of the FA, the abundance of current ripples and parallel lamination, and similarity to prodelta deposits described by Fielding (2010). Large-scale soft-sediment deformation features are interpreted to indicate seismically induced mobilization of sediment downslope through mass movement (cf. Syvitski and Schafer 1996; Hilbert-Wolf and Roberts 2015). Smaller-scale convoluted structures that commonly occur in this FA suggest localized slumping of sediment from the delta slope into deeper waters (e.g., Zavala et al. 2006). The presence of rippled, convolute-laminated intervals and isolated outsized (very coarse sand- to pebble-size) clasts interpreted to be "storm rollers" suggests reworking of slumped sediments by wave-influenced turbidity currents. Collectively, these depositional features are related to traction-plus-fallout processes, generated by turbulent hyperpycnal flows with high suspended loads (cf. Plink-Björklund and Steel 2004; Zavala et al. 2006).

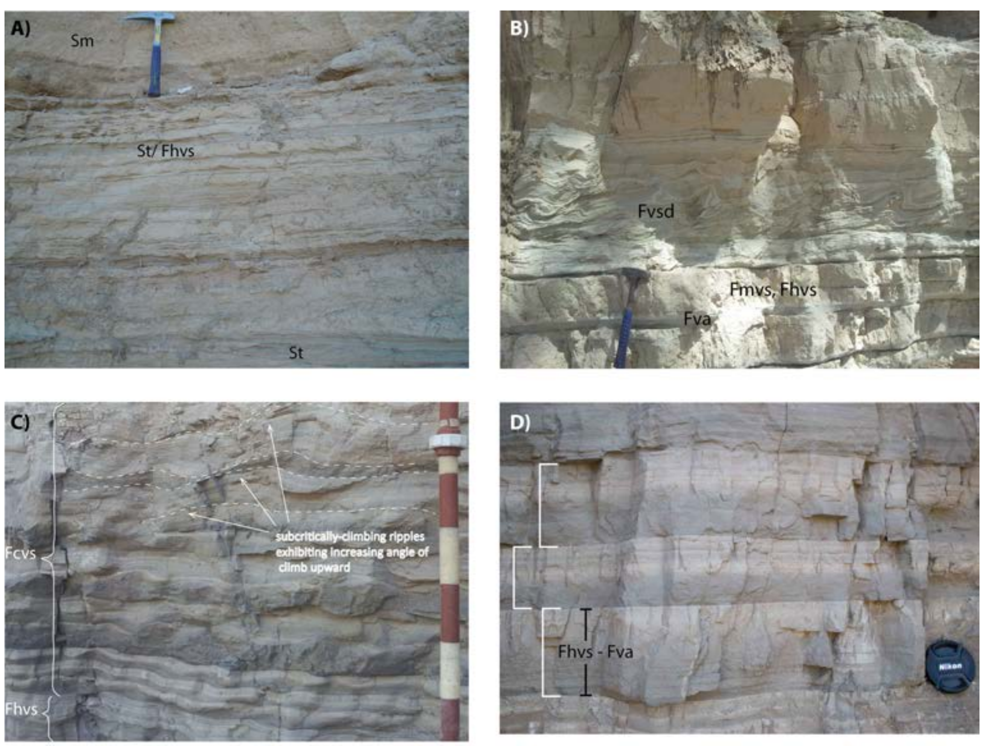

Fig. 4.—Upper Lake Beds fine-grained facies. **A)** Interbedded, tabular, cross-stratified sandstone (St) and massive or horizontally-laminated volcanic siltstone (Fhvs). **B)** Massive to

convoluted-beds of volcanic siltstone and ash; Fmvs, Fvsd and Fva facies, horizontally and current ripple-laminated volcanic siltstone and ash (Fhvs, Fcvs and Fva). **C)** Tabular, horizontally- and ripple-laminated volcanic siltstone (Fhvs, Fcvs). **D)** Close-up of horizontally-laminated, very fine-grained siltstone-to-ash (illustrated in white) bed series interpreted as hyperpycnites.

FA11: Tabular, Massive, Horizontally Stratified Organic Mudstone

This facies association consists of up to 5-m-thick, multistory tabular and laterally extensive (at least 7 km) organic-rich mudstone intervals (Fcf, Fl) that are commonly interbedded with thin, parallel- to ripple cross-laminated very fine-grained sandstone (Sr) and siltstone (Fl) facies (Tables 1 - 3; Fig. 5A - D). FA11 is the most abundant FA in the study area, and it forms the basal portion of the ULB in the well exposed sections near Ikuha and Ilasilo. Both sandstone and siltstone facies are well sorted, fine upward, and exhibit sharp to gradational bounding surfaces.

Up-section, FA11 is defined by interbedded, alternating volcanic ash (Fva) and volcaniclastic siltstone (Fhvs, Fvso,) facies (Fig. 5A). Both facies are organic-rich in the lower portion of this FA, and exhibit upward increase in bed thickness. The volcanic ash beds range between 5 and 20 cm in thickness; bed thickness of volcaniclastic siltstone ranges between 15 and 60 cm. Locally, FA11 is incised by thick conglomeratic sandstone deposits of FA 6. FA11 contains abundant fish, diatoms (Fig. 6), and locally carbonized wood fragments (Fig. 5D).

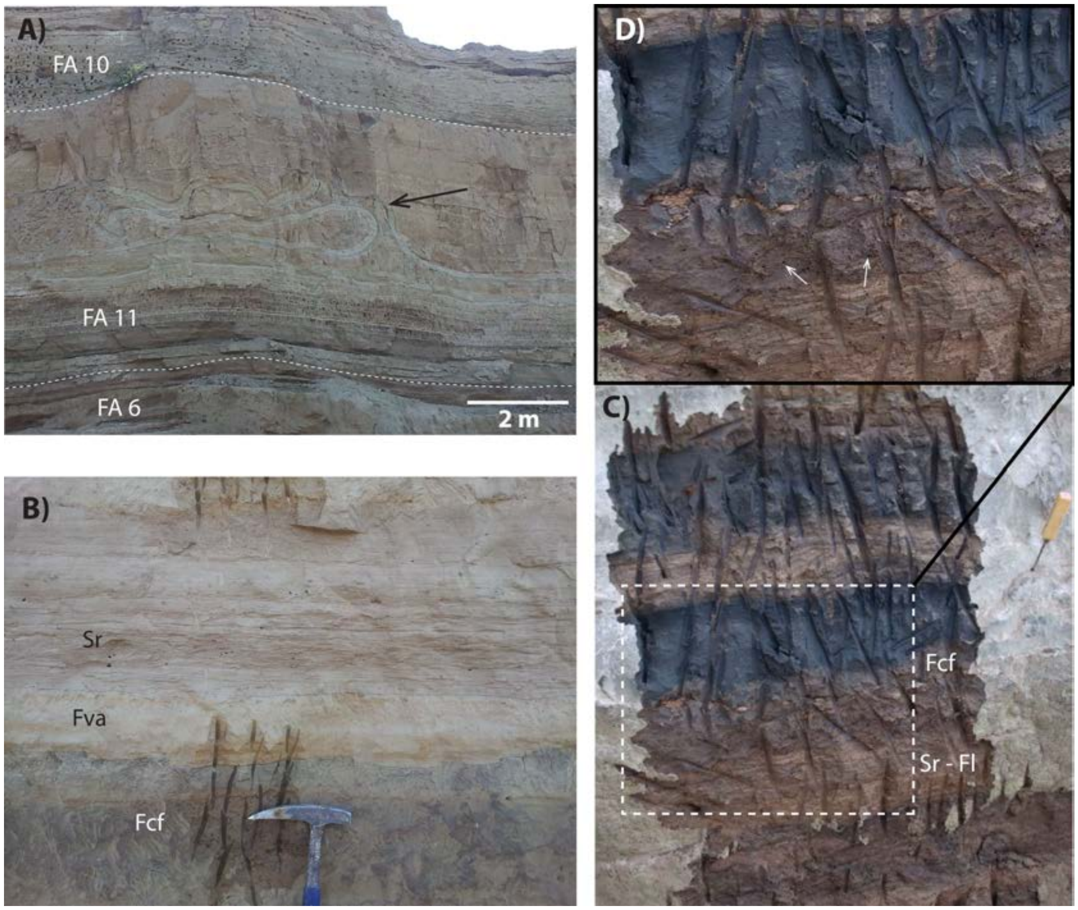

Fig. 5.—Upper Lake Beds fine-grained facies. **A)** Organic-rich volcanic siltstone (Fvso) with large-scale soft sediment deformation (arrow) and interbedded volcanic siltstone (Fvsd) and cross-stratified volcanic sandstone (Stv). **B-C**) Massive, tabular beds of horizontally-stratified organic-rich mudstone (Fcf), volcanic ash (Fva) and ripple cross-laminated fine-grained sandstones (Sr). **D)** Close-up of carbonized wood fragments (arrows).

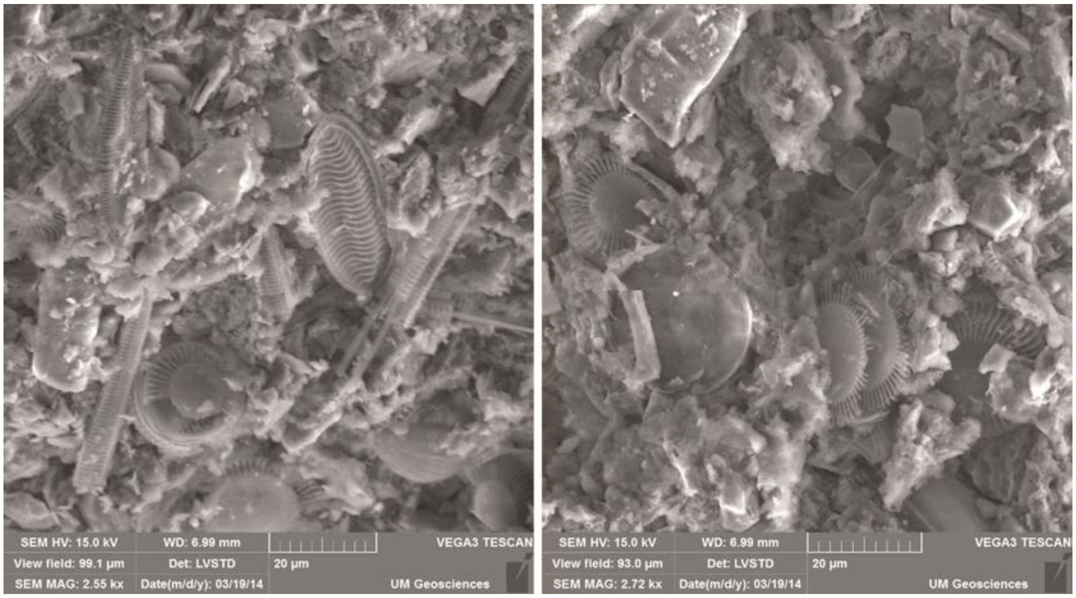

Fig. 6.—Secondary electron (SEM) images of organic-rich, diatomaceous mudstone (dark unit in dashed box, Fig. 5C) collected from the basal unit of the Ilasilo 6 section.

Interpretation.—Based on its generally fine-grained nature and well preserved, laterally extensive horizontal stratification, and abundance of diatoms, FA11 is interpreted as low-energy deposits formed by suspended-load fallout and land-generated hyperpycnal flows in a sub-wave-base profundal environment (e.g., Kataoka 2005; Fielding 2010). The excellent preservation of diatom fossils and the organic-rich composition of the lower intervals of FA11 suggest deposition under conditions of low oxygen, consistent with this interpretation. The interbedded siltstone and sandstone beds in the upper part of this facies fine upward and contain unidirectional ripple cross-lamination and rare climbing ripples, suggesting rapid sedimentation by low-density turbidity currents (cf. Fouch and Dean 1982). These flows are interpreted to be the basinward extension of river-generated hyperpycnal underflows (cf. Zavala et al. 2006), consistent with the presence of terrestrial plant (wood) remains.

The absence of prominent erosional surfaces and the upward increase in thickness of individual beds in this FA resulted from an overall upward increase in sediment supply associated with volcanic eruptions and subsequent downslope remobilization of unconsolidated volcaniclastic material (e.g., Kokelaar 1992). In places, the upper portion of FA11 is highly bioturbated and characterized by calcareous nodules and rootlets, suggesting that the FA11 profundal units were ultimately exposed to surface conditions by a major drop in base level. The recurrence of this FA across the ULB stratigraphy is interpreted to reflect multiple lake-level fluctuations.

DEPOSITIONAL SYSTEMS

Detailed facies analysis of the upper Lake Beds indicates deposition on a dynamic fluvial - lacustrine setting (Figs. 7 - 10). Herein, three main depositional systems are recognized. These are: (1) the alluvial to fluvial channel system; (2) the delta system; and (3) the profundal lacustrine system.

Alluvial to Fluvial Channel Deposystem

This deposystem comprises thick alluvial deposits developed along the basin margin, particularly in the Songwe, Ifisi, and Ikumbi areas. Alluvial deposits pass laterally into proximal fluvial channel belts with minor floodplain paleosols and wetlands.

The alluvial deposits are dominated by thick (up to 9 m), cobble to boulder conglomeratic bodies (FA1) with basal angular unconformities and high erosional relief. Clast packing and texture indicates rapid sedimentation by high-density pseudoplastic debris flows (inertial bedload or turbulent flows). In the Ifisi and Songwe areas, basal ULB alluvial deposits rest with angular unconformity directly upon folded Cretaceous strata of the Red Sandstone Group (Figs. 3, 7).

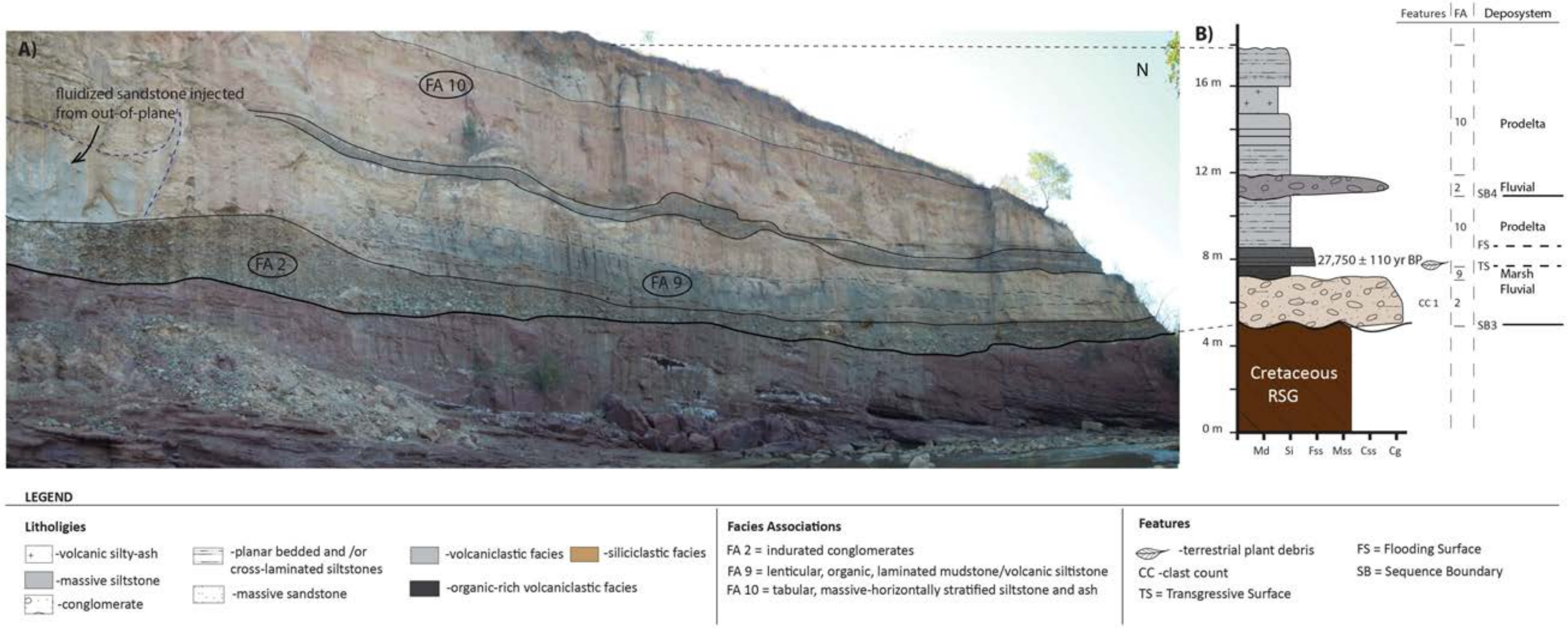

FIG. 7.—Songwe section 1 along the upper Songwe River. **A)** Outcrop photograph of the Songwe section 1, dominated by fluvial channel lag (Gcme), and marsh and lacustrine (Fvso and Fva) deposits (FAs 2, 9 and 11). Section is exposed along the Songwe River Valley in the southeastern part of the study area. **B)** Measured section (8°54′36″S, 33°12′36″E).

Braided-stream deposits in the ULB are characterized by multistory conglomerate-filled channels (FA2), interbedded and intercalated with tabular to lenticular volcanic sandstone units as well as scour-filled, organic-rich siltstone beds, interpreted to be floodplain (FA8) and wetland marsh (FA9) deposits. The vertical stacking of lenticular conglomerate bodies (FA2), especially near the rift margins, suggests channel reactivation (cf. Benvenuti 2003). Floodplain deposits, including small ponds or wetlands, developed both on the braidplain channel systems and along the margins of the channel belt during low-flow stages and following channel abandonment (cf. Benvenuti 2003; Fielding 2010).

A clear example of the alluvial-plain to fluvial-channel deposystem is observed in the Songwe section 1, where organic-rich, laminated FA9 deposits onlap directly onto a buttress unconformity that is interpreted to have developed following base-level fall and deep channel incision (see Fig. 2D in Hilbert-Wolf and Roberts 2015). The upper parts of these units are highly bioturbated, characterized by root traces, and marked by prominent erosional upper contacts, suggesting that subaqueous sedimentation on the floodplain was followed by a period of subaerial exposure and paleosol development. Locally, in the Songwe - Ifisi area, thick calcareous paleosols indicate more intense pedogenesis, presumably under seasonal or periodic aridity.

Delta System

The delta system is interpreted to have developed between the alluvial to fluvial channel deposystem and the profundal (deep lake bottom) deposystem. Lower-delta-plain, delta-front, and prodelta subenvironments are distinguished in the delta deposystem and defined by FA7, 5, and 10, respectively (Figs. 8 - 10). This deposystem is recognized extensively throughout the ULB in the Ilasilo and Ikuha areas, and is recorded at various levels across the stratigraphy.

Lower delta plain.—Lower-delta-plain deposits are not common in the ULB, and are documented at only one locality (Ilasilo section 2) in the Ilasilo area (Fig. 9). They consist of alternating fine-grained sandstone and volcanic siltstone beds (Sr, Fhvs and Fmvs: FA7) suggesting alternating low-energy deposition by unconfined traction currents and settling of suspended sediments (cf. Zavala et al. 2006). Abundant pyritized fish bones suggest bottom-water anoxia, perhaps associated with low-energy swampy conditions in the distributary channels (cf. Dunham 1961). However, the presence of fossilized termite galleries and nests in other portions of this unit indicate subaerial exposure and pedogenesis, consistent with levee subenvironments on the lower delta plain (cf. Mazzullo 1973; Fielding 2010).

Delta front.—Delta-front deposits, characterized by FA5, are easily recognized by their thick, large-scale low-angle (<30°) dipping foresets (Fig. 8). In a number of areas steeply dipping (>30°) foresets are observed near the rift flanks, where they are interpreted to be Gilbert-type deltas (FA3: Fig. 8A). Delta-front deposits range from volcaniclastic pebbly sandstone to medium- and coarse-grained sandstone, to fine-grained sandstone and volcanic siltstone (Fig. 8B). Fish bones and a wide variety of freshwater ostracodes and molluscs are common in these deposits (Fig. 3F; see also Cohen et al. 2013). Stratigraphic relationships with underlying and overlying prodelta (FA10) and delta-plain (FA6, 7) deposits in some areas (Figs. 8B, 10) conform to a classic progradational delta system (cf. Fielding 2010; Olariu et al. 2010).

Individual sedimentary units in these delta-front deposits are characterized by alternating traction and fallout depositional features, strongly suggesting bedload deposition from collapsing hyperpycnal flows (cf. Zavala et al. 2006). Paleocurrent analysis of trough cross-stratified sandstone units and low-angle delta clinoform sets indicate north and northeast directions in the delta front deposits in the Ilasilo area, and to east to southeast directions around Ikuha. These results suggest that delta-fronts built out both normal to and parallel to the Lupa bounding fault (Fig. 1). Based on paleocurrent datasets, these deltaic successions are interpreted to have been deposited by distributary channels in river-dominated ”bird-foot” deltas constructed into Lake Rukwa from rivers draining hinterlands to the northeast, southwest, and southeast.

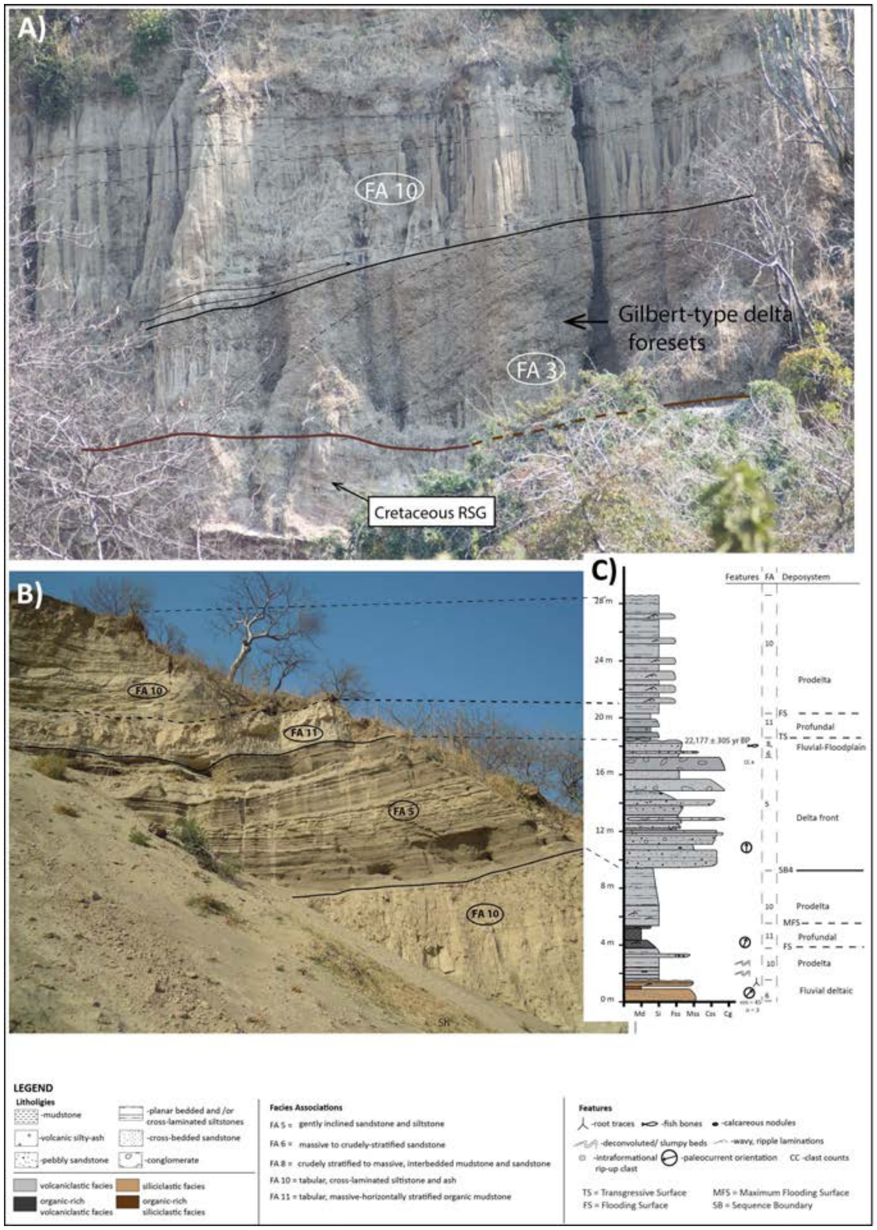

FIG. 8.—Illustration of delta front deposits. **A)** Outcrop photo of fluvial deltaic deposits exposed along the western rift margin, southeast of Malangali village (see Fig. 2). Note inclined bedding of conglomerate and pebbly sandstone units (FA3: Gilbert-type delta foresets). Foresets dip north and down-lap with angular unconformity onto eroded Cretaceous Red Sandstone Group strata. **B)** Gently inclined pebbly to fine grained sandstone and siltstone at Ilasio 3 section (FA5; see close ups in figure 4B-D). Note the massive, tabular horizontally- and cross-stratified volcanic siltstone and ash (FA10 and FA11). **C)** Measured section (8°39′22″S, 33°01′47″E).

Prodelta.—The prodelta environment is distinguished by tabular parallel- to ripple cross-laminated volcanic siltstone and ash beds that together constitute FA10 (Figs. 8 - 10). Sedimentation was dominated by hyperpycnal flows that reflect alternation of tractive and fallout, medium- and low-energy depositional conditions. These hyperpycnal flows may have originated from sheet-flooding events during a prolonged humid phase, as suggested by Haberyan (1987) during this time, and/or triggered by seismic activity related to modern tectonic development of the EARS (Delvaux et al. 1998). However, the dominance of volcanic detritus (ash, pumice) in these deposits suggests a strong linkage with periods of active volcanism and basinwide mobilization and reworking of volcaniclastic sediment down-slope (e.g., Cuitiño and Scasso 2013). Abundant millimeter- to centimeter-scale soft-sediment deformation features and ubiquitous climbing ripples in prodelta hyperpycnites suggests repeated, rapid sedimentation events and high sediment supply, as would be expected during periods of widespread explosive volcanism in the nearby Rungwe Volcanic Province.

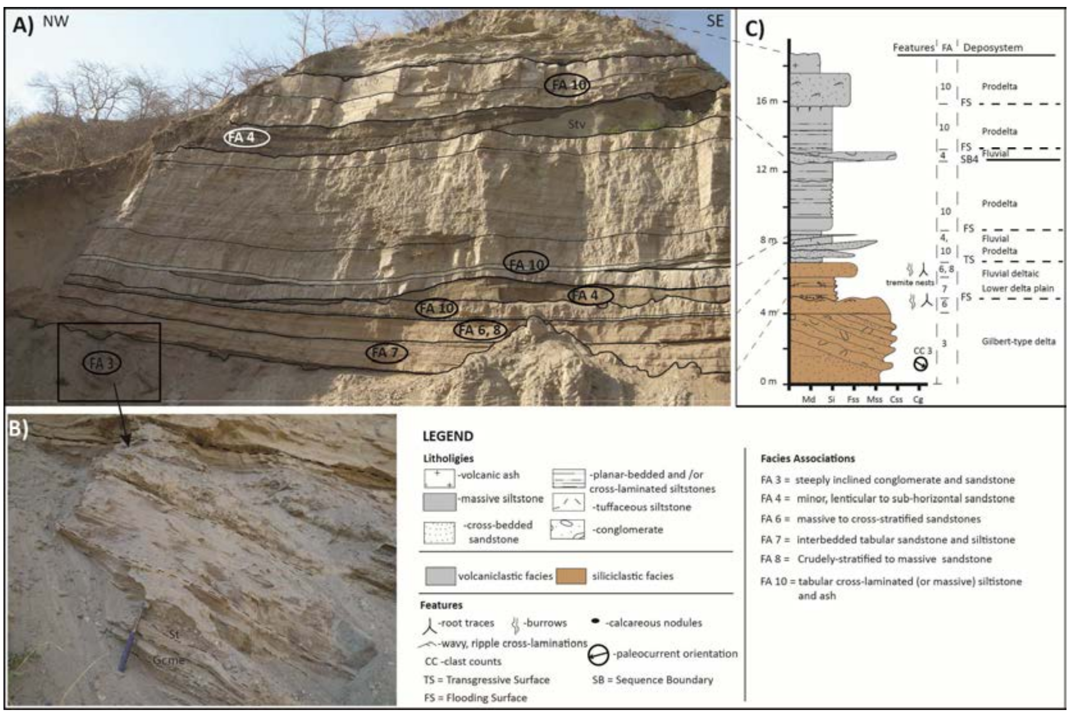

FIG. 9.—Ilasilo section 2, located along a tributary to the Songwe River. **A)** Outcrop photo of well exposed fluvial-deltaic deposits. Inset box shown in C. **B)** Close up view of steeply dipping Gilbert-type delta forests composed of conglomerate and sandstone beds (Gcme and St facies; FA3). **C)** Measured section (8°39′13″S, 33°01′42″E).

Profundal Lacustrine

The third depositional system documented in the ULB is defined by profundal deposits of FA11, which are best exposed in the Ilasilo 6 section (Fig. 10). They are characterized by laterally extensive, multistory organic-rich mudstone units that are commonly interstratified with thin beds of ripple cross-laminated siltstone and very fine-grained sandstone. The inclusion of both volcanics-dominated sediments and siliciclastics-dominated sediments in the profundal lacustrine deposystem demonstrates a mixed source provenance for the recent basin-fill sources. The overall fine-grained, thinly laminated nature of these thick profundal deposits resulted dominantly from low-energy suspension fallout processes in a sub-wave-base lacustrine environment, with periodic land-generated hyperpycnal currents. This interpretation is consistent with an abundance of pyritized fish bones and finely disseminated organic material, including plant hash, suggesting terrestrial input into anoxic bottom waters (cf. Zavala et al. 2012). The typically horizontal stratification of the profundal deposits in the ULB suggests that deposition transpired on a relatively flat lake floor.

.

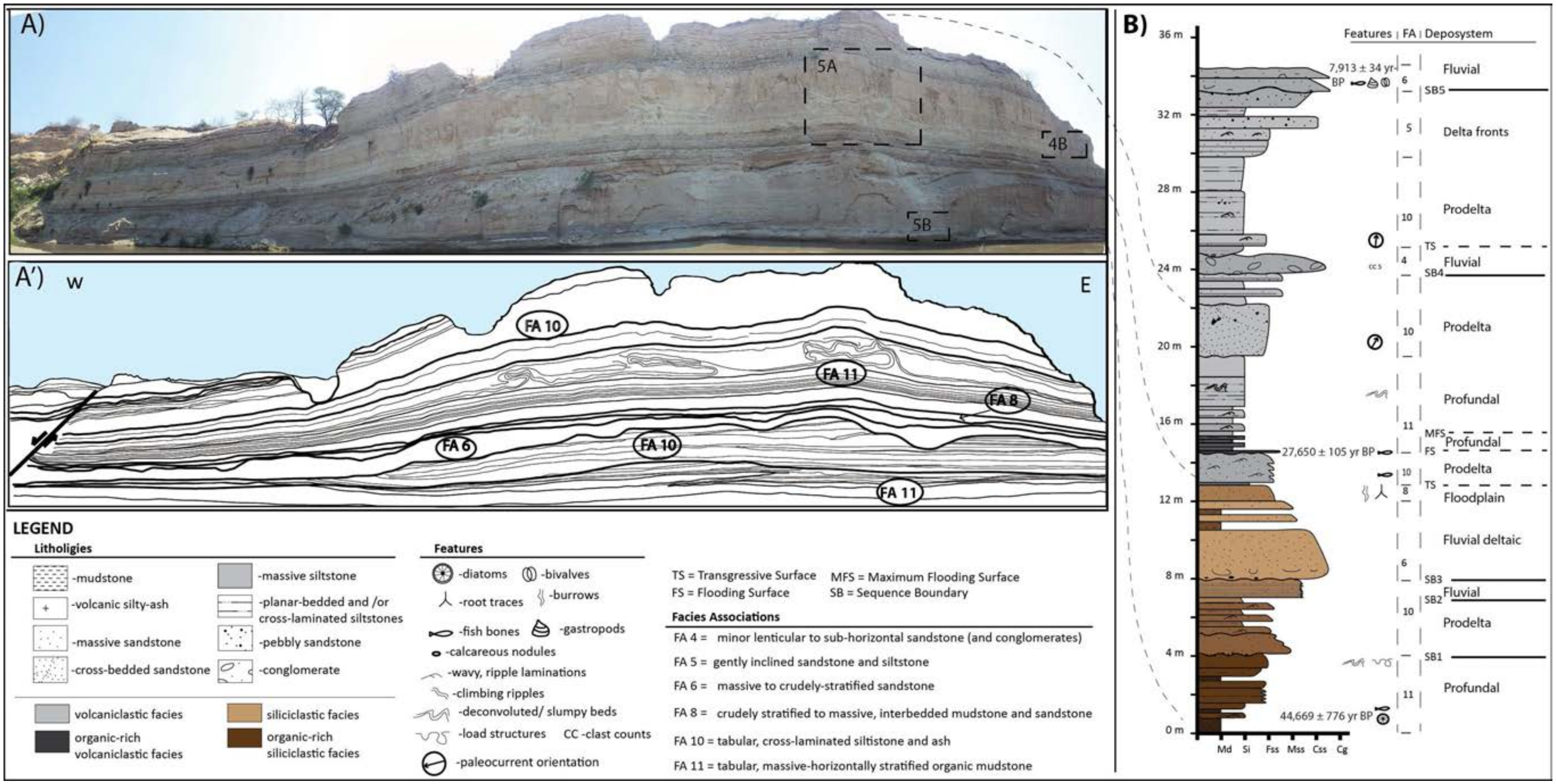

Fig. 10. Ilasilo section 6, located along the Songwe River. **A)** Outcrop photo of the well-exposed stratigraphy (inset box is shown in Figs 5A-B, 4B). **B)** Measured section (8°38′07″S, 33°00′47″E).

CONGLOMERATE AND SANDSTONE PETROLOGY

Composition of Conglomerate Lithoclasts

Pebble counting in conglomerate beds was performed on five samples and reveals both spatial and stratigraphic variations in lithoclast composition in the ULB (Fig. 11). Alluvial and fluvial-channel-lag conglomerate units (FA1 and FA2) in the lower portion of the ULB at the Songwe, Ikumbi, and Ifisi areas are composed of exclusively metagranitoid, vein quartz, and metavolcanic clasts. In contrast, at higher stratigraphic levels and in more distal environmental settings, conglomerate beds in delta-plain, Gilbert-delta, and proximal delta-front deposits at the Ilasilo and Ikuha areas are characterized by significant input of recycled intraformational and extraformation-sandstone, volcanic siltstone, and pumice clasts. These results indicate that in more proximal environments, alluvial conglomerates are dominantly sourced from metamorphic and granitoid basement rocks, most likely Paleoproterozoic Ubendian belt and Precambrian basement rocks from nearby rift flanks. The shift to mostly volcanic and intraformational sedimentary rip-up clasts up-section and in more distal environments is interpreted to reflect the introduction of penecontemporanous volcanic sources that resulted in the trapping of coarse-grained extrabasinal clastics near the basin margins (cf. Heller and Paola 1992).

Sandstone Petrology

Sandstone compositions in the ULB are highly variable, with siliciclastic to volcaniclastic end members. Considerable variation in grain size and sorting also occurs (Fig. 12A - F). Siliciclastic sandstone units are typically brownish (coloured), ranging from pale red (10R 6/6) to pale yellowish brown (10YR 6/2), and quartzolithic to feldspatholithic in composition. Siliciclastic sandstone units occur mainly in the lower parts of the stratigraphy, mostly as lower-delta-plain deposits (FA7), with some interstratified fluvial channel deposits (FA 6).

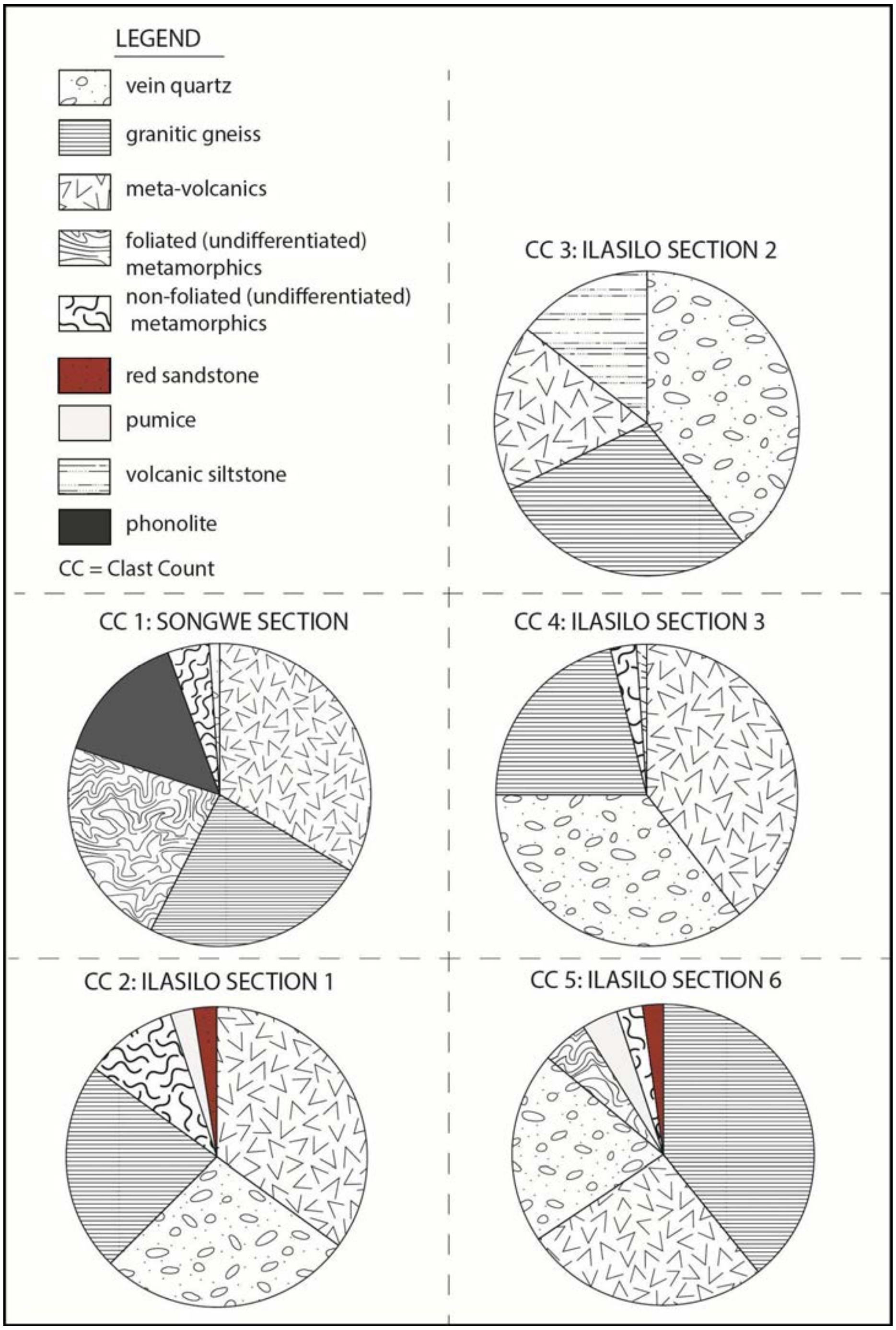

Fig. 11.—Pebble count results for conglomerate beds in the upper Lake Beds, based on 50 cm^2 grid counts.

Volcaniclastic sandstone units range from yellowish gray (5Y 7/2), medium light-gray (N6), to medium dark-gray (N5), and range from fine- to coarse-grained sand with floating pebble clasts composed of pumice, mafic volcanic fragments, and minor quartz feldspars and volcanic siltstone rip-ups. Many volcaniclastic sandstone units also contain abundant carbonized plant material.

Four siliciclastic and two volcaniclastic sandstone samples were collected from relatively indurated intervals for thin-section analysis. The results are discussed separately below for siliciclastic and volcaniclastic petrofacies.

Siliciclastic sandstone petrofacies.—Siliciclastic sandstone petrofacies are typically moderately to well sorted and composed of very fine- to coarse-grained sand and isolated pebbles (Fig. 12E, F). Grains range from angular to subrounded and are dominated by (in the order of their abundance): quartz, alkali feldspars, plagioclase and lithics, including granitic gneiss, mafic volcanic, metavolcanic, and sedimentary rock fragments. Accessory minerals include calcite, mica, and dense minerals dominated by magnetite and garnet. Matrix ranges between 2% and 40%, and porosity ranges between 8% and 16%. Cement varies between 5% and 10%, and is dominated by hematite and clay.

Sandstone framework compositions were analyzed by point counting, using a modified Gazzi-Dickinson method (Ingersoll et al. 1984). The results show that siliciclastic sandstone samples from the ULB are generally compositionally immature, with total quartz (including chert and polycrystalline and monocrystalline quartz) ranging from 58 to 79%, feldspars (alkali and plagioclase) ranging between 15 and 26%, and lithics (volcanic, metamorphic, sedimentary fragments) ranging from 12 to 40%. On Qt-F-L plots, the subarkosic, sublitharenitic, lithic arkosic, and litharenitic fields each are represented (Fig. 12). This compositional immaturity is interpreted to reflect nearby sediment sources and minimal physical or chemical weathering.

The most likely sediment sources for these siliciclastic sandstone units include granitoids, metagranites, and metavolcanics from the uplifted Proterozoic Ubendian metamorphic rocks and Archean granitoids along the rift flanks. This interpretation is consistent with pebble-count results from conglomerate beds in lower parts of the upper Lake Beds stratigraphy (Fig. 11).

Volcaniclastic sandstone petrofacies.—Thin-section analysis provides a basis for subdividing the volcaniclastic sandstone petrofacies into two end members: (1) the crystal-lithic tuffaceous sandstone subfacies (Fig. 12A, B); and (2) the glass (shards + pumice)-dominated tuffaceous sandstone subfacies (Fig. 12C, D). The crystal-lithic-tuff subfacies consists of subangular to rounded volcanic lithic fragments, quartz, fresh plagioclase, rare biotite, and dense minerals. Individual grains range from fine- to coarse-grained sand. The glass-dominated tuffaceous sandstone subfacies comprise over 65% pumice and glass shards, suggesting derivation from weakly reworked primary vitric tuffs. Roughly 40 to 55% of the glass consists of well-rounded pumice ranging in size between 0.05 mm (vf) and 0.56 mm (m-c). The remainder of the glass consists of coarse-silt- to fine-sand-size shards, suggesting derivation from abrasion of pumice clasts. The detrital component of the glass-dominated subfacies makes up only ~10% of the rock and is composed of volcanic lithic fragments, quartz, fresh plagioclase, and minor mica. Based on these textural and composition features, the volcaniclastic sandstone petrofacies in the ULB are interpreted to be sourced from reworked proximal to distal pyroclastic flow deposits that originated from the Rungwe Volcanic Province (cf. Ebinger et al. 1989).

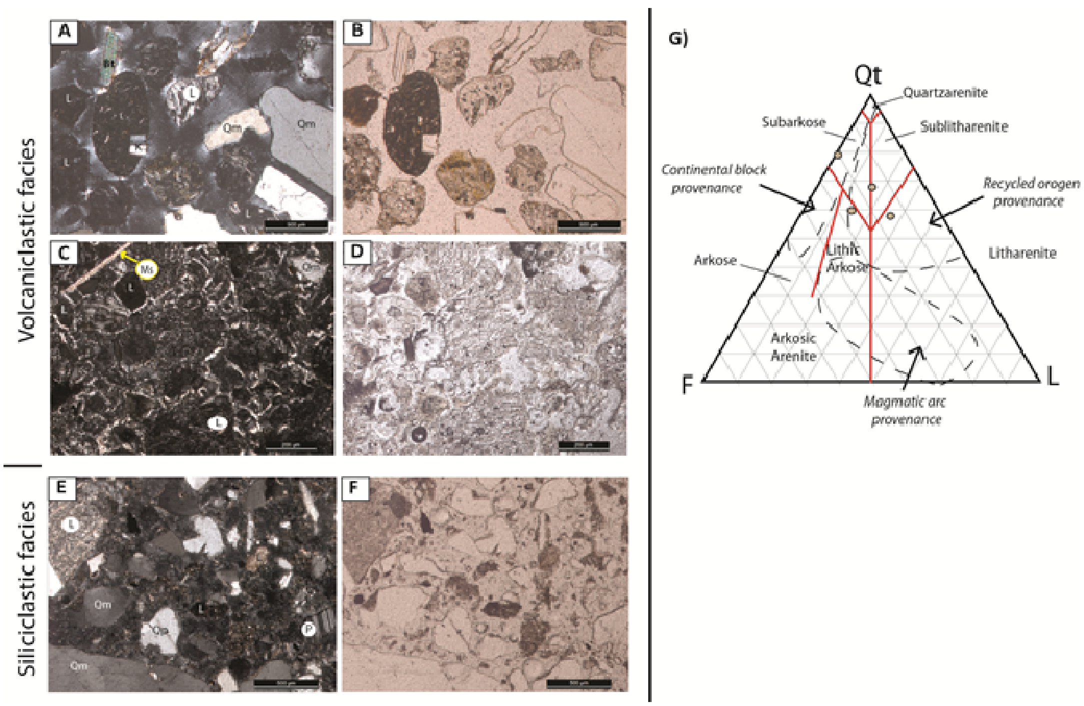

Fig. 12.—**A-F)** Photomicrographs of the volcaniclastic sandstone; crystal-lithic tuff, (A-B: 10x, XPL and PPL, respectively), and vitric tuff (C-D: 5x, XPL and PPL, respectively), and Siliciclastic; sublitharenite (quartzo-feldspatho-lithic) sandstone from upper delta plain (E-F: 10x, XPL and PPL, respectively), **G)** Sandstone point count data plotted following the

methodology of Gazzi-Dickinson (Ingersoll et al. 1984) and sandstone classification (after Pettijohn et al., 1987).

Field observations and petrographic composition analyses of conglomerate and sandstone units of the ULB (Figs. 11, 12) permit the characterization into siliciclastics-dominated facies (fluvial channels and delta-plain deposits) and volcaniclastics-dominated facies (lacustrine to fluvial - deltaic deposits) (Fig. 13). In addition, variable sediment provenance serves as a useful lithostratigraphic correlation tool.

RADIOCARBON DATING

The chronology of the upper Lake Beds succession herein is refined by reporting new radiocarbon ages and discussing these results along with recent ^{14}C ages reported by Cohen et al. (2013). In the current study, five organic-rich siltstone samples and one aragonitic unionoid bivalve shell sample were collected from various areas and stratigraphic positions and carbon dated via the AMS method at the Beta Analytic Laboratory, Miami, USA (Table 4). Sample preparations involved sieving to <180 microns to remove any root or macrofossils and acid washing (or acid etching for bivalve shells) to remove carbonates.

New Radiocarbon Ages and Geochronology of the ULB

New radiocarbon ages obtained from this study are presented in Table 4 and collectively indicate that outcrop exposures of the ULB in the Rukwa Rift were deposited between ~45 and 7.9 ka. Notably, two other new radiocarbon samples from highly unusual, large-scale soft-sediment deformation features at the Songwe 1 and Ilasillo 6 sections were recently reported in Hilbert-Wolf and Roberts (2015) as part of a separate study on paleoseismicity in the Rukwa Rift. Significantly, large-scale soft-sediment deformation features yielded identical ages (within error) of 27,750 ± 110 Cal yr BP for sample 62312-6 (from 8 m above the base of the Songwe section 1) and 27,650 ± 105 Cal yr BP for sample 71014-2 (15 m above the base of the Ilasilo section 6).

Cohen et al. (2013) reported a number of other radiocarbon ages from across the Rukwa Rift Basin, including one sample (DD736/2009-17; Songwe Gully) herein referred to as Ilasillo section 1. They obtained an age of 22,010 ± 320 Cal yr BP for this sample, consistent with the age of 22,177 ± 305 reported in this study for sample 71513-10, collected at the same stratigraphic interval from Ilasilo section 3. Cohen et al. (2013) also reported radiocarbon ages between ~7 and 11 ka from the Galula area, which we can correlate with the upper part of the stratigraphy in our Ilasillo sections, and for which we obtained a similarly young age of 7.9 ka for sample 7913-10 (see Fig. 13). The youngest age reported for the ULB by Cohen et al. (2013) was 5.5 ka from north of Lake Rukwa.

Table 4. AMS radiocarbon age results for six samples obtained in this study.

Sample Number	Location	Depositional Environment	Material	Conventional Radiocarbon Age (BP)	$\delta^{13}C$	Calibrated (Cal BP) Age 68% (1 sigma)
71813-1	1.5 m from the base of the Ilasilo section 6; 8°38′07″S, 33°00′47″E	Profundal lacustrine	Organic sediment	41150 ± 500	-17.5‰	44669 ±776
71814-2	6 m above the base of the Ikuha section 2; 8°41′49″S, 33°13′12″E	Profundal lacustrine	Organic sediment	30350 ± 170	-15.3‰	34478 ± 162
71814-4	17 m above the base of the Ikuha section 2; 8°41′49″S, 33°13′12″E	Prodelta	Organic sediment	29230 ± 160	-15.7‰	33671 ± 312
71313-1	11 m above the base of the Ilasilo section 1; 8°39′34″S, 33°01′48″E	Profundal lacustrine	Organic sediment	23680 ± 100	-15.8‰	28602 ± 390
71513-10	19 m above the base of the Ilasilo section 3; 8°39′22″S, 33°01′47″E	Fluvial deltaic	Organic sediment	18570 ± 60	-20.7‰	22177 ± 305
7913-10	~36 m above the base of the Ilasilo 6 section; 8°38′07″S, 33°00′47″E	Fluvial deltaic	Bivalve shells	7080 ± 30	-2.4‰	7913 ± 34

Dates are reported as radiocarbon years before present (i.e., AD 1950). By international convention, the modern reference standard was 95% the ^{14}C activity of the U.S. National Institute of Standards and Technology (NIST) Oxalic Acid (SRM 4990C) and calculated using the Libby ^{14}C half-life (5568 years). Quoted errors represent 1 relative standard deviation statistics (68% probability) counting errors based on the combined measurements of the sample, background, and modern reference standards. Measured $^{13}C/^{12}C$ ratios ($\delta^{13}C$) were calculated relative to the PDB-1 standard. The conventional radiocarbon age represents the measured radiocarbon age corrected for isotopic fractionation, calculated using the δ ^{13}C. Calendric ages (Cal yr BP) are calibrated from conventional radiocarbon ages using CalPal© online, using the CalPal_2007_HULU calibration curve.

The radiocarbon results presented here and integrated with previously published dates from outcrop and shallow core samples strongly indicate that the strata described as the upper Lake Beds in this study are late Quaternary (<50 ka) and younger in age. Importantly, the previously proposed division of the Lake Beds in the Songwe and Galula (Ilasilo) areas, into "older" and "younger" mappable units (Grantham et al. 1958) is not supported by the extensive radiocarbon dating and stratigraphic correlations reported here and by Cohen et al. (2013). Rather, these results indicate a close late Quaternary age correspondence between the two mapped units. The previously considered 'older vs "younger" stratigraphic subdivisions is shown here to more accurately represent generally age-equivalent lateral facies transitions associated with a complex fluvio-lacustrine system.

SEQUENCE STRATIGRAPHIC FRAMEWORK

Nine stratigraphic sections were measured across three main study areas (Fig. 2), and dozens of additional localities were investigated during the course of this study in order to understand the stratigraphic relationships and paleoenvironments of the ULB. Sections range from ~19 - 50 m thick, and span a regional composite thickness of >55 m, representing deposition between ~45 and ~5 ka (Fig. 13). Several key stratigraphic surfaces were identified along with landward- and basinward-stepping facies transitions, which collectively were used to interpret a sequence stratigraphic framework for the ULB in the southern end of the Rukwa Rift Basin.

Depositional sequences are identified following methodology and nomenclature proposed by Catuneanu et al. (2011), which emphasizes a flexible model-independent approach to sequence stratigraphy. Sequence boundaries are identified by subaerial unconformities and regional erosion surfaces in the updip areas, and their corresponding abrupt basinward facies shift (correlative conformities) in the downdip areas. Parasequences are recognized as relatively conformable succession of genetically related facies (facies associations), bounded by flooding surfaces. Five sequence boundaries, and their corresponding abrupt basinward facies shifts, along with multiple flooding surfaces are recognized in outcrop. These surfaces are used to document six depositional sequences in the ULB (Figs. 13 - 15). Following the continental nature of the Lake Beds succession, we apply the concepts of a lake-type basin stratigraphic model of Carroll and Bohacs (1999) and Bohacs et al. (2000) to infer changes in lake-type basins through time and assess controls on sedimentation by analyzing vertical stacking patterns of the strata and spatial distribution of the constituent depositional system tracts across the study area. This interpretive framework better captures the greater sensitivity of lake-basin systems (compared to marine systems) to changes in the rate at which accommodation space is filled by sediment and water. In the lake-basin model, base-level position is mainly a function of the balance between tectonics and climate change, and its influence on lake-basin sedimentation patterns (Carroll and Bohacs 1999; Bohacs et al. 2000; Renaut and Gierlowski-Kordesch 2010).

The six sequences documented in the ULB strata are described in stratigraphic order, from bottom to top, along with interpretations of lake-type basins and the relative influence of tectonic, climatic, and sediment-supply factors on sequence development.

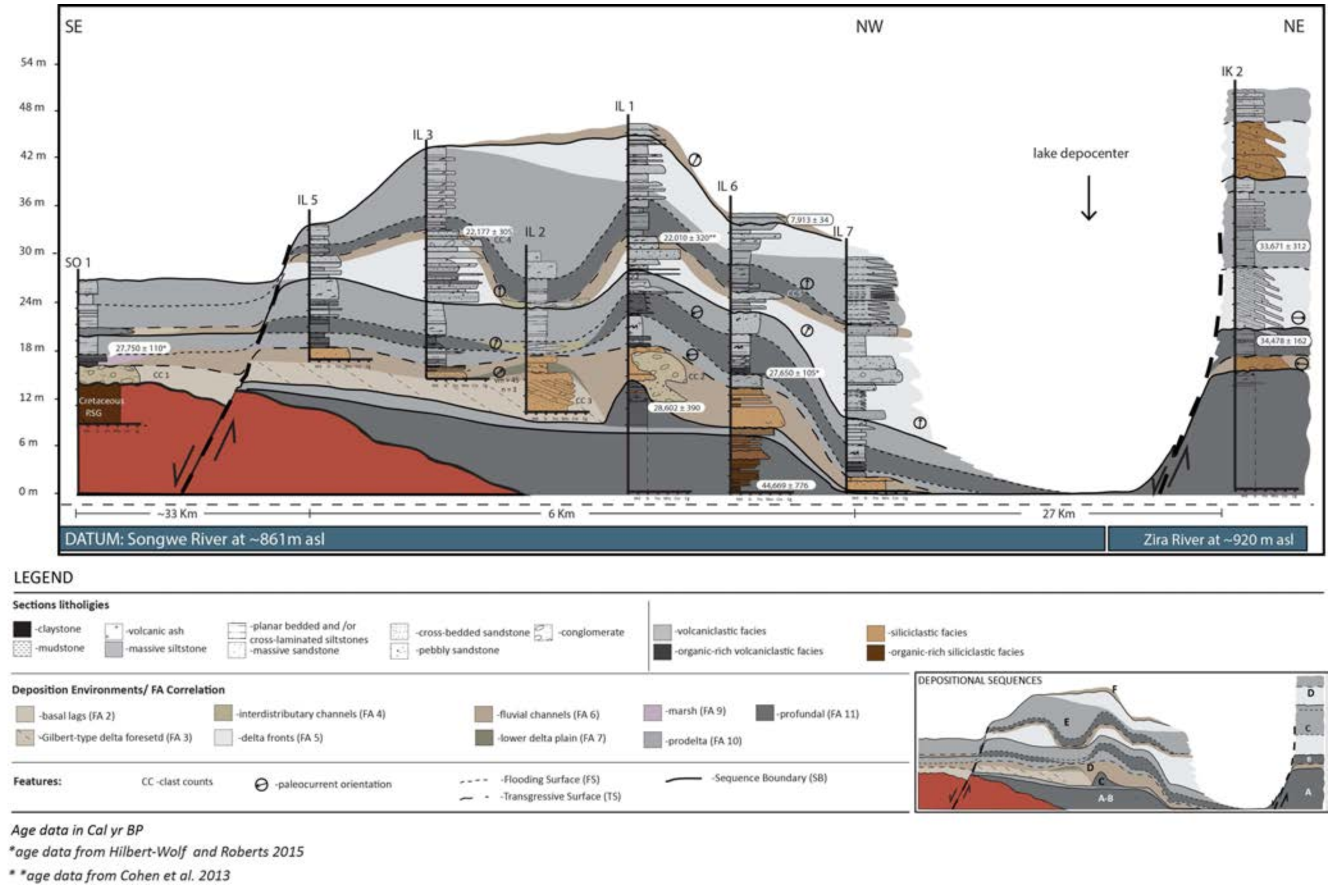

Fig. 13.—Stratigraphy and facies correlation of measured sections through the upper Lake Beds on the southern end of the Rukwa Rift Basin. Interpreted depositional sequences are also shown.

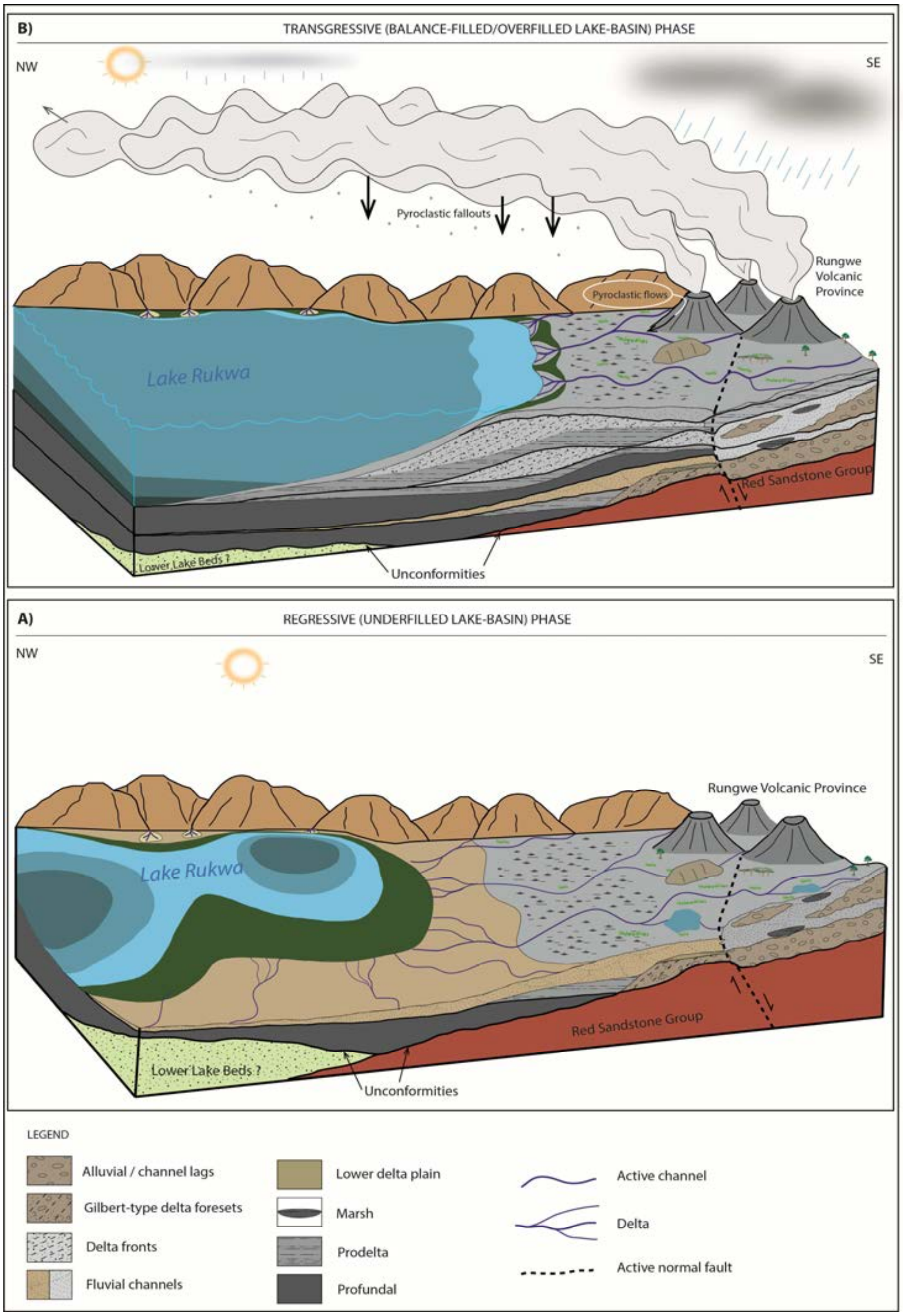

Fig. 14.—Paleoenvironmental reconstruction of the upper Lake Beds in the Rukwa Rift Basin during the: **A)** climate-driven regressive, underfilled lake-basin type phase; vs. **B)** the transgressive, balance-filled/overfilled lake-basin type phase. Reconstructions also highlight variation of sediment input from explosive volcanism (volcaniclastic units) vs. weathering and erosion of the uplifted basement rocks (siliciclastic units).

Sequence A

Sequence A is the lowermost sequence defined for the ULB and is incompletely exposed. It represents transgressive and highstand systems tracts comprising profundal lacustrine (FA11) and prodelta (FA10) deposits (Figs. 5B - D, 8, 13, 15), developed between ~50 and 43 ka. The stacking pattern of the strata in Sequence A corresponds to the fluctuating-profundal facies association of the lake-type basin model. Sequence A ranges in thickness from 2 to 6 m and crops out mainly in the Ilasilo and Ikuha areas. The lower portion of the sequence is dominated by siliciclastic shales, whereas its upper portion is dominated by volcanic siltstone. This change in sediment composition is consistent with the introduction of a large supply of sediment from primary and/or reworked pumice and volcanic ash during episodes of explosive volcanism documented between ~49 and ~42 ka in the Rungwe and Kyejo volcanic centers (Fig. 15; Ebinger et al. 1989, 1993; Ivanov et al. 1999; Fontijn et al. 2010. 2012). The transition from profundal (FA11) to prodelta (FA10) deposits is interpreted to reflect progradation and rapid filling of accommodation in the basin due to the high influx of volcaniclastic sediment. Sequence A is capped by an erosional scour surface that represents a subaerial unconformity or regressive surface (SB1).

Based on its facies stacking patterns, Sequence A is interpreted to record a balanced-fill lake-type basin phase and establishment of a relatively deep lake and subsequent base-level fall to underfilled lake basin. Deposition in the lower portion (transgressive systems tract) of the sequence is interpreted to have resulted from approximately proportional rates of influx of water + sediment fill versus accommodation generation (cf. Carroll and Bohacs 1999). Elevated base level during the early stage of deposition of this sequence is interpreted to reflect wet climatic conditions during this time. Sedimentation in the upper portion of Sequence A (the highstand system tract) and associated base-level fall is interpreted to record continued filling of accommodation created as a result of active rifting in the basin and associated contemporaneous volcanic activity in the Rungwe Volcanic Province (cf. Ebinger et al. 1989, 1993).

Sequence B

Sequence B consists of ~5-m-thick parasequence set of fluvial deltaic (FA6) and profundal lacustrine (FA 11) deposits that accumulated above sequence boundary 1 (SB1) and separated by a transgressive surface. The basal fluvial deltaic interval is interpreted to represent a lowstand system tract, whereas the upper profundal lacustrine deposits represent the succeeding transgressive system tract. Sequence B is well preserved in the Ikuha and Ilasilo areas, and is roughly constrained to have developed between ~42 and 34 ka. Sequence B also records a marked compositional shift from siliciclastic-dominated in the lower fluvial deltaic facies to volcaniclastics-dominated in the upper profundal facies. This set of relationships is interpreted to represent a transition from erosion of uplifted metamorphic rift flanks, to deposition or reworking of volcanic or reworked pyroclastics. Most likely this transition was associated with onset of the ~42 ka explosive volcanic episode recorded in the Rungwe Volcanic Province (Fontijn et al. 2012). Sequence B is capped by an erosional surface and abrupt basinward shift in stratal stacking patterns interpreted to represent a significant base-level fall and subaerial exposure prior to deposition of Sequence C.

Sequence B is interpreted to correspond to local climate-induced base-level rise and increasing precipitation-to-evaporation rates associated with a shift from dry to wet conditions. During this time, water + sediment fill in the Rukwa basin likely exceeded potential accommodation space. Sequence B is interpreted to record a transition from underfilled lake basin during the onset of this sequence to a balanced-fill lake basin which dominated for most this sequence (cf. Carroll and Bohacs 1999).

Sequence C

Preserved in the Ikuha and Ilasilo areas, Sequence C represents a complete sequence comprising proximal deltaic (FA5), prodelta (FA10), and profundal lacustrine (FA11) deposits. Sequence C was deposited between ~33 and 28 ka. In the Ikuha area, two flooding surfaces are recognized, separating several parasequences of Sequence C (Fig. 13), which is bounded above by an erosional sequence boundary (SB3) that records an abrupt basinward shift of fluvial deltaic facies associated with the onset of sequence D. Sequence C is dominated by volcanic hyperpycnites interpreted to record high sedimentation rates due to the availability of primary and reworked pyroclastic sediments. Rapid base-level rise and deposition of volcanic to volcaniclastic hyperconcentrated flows into prodelta and profundal environments are interpreted to have resulted from sustained flooding events associated with relatively long-lived wet climatic periods that resulted in a balanced or overfilling of the Rukwa basin by water + sediment. Paleocurrent data reveal internal fluvial and deltaic drainage into the basin center throughout the deposition of sequences A, B, and C, suggesting that the Rukwa Rift Basin actively focused sediment delivery during the deposition of these sequences.

Sequence D

Sequence D is widespread across the study area and is interpreted to reflect regional establishment of fluvial - lacustrine conditions during ~27 to 22 ka (Figs. 2, 13, 15). Proximal deltaic deposits and fluvial channels (FA2) at the base of this sequence are interpreted to be lowstand-systems-tract (LST) deposits and are capped by a highly bioturbated surface interpreted to indicate base-level fall (cf. Scott and Smith 2015) prior to transgression and transition to lacustrine prodelta (FA10; transgressive system tract) and profundal (FA11; highstand system tract) depositional systems. A sequence-bounding erosional unconformity caps Sequence D (SB4: Figs. 7, 13, 15) and is interpreted to represent subaerial exposure during rapid lake-level fall. The timing of this event is consistent with a lake regression event reported by previous workers (e.g., Barker et al. 2002; Thevenon et al. 2002) to have occurred between ~23 - 20 ka, during the Last Glacial Maximum, and hence climate was probably the dominant control on the development of this sequence boundary. Sequence D exhibits a provenance shift similar to that observed in Sequences A and B, in which the lower interval is siliciclastics dominated and sourced from nearby rift flanks, and the upper transgressive portion of the sequence is volcaniclastics dominated and associated with rapid erosion and transport of volcanic detritus. Penecontemporaneous volcanism likely included both primary ash flows and falls associated with a period of renewed explosive volcanism in the nearby Rungwe Province. The scarcity of volcanic sediments in the lower portion of Sequence D is consistent with a period of volcanic quiescence documented for the Rungwe Volcanics between ~42 ka and 20 ± 6 ka (Fontijn et al. 2010, 2012) (Figs. 14, 15). The vertical facies stacking pattern and widespread deposition of this sequence is interpreted to record deposition in an overfilled-lake-type basin. Shoreline transgression occurred around 27.6 ka (Fig. 15), broadly consistent with findings from shallow core investigations in Lake Rukwa suggesting base-level rise and significant expansion of Lake Rukwa during the late Pleistocene and early Holocene (e.g., Kennerley 1962; Haberyan 1987; Talbot and Livingstone 1989; Thevenon et al. 2002), overflowing into Lake Tanganyika through the Karema Gap (see Figures 2 and 3 in Cohen et al., 2013). Sequence D is also interpreted to have been controlled by a combination of climate change and sediment supply linked to volcanic activity in the Rungwe Province. The occurrence of widespread, large-scale soft-sediment deformation features in the upper half of this sequence also suggests that significant fault movement in the basin occurred during this time. Associated seismicity may have triggered hyperpycnal flows into paleo - Lake Rukwa (cf. Hilbert-Wolf and Roberts 2015).

Sequence E

Sequence E is spatially widespread, and is characterized by rapid lake deepening and filling, and a volcaniclastic provenance. Sequence E was deposited between <22 and ~8 ka. In ascending stratigraphic order, Sequence E comprises three progradational parasequences consisting of fluvial deltaic (FA5), profundal (FA11), and distal delta front of FA5 deposits. Each parasequence is capped by a flooding surface (Figs. 3B - D, 8B). The sequence is marked by an erosional unconformity (SB5) at its top, indicating abrupt lake base-level fall. The presence of abundant, widespread high-density turbidites in Sequence E is attributable to elevated water supply to the basin associated with waning of Last Glacial Maximum and the establishment of widespread pluvial conditions reported between ~16 and 5 ka (cf. Haberyan 1987; Talbot and Livingstone 1989; Barker et al. 2002; Thevenon et al. 2002). Coeval episodes of explosive volcanism in the Rungwe Province reported at 20 ka and ~12 - 10 ka (Fig. 15; Ivanov et al. 1999; Fontijn et al. 2010, 2012) supplied abundant labile volcanic sediments to the landscape. Based on vertical facies stacking pattern and lateral widespread, Sequence E is interpreted to record the establishment of an overfilled lake basin, which is consistent with the last widespread lake highstand reported to have occurred at ~13.5 ka (Barker et al. 2002; Thevenon et al. 2002; Cohen et al. 2013). The development of this sequence is associated with high rates of sediment and water supply that likely exceeded available accommodation.

Sequence F

Sequence F represents the youngest stratigraphic sequence in the ULB, deposited ~7 ka to recent, and is characterized by a relatively thin (<3 m) lowstand system tract. It comprises a succession of fluvial deposits (FA6) that are best exposed in the Ilasilo area. The base of this sequence is characterized by incised volcanics-rich fluvial channels that are infilled with distinctive channel lag deposits composed of abundant mollusc shells and heavily abraded fish bones (Fig. 3F). The deposition of Sequence F is interpreted to reflect the establishment of an underfilled lake basin, and is associated with arid conditions during the middle Holocene (cf. Haberyan 1987; Thevenon et al. 2002). Radiocarbon ages reported here and by Cohen et al. (2013) from the Ilasilo and Galula areas, respectively, suggest that this final sequence was deposited between 7.9 and 5.5 ka. Deposits of Sequence F are currently exposed some 110+ meters above the current lake level, indicating that a significant base-level fall occurred in the area during the last 5.5 ka and that the modern Rukwa Rift Basin is currently underfilled.

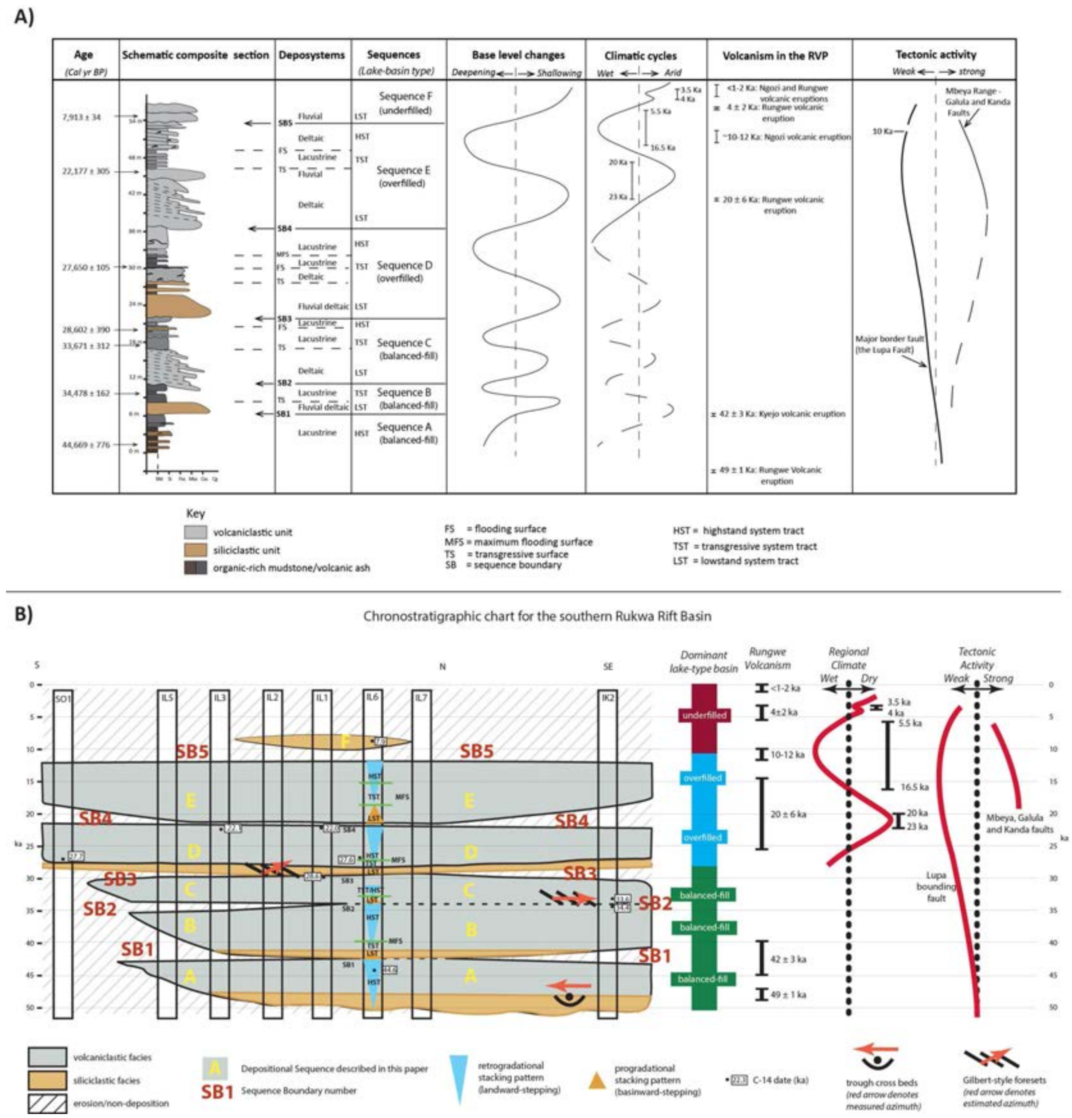

Fig. 15.—**A)** Schematic stratigraphic section of the upper Lake Beds with sequence stratigraphic interpretations and inferred controls on sedimentation. Climatic cycles, volcanism, and tectonic activity are shown through time and correlated to the composite stratigraphic section. Figure based on data from Haberyan 1987; Ebinger et al. 1989, 1993 Delvaux et al. 1998; Ivanov et al. 1999; Barker et al. 2002; Thevenon et al. 2002; Barker et al. 2003 Fontijn et al. 2010, 2012 (solid line traces), and interpretations (dashed line traces), **B)** Chronostratigraphic chart for the upper Lake Beds outcrop exposures in the southeastern RRB illustrating the major sequences, alternating volcaniclastic vs siliciclastic petrofacies and periods of explosive volcanism.

TECTONIC, CLIMATIC, AND VOLCANIC CONTROLS ON SEQUENCE DEVELOPMENT IN THE UPPER LAKE BEDS

Depositional controls on the upper Lake Beds succession in the Rukwa Rift Basin reflect a complex interplay of rift tectonics, climate change, and explosive volcanism in the nearby Rungwe Volcanic Province (Figs. 14, 15). This investigation subdivides the ULB into six depositional sequences (A - F) that reflect episodic lake cyclicity (base-level rises and abrupt falls) throughout the late Quaternary. The sequence stratigraphic analysis conducted herein reveals that the Rukwa Rift Basin evolved through time from a balance-filled lake basin (Sequence A - C); to an overfilled lake basin, characterized by basin-wide lake expansion (Sequences D and E); to rapid base-level fall, lake contraction, and establishment of an underfilled-lake-basin type beginning with deposition of fluvial and lacustrine facies associated with Sequence F, which persist today. Below, the relative influence of tectonics, climate, and sediment supply (i.e., volcanism vs. basement provenance) on sedimentary processes and sequence development in the ULB is discussed.

Climatic Control

Climate is considered to have exerted a first-order control on sequence development in the upper Lake Beds succession. Rapid base-level changes, several of which involved fluctuations of several hundred meters over millennial time scales, reflect strong climate influence associated with both regional and local climate change. The cyclicity and sequence stratigraphy interpreted herein for the ULB corresponds well with previous limnological investigations of Lake Rukwa; however, these records extend back only to ~23 ka (Fig. 15). This study reveals that earlier phases of ULB deposition (Sequences A - C) record balanced-fill lake basins. Following this, two major depositional cycles (Sequences D and E) record the overfilled deep lakes. At times the influx of water was high enough to overtop the basin sill and Lake Rukwa temporarily expanded to form a brief connection with Lake Tanganyika (Haberyan 1987; Talbot and Livingstone 1989; Delvaux et al. 1998). In particular, the widespread occurrence of hyperpycnites across the basin and throughout the succession is associated with a high supply rate of both sediment and water, which are equally attributed to long-term wet climatic conditions and voluminous sediment supply from primary and reworked volcanics.

Volcanic Control

Although millennial-scale climate change likely exerted the main control on precipitation - evaporation balance and the flux of water through the basin, rapid filling of available accommodation space was most likely driven by short periods of intense volcanism in the rift. Hence, volcanism is also considered to be a major control and important factor on sedimentary processes and sequence development in the ULB. This study has shown clearly that periods of intense volcanic activity in the Rungwe Volcanic Province played a key role in the depositional style and sediment packages observed throughout the ULB. Furthermore, the ULB stratigraphy is characterized by alternating patterns of siliciclastics- and volcaniclastics-dominated strata. This varied sedimentary composition reflect shifts in sediment source that are linked to alternating periods of volcanism in the Rungwe vs. periods of volcanic quiescence and sedimentation from weathering and erosion of the uplifted basement rocks along the basin margin.

Whilst the deep wells, Ivuna-1 and Galula-1, show that most deeper Lake Beds sandstones are quartzo-feldspathic, the petrofacies of the ULB are 80% volcaniclastic; dominated by tuffaceous sandstone composed of relatively juvenile (weakly reworked) pyroclastic material including abundant pumice. This suggests syn-eruptive, volcanic-induced sedimentation in the basin, probably involving both primary air-fall and ash-flow deposits (e.g., Smith et al. 2002), as well as considerable reworking of these deposits. Both syn- and inter-eruptive stratigraphic intervals are dominated by thick successions of stacked hyperpycnites that developed within broad fluvial-lacustrine systems tracts (e.g., Sequences C - F), in response to voluminous input of an abundant, easily erodible supply of volcanic ash and pyroclastic deposits. Recent work on the Rungwe, Masoko, and Ngozi volcanoes in the Rungwe Volcanic Province has shown a particularly explosive history over the last 49 ka, including major eruptive episodes at 49 ka, 42 ka, 20 ka, and 4 - 1 ka (Ivanov et al. 1999; Fontijn et al. 2010, 2012). Based on facies analysis, sequence stratigraphy and the timing of eruptive episodes, explosive volcanism from the penecontemporaneous Rungwe Volcanic Province appears to have acted as a major source of the voluminous and rapid and easily erodible supply of volcaniclastic and pyroclastic material to the sequence development in the late Quaternary ULB.

Tectonic Control (Faulting and Seismicity)

Faulting exerts a first-order control on the development of the lake basins in rift systems (Yuretich 1982). Tectonic movements in such basins can affect hydrology by controlling basin shape and depth (accommodation), watershed geology (sediment input), and drainage patterns by defining the sill height or spill point of the basin (Renaut and Gierlowski-Kordesch 2010). However, tectonic movements occur over relatively long time scales. This study reveals that the ULB units exposed in outcrop were deposited over a span of just ~40 ka, although a much thicker succession of Lake Beds strata recorded in well logs and seismic reflection profiles suggests a much longer depositional history (e.g., Morley et al. 1999). The initiation of the Lake Beds sedimentation is clearly tied to a long history of rifting in the Rukwa Rift (Ebinger et al. 1989, 1993).

The upper Lake Beds strata are characterized by abundant small-scale, as well as several examples of very large-scale, soft-sediment deformation features that are interpreted to be of seismogenic origin and demonstrate synsedimentary faulting during the late Quaternary (FA10: Figs. 4B, 5A, 10A) (Hilbert-Wolf and Roberts 2015). The occurrence of tectonic movements during the last stages of basin evolution is also consistent with findings by Ceramicola et al. (1997) and Morley et al. (2000), who documented Holocene faulting in the basin using high-resolution seismic reflection records. This active seismicity may have influenced sedimentation patterns in the Lake Beds, perhaps leading to the abundance of seismites and hyperpycnites in the upper Lake Beds. However, it is unlikely that these high-frequency fault movements exerted the major control on base level in the Rukwa Rift Basin over such a short time scale (~40 ka) because the magnitude of base-level change is too great and its frequency too high.

CONCLUSIONS

Detailed lithofacies mapping, along with radiocarbon dating and petrologic investigations of the upper Lake Beds in the Rukwa Rift Basin, southern Tanzania, provide the basis for interpretation of depositional environments and sequence stratigraphy and assessment of the relative roles of tectonism, climate, and volcanism on sedimentation. A total of 24 lithofacies and 11 facies associations are described and used to interpret a mosaic of depositional environments associated with three main depositional systems: (1) alluvial to fluvial channel system; (2) delta system; and (3) profundal lacustrine system.

The exposed ULB represent six (different) depositional sequences (A - F), which are characterized by alternating landward- and basinward-stepping stratal stacking patterns and sequence-bounding unconformities. Base-level changes and subsequent sedimentary sequence development in the ULB appears to be controlled largely by interplay between climate change and sediment supply, which was strongly influenced by synchronous, episodic volcanism in the Rungwe Volcanic Province. Siliciclastics- and volcaniclastics-dominated depositional sequences record shifts in provenance associated with episodic explosive volcanism. These provenance shifts reflect alternating episodes of rapid sedimentation due to pyroclastic fallout and secondary reworking of pyroclastic deposits versus slower sedimentation associated with weathering and erosion of the uplifted metamorphic and granitoid basement rocks along the rift flanks.

Based on the new ^{14}C age datasets obtained from this study, as well as previous published dates (Cohen et al. 2013), the top of the ULB sequence exposed in outcrop is assigned a late Quaternary age, ranging between ~45 and ~5 ka. However, a more full treatment of the stratigraphy and nomenclature of entire Lake Beds succession await more thorough dating and analysis of the expansive stratigraphy of the Ivuna-1 and Galula-1 wells, as well as a thorough investigation of as yet undescribed strata overlying the Cretaceous Galula Formation and underlying ULB strata on the western margin of the rift system.

Acknowledgments

We are grateful to the Tanzania Petroleum Development Corporation (TPDC) and Heritage Oil Rukwa Tanzania Ltd. for providing a PhD bursary to the lead author (CM) and funding to conduct three field seasons in the rift. This research was also supported by the US National Science Foundation (EAR_1349825, BCS_1127164), the National Geographic Society (CRE), and the post-graduate research fund from James Cook University. We are indebted to the staff of Heritage Oil Rukwa Tanzania Ltd in the Dar es Salaam office for support in the fieldwork logistics. We thank H. Hilbert-Wolf, N. Boniface, J. Edmund, P. O'Connor, N. Stevens, Z. Jinnah, and the rest of the RRBP team members for their field assistance and valuable discussions. Finally, we thank the Associate Editor J. Scott and reviewers (A. Cohen and D. Delvaux) for constructive reviews that improved this manuscript.

Chapter 2

Sedimentology and paleoenvironments of a new fossiliferous late Miocene-Pliocene sedimentary succession in the Rukwa Rift Basin, Tanzania

Keywords: Sedimentology; Neogene; Rukwa; Tanzania; Facies

ABSTRACT

This paper presents a detailed sedimentologic investigation of a newly identified, fossiliferous late Neogene sedimentary succession in the Rukwa Rift Basin, southwestern Tanzania. This synrift deposit is a rare and significant new example of a fossiliferous succession of this age in the Western Branch of East Africa Rift System. The unit, informally termed the lower Lake Beds succession, is late Miocene to Pliocene in age based on cross-cutting relationships, preliminary biostratigraphy, and U-Pb geochronology. An angular unconformity separates the lower Lake Beds from underlying Cretaceous and Oligocene strata. Deposition was controlled by rapid generation of accommodation space and increased sediment supply associated with late Cenozoic tectonic reactivation of the Rukwa Rift and synchronous initiation of the Rungwe Volcanic Centre. The lower Lake Beds, which have thus far only been identified in three localities throughout the Rukwa Rift Basin, are characterized by two discrete lithologic members (herein A and B). The lower Member A is a volcanic-rich succession composed mostly of devitrified volcanic tuffs, and volcaniclastic mudstones and sandstones with minor conglomerates. The upper Member B is a siliciclastic-dominated succession of conglomerates, sandstones, mudstones and minor volcanic tuffs.

Detailed facies analysis of the lower Lake Beds reveals various distinctive depositional environments that can be grouped into three categories: 1) alluvial fan; 2) fluvial channel; and 3) flood basin environments. The latter is characterized by volcanoclastic-filled lakes and ponds, abandoned channel-fills and pedogenically modified floodplains. Member A represents a shallow lacustrine setting filled by tuffaceous sediments, which grade up into a system of alluvial fans and high-energy, proximal gravel-bed braided rivers. An unconformity, identified by a pedogenically modified (calcretized) conglomerate unit marks the contact between the two members. Member B shows an upward transition from a high-energy, gravel-bed braided river system to a sandy braided river system with increasingly abundant floodplain deposits and well-developed paleosols. Vertebrate fossils are sparse in member A, but common in member B, preserved both within pedogenic soil horizons and as isolated elements and microsites within fluvial channel facies associations. Faunal remains include fishes, turtles and crocodylians, along with well-preserved mammal cranial and post-cranial remains. In addition, freshwater gastropod shells are locally present in member A, and continental trace fossils, including abundant fossilized termite nests, are present in both members.

1. Introduction

The Cenozoic East African Rift System (EARS) is well-known for its extensive exposures of richly fossiliferous sedimentary deposits and rift-related volcanism. The distribution of vertebrate fossils, including hominin remains, is known primarily from sedimentary deposits in the Eastern Branch of the EARS (e.g., the Ethiopian, Kenyan and Gregory rifts; Brown and Feibel, 1986; Dunkelman, 1986; Fleagle et al., 1991; Hautot et al., 2000; Feibel, 2011). The most famous Miocene-Pleistocene fossil sites in the EARS include Olduvai Gorge and Laetoli in northern Tanzania, the Omo-Turkana basin along Ethiopia-Kenya border, in addition to the Middle Awash, Gona, Hadar and Konso areas within the southern Afar depression of northwestern Ethiopia (e.g., Leakey and Leakey, 1964; Bishop, 1978; White and Suwa, 1987; Leakey et al., 1995; Haile-Selassie et al., 2015). The other major locations in Africa where fossil assemblages of this age with abundant vertebrate faunas and early hominin remains have been discovered is in the Cradle of Humankind just outside of Johannesburg, South Africa. Here, fossil cave sites such as Sterkfontein, Swartkrans, Kromdraai, Drimolen, Gondolin, Gladysvale, Malapa and Rising Star have produced a wealth of Plio-Pleistocene fossils (Lockwood and Tobias, 1999; Menter et al., 1999; Susman and de Ruiter, 2004; Pickering et al., 2007; Berger et al., 2010, 2015; Berger, 2012; Herries and Adams, 2013; Dirks et al., 2010, 2015).

The search for fossiliferous strata documenting this important time interval reaches beyond just South Africa and the Eastern Branch of the EARS, as demonstrated by fossil discoveries in the Lake Chad Basin of Central Africa that extend the record of human evolution back to ~7 Ma ago (Brunet et al., 2002, 2005). However, despite decades of paleontologic exploration, only a handful of fossiliferous Miocene-Pleistocene sedimentary deposits have been documented from the Western Branch (Albertine Rift) of the EARS (Pickford et al., 1993; Bromage et al., 1995; Crevecoeur et al., 2014). These rare Western Branch sites are largely limited to the northern part of the rift branch between Lake Albert and Lake Edward, where lower Miocene to Pleistocene deposits have been described from both the DRC and Uganda. In particular, the Semliki Valley to the south of Lake Albert in Uganda (Pickford et al., 1993), and Ishango on the north side of Lake Edwards (Crevecoeur et al., 2014), have both produced abundant faunal remains, which together form part of a fairly extensive succession of fossiliferous lower Miocene-Pleistocene fluvio-lacustrine strata in this region (Roller et al., 2010). To date, the only significant fossil locality of this age in the southern portion of the EARS is in the northern Malawi Rift Basin, a segment of the Western Branch of the East African Rift System (Beltzer and Ring, 1995; Roller et al., 2010). The Uraha, Mwenirondo, Malema and Mwimbi sites on the northwestern shores of Lake Malawi preserve a number of relatively isolated, fossiliferous, fluvio-lacustrine, Plio-Pleistocene deposits defined as the

Chiwondo beds, which have produced abundant faunal remains, along with a single hominin dentary and other isolated jaw fragments (Clark et al., 1970; Bromage et al., 1985, 1995a, b; Rozzi et al., 1997; Sandrock et al., 2007; Kullmer et al., 2011; Stewart and Murray, 2013).

The late Cenozoic, between 10 Ma and Recent, represents a critical time period in African history, characterized by major environmental and climatic changes associated with the development of the East African Rift System and uplift of southern and eastern Africa (Potts, 1998; deMenocal, 2004; Sepulchre et al., 2006; Maslin and Christensen, 2007; Trauth et al., 2007). It has been suggested that tectonic rifting has played an important role in faunal evolution in Africa, particularly by creating diverse landscapes with dispersal corridors and settings conducive to the development of major river systems and lakes where a mosaic of African species are thought to have lived and evolved (Brown, 1981; Feibel et al., 1991; Potts, 1998; Ashley, 2000; Trauth et al., 2007). Additionally, tectonic rifting is associated with volcanism and high subsidence rates that provide excellent conditions for the production and deposition of sediments, and hence rapid burial of floral and faunal remains (WoldeGabriel et al., 2000; Stollhofen et al., 2008). Rift basins are therefore, important archives of high-resolution tectonic, climatic and environmental data.

Nowhere has the importance of such changes in Africa been of more interest than in the study of the East African Rift System, which has long focused on the interplay between tectonic, environmental and climatic changes for understanding the evolutionary and ecological patterns and distribution of flora and fauna on the continent since the late Miocene (e.g., Vrba, 1988; deMenocal, 1995; Stanley 1995; Potts 1998; Kingston, 2007; Maslin and Christensen, 2007; Trauth et al., 2007; Muslin et al., 2014). A key aspect of expanding our understanding of the evolution of East African landscapes and ecosystems depends upon recognition and discovery of new outcrop exposures, particularly in previously under-studied or unknown basins. Whereas late Neogene deposits in the Eastern Branch of the East African Rift System have been extensively explored and studied, many parts of the Western Branch of the EARS have yet to be extensively explored and documented. In this paper, we document a vertebrate, invertebrate and trace fossil-bearing late Neogene stratigraphic succession in the Rukwa Rift Basin of southwestern Tanzania, informally referred to here as the lower Lake Beds succession. This study was conducted as part of the Rukwa Rift Basin Project (see Roberts et al., 2004, 2010, 2012; O'Connor et al., 2006, 2010; Stevens et al., 2008, 2013), which is focused on the discovery and documentation of the palaeontologic history of the rift over the last 100 million years in combination with refining the tectonic and sedimentary history of the basin. The purpose of this paper is to describe the distribution and detailed sedimentology of the lower Lake Beds Succession and to provide a preliminary stratigraphic and paleoenvironmental context for this newly recognized Neogene vertebrate fossil locality in East Africa.

2. Regional Geology and Background

The northwest-trending Rukwa Rift Basin (RRB) is part of the Western Branch of the East African Rift System, situated between the Tanganyika and Malawi rifts in southwestern Tanzania (Fig. 1). The basin is about 360 km long and 40 km wide, bounded to the northeast by the linear Lupa border fault and Tanzania Craton, to the southwest by the Ufipa fault and uplifted Ufipa block, and to the south and southwest by the Rungwe volcanics and Mbozi block, respectively (Ebinger et al., 1989; Kilembe and Rosendahl, 1992). The RRB has a half-graben architecture, and is flanked by uplifted Paleoproterozoic metamorphic basement rocks of the Ubendian shear belt (Quennell et al., 1956; Daly et al., 1985; Lawley et al., 2013).

The Rukwa Rift was initiated during the Paleozoic by reactivation of Paleoproterozoic to Neoproterozoic sinistral shear zones in the NW-SE trending Ubendian Belt (Theunissen et al., 1996). Structural development of the RRB has provoked debate among researchers. The RRB was first proposed to have formed as a strike-slip pull-apart basin in an oblique, northwest-southeast extensional setting based on interpretations of linear map geometry and oblique orientation to the general north-south trend of EARS, as well as from satellite images and seismic profiles (Chorowicz and Mukonki, 1979; Kazmin, 1980; Tiercelin et al., 1988). The oblique opening model was later supported by outcrop-based structural studies that indicated dominantly low angle, dextral kinematics along the Lupa Fault (Wheeler and Karson, 1994). However the basin geometry and listric fault shape observed in seismic reflection data does not fit a pull-apart basin, and other workers have suggested east-west to northeast-southwest extension, and oblique opening of an extensional rift basin, influenced by northwest-southeast trending pre-existing fabric in the basement (Ebinger, 1989; Morley et al., 1990; Mbede, 1993). Thus, a general E-W extension model was proposed, dominated by normal faulting sub-orthogonal to the trends of the rift segments (orthogonal opening model: Ebinger, 1989; Morley et al., 1992; Delvaux, 2001; Delvaux and Barth, 2010; Morley, 2010).

The orthogonal opening model for the Rukwa Rift Basin is supported by more recent work on the ancient and active faults along the Ufipa Plateau. Based on detailed active tectonic studies, brittle kinematics and paleostress investigations, Delvaux et al. (2012) has shown that extension occurred sub-orthogonal to the NW-SE rift trend in a normal faulting regime. These workers hypothesized the existence of two brittle regimes that pre-date the late Neogene development of the East African Rift System. According to Delvaux et al. (2012), the oldest brittle regime initiated sometime prior to the late Carboniferous, and is characterized by eastward thrusting with compression sub-orthogonal to the trend of the Ubende Belt and subsequent rift segmentation. This deformation episode was associated with the interaction between Bangweulu Block and the Tanzanian Craton during the late stages of the Pan-African orogeny (Ebinger 1989; Morley et al., 1990; Delvaux et al., 2012). The youngest brittle stage, which is characterized by N-S transpression and related dextral fault movements, is linked to Mesozoic far-field stresses associated with rifting along the southern passive margin of Gondwana (Delvaux et al., 2012).

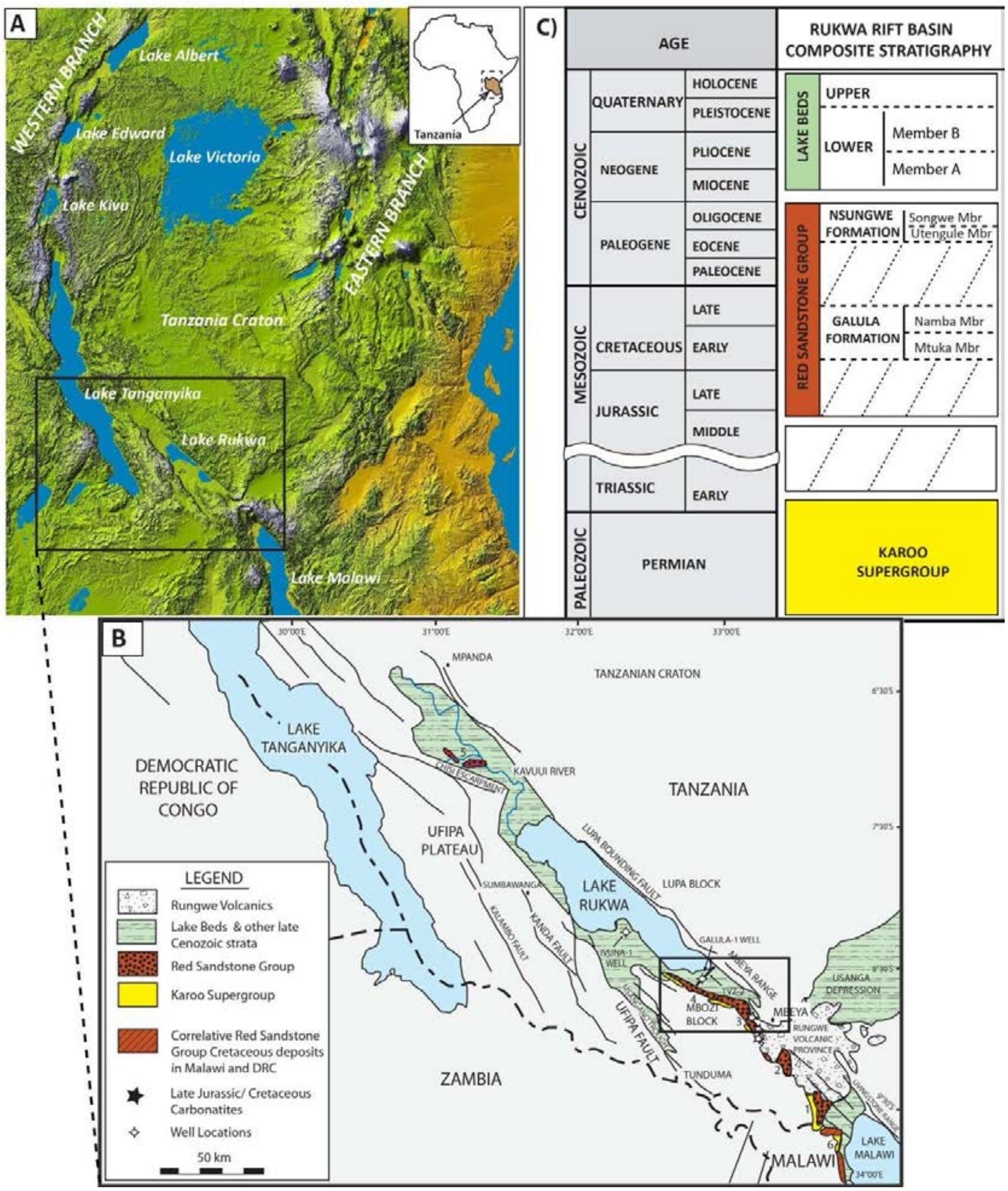

Figure 1. **A)** Map showing study area in southwestern Tanzania. **B)** Geological map of the Rukwa Rift Basin showing tectonic elements and distribution of rock units. Inset box is shown in Fig. 2A. **C)** Composite stratigraphy of the Rukwa Rift Basin (modified from Roberts et al., 2010).

Seismic and gravity surveys conducted in the RRB during 1980s and 1990s, along with the drilling of two hydrocarbon exploration wells (Galula-1 and Ivuna-1 drilled in 1987), revealed up to 8-11 km of sedimentary fill in the basin, making it one of the thickest continental sedimentary basins in Africa (see figs. 8-11 in Morley et al., 1999). Analysis of the seismic profiles coupled with well data and surface geology show that the RRB has undergone at least four episodes of rifting, including: (1) a Permo-Triassic event, which resulted in the deposition of Karoo Supergroup equivalent strata (Kilembe and Rosendahl, 1992; Morley et al., 1999); (2) a Cretaceous rifting event that deposited the fluviatile Galula Formation, a unit that is subdivided into two distinct members (lower part of the Red Sandstone Group: Roberts et al., 2004, 2010, 2012); (3) a late Oligocene event that resulted in a short-lived, richly fossiliferous fluvio-lacustrine depositional sequence (Nsungwe Formation, upper part of the Red Sandstone Group), which was accompanied by alkaline volcanism (Roberts et al., 2004, 2010, 2012); and (4) late Miocene to Recent rifting and deposition of the Lake Beds succession, accompanied by voluminous bimodal volcanism in the Rungwe Volcanic Province (Grantham et al., 1958; Ebinger et al., 1989; Wescott et al., 1991).

The Lake Beds succession, which represents the youngest stratigraphic interval in the RRB, is widespread and relatively thick, reaching up to 4 km (see Kilembe and Rosendahl, 1992). In the southern RRB, Lake Beds deposits are well exposed in the Ilasilo-Galula, Ikuha and Ikumbi areas, as well as in the Songwe Valley and along the Chambua, Hamposia, Namba and Chizi river drainages (Fig. 2A). The Lake Beds deposits unconformably overlie the late Oligocene Nsungwe Formation or the Cretaceous Galula Formation of the Red Sandstone Group (Roberts et al., 2010). The Lake Beds units were first described by Grantham et al. (1958) as conglomerates, sandstones and mudrocks associated with fluvial-floodplain and lacustrine environments. Grantham et al. (1958) informally subdivided the Lake Beds into lower and upper units, based on structural and lithological features. According to Grantham et al. (1958), the lower (older) unit consists of gently NE-dipping sandstone and overlying volcanic siltstone, whereas the upper (younger) unit is characterized by flat-lying beds of conglomerate, pumice tuff and limestone. Earlier efforts to determine the depositional age of the Lake Beds involved contentious microfloral analysis of the Ivuna-1 and Galula-1 well cuttings, which suggested a late Pliocene-Holocene age for the large portion of the Lake Beds (e.g., Wescott et al., 1991). Radiocarbon dating of shallow (12.8 m thick) sediment cores suggested a Quaternary age for this uppermost interval of the strata (e.g., Haberyan, 1987).

Unfortunately, however, there remains no formal stratigraphy for the Lake Beds. To date, the exposed Lake Beds deposits documented by various research teams in the Rukwa Rift have been restricted to the latest Quaternary portion, which is largely devoid of vertebrate fossils except isolated fish elements (Sherwood and Kingston, 2002; Cohen et al., 2013). Over the last few decades, the Lake Beds have also been the focus of brief and unsuccessful exploration focused on identifying new hominin-bearing deposits in this part of the East African Rift System (e.g., Sherwood and Kingston, 2002).

More recently, detailed sedimentologic, geochronologic and biostratigraphic investigations of the uppermost units of the Lake Beds succession have been performed (Cohen et al., 2013; Mtelela et al., 2016). These investigations have largely confirmed a latest Pleistocene-Holocene age between 45 and 5 ka for all known exposures of the Lake Beds strata in both the northern and southern outcrop extents across the basin (Mtelela et al., 2016). Indeed, sedimentologic investigations conducted by Mtelela et al. (2016) reveal that the “upper” and “lower” Lake Beds as defined and mapped by Grantham et al. (1958) does not represent a true lithostratigraphic subdivision. Rather, these stratigraphic interpretations represent lateral facies changes (sub-environments) within a widely variable fluvial-lacustrine deposition system, and the term upper Lake Beds Succession has been suggested for all of these strata (Mtelela et al., 2016).

However, interpretations of 2-D seismic data across the basin shows that the Lake Beds succession sits above slightly incised and deformed beds of the Red Sandstone Group in a half-graben basin (Kilembe and Rosendahl, 1989; Morley et al. 1999), with bedsets gently dipping and fanning towards the main bounding fault in a north-to-northwest direction. As such, the western rift margin represents a likely site for containing exposures of the basal portion of the Lake Beds stratigraphy, particularly considering the present day low surface level of Lake Rukwa. Indeed, during the course of the recent sedimentological and paleontological investigations of the upper Lake Beds, conducted as part of the Rukwa Rift Basin Project, our research group identified a series of new and previously unrecognized sedimentary deposits cropping out between the Red Sandstone Group and upper Lake Beds deposits in isolated areas within the rift. It appears that recent rifting and uplift have exposed older sedimentary units along the western margin of the basin, in the Songwe Valley (south of the lake) and along the Hamposia, Chizi and Ikumbi River drainages.These strata are termed here the lower Lake Beds (LLB). Perhaps due to the irregular nature of exposures and the blanketing nature of upper Lake Beds strata, exposures of the LLB (described in this paper) were not recognized or mapped during the first regional geologic mapping by Grantham et al. (1958). The total outcrop extent of this unit is unknown and awaits further exploration. The LLB deposits have been folded and faulted along with the Red Sandstone Group strata, clearly differentiating them from the undeformed, horizontally bedded upper Lake Beds strata (Fig. 2-4). The sedimentology and paleontology of the LLB (discussed below) is distinctly different from that of both the Oligocene and Cretaceous Red Sandstone Group deposits and the overlying upper Lake Beds strata. Detailed biostratigraphic assessments, to be presented elsewhere (N. Stevens, pers.

comm.), and geochronologic data (Hilbert-Wolf et al., 2013, in press) indicate a late Miocene to Pliocene age for these deposits.

3. Methods

A GPS set to the Tanzanian datum (Arc 1960), Jacob's Staff, laser range finder, and Brunton compass were utilized for mapping and measuring stratigraphic sections along the upper Hamposia, Chizi and Ikumbi Rivers, where deep channel incision has resulted in well-exposed cliff face exposures of the LLB (Fig. 2). Topographic maps and the Mbeya 244 quarter-degree geologic map (Grantham et al., 1958) were used as base maps. A Munsell rock colour chart was used to determine rock colour codes. A Brunton compass was also used to measure bedding trends and palaeocurrent orientations on three-dimensionally exposed ripple, planar and trough cross-stratified beds. Lithofacies were identified and documented based on key sedimentologic aspects, including: lithology, texture (grain-size, shape and sorting), sedimentary and biogenic structures, and fossil content.

Facies analysis was conducted for the lower Lake Beds following the methodology outlined by Mtelela et al. (2016) for the upper Lake Beds. Lithofacies nomenclature and codes used in this study are modified after Miall (1996), to illuminate the distinctive characteristics of the Lake Beds. In particular, we use the terms *tuffaceous conglomerate*, *tuffaceous sandstone* and *bentonitic mudstone* (and their respective codes) for secondary, reworked pyroclastic sedimentary rocks comprised of dominantly pebble-, sand-, and clay-sized sediments, respectively. Pebble counts were performed in the field on conglomerate beds at different levels in the stratigraphy to characterize lithoclast composition and supplement sandstone petrology. Representative sandstone samples were collected for thin-section analysis. The detrital mineral composition of siliciclastic sandstone in thin sections were statistically analyzed by a point counting technique, following a modified Gazzi-Dickinson method (Ingersoll et al. 1984), to determine percentage proportions of chiefly quartz, feldspar and rock fragments. For each sandstone thin sections, a total of 350 sand-sized grains were counted.

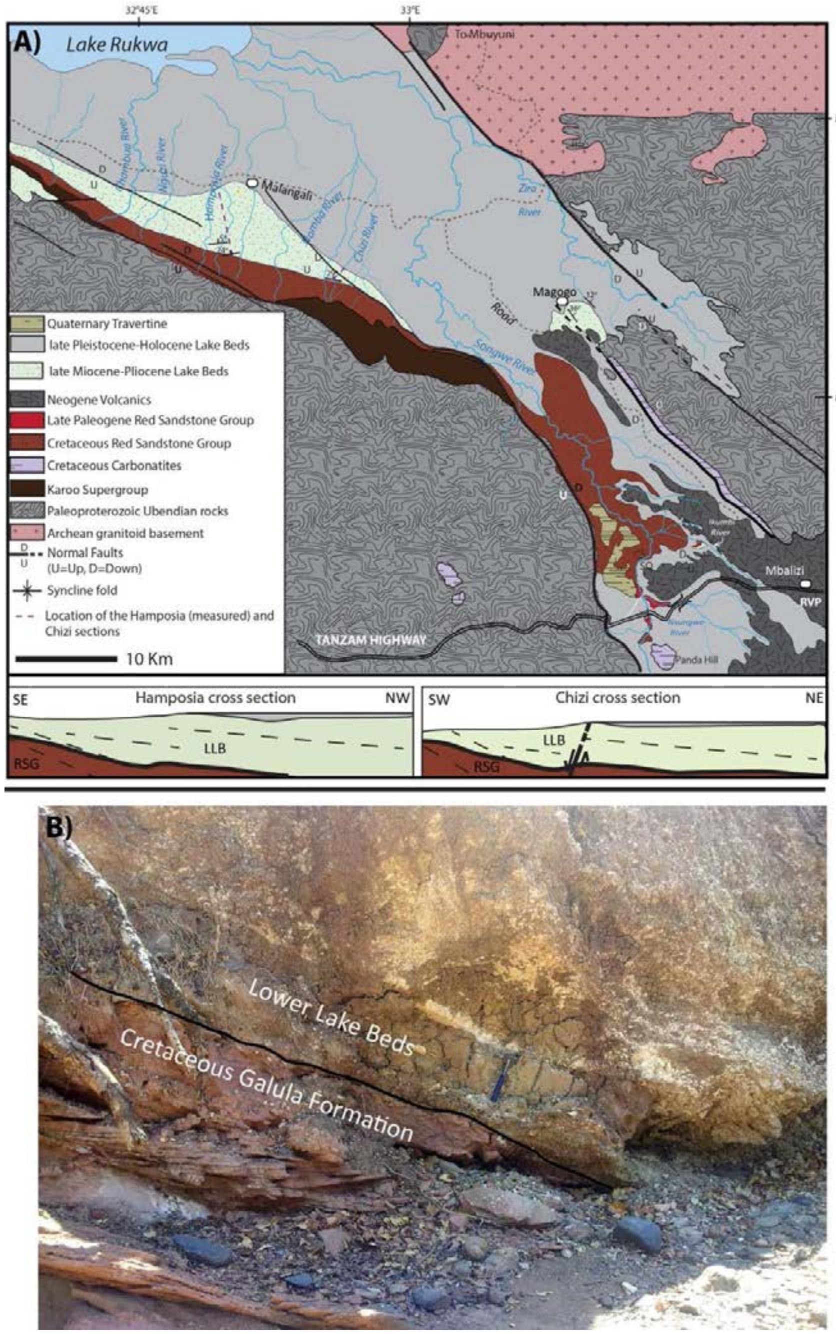

Figure 2. **A)** Geologic map of the southern Rukwa Rift Basin, highlighting the distribution of the lower Lake Beds succession along the present-day Chambua, Nguzi, Hamposia, Namba and Chizi river drainages, as well as in the Ikumbi and Magogo areas. Other lithologies and structures are adopted from Grantham et al. (1958) and Roberts et al. (2010). **B)** Unconformable contact between lower Lake Beds and the Cretaceous Red Sandstone Group rocks along the Chizi River. Note that both the Cretaceous and lower Lake Beds strata are dipping in the same direction; however there is a slight angular unconformity that marks the contact between the two units.

4. Lithostratigraphy

An ~156 m thick stratigraphic section was measured along the Hamposia River drainage. The lithostratigraphy presented below is based primarily on observations and data collected along this section. However, correlations can be made with strata observed in the other areas, particularly in the Chizi River drainage (Fig. 2). Along the outcrop belt on the western side of Lake Rukwa, the LLB strata rest unconformably on top of the Cretaceous Galula Formation. The basal contact is clearly exposed in cliff-face exposures along both the Chizi and Hamposia rivers. Along the Hamposia and Chizi Rivers, the LLB unconformably overlies the Galula Formation, and dips roughly 18° and 26° towards the NNW and NE, respectively. Along the Ikumbi River, the LLB overlies the Nsungwe Formation, and dips ~6° towards the ENE. At the Hamposia River section, the contact is located at 8°37′54″S, 32°49 ′10″E, near the village of Mpona, where the LLB dips 18° to the NW, and the underlying Galula Formation dips 24° NW (note very similar strike orientations). The LLB and the Cretaceous strata appears to have been faulted together following deposition of the LLB, but prior to deposition of the Quaternary-Holocene upper Lake Beds strata, which were deposited horizontally above the dipping Galula Formation and LLB strata. The top of the LLB section along the Hamposia River ends at 8°34′35″S, 32°49 ′49″E, near the vehicle bridge close to Malangali village. At the Ikumbi Section, and in several places within the Songwe area, the LLB also overlie dipping bedding of the late Oligocene Nsungwe Formation (Roberts et al., 2010, 2012; Spandler et al., 2016). In the Ikumbi section, horizontally-stratified ULB units have erosionally incised into both the LLB and the underlying Nsungwe Formation. In the Magogo area, the LLB is steeply dipping and it is unclear what portion of the LLB stratigraphy is exposed. There is no basal contact with the Red Sandstone Group exposed around Magogo, but a basal carbonate unit does occur there that is not observed elsewhere in the study area.

In the Hamposia river section, distinct lithological variations between the lower and upper portions of the LLB stratigraphy, coupled with the presence of major unconformity surfaces within the LLB, permit the subdivision of the LLB into two informal stratigraphic units: lower Member A and upper Member B (Fig. 3). At present, there is insufficient exposure and regional understanding of the stratigraphy to extend these subdivisions to the LLB strata that crop out in the Magogo area and Songwe Valley (e.g., Ikumbi area). Hence, the informal lithostratigraphy presented here is limited to exposures of the LLB along the southwestern margin of Lake Rukwa. Establishment of a formal stratigraphic subdivision and nomenclature for the entire Lake Beds succession awaits a basin-wide synthesis and integration of outcrop based and subsurface (Ivuna-1 and Galula-1 wells) dating of these units recently reported by Hilbert-Wolf et al. (in press).

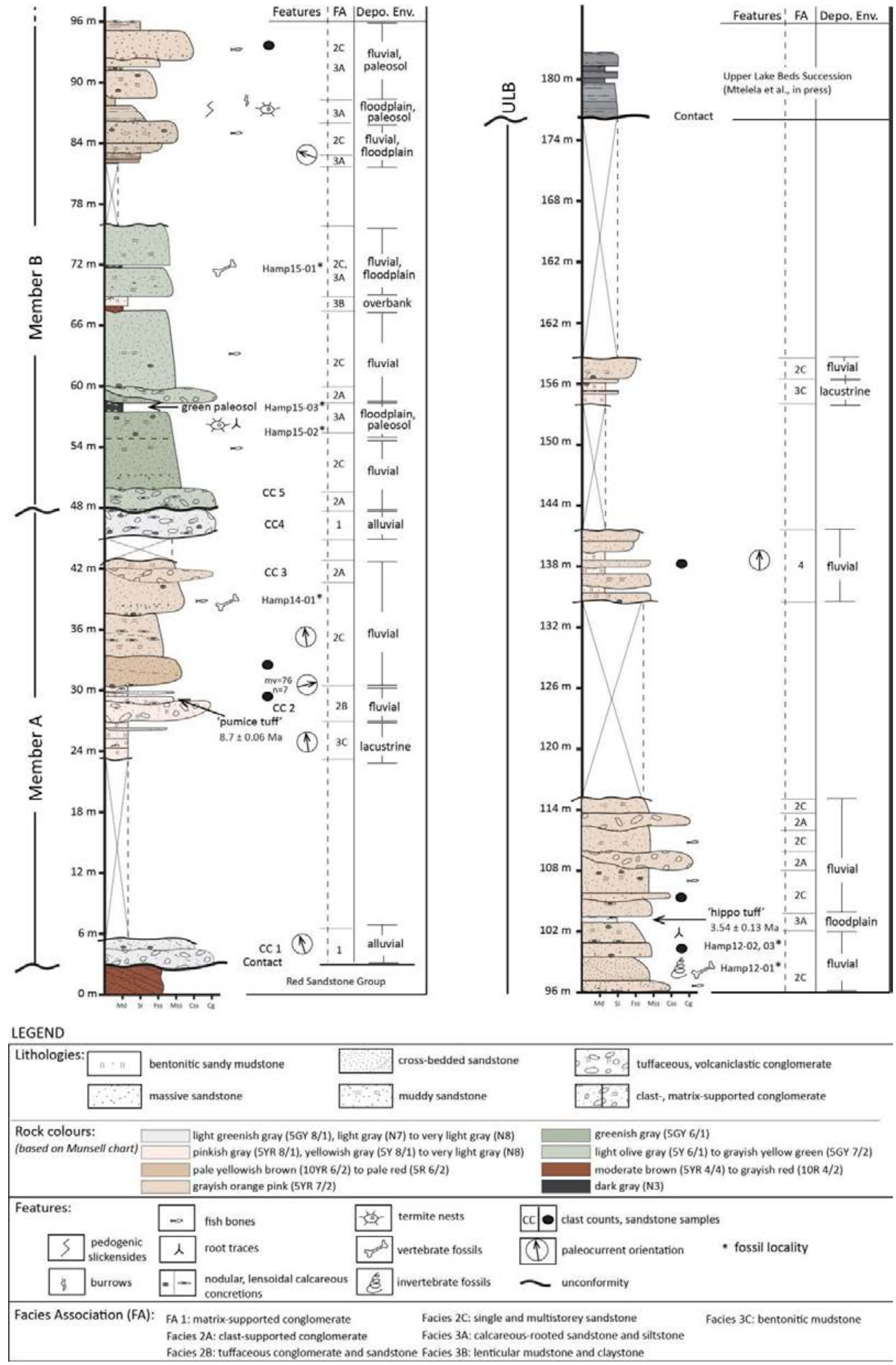

Figure 3. Lower Lake Beds stratigraphic section measured along the Hamposia River drainage, from 8°37′54″S, 32°49 ′10″E to 8°34′35″S, 32°49 ′49″E. U-Pb age data for the Pumice Tuff and Hippo Tuff beds are from Hilbert-Wolf et al. (in press).

4.1. Member A

Informal member A is defined as the dominantly tuffaceous lower portion of the LLB that rests unconformably on the Galula or Nsungwe formations. Along the Hamposia River, member A is ~40 m thick and capped by deeply weathered paleosol horizon that is cut by a high-relief erosional unconformity separating it from the overlying fluvial strata of member B (Fig. 3). The basal 23 m of member A is characterized by a distinctive siliciclastic-dominated facies consisting of tabular to lenticular quartz pebble conglomerate, resting unconformably above the Red Sandstone Group. Paleocurrent observations and the few possible measurements suggest deposition by NW directed longitudinal fluvial channels. This basal interval is significant in that it also lacks volcanic detritus or pyroclastic units. The middle interval of member A transitions sharply to a volcanic-rich succession of tuff, tuffaceous conglomerate and bentonitic mudstone. The upper-most part of member A transitions back to a more siliciclastic-rich succession of muddy sandstone and conglomerate. However, the matrix and some of the clasts of these upper sandstone and conglomerate units retains a volcanic nature with abundant bentonitic mudstone and devitrified volcanic ash.

Conglomerate units at the bottom and top of member A are vein-quartz dominated. Individual beds are typically characterized by an upward transition from a primarily clast-supported to a matrix-supported towards the top. Siliciclastic sandstone framework grain compositions vary from quartzose to quartzo-feldspathic (subarkosic), and vary in color between very light gray (N8), pale red (5R 6/2) and grayish orange pink (5YR 7/2). Volcaniclastic lithofacies that dominate the middle of member A are composed of a combination of primary pyroclastic deposits and re-sedimented volcanic-rich sedimentary deposits. The pyroclastic deposits are primarily unwelded, pumice-rich ash flow tuff and ash fall tuff lithofacies. In most cases, the primary volcanic glass is weathered and has devitrified or partially devitrified into smectitic clays. The strike and dip change up-section due to post-depositional faulting, from 82°/18° NNW at the base, to 20°/7° WNW in the upper part of the section through this unit. Fossils recovered from member A are limited to isolated fish bones and fragments of large mammal bones that occur in the beds of siliciclastic sandstone lithofacies towards the upper part of this unit.

4.2. Member B

Informal member B is considerably thicker (~110 m thick in outcrop) than member A, and is defined as the siliciclastic-dominated interval above the unconformity at the top of member A. In the type section along the Hamposia River described in this study, the dip of member B shallows considerably up-section to almost zero. Member B can be followed for ~5-

6 km along the Hamposia river drainage, from the Mpona area to the western part of the Malangali village. In many places along this river section, the overlying upper Lake Beds succession erosionally overlies member B with an angular unconformity.

Deposits of member B are characterized by alternating, multistory clast-supported conglomerate and sandstone bodies that are locally interbedded or intercalated with thin (< 60 cm thick) beds of fine-grained sandstone, siltstone, mudstone, and rare volcanic ash beds (10-20 cm thick). Conglomerate deposits are commonly massive tabular-lenticular bedded, typically cobble-sized and polymictic in composition. Sandstone lithofacies are generally quartzo-feldspathic (subarkosic), but vary in color from greenish gray (5GY 6/1) or grayish yellow green (5GY 7/2) to grayish orange pink (5YR 7/2). A distinctive feature of this unit is the presence of well-developed paleosols with calcium carbonate accumulations (Bk horizons). Bedding is gently tilted across the middle portion of member B, dipping 5°-7° towards the north-northwest and west-northwest.

Member B is considerably more fossiliferous than member A and preserves abundant freshwater and terrestrial vertebrate remains in sandstone units. Isolated fish, crocodile and turtle remains are prolific in certain horizons throughout most of member B. In contrast, isolated large, exceptionally well-preserved mammalian and crocodilian cranial and post-cranial remains are locally abundant from both mudstone and sandstone bodies near the base and middle of member B.

5. Facies Analysis

Fourteen sedimentary lithofacies were identified for the LLB in the Rukwa Rift Basin (Tables 1 and 2). Based on the repeated association of certain lithofacies together with distinctive internal and external geometries and diagnostic vertical and lateral facies relationships, seven facies assemblages were recognized and categorized into three genetically-related facies associations (FAs): alluvial fan deposits (FA1), fluvial channel deposits (FA2), and floodbasin deposits (FA3). In order of descending grain size, the specific facies assemblages include: matrix-supported conglomerates (FA1), clast-supported conglomerates (Facies 2A), tuffaceous conglomerate and sandstone (Facies 2B), single and multi-storey sandstone (Facies 2C), calcareous, rooted sandstone and siltstone (Facies 3A), lenticular mudstone and claystone (Facies 3B) and bentonitic mudstone (Facies 3C). Each of these FAs is described in detail below, followed by interpretation of their depositional processes and environments (summarized in Table 3).

Table 1. Coarse-grained lithofacies in the late Miocene-Pleistocene Lower Lake Beds.

Code	Lithofacies	Texture and Composition	Structures and Features	Color	Interpretation
Gcm	Clast-supported conglomerate	Clasts: pebble-to boulder-sized; comprised of vein quartz, metamorphic granitoids and meta-volcanic;poorly-sorted:sub-angular to rounded Matrix: fine to medium-grained muddy sandstone	Massive to crudely-bedded; ungraded to weak normal grading	-	Unidirectional high energy deposits.
Gmm	Matrix-supported conglomerate	Clasts: pebble–to cobble-sized; monomictic: Vein quartz dominated or polymictic: comprising vein-quartz, metamorphic granitoids and meta-volcanics; typically poorly-sorted; Sub-angular to well rounded. Matrix: carbonaceous sandy mudstone or muddy sandstone	Typically massive; ungraded	Light greenish gray (5GY 8/1), very light gray (N8)	Unidirectional high-energy deposits.
Gmv	Volcaniclastic conglo-merate	Clasts: pebble- and less common cobble-sized; exclusively pumice in composition;poorly-sorted;sub-round to rounded Matrix: devitrified bentonitic ash	Massive; reversely graded	Pinkish gray (5YR 8/1), yellowish gray (5Y 8/1	High-energy fluvial reworked pyroclastic or epiclastic deposits.
Smp	Massive pebbly sand-stone	Medium-grained muddy sand- to pebble-sized; moderate-poorly-sorted; quartzo-feldspathic in composition, with vein quartz dominated granules and pebbles; sub-angular to rounded; commonly characterized by discontinuous 10-15 cm thick, lensoidal carbonate concretions.	Massive to crudely-stratified; fish bones locally.	Light greenish gray (5GY 8/1), pale red (5R 6/2)	Unidirectional medium- to high energy deposits

Smv	Massive tuffaceous sandstone	Medium- to very coarse-grained sand and granules; moderate –well-sorted; sub-round to well-rounded; comprises pumice and vitric ash	Typically massive	Light gray (N7), very light gray (N8)	Unidirectional medium- to high- energy *epiclastic* deposits
Spv	Planar cross-stratified Vitric-tuffaceous sandstone	Medium- to coarse-grained sand; moderately- to well -sorted; sub-round to well-rounded; comprises of pumice and vitric ash.	Planar cross-stratified	Light gray (N7), very light gray (N8)	Unidirectional medium- to high- energy reworked pyroclastic deposits.
Sm	Massive sandstone	Fine- to coarse-grained sand; quartz and feldspar dominated; moderately-poor sorted; sub-angular to rounded	Massive or crudely-stratified; isolated carbonate nodules abundant fish bones locally	Pale yellowish brown (10YR 6/2), grayish yellow green (5GY7/2), grayish orange pink (5YR 7/2), light olive gray (5Y 6/1), greenish gray (5GY 6/1)	Unidirectional low- to medium-energy deposits.
Sh	Horizontally-stratified sandstone	Fine- to medium-grained sand; moderate- well-sorted; sub-angular to rounded; quartz and feldspar dominated	Horizontally-stratified	Light greenish gray(5GY 7/1), grayish orange pink (5YR 7/2)	Unidirectional low- to medium-energy deposits
St	Trough cross-stratified sandstone	Muddy, fine- to medium-grained sand; moderately-sorted; sub-angular to rounded.	Trough cross-stratified; fish, crocodile and hippo remains	Grayish yellow green (5GY 7/2), pale yello-wish brown (10YR 6/2)	Unidirectional low- to medium-energy deposits

Table 2. Fine-grained lithofacies in Late Miocene-Pleistocene Lower Lake Beds.

Code	Lithofacies	Texture and Composition	Structures and Features	Colour	Interpretation
Fhvs	Horizontally -stratified volcanic siltstone	Ash and silt-sized grains; with rare floating pumice sands	Horizontally stratified; crudely bedded in places	Medium dark-gray (N5) to light gray (N7)	Subaqueous pyrocla- stic flow/fallout deposits.
Fcvs	Current-rippled volcanic siltstone	Ash and silt-sized grains; with isolated pumice sands and granules.	Current and wave ripples	Medium dark-gray (N5) to light gray (N7)	Water-reworked pyroclastic flow deposits
Fr	Rooted fines	Muddy, silt- to fine-grained sand; moderately-sorted; locally contain isolated floating pebbles;	Massive: primary structures destroyed; calcified roots, calcareous nodules	Light greenish gray (5GY 8/1), pale red (5R 6/2)	Low-energy suspen- sion deposits, paleo-sol
Fl	Finely-laminated mudstone, claystone	Clay- to silt-sized; rare isolated granules and pebbles; overall moderate-well-sorted	Fine-laminations; blocky weathering; rare isolated calcareous nodules	Moderate brown (5YR 4/4), grayish red (10R 4/2), very light gray (N8)	Low-energy suspen- sion or traction deposits.
Fcf	Massive fines	sandy mud, silt and clay; moderate- well-sorted; locally organic	Typically massive; locally characterized by calcareous nodules	Grayish red (10R 4/2), very light gray (N8), dark gray (N3)	Low-energy suspen- sion or overbank flood deposits.
Fbr	Ripple-laminated bentonitic sandy mud-stone	Sandy ash- to silt-sized; composed of devitrified (bentonized) ash and pumice	Wavy, asymmetric ripple cross-lamination; local climbing ripples.	Pinkish gray (5YR 8/1), light gray (N7), very light gray (N8)	Subaqueous low-energy water-lain pyroclastic flow deposits
Fbh	Horizontally -, crudely-stratified bentonitic sandy mudstone	Sandy-silty clay; moderate-well- sorted; devitrified (bentonized) fine ash and pumices grains; lightly organic; rare calcareous nodules	Horizontally to crudely stratified; mud cracks	Pinkish gray (5YR 8/1), light gray (N7), very light gray (N8)	Pyroclastic flow deposits Subaqueous low-energy pyroclastic/epiclastic suspension fallout deposits, with periodic sub-aerial exposure.

Table 3. Facies associations and depositional environments of Late Miocene-Pleistocene Lower Lake Beds.

Facies Association	Facies	Diagnostic Features	Architectural Elements	Depositional Process	Macrofossil	Depositional Environment
FA 1 - Alluvial deposits:						
FA 1 *(massive, matrix-supported conglomerate and subordinate sandstone)*	Gmm, Sm	Coarse-grained; massive; poorly-sorted; crudely upward fining; matrix upward fining; matrix	SG, CH	Gravity settle-out from sheet floods or debris flows.	-	Alluvial plain
FA 2 - Fluvial channel deposits:						
Facies 2A	Gcm, Smp, Sm	Muddy, coarse-grained sand-stone and conglomerate;poorly-sorted;massive or crudely-stratified; ungraded- to weakly normal-graded; erosive lower bounding surface	SG, CH	Debris flow, sheet flooding		Channel lags
Facies 2B	Gmv, Spv, Smv, Fhvs ,Fcvs, Fcf	High degree of sediment rounding; reverse grading; moderately-poorly-sorted; interbedding of fine-grained devitrified ash and coarse-grained pumiceous sandstone	CH, FF(CH)	Debris flows, sheet floods, and suspension saturation settling of diluted hyperconcent-rated flows	-	Fluvial/interfluvial channels.
Facies 2C	Smp, Sm, Sh, St	High degree of sediment	SG, CH, SB	Debris flows, sheet	Fish, hippo and	Fluvial channels

		rounding; upward fining erosive (lower bounding) surfaces		flooding, sediment-gravity fallout	crocodile remains	
FA 3 - Flood basin deposits						
Facies 3A	Sm, Fr	Massive – primary sedimentary structures destroyed; calcified roots; calcareous nodules	SB, FF	Fluvial channels, susp- pension and sediment-gravity fallouts	Trace fossils	Floodplain, paleo-sols.
Facies 3B	Fl, Fcf, Fbh	Fine-grained sediments; finely laminated or massive; concave- up lower bounding surface	FF, FF (CH)	Suspension fallout	-	Abandoned chan-nell fills
Facies 3C	Fbh, Fbr	Fine-grained sediments; plane or concave-up lower surface; finely-laminated; locally slightly organic/bioturba ted;	FF, FF(CH), CH	Fluvial and interfluvial channel-fill, suspension fallout	-	Small lakes/ponds

Architectural elements; SG = sediment-gravity flow, CH = channel fill, SB = sand bedform, FF = floodplain fines, including paleosol and overbank (after Miall, 1996).

5.1. Facies association 1 – alluvial fan deposits

FA1 consists of 1.5-2.5 m thick tabular, matrix-supported conglomerate (Gmm) that mostly occurs as single beds or as beds that fine upward into massive sandstone facies (Sm) (Table1, 3; Fig. 4A-B). FA1 is commonly defined by high-relief (>0.5 m) erosional-scours along bedding soles and/or tops. Conglomerate deposits (Gmm) are typically massive and characterized by poorly-sorted, sub-angular to sub-rounded pebbles and cobbles. Clast composition is dominated by vein-quartz and quartzite. The most characteristic feature of this FA is a matrix support, which is typically sandy mud; however, zones of clast-supported conglomerate (Gcm) are locally present. Both conglomerate (Gmm) and sandstone (Sm) facies of this FA are whitish in color, ranging from light greenish gray (5GY 8/1), light gray (N7) to very light gray (N8). In places where FA1 occurs as a single thick conglomerate bed, crude upwarding fining is observed. Paleocurrent data deduced from pebble imbrication indicates northwest paleoflow. Calcium carbonate cement and nodular accumulations are very common in FA1, and are particularly dense towards the upper contacts. There are no fossils recovered from this FA.

Figure 4. **A)** Outcrop photo of well-exposed alluvial-fluvial deposits along the Hamposia River section, one of more than 8 channel cut outcrops along this drainage (ranging between 6 and 24 m tall cliffs), with illustrations of facies associations and major unconformity surfaces in the Lake Beds. **B-C)** Lower Lake Beds coarse-grained facies, including: massive, matrix-supported

conglomerate (Gmm; **B**) and clast-supported conglomerate (Gcm; **C**). Note: arrow in figure 4A points to a high-relief erosional surface capping a thick calcareous paleosol, separating the lower and upper units (Member A and B) of the LLB succession.

5.2. Interpretation: FA1

FA 1 is interpreted to represent alluvial fan deposits based on texture and compositional features, including matrix composition, angularity of the clasts, poor sorting and crude upward fining. The overall coarse-grained nature, poor sorting and muddy matrix in the conglomerate are all indicative of high-energy bedload deposition by gravity-fallout processes associated with sheet floods or pseudoplastic debris flows (cf. Nemec, 1990; Leleu et al., 2009; Oyanyan et al., 2012). The common tabular geometry and moderately mature (texturally) nature of these debris flow deposits suggest alluvial sedimentation on the medial reaches (alluvial plain) of a channel system, where alluvial processes transition to proximal braided fluvial processes. The upward fining sandstone intervals of FA1 are interpreted to reflect waning flows of discrete flooding events.

Similar deposits in other areas have been interpreted to result from rapid uplift, weathering and erosion along faulted (rift) margins (Miall, 1981). The presence of dense calcium carbonate accumulations in these deposits likely indicates calcic Bk paleosol horizon, reflecting prolonged periods of aridity following the deposition (cf. Mack et al., 1993; Tanner, 2003). This interpretation is consistent with the observed high-relief erosion surfaces associated with this FA, which indicates hiatuses in sedimentation.

5.3. Facies association 2 – fluvial channel deposits

5.3.1. Facies 2A: clast-supported conglomerate

Facies 2A is relatively common in the study area, and dominated by 1-10 m thick tabular to lenticular clast-supported conglomerate (Gcm), interbedded or intercalated with minor matrix-supported conglomerate (Gmm) and sandstone facies (Smp, Sm, St) (Table 1, 3; Fig. 4A, C). Conglomerate beds pinch out laterally over a few meters to tens of meters. Bounding surfaces are typically erosional along bedding soles and gradational bedding tops. The conglomerate is typically massive or crudely stratified with weak normal grading and poorly-sorted pebble- to cobble-sized clasts and rare boulders. Conglomerates are polymictic, comprised of varied proportions of vein-quartz, meta-granitoids and meta-volcanic clasts. The matrix is typically fine- to medium-grained sandstone or, in places, very coarse-grained muddy sandstone. Facies 2A dominates the middle portion of the measured stratigraphic sections along the Hamposia and Chizi River drainages, where facies 2A alternates with thick sandstone units of facies 2C. Scarce paleocurrent indicators suggest flow dominantly towards the north and northwest.

Facies 2A yields rare to abundant vertebrate fossil remains, particularly in the middle to upper portion of the stratigraphy, dominated by microsites and isolated cranial and post-cranial remains, although rare sites with associated bone concentrations also exist (Fig. 6C). The most abundant faunal remains are fish and aquatic vertebrates. Rare bivalves and gastropods are present. No wood or plant remains have been recovered from this facies, or from anywhere in the LLB.

5.3.2 Interpretation: Facies 2A

Based on its coarse-grained nature, poor sorting, erosive basal surfaces, geometry and lateral relationship with facies 2C, and absence of sedimentary structures, facies 2A is interpreted to represent basal lag and gravel bar deposits associated with large braided fluvial channels. This interpretation is consistent with the presence of common freshwater fossils. The intercalation of lenticular conglomerate and sandstone bedforms reflects hydrodynamic changes and lateral migration of channel-margins (e.g., Bridge et al., 2000; Umazamo et al., 2012), consistent with fluvial channel flow on the braidplain environments (Miall, 1996). The recurrence of facies 2A and alternation with sandstone deposits of facies 2C suggests multi-phase channel development.

5.3.3. Facies 2B: tuffaceous conglomerate and sandstone

Facies 2B deposits are typically 3-4 m thick and consist of dominantly matrix-supported tuffaceous conglomerate (Gmv) and volcaniclastic sandstones (Spv, Smv) (tables 1-3; Fig. 5A-C). These facies are best developed along the Hamposia section, between 27 and 31 m above the basal contact with the Red Sandstone Group. The thickness of individual beds of facies 2B ranges from 25 cm to ~2 m. Upper and lower contacts are typically erosional. Tuffaceous conglomerate is typically massive, poorly sorted, and inversely graded. It is composed almost exclusively of pebble- to cobble-sized clasts of mostly reworked tuffaceous mudstone intraclasts and pumice clasts (devitrified now), which are sub-angular to round. Tuffaceous sandstone beds are massive (Smv) to planar cross-bedded (Spv), and composed of medium to coarse and very coarse sand-sized pumice particles and fine ashy matrix, most of which has devitrified into clay, further lithifying these beds.

In many places, tuffaceous sandstone (Spv, Smv) is intercalated and/or interbedded with thin, tabular to lenticular beds of wave and ripple- or horizontally-stratified tuffaceous siltstone (Fcf, Fcvs, Fhvs; Fig. 5C-D). Deposits of this facies have distinctive pinkish gray (5YR 8/1), yellowish gray (5Y 8/1) or very light gray (N8) colours. Paleocurrent data measured on well-exposed tabular cross-stratification reveals northeast paleoflow. Contacts between conglomeratic lower portions of facies 2B and sandy-dominated upper intervals are typically erosional, and commonly marked by discontinuous, thin lenticular beds of calcium carbonate and calcareous nodular sandy concretions. Mud cracks are common in matrix of conglomerate and sandstone, and in the mudstone beds. Similar to FA1, there are no fossils recovered from facies 2B.

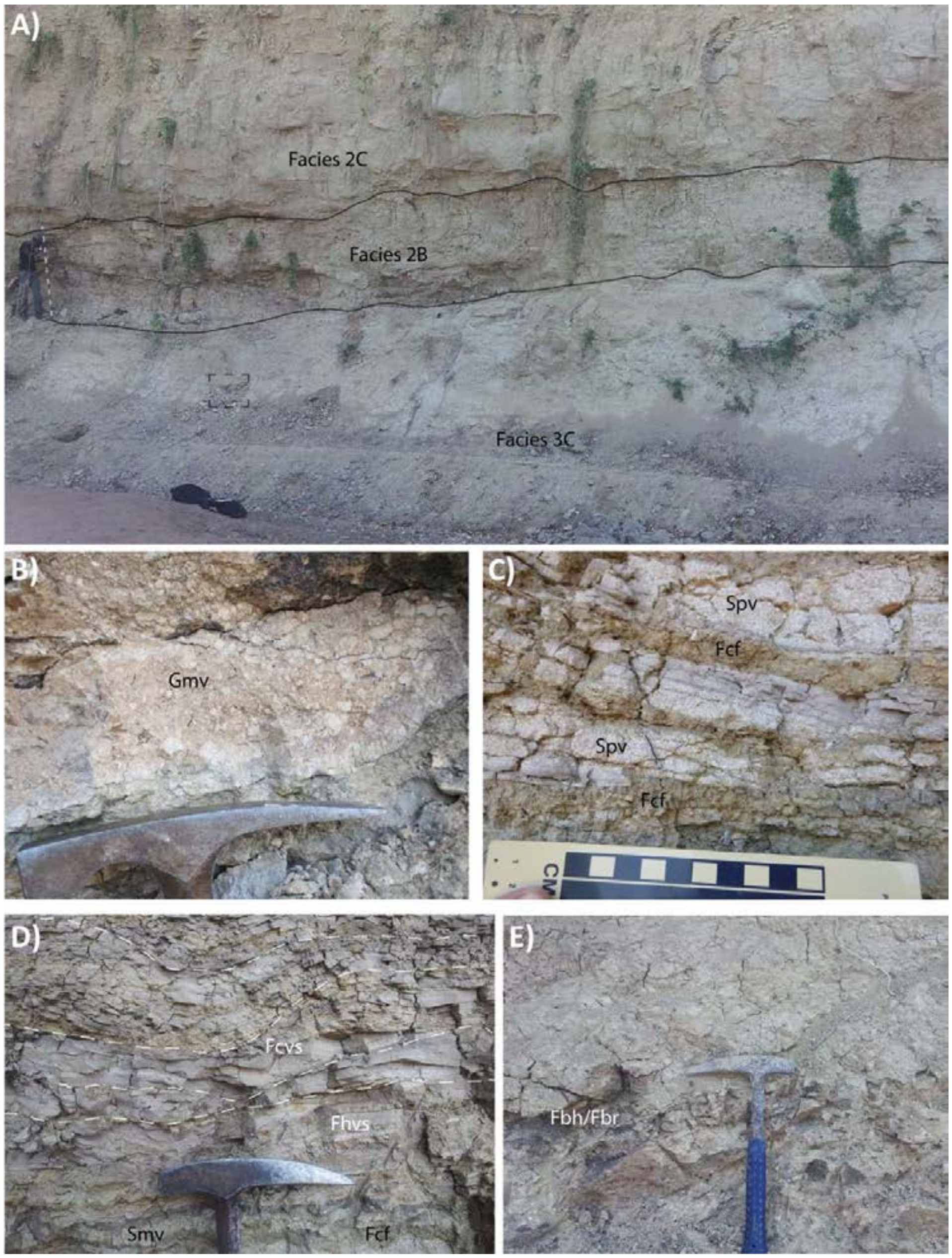

Figure 5. **A)** Outcrop photo of fluvial-floodbasin/lacustrine volcanic and volcaniclastic flow deposits along the Hamposia river drainage, near Mpona village. **B-E)** Close-ups images of: volcaniclastic conglomerate (Gmv; **B**); planar cross-stratified vitric-tuffaceous sandstone (Spv;

C); current-ripple laminated and horizontally-stratified volcanic siltstone (Fcvs, Fhvs; **D**); and horizontal- and ripple-laminated bentonitic sandy mudstone (Fbh, Fbr; **E**).

5.3.4. Interpretation: Facies 2B

Facies 2B is interpreted to represent fluvially reworked pyroclastic deposits. This interpretation is based on the high degree of sediment rounding and the interbedding of coarse-grained tuffaceous sandstone with devitrified ash (bentonite) and bentonitic mudstone deposits (e.g., Bhat et al., 2008). The ash-rich matrix and poorly-sorted nature of the conglomerate is indicative of debris flow-driven sedimentation. The deposition of this basal conglomerate resulted from sediment gravity settle-out during waning flow of a fluvial channel. A number of mechanisms have been put forth by various researchers to explain the reverse grading observed in some pyroclastic fallout and flow deposits (cf. Duffield et al., 1979 and references therein). The most plausible mechanism for the reverse-grading observed in these water-lain coarse pyroclastic deposits is related to clast density during gravity-debris-fallout, where large clasts were partially saturated and sank more slowly than smaller clasts (Sparks and Wilson, 1976). The presence of erosional upper surfaces of conglomeratic units and associated discontinuous carbonate lenses suggest channel abandonment and subaerial exposure. Deposition in the upper (sandstone-mudstone) interval of facies 2B most likely resulted from remobilized pyroclastic flow/fallout deposits from diluted hyperconcentrated fluvial flows (Bhat et al., 2008). The presence of wavy and ripple cross-laminated intervals (Fig. 4D) indicate current and wave-influenced deposition, suggesting sedimentation by subaqueous interfluvial channels or volcanic-clogged subaerial channels. This interpretation is generally supported by preliminary paleocurrent observations that suggest different paleoflows in these deposits. Sandstone units within facies 2B resulted from relatively high-energy traction currents, whereas mudstone units were deposited by suspension settle-out during the waning stages of flows.

5.3.5. Facies 2C: single and multi-storey sandstone bodies

Facies 2C is the most abundant FA in the upper interval of the LLB, and occurs repetitively within the stratigraphic sections along the Hamposia, Chizi and Ikumbi rivers. Facies 2C is defined by up to 7 m thick sequences composed of single or multiple sandstone bedsets of Sm, Smp, Sh and St, locally with gravel lenses (Gcm) (tables 1 and 3; Fig. 6). Individual beds range from 50 cm to ~5 m thick. In most cases, facies 2C is characterized by a basal erosional contact and upward fining coarse- to medium-grained sandstone that is pebbly in places. Top surfaces are gradational to sharp, and are overlain by deposits of facies 3A. Facies 2C is locally eroded by, and overlain by, conglomeratic deposits of facies 2A. In places, individual beds and bedsets are bounded by 5-10 cm thick, discontinuous zones with carbonate concretions. Sandstones range in colour from brown, light brown to light green (see Munsell's rock colour codes in Fig. 3). Locally, facies 2C deposits are interbedded with lenticular, concave-up and laterally discontinuous mudstone beds and devitrified ash deposits of facies 3B.

Sandstone units of facies 2C are typically moderately to poorly sorted, and characterized by sub-angular to sub-rounded grains. Paleocurrent orientations are preliminary due to paucity of field measurements; however, general observations of bedset dip-directions indicate northerly (350-360o) paleoflow. Sandstone is typically quartzo-feldspathic in composition, locally containing isolated calcareous concretions. Facies 2C is fossiliferous, containing abundant fish bones, turtle, crocodilian, and large mammals (Fig. 6C and D) remains.

Figure 6. **A)** Photograph of a fossil-bearing, sand dominated fluvial channel deposits (FA2: Facies 2C) from the Hamposia section. **B-D**) Close-ups images of termite nest trace fossil (**B**), mammal fossils (**C-D**) that occurs in FA2. Note an arrow in figure 6A pointing to a volcanic tuff bed (Hippo Tuff) dated at 3.54 ± 0.13 Ma (Hilbert-Wolf et al., in press).

5.3.6. Interpretation: Facies 2C

Single and multi-story sandstones of facies 2C are interpreted as fluvial channel deposits based upon their erosive basal contacts, textural features (sediment rounding and upward-fining), sedimentary structures and geometry. The typical upward fining trend from coarse-grained pebbly sandstone at the base to fine-grained sandstone at the top reflects typical channel-like vertical sediment accretion, associated with waning flow conditions within the channel. Facies 2C records a range of both normal flow and flood stage stream conditions. Flood stage conditions reflect rapid sediment deposition by gravitation collapse of bedload sediment from a flood-related debris channel flows as suggested by muddy and overall poor sediment sorting as well as thick and generally massive nature of many beds (Miall, 1996). However, in other portions of the stratigraphy, facies 2C more likely records more stable, continuous sedimentation from long lived perennial fluvial channels. The presence of abundant aquatic fauna (e.g., fish, turtles, crocodiles, and hippos) supports this interpretation. The spatial and temporal association of facies 2C with facies 3B and facies 2A deposits reflects subaerial exposure, channel abandonment and subsequent channel reactivation. Paleocurrent data and the association of these tabular and lenticular sandstone deposits with overbank channel-fill related deposits of facies 3B is interpreted to reflect deposition within a braided fluvial channel setting.

5.4. Facies association 3 – flood basin deposits

5.4.1. Facies 3A: calcareous, rooted sandstone and siltstone

Facies 3A is uncommon in the LLB and is characterized by 0.6-4 m thick, massive sandstone, siltstone and mudstone deposits (facies Sm, Fr, Fcf: tables 1-3; Fig. 7A-B). The deposits occur as tabular to lenticular bedsets that are commonly defined by a sharp planar base and variably erosional to gradational top surfaces, upward fining and transitions into overlying mudstone beds. Facies 3A units extend laterally for meters to tens of meters, interfingering with facies 2C. Sandstone units (Sm) are medium- to fine-grained, moderately-sorted and quartzo-feldspathic in composition. Siltstone and mudstone units (facies Fr, Fcf) are commonly interbedded with thin, discontinuous lenses of calcium carbonates. Deposits of facies 3A tend to be heavily bioturbated with abundant calcified rootlets, burrows and nodular calcareous concretions. Rootlets vary in morphology between vertical and horizontal, and range in thickness from mm to few cm in diameter.

5.4.2. Interpretation: Facies 3A

On the basis of lithofacies, geometry, and lateral relationship with major sandstone deposits (facies 2C), facies 3A deposits are interpreted to result from vertical sediment aggradation within a wide floodplain setting (e.g. Michaelsen et al., 2000). The massive nature of the deposits in this FA indicates that primary depositional structures were destroyed due to bioturbation. The presence of calcified rhizoliths and calcium carbonate concretions indicate that vegetation and associated soil development took place in a subaerial setting following deposition. Soil development is interpreted to have taken place in semi-arid climatic conditions, as evident by the presence of calcareous concretions and calcium carbonate lenses interbedded with mudstone facies in the upper parts of this facies.

5.4.3. Facies 3B: lenticular, concave-up mudstone and claystone

This FA is composed of 0.8 to ~1 m thick, lenticular units of claystone and mudstone (Fcf and Fl) that are locally interbedded with thin (<20 cm) siltstone beds (Fl) (tables 1, 3; Fig. 7C-D). These deposits are characterized by erosive, concave-up lower bounding surfaces and typically sharp upper contacts. Deposits of this facies occur in erosional scours that are most typically found above thick sandstone deposits of facies 2C. Individual beds in this FA range from 10-60 cm in thickness. Mudstone and claystone units are commonly moderate brown (5YR 4/4) or grayish red (10R 4/2). Claystone beds of this FA are typically brown in colour and massive, whereas the siltstone units are finely-laminated and locally contain isolated calcium carbonate concretions.

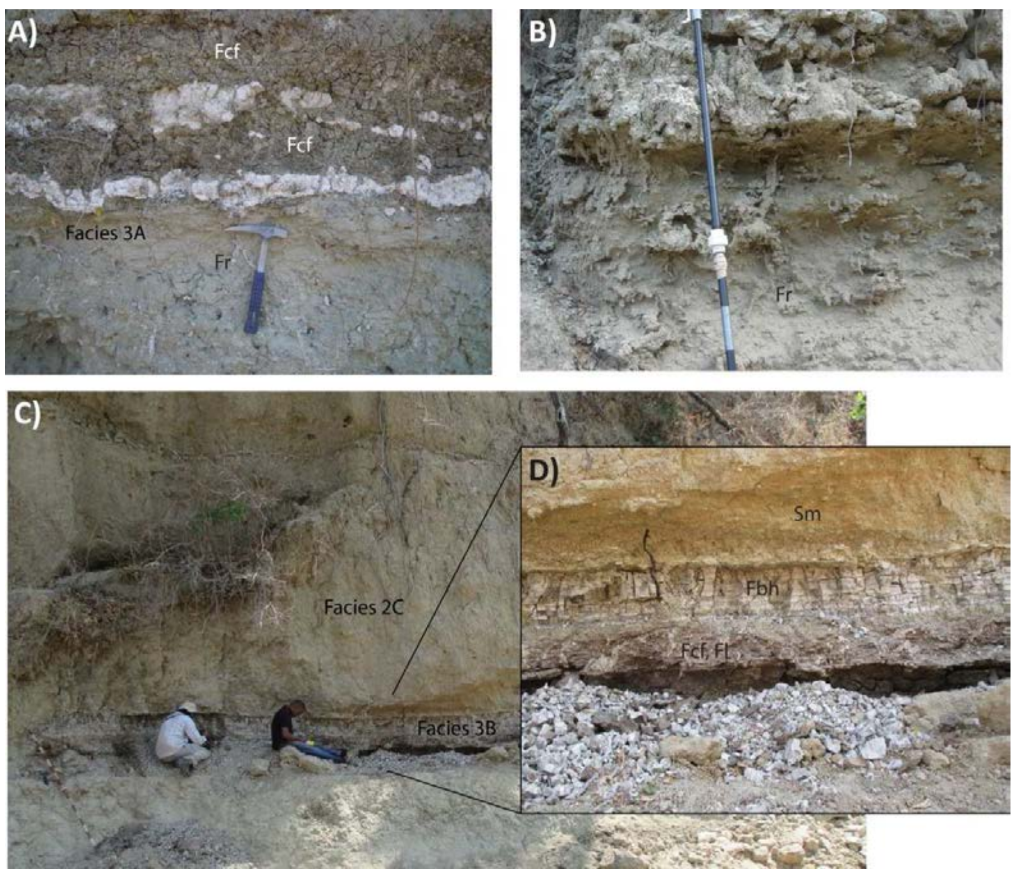

Figure 7. Lower Lake Beds fine-grained facies. **A-B)** Calcareous, rooted sandstone, siltstone and mudstone (Facies 3A: Sm, Fr, Fcf facies). **C)** Lenticular, concave-up mudstone and claystone deposits (Facies 3B) interbedded with sandstone deposits of Facies 2C. **D)** Close-up images of Facies 3B; massive, finely-laminated mudstone and claystone (Fcf, Fl facies).

5.4.4. Interpretation: Facies 3B

Facies 3B is interpreted to record low-energy, abandoned channel-fill deposition by suspension settling out of fine-grain sediments. This interpretation is mainly based on the fine-grained texture and concave-up geometry, as well as their spatial relationship with sandstone deposits of facies 2C. The presence of calcareous concretions in some intervals of this FA is interpreted to indicate periodic subaerial exposure and development of horizonated paleosols.

5.4.5. Facies 3C: bentonitic mudstone, bentonite and unweathered volcanic ash

This facies association is well-developed in the lower portion of the LLB and is less common stratigraphically up-section. Deposits of facies 3C form up to 4 m thick sheet-like packages of bentonitic mudstone, pure bentonites and unweathered ash beds (Fbh, Fbr, Fhvs; Table 1, 3; Fig. 5A, E), which are apparently laterally extensive. These mudstone units tend to be quite sandy and are dominantly composed of devitrified fine-grained ash and sub-rounded to well-rounded, silty- to very fine sand-sized pumice grains. They range in colour from pinkish gray (5YR 8/1), to yellowish gray (5Y 8/1) to very light gray (N8). Basal surfaces are poorly-exposed, but appear to exhibit concave-up geometry. The upper contact of this FA typically displays erosional scour from above (typically by FA 4). Individual beds of facies 3C range from 20 cm to 1.5 m, and include alternating parallel- and asymmetric ripple cross-laminated intervals. The lower interval of this FA appears to be massive and bioturbated. Intercalations of thin, lenticular, fine-grained sandstone (Sh) were observed near the upper limit of this FA.

5.4.6. Interpretation: Facies 3C

Based on the fine-grained size, thinly-laminated nature, geometry, and lateral extent, facies 3C is interpreted to record low-energy sedimentation within subaqueous flood basin ponds or small lakes (e.g., Talbot and Allen, 1996; Leleu et al., 2009; Umazamo et al., 2012). Textural features such as a high degree of rounding of individual silt- to fine-sand grains suggest sediment derivation from fluvial-reworked pyroclastic deposits in the hinterlands (e.g., Cas and Wright, 1987; Nichols and Fisher, 2007; Bhat et al., 2008). Horizontally laminated beds (facies Fbh) were deposited by sediment settling from suspension. Ripple cross-laminated intervals of facies 3C suggests deposition from land-generated unidirectional and/or subaqueous current flows (e.g., Zavala et al., 2006, 2011; Cuitino and Scasso, 2013). The deposits record a shallowing-upward trend, as demonstrated by overall coarsening upwards of this FA and intercalations of thin lenticular sandstone beds towards the upper limit of facies 3C, as well as spatial and temporal relationship with the overlying tuffaceous conglomerate deposits of facies 2B.

6. Sedimentary Petrology

6.1. Conglomerate lithoclast composition

Pebble-counting was performed on five conglomerate beds (samples CC1 to CC5; Figs. 3, 8), where all clasts >2cm in diameter were counted within a 50 cm^2 grid over each bed. The lithoclast compositions were grouped into five distinctive lithologic categories: pumice, vein quartz, granitic gneiss, meta-volcanics, foliated- and unfoliated metamorphic clasts.

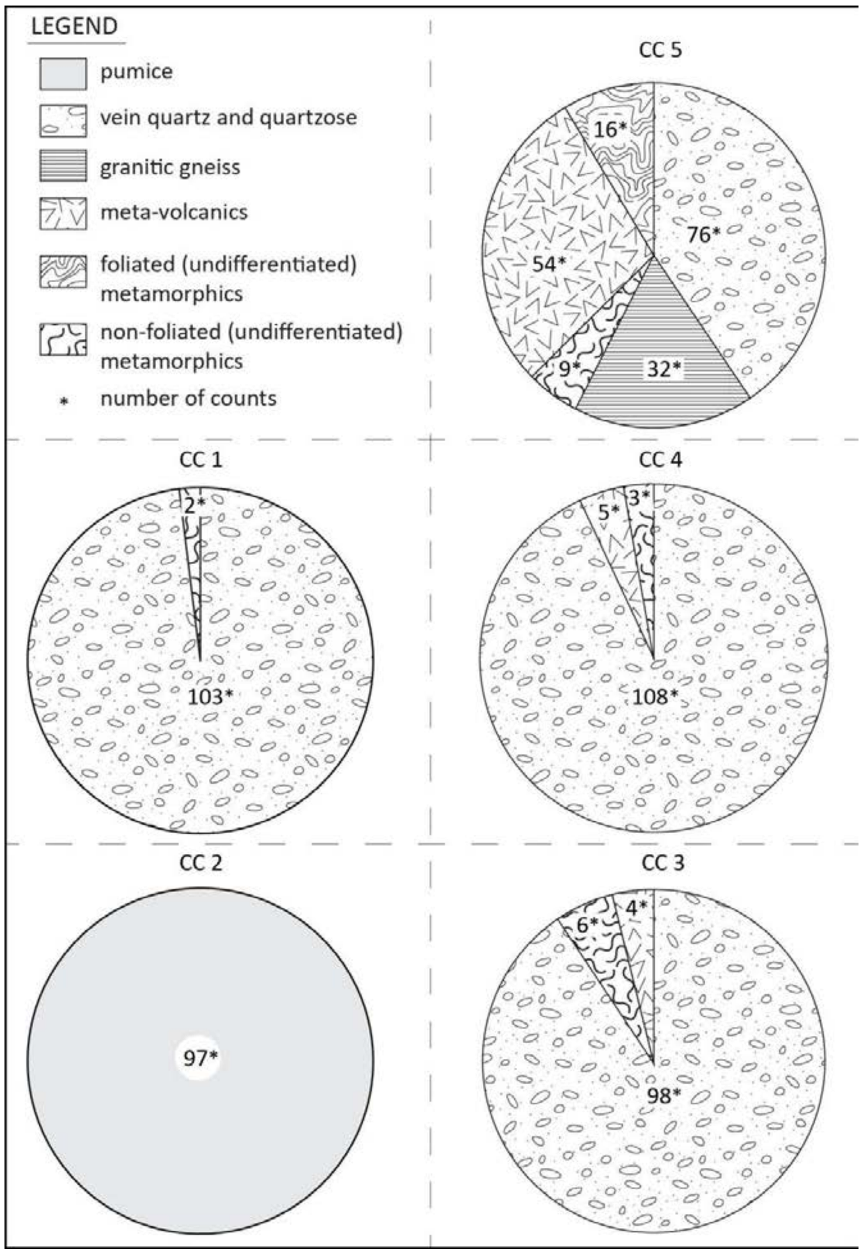

Figure 8. Conglomerate pebble count results (CC1-CC5) for the LLB.

The results show a major compositional shift mid-way through the stratigraphy that corresponds with the presence of a major erosional unconformity and calcrete horizon at ~45-48 m above the basal contact (Fig. 3). Below this horizon, siliciclastic conglomerate beds are dominated by vein-quartz clasts as demonstrated by clast-count samples CC1, CC3, and CC4. Statistically, lithoclast composition in the conglomerate beds of this lower interval shows that vein-quartz pebbles and cobbles make up 93-98% of the total counts, whereas the other 2-7% is composed of non-foliated metamorphic clasts. In contrast, above the unconformity, conglomerates beds are typically polymictic in composition. Although only one sample was counted formally (sample CC5: Fig. 8), visual inspection of conglomerate clast composition in the field and through analysis of field photographs indicate that other conglomerate units above the unconformity, which were difficult to access, differ significantly in composition from those below this surface. The clast composition of sample CC5 is as follows: vein quartz and quartzite (~41%), meta-volcanic (~29%), granitic gneiss (17%), foliated metamorphic (6%) and non-foliated metamorphic (6%).

Besides the variation in siliciclastic conglomerate provenance between the lower and upper portions of the strata, the LLB succession is also characterized by volcaniclastic provenance variation across the stratigraphy. The lower stratigraphic interval contains volcaniclastic (tuffaceous) conglomerate deposits along with associated tuffaceous sandstone, vitric ash and bentonitic mudstones (Facies 2B). The tuffaceous conglomerate, which occur as a single bed and represented by sample CC2, is 100% pumice pebbles and cobbles that are cemented by a tuffaceous matrix, vitric ash and sandy to silt-sized pumice (Fig. 3, 5B, 8). Whereas the tuffaceous conglomerate bed is limited to this lower portion of the stratigraphy, the associated volcanic and volcaniclastic deposits decrease dramatically up-section, above the unconformity surface.

6.2. Sandstone petrology

Sandstone compositions in the LLB from the Hamposia River section vary between volcaniclastic and siliciclastic end members (Fig. 3 and 9). Volcaniclastic sandstones are less common, and occur as thin tabular or lenticular beds of pumice tuff (tuffaceous sandstone facies: facies 2B) that are limited to the lower part of the section. Siliciclastic sandstone compositions dominate the middle to upper part of the stratigraphic succession, and are associated with fluvial channel deposits (FA 2: facies 2C). Because of the very poorly indurated nature of the sandstones in the LLB, only a small suite of thin sections were made. Hence, the sandstone petrology must be considered preliminary and is largely based on hand sample description and analysis of five representative thin sections of the siliciclastic sandstone units, collected from across the stratigraphic section. A clear bias to this study has been the challenge of constructing quality thin sections of the volcaniclastic sandstone lithofacies, which are clay-rich and poorly cemented. Impregnation was devised to overcome this, but didn't help produce enough thin section samples as most of the samples continually polished to nothing, only leaving a few grains in the center to examine. However, volcaniclastic composition of these sandstone units is clear in limited thin sections and hand samples, and careful field observations confirm that this petrofacies is almost exclusively confined to the lower part of the LLB.

Siliciclastic petrofacies: On a Qt-F-L diagram (Fig. 9E), all thin-sectioned samples plot in the subarkose field. The results show that total quartz (including monocrystalline plus polycrystalline quartz) ranges from 75-81%; total feldspar (alkali and plagioclase) ranges between 12 and 23%; and total lithics range between 3-7%. The quartz grains exhibit both straight extinction and undulatory extinction. In all samples, monocrystalline quartz is dominant (66-89%) over polycrystalline quartz (11-33%). Plagioclase (constituting 7-17%; average 13%) dominates over potassium feldspars (3-9%; average 6%). Both plagioclase and potassium feldspar grains are mostly fresh, although there is a small component that does exhibit minor chemical alteration. These grains are primarily replaced by hematite along the edges. Lithics are dominated by metamorphic rock fragments (granitic gneiss and unfoliated meta-granitoids). Accessory minerals represent a few percent of the total grain fraction and include dense minerals (dominantly magnetite and garnet) and mica. Matrix varies from 4-10%, and porosity ranges between 6% and 10%. Cement varies between 8% and 18%, and is dominantly authigenic clays and hematite. Although the analyzed sandstone samples contain 8-18% cement, most sandstone units are less well cemented and moderately indurated.

Volcaniclastic petrofacies: As noted above, the volcaniclastic sandstone lithofacies produced few usable thin sections. However, it is clear that these samples range from nearly purely volcanic in nature to highly reworked with a large quartzose sand composition. Qualitative observations of thin-sectioned representative samples (Fig. 9F-G) reveals that volcaniclastic sandstone comprises dominantly pyroclastic material, most of which has weathered to clay minerals. However, relic pumice fragments are the most commonly observed framework grains and ranges from silt- to very coarse-grained sand sized. The second most abundant clast type are what appear to be lithic volcanic or volcaniclastic fragments composed of reworked volcanic siltstone and welded tuff fragments (Fig. 9F). Quartz and feldspar grains are locally abundant, and range from silt to fine grained-sand sized (Fig. 9G). Heavy minerals (mostly magnetite) and mica constitute minor proportions.

Volcaniclastic sandstone lithofacies are almost exclusively observed in the field in the lower part of the LLB, between the 23 and 31 meter levels. A shift is observed in the siliciclastic conglomerate and sandstone petrology at the major erosional unconformity at 48 m level (Fig. 3). Below the boundary, in the volcaniclastic dominated succession, the siliciclastic sandstone lithofacies are typically quartzose at the base, and become more quartzo-feldspathic stratigraphically up-section, particularly above the boundary. Basal quartzose sandstone beds are whitish or very light gray (N8) in color, whereas quartzo-feldspathic sandstone varies between brownish (pale yellowish brown, 10YR 6/2 to grayish orange pink, 5YR 7/2) and greenish (greenish gray, 5GY 6/1 to grayish yellow green, 5GY 7/2). This compositional change, which is readily observable in the field, can also be depicted from the petrographically analysed samples. Despite the fact that all samples plot on subarkose field on a Qt-F-L diagram, one sample collected from the lower interval (volcaniclastic interval), just below the unconformity surface, shows slightly higher abundance of quartz grains than the other samples collected above this horizon.

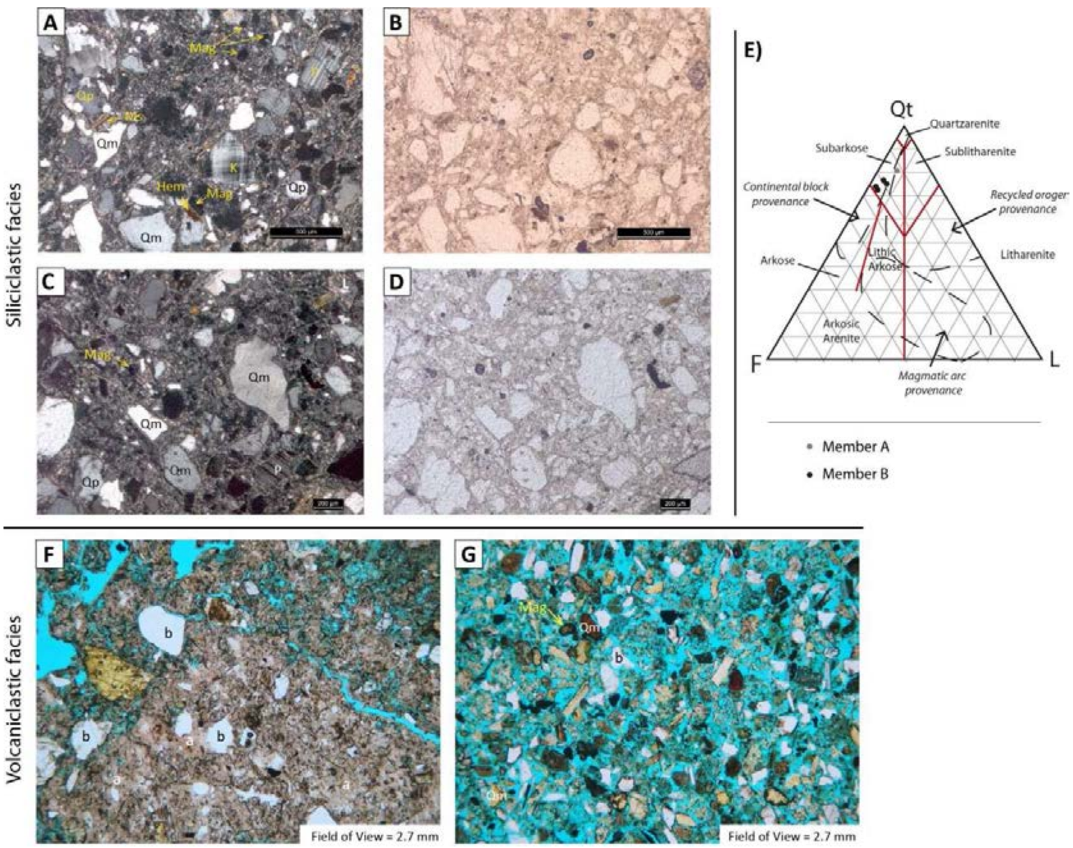

Figure 9. Photomicrographs of the representative sandstone facies: microscopically-analyzed siliciclastic sandstone at crossed polarized **(A, C)** and plane polarized **(B, D)** light, with sandstone point count data plotted **(E)** (sandstone classification after Pettijohn et al., 1987); tuffaceous sandstone facies in plane polarized light **(F, G)**, comprising dominantly volcanic glass (a) and pumice grains (b).

7. Faunal overview

Both members of the LLB strata preserve fossils, however, only fragmentary vertebrate specimens have been recovered from Member A. Member B is highly fossiliferous, with a total of 44 fossil specimens recovered as part of geological reconnaissance efforts in the (seven) most productive localities. Identifiable specimens (n = 29) are dominated by fishes (62%) and large crocodylians (21%), with smaller numbers of large bodied mammals (10%), turtles (3%) and mollusks (3%) (Fig. 10). Specimens range in size from <2 mm to over 60 cm in length. A detailed faunal description of the LLB materials is underway (N. Stevens, pers. comm.). Discoveries to date appear consistent with a marginal wetland located within a seasonally arid environment. This interpretation is supported by the predominance of aquatic taxa in the preserved fauna (N. Stevens, pers. comm.), coupled with sedimentary evidence for sedimentary evidence of fluctuation in fluvial discharge in the channels, and evidence of periodic or possibly seasonal aridity in the floodplain (i.e., calcic paleosols).

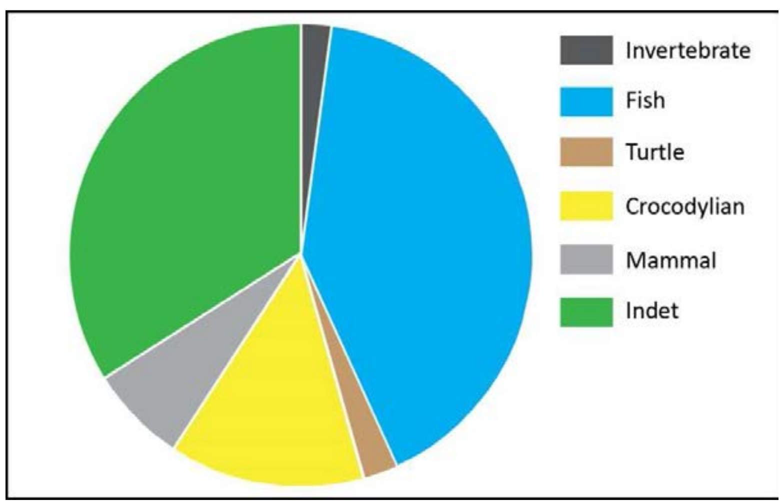

Figure 10. Faunal composition based on fossils from Member B.

8. Sequence stratigraphic framework

We identify depositional sequences in the lower Lake Beds succession following a model-independent approach to sequence stratigraphy proposed by Catuneanu et al. (2011). In this study, a 156-m-thick stratigraphic section was measured along the western margin of the Rukwa Rift through the Hamposia River drainage (Fig. 2, 3). This section preserves two distinctive depositional sequences in the lower Lake Beds succession in the RRB, which correspond closely with lithostratigraphic subidivisions (members A and B) defined for lower Lake Beds (Fig. 11). Vertical stratal stacking patterns of the two sequences, termed Sequence I and Sequence II, reflect: 1) the transition of depositional environments from alluvial/fluvial-lacustrine to fluvial-floodplain dominated; 2) a shift in sedimentary provenance from volcaniclastic- to siliciclastic-dominated intervals; and 3) an apparent transition between sub-humid and semi-arid climatic conditions. Suggested climate changes are based on sandstone composition shifts from dominantly quartzose in Sequence I, to quartzo-feldspathic in Sequence II (cf. Roller et al., 2010), and a distinct increase in the presence and abundance of well-developed paleosols between the two sequences. A sequence bounding erosional unconformity (SB) is placed at the 48 m level in the Hamposia section, which clearly defines the contact between sequences I and II (Fig. 3, 11). We integrate the sedimentology and sedimentary petrology reported above, coupled with newly reported radioisotopic ages for the LLB (Hilbert-Wolf et al., in press), evidence for the timing and intensity of volcanism in the Rungwe Volcanic Province (Ebinger et al., 1989, 1993; Fontijn et al., 2012), and late Miocene to Pleistocene climate records for eastern Africa (deMenocal, 1995, 2004; Trauth, 2007; Roller et al., 2010) to understand and interpret controls on sedimentation in these two sequences.

8.1. Sequence I

Hilbert-Wolf et al. (in press) applied U-Pb geochronology to date two tuffs in the LLB, indicating that sequence I was deposited during the late Miocene, commencing by *ca* 8.7 ± 0.06 Ma. Sequence I represent the lower 48 m thick stratigraphic interval of the LLB, and corresponds to lithostratigraphic member A (Figs. 3, 11). It is interpreted as an aggradational parasequence set of alluvial-fluvial (FAs 1 and 2) and lacustrine/floodbasin (Facies 3C) deposits that represent lowstand and highstand systems tracts, respectively. Sequence I is characterized by a basal low accommodation alluvial fan system that rapidly transitioned up section into a shallow, volcanically influenced lacustrine system with associated fluvial-deltaic deposition. This sequence most likely developed as a result of renewed rifting and increasing generation of accommodation space and increased sediment supply during the initiation of the Rungwe Volcanics. Facies stacking patterns support this concept. However, the basal ~3-23 m of this sequence is distinctly different from that of the rest of the sequence, dominated by a super-mature quartzose conglomerate reminiscent of the base of the Nsungwe Formation (basal few meters of the Utengule Member; Roberts et al., 2010). Roberts et al. (2012) interpreted the super-mature quartzose composition of the base of the Nsungwe Formation to reflect a major fluvial pediment surface associated with regional uplift during the initial development of the African Superswell. These workers documented a shift in detrital zircon provenance patterns, briefly reflecting a shift southward to northward provenance and paleoflow conditions. No such detrital zircon provenance patterns are recorded for this interval, but the similarity between the base of the Nsungwe and the base of the sequence I of the LLB is distinctive and is interpreted to represent a similar fluvial pediment surface associated with initiation of the LLB and reactivation of the rift system. This basal, super-mature quartzose interval of Sequence I is interpreted to represent a low-accommodation lowstand systems tract (LST) that developed as a result of initial reactivation of the Rukwa Rift around 8.7 Ma (Hilbert-Wolf et al., in press). These quartzose siliciclastic deposits are most likely sourced from quartz vein/pegmatitic, granitic and meta-granitoid terranes of the Archean Tanzanian Craton and Paleoproterozoic Ubendian belt (Quennell, 1956; Quennell et al., 1956; Daly et al., 1985), and probably partly recycling of the underlying Cretaceous RSG (Roberts et al., 2004, 2010). These deposits are capped by a calcareous paleosol horizon, which is more exposed in the basal LLB section along the Chizi River drainage (Fig. 2B). This distinctive paleosol horizon is interpreted to indicate subaerial exposure (cf. Scott and Smith, 2015) prior to rapid generation of accommodation and subsequent transition to a transgressive lacustrine/flood basin depositional system. This transition is also associated with a provenance shift from super mature quartzose conglomerate to immature volcaniclastic sandstones and siltstones. The sedimentary provenance shift and the deposition of primary and reworked pyroclastic deposits (FA2: facies 2B; and FA3: facies 3C) is associated with the first stage of late Cenozoic volcanism in the Rungwe Volcanic Province, between 9.2 and 5.4 Ma (Ebinger et al., 1989, 1993; Fontijn et al., 2012; Hilbert-Wolf et al., in press). A well-developed calcic paleosol caps the top of Sequence I.

The initial phase of super-mature alluvial sedimentation (LST) is envisaged to have developed as a result of uplift, weathering and erosion along the faulted basin margins during the opening phase of basin reactivation. This most likely resulted in pediment development prior to initiation of the Neogene EARS rifting cycle in the Western Branch (Ebinger, 1989; Ebinger et al., 1989). The transition from a fluvial pediment at the base of the sequence to a mosaic of small lakes and wetlands rimmed by proximal fluvial-deltaic channels (Facies 3C: ~23-27 m stratigraphic interval; Fig. 3, 11) is interpreted to have resulted from an increase in the generation of accommodation space as rifting continued, contemporaneously with the initiation of the Rungwe Volcanic Province (Ebinger et al., 1989, 1993). A strong link to the initiation of the Rungwe volcanics is supported by the rapid influx of primary ash falls/flows and fluvially reworked (secondary) pyroclastic materials in this sequence. U-Pb dating of several of the volcanic tuffs in the LLB suggests a late Miocene age (8.7 ± 0.06 Ma) for the initiation of both volcanism and sedimentation in the RRB (Hilbert-Wolf et al., in press), which is consistent with the age of the oldest volcanics dated in the Rungwe Volcanic Province by Ebinger (1989) and Ebinger et al. (1989). The uppermost portion of this sequence suggests decreasing volcanic input and transition to siliciclastic sand-dominated channel systems, suggesting a decrease of accommodation space in the basin. This is interpreted to indicate rapid filling of available accommodation space, followed by slow generation of accommodation and reduced sediment supply, perhaps associated with a period both volcanic and tectonic quiescence.

8.2. Sequence II

Sequence II is ~108 m thick and is characterized by fluvial channel-dominated deposits. Sequence II is interpreted to represent a regressive or lowstand system tract (LST) associated with a transition from a lacustrine to fluvial depositional system. Preliminary geochronologic and biostratigraphic data suggest that the deposition of Sequence II was initiated in the Pliocene (~4-3.5 Ma; Hilbert-Wolf et al., in press). Sedimentation may have continued into the Pleistocene; however no upper age brackets have been established for the top of this sequence. Channel deposits (FA2: facies 2A, 2C) in this sequence indicate a transition from high-energy, gravel-bed braided river systems to sandy braided river systems (Figs. 3 and 5). Floodplain deposits (FA3: facies 3A) are abundantly preserved and are characterized by well-developed paleosol horizons. Volcanic and volcaniclastic deposits are considerably less abundant in this sequence, and are limited to relatively thin beds of vitric tuff. The deposition of these volcaniclastic facies is associated with the second stage of late Cenozoic volcanism in the nearby Rungwe Volcanic Province that is constrained between 3 and 1.6 Ma (Ebinger et al., 1989, 1993; Fontijn et al., 2012). However, U-Pb ages obtained from these tuff beds (Hilbert-Wolf et al., in press) suggests that the second phase of volcanism in the Rungwe Province most likely extended back to ~4-3.5 Ma.

Sequence II is interpreted to have developed as a result of slow, but continuous generation of accommodation space that exceeded the rate of water and sediment infill. The generation of accommodation space in the basin is interpreted to have resulted from renewed rifting during the Pliocene-Pleistocene, which is associated with second episode of explosive volcanism in the RVP (Ebinger et al., 1989, 1993; Fontijn et al., 2012). This interpretation is also supported by cosmopolitan composition of siliciclastic sandstones and significant input of meta-volcanic and meta-granitoid clasts in conglomerate deposits of this sequence, suggesting unroofing (uplift, weathering and erosion) of metamorphic rocks along the rift flanks. The latter are most likely associated with the Paleoproterozoic Ubendian Belt (Daly et al., 1985). Base level fall and subsequent development of calcareous paleosol horizons, in addition to a relatively higher abundance of feldspars in siliciclastic sandstone of this sequence suggest generally arid climatic conditions during the deposition of this sequence, which is consistent with regional aridification trends reported elsewhere in eastern Africa during this time (e.g. deMenocal, 1995, 2004; Trauth, 2007; Roller et al., 2010).

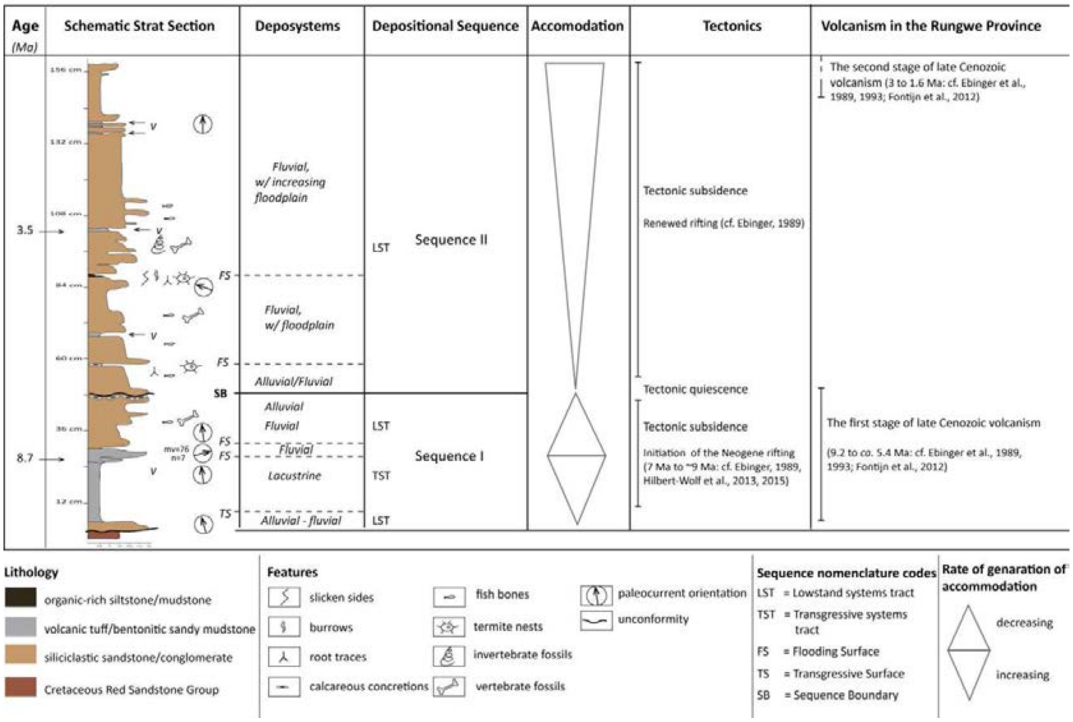

Figure 11. Schematic stratigraphic section of the lower Lake Beds with sequence stratigraphic interpretations and inferred controls on sedimentation. Note, depositional sequences correspond directly with informal lithostratigraphic members A and B in figure 3.

9. Conclusions

We describe a newly discovered Miocene to Pliocene succession in the Rukwa Rift Basin of southwestern Tanzania, herein informally referred to as the lower Lake Beds. A detailed investigation of the stratigraphy and sedimentology of the deposits was conducted along the Hamposia River and other nearby drainages. Fourteen lithofacies were identified and categorized into seven genetically-related facies associations (FAs). A synthesis of vertical stacking patterns and lateral relationships of facies associations, along with sedimentary petrology and vertebrate fossil remains leads to a recognition of three main deposition environments: (1) alluvial environments, (2) fluvial channel environments, and (3) flood-basin environments, characterized by volcanic-filled lakes and ponds, abandoned channel-fills and floodplains. Petrologic investigations reveal a shift between volcaniclastic and siliciclastic provenence in the lower portion of stratigraphy, to siliciclastic sandstones and polymictic conglomerates in the upper interval. This provides the basis for informally subdividing the succession into a volcaniclastic-dominated lower member A, and an overlying, siliciclastic dominated member B. Establishment of a formal stratigraphic subdivision and nomenclature for the Lake Beds Succession awaits further exploration across the basin to determine outcrop extent of the lower Lake Beds Succession, and a better outcrop-based and subsurface dating of these units.

Acknowledgements

We thank the Tanzania Petroleum Development Corporation (TPDC) and Heritage Oil Rukwa Tanzania Ltd. for providing a PhD bursary to the lead author (CM) and funding to conduct fieldwork in the Rukwa Rift Basin. This research was also supported by the US National Science Foundation (EAR_1349825, BCS_1127164), the National Geographic Society (CRE), and the post-graduate research fund from James Cook University. We are indebted to the staff of Heritage Oil Rukwa Tanzania Ltd in the Dar es Salaam office for support in the fieldwork logistics. We thank N. Boniface, J. Edmund, Z. Jinnah, and the Rukwa Rift Basin Project team members for their field assistance and valuable discussions. And lastly but not least, we are grateful to the Editor D. Delvaux and reviewers (including A. Cohen and R. Tucker) for constructive feedback that improved the manuscript.

Chapter 3

Preliminary sedimentology and stratigraphy of the enigmatic middle Lake Beds succession (Pleistocene?) in the Rukwa Rift Basin, Tanzania

Keywords: Facies Analysis; Pleistocene; Rukwa Rift Basin

ABSTRACT

This chapter builds upon detailed sedimentologic and stratigraphic analyses of the upper and lower portions of the Lake Beds succession by providing a preliminary overview of a series of isolated, enigmatic deposits exposed across the southern Rukwa Rift Basin, informally termed the middle Lake Beds. The middle Lake Beds are characterised herein as a series of isolated outcrop exposures with uncertain age relationships, but occurs stratigraphically between the lower and upper Lake beds units, and can be divided into five different lithostratigraphic units or informal members. The middle Lake Beds units include at least 36 m-thick lacustrine (limestone) unit (member A), which is sharply overlain by a thin (< 15 m-thick) volcaniclastics succession of alluvial sandstones, siltstones, mudstones and thin conglomerates (member B). These two members crop out in the Magogo area, and are lithologically distinct from other middle Lake Beds units in the basin. Members C and D are identified further to the south, in the Songwe Valley, where a series of faulted well-sorted siliciclastic fluvial sandstones (member C) crops out around the vicinity of the Mbeya Cement Company, as well as to the east of the cement quarry. Two maximum age constraining detrital zircons from this unit yielded Middle Pleistocene ages (~1-2 Ma), consistent with assertions that this unit lies stratigraphically between the lower and upper Lake Beds sequences. Nearby, along the Ikumbi River, several kilometers to the east of the Cement Quarry, tuffaceous/ash-rich siliciclastics fluvial sandstones and conglomerates are exposed in a series of river cuts. These deposits may represent a lateral facies relationship with member C; however, because of their distinctive volcanic provenance and significantly coarser grain-sizes, they are presently assigned a new member (member D). A final thin lacustrine volcaniclastics siltstone unit, termed member E, preserving beautiful leave macrofossils was documented in the far south of the basin, near Tukuyu. This thin stratigraphic unit is situated between two basalt flows, with the overlying flow dated (via Ar/Ar) at ~500 ka.

Facies analysis reveals that the middle Lake Beds units were deposited within a complex array of depositional environments, ranging from alluvial fan and fluvial channels, floodplains to shallow lakes. The observed lithological variability in facies across the middle Lake Beds strata suggests that deposition was most likely transpired during tectonically active periods, at times contemporaneously with explosive and effusive volcanism associated with the Rungwe Volcanic Province. Although most deposits can be confidently placed between the lower and upper Lake Beds, the relative stratigraphic placement of these informal members, relative to one another is based on preliminary mapping and limited geochronologic data. Due to the limited and poor exposure of these deposits across the basin, the stratigraphy presented here must be considered preliminary until more extensive investigations of these enigmatic deposits can be conducted, which will require a significant amount of additional fieldwork, including exploration across new portions of the basin and dating.

1. Introduction

The late Cenozoic Lake Beds succession of the Rukwa Rift Basin (RRB) was deposited in response to modern tectonic development of the East African Rift System (EARS) (Ebinger et al., 1989; Wescott et al., 1991; Mtelela et al., in review), yet it represents the least studied and youngest tectono-sedimentary unit in the basin. Rifting history in the RRB goes back to late Carboniferous-Permian, and was initiated due to reactivation of Paleoproterozoic-Neoproterozoic Ubendian shear zones (Theunissen et al., 1996). There is a consensus that the Rukwa Rift opened in a general E-W direction, sub-orthogonal to the NW-SE rift trend of normal faulting regime (Ebinger 1989; Morley et al., 1990; Delvaux et al., 2012). The Rukwa Rift has undergone at least three other tectonic rifting episodes preceding the late Cenozoic East Africa rift event, including: a Permo-Triassic event that deposited Karoo Supergroup (Kilembe and Rosendahl, 1992; Morley et al., 1999); and a Cretaceous and late Oligocene rifting events that deposited the Red Sandstone Group, Galula and Nsungwe formations, respectively (Roberts et al., 2004, 2010, 2012). Geologic studies and seismic profiles reveal that the RRB has half-graben geometry, with sedimentary strata thickening north-easterly towards the depocenters and the main border fault (Lupa Fault) located in the eastern margin of the basin (Pierce and Lipkov, 1988; Kilembe and Rosendahl, 1992; Morley et al., 1992, 1999, 2000). The western margin of the rift is characterized by uplifted Ufipa Block, along with a series of active fault lines including the Kalambo, Kanda, Songwe and Mbeya faults (Fig. 1; Delvaux et al., 1998, 2012), where active erosion occurs, and a large part of paleo- and modern fluvial systems originate from (see Chapter 1 and 2: Mtelela et al., in press, in review).

The Lake Beds succession unconformably overlies the older Cretaceous Galula Formation or the late Oligocene Nsungwe Formation, and in places it rests directly above Permo-Triassic Karoo rocks (Fig. 1; Roberts et al., 2004, 2010, 2012). The Lake Beds were first mentioned by Grantham et al. (1958) during regional geologic mapping of the southern part of the rift, in which they described conglomerate, sandstone and mudrocks associated with fluvial, floodplain and lacustrine environments. Since then, the Lake Beds have received very little geologic attention until very recently; when Cohen et al., (2013) began work on invertebrate biostratigraphy, and members of our team (Rukwa Rift Basin Project) began conducting extensive geologic mapping, sedimentology and geochronologic investigations of the Lake Beds succession (Hilbert-Wolf and Roberts, 2015; Hilbert-Wolf et al., in press; Mtelela et al., in press, in review). Indeed, the understanding of the sedimentology and stratigraphy of the Lake Beds succession has evolved considerably since the beginning of this project, and has resulted in: (1) identification and sedimentologic description of at least three major depositional successions, termed the upper, middle (focus of this chapter), and lower lake beds; (2)

improved chronostratigraphy of these units; (3) refined understanding of the timing and relationships between sedimentation and climate, tectonics and volcanism; and (4) discovery of a series of important and previously unknown Miocene-Pleistocene vertebrate fossil localities in the East African Rift System.

The lower Lake Beds succession crops out along the uplifted western margin of the rift (Fig 1; see also Chapter 2), where a well-developed angular unconformity can be observed between it and the Red Sandstone Group. Hilbert-Wolf et al. (in press) dated a basal ashbed from this unit, confirming a late Miocene age for the lower Lake Beds, which is consistent with proposed initiation of the final sedimentary succession in the rift and the initiation of the Rungwe Volcanic Centre (Ebinger 1989; Kilembe and Rosendahl, 1989; Morley et al., 1990, 1999; Delvaux et al., 2012). Grantham et al. (1958), who first mapped the distribution of the Lake Beds strata, appear to have only recognized what we now refer to as the upper Lake Beds, and did not fully appreciate the complexity of this geologic sequence. These workers suggested an informal subdivision of the Lake Beds into lower and upper units, however Mtelela et al. (in press; Chapter 1) demonstrated that this subdivision represented lateral facies changes between the upper Lake Beds, rather than a stratigraphic subdivision. This is a situation that closely mimics the complexity of the Red Sandstone Group in the rift, which was mapped as a single depositional unit and alternatively considered to be Cretaceous or Miocene by various workers. However, more detailed sedimentological investigations by Roberts et al. (2004, 2010, and 2012) demonstrated a more complex depositional history, represented by at least two formations, each with two distinct members, spanning the Cretaceous-Paleogene.

During the course of our extended geologic mapping of the Lake Beds, we repeatedly encountered isolated lithostratigraphic units that looked similar, but different to the lower Lake Beds unit and to parts of the Red Sandstone Group (and distinctly different from the upper Lake Beds). It slowly became clear that these isolated series of small, often fault-bounded units observed in the Magogo area, the Songwe Valley, along the Ikumbi River (Fig. 1), and as far south as the Tukuyu area, could not be linked to any known depositional units in the rift, but were clearly located below the horizontally bedded Upper Lake Beds, and above the lower Lake Beds. The relationship between these units is complex and still poorly understood, however, preliminary radioisotopic dates obtained from detrital zircons and basalt flows capping these deposits (e.g., Tukuyu) indicate that these various units are most likely early to mid-Pleistocene in age. Herein, we use the term middle Lake Beds to refer to this series of previously unmapped stratigraphic units in the rift. The focus of this study is to describe the distribution and sedimentology of these deposits and develop a preliminary, informal lithostratigraphic framework for the middle Lake Beds strata. In addition, facies analysis is utilised to reconstruct the depositional environments associated with each of the informal members of the middle Lake Beds succession.

2. Methods

Geologic mapping of the Lake Beds succession was performed using topographic maps and the Mbeya 244 quarter-degree geologic map of Grantham et al. (1958) as base maps, with GPS set to the Arc 1960 datum. A Jacob's staff, and Brunton compass were used for measurement of stratigraphic sections. Sedimentological analyses of the middle Lake Beds, including palaeocurrent measurements, facies and architectural element analysis followed techniques and methodology outlined in Chapters 1 (Mtelela et al., 2016) and 2. Lithofacies were identified primarily based on textural, composition, and sedimentary structures. Assemblages of genetically-related facies were grouped into distinctive facies associations.

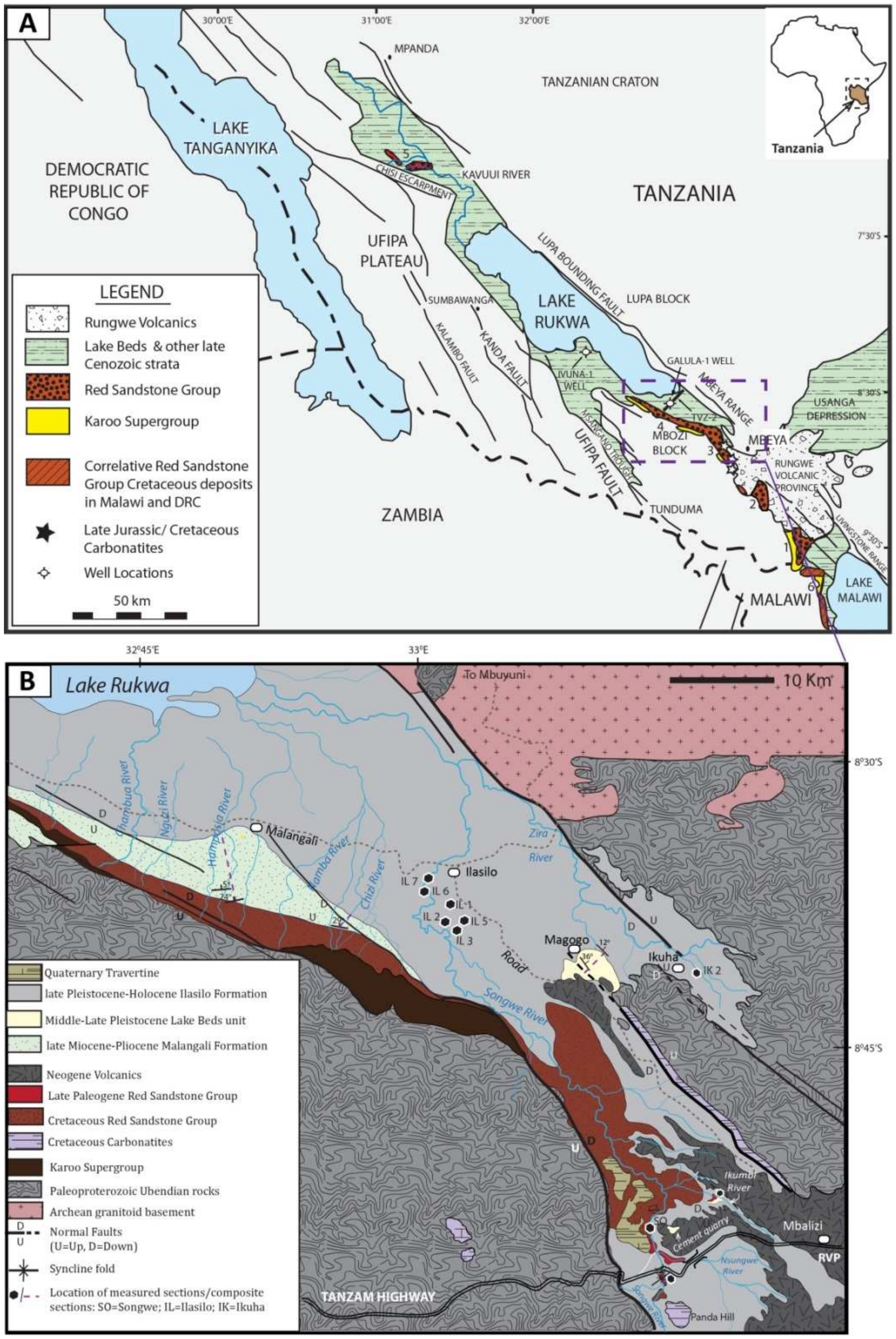

Fig. 1. **A)** Geologic map of the Rukwa Rift Basin showing tectonic elements, distribution of rock units and location of the study area (insert box). **B)** Geologic map of the southern Rukwa Rift Basin (study area), showing the distribution and location of measured section through the lower, middle and upper Lake Beds in the following key areas: (1) Along the Songwe River (Songwe and Ilasilo areas), (2) to the east of the main Songwe River (Cement Quarry and Ikumbi areas); (3) along the Hamposia and Chizi rivers (Malangali area); and (3) in the headwaters and tributaries of the Zira River (Magogo and Ikuha areas). Note that the base map is after Grantham et al. (1958) and Roberts et al. (2010).

3. Distribution of the middle Lake Beds strata

The Lake Beds succession was mapped by Grantham et al. (1958) and subsequent workers, who demonstrated that it covers much of the Rukwa Rift Basin. Recent work by Cohen et al. (2013), and in this project, are largely in agreement with Grantham et al. (1958) that the vast majority of the mapped Lake Beds deposits are late Quaternary, and correspond to what is termed in Chapter 1 as the upper Lake Beds (Ilasillo Formation; see Chapter 4). In contrast, the Miocene to Pliocene (and possibly Pleistocene) lower Lake Beds (Malangali Formation; see Chapter 4) is extremely limited in outcrop distribution, with only two well-exposed outcrop areas (along Chizi and Hamposia River drainages) along the southwestern margin of the rift.

Part of the reason that the middle Lake Beds was the last portion of the Lake Beds stratigraphy to be identified is that it appears to be limited to a series of isolated, typically fault-bounded units that show considerable lithological variability. Middle Lake Beds exposures are currently recognized in the following areas:

3.1. Magogo Area

Along a tributary to the Zira River (Fig. 1), a ~60 m thick, steeply dipping middle Lake Beds section crops out around Magogo area, which is overlain by horizontally bedded upper Lake Beds deposits. Here, two lithostratigraphic units are recognized and assigned to the middle Lake Beds: (1) a lower limestone unit and (2) an upper volcanoclastic sandstone and mudstone dominated unit (Fig. 5). No lower contact is observed, but both units are dipping and appear to represent a continuous stratigraphic sequence with a sharp, unconformable contact between the two units.

3.2. Songwe Valley - Mbeya Cement Quarry

The middle Lake Beds also occur in the Songwe Valley, to the east of the Songwe River within the Mbeya Cement quarry and exposures in the valley directly to the east of the quarry (Fig. 2). In the Mbeya Cement quarry, the Lake Beds are characterized by reddish coloured siliciclastic-dominated sandstones that unconformably overlie a purple and whitish coloured sandstone unit. It is not clear yet whether the latter purple and white sandstone represents the late Oligocene Nsungwe Formation or Cretaceous Galula Formation of the Red Sandstone Group. Indeed around the quarry, the Lake Beds strata resemble the Red Sandstone Group in colour and sedimentologic characteristics. However, two detrital zircon (U-Pb) samples obtained from this section revealed early Pleistocene maximum depositional ages (~ 2 Ma and ~1 Ma grain ages; Hilbert-Wolf, H., pers. Com). This is the only time in which detrital zircons of this age have been found in the Rukwa Rift (Hilbert-Wolf et al., in press), and this strongly suggests that these strata are post-lower Lake Beds, and hence, belong to the enigmatic middle Lake Beds. Much of the sandstone strata across the quarry are affected by normal faulting. The middle Lake Beds unit around the Mbeya Cement quarry are overlain by Quaternary Travertine and horizontally bedded volcaniclastic upper Lake Beds Strata (Fig. 6).

3.3. Ikumbi River

An exposure of possible middle Lake Beds strata is also mapped on the far east side of the Songwe Valley, along the Ikumbi River (Figs. 1 and 2). At the Ikumbi section, the middle Lake Beds strata are at least 20 m thick, and comprise volcanic ash-rich siliciclastic sandstone and conglomerate deposits that unconformably overlie a newly dated exposure of the late Oligocene Nsungwe Formation (Spandler et al., 2016). Both the middle Lake Beds succession and Nsungwe Formation strata are bounded by the Mbeya Fault to the northeast. The middle Lake Beds succession is stratigraphically overlain by distinctive, volcanic-ash rich upper Lake Beds strata along the Ikumbi River.

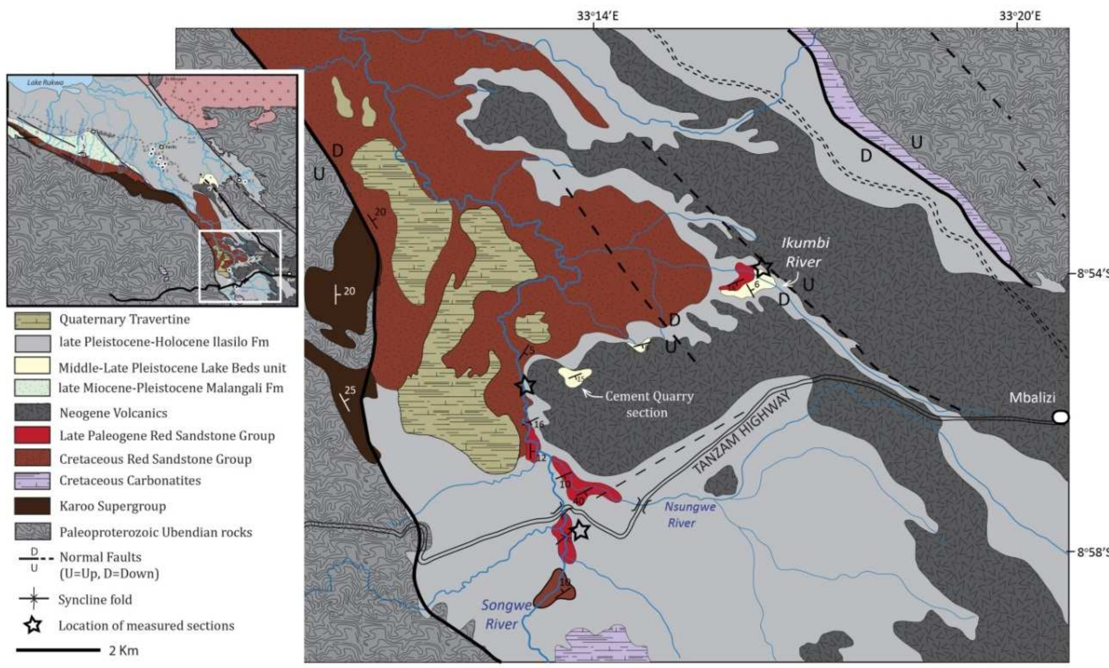

Fig. 2. Geologic reference map of the study area (upper-left), and a close-up of the south-eastern part of the study (insert box in the reference map), showing middle Lake Beds exposures along the Songwe Valley and Ikumbi River. Note, the Tukuyu middle Lake Beds exposure is located ~80 km southeast of Mbalizi town, below Kaparogwe Falls.

3.4. Kaparogwe Falls

Abundant sedimentary exposures exist south of the town of Tukuyu, many of which may represent middle Lake Beds deposits. However, due to time and logistical constraints, only a single locality has been studied in sufficient detail to report here. This locality is found below the lip of the popular tourist locality known as Kaparogwe Falls (~14 km south of Tukuyu town), which is characterised by a single ~3 m thick intra-basalt flow siltstone and sandstone sequence (Figs. 3 and 7). The southern-most middle Lake Beds deposits at Kaparogwe Falls overlie the Cretaceous Galula Formation and a basaltic flow laterally along the strike, and also capped by a basalt flow, which is dated at ~500 ka (A. Deino, pers. comm.). The Lake Beds strata form concave-up pod-like geometry, encased between the two basaltic flows. It is suspected that other middle Lake Beds equivalent deposits exist in the area; however, only a single "tourist" visit was made to this area during the course of this project, hence excellent potential exists for future work in the far southern portion of the basin.

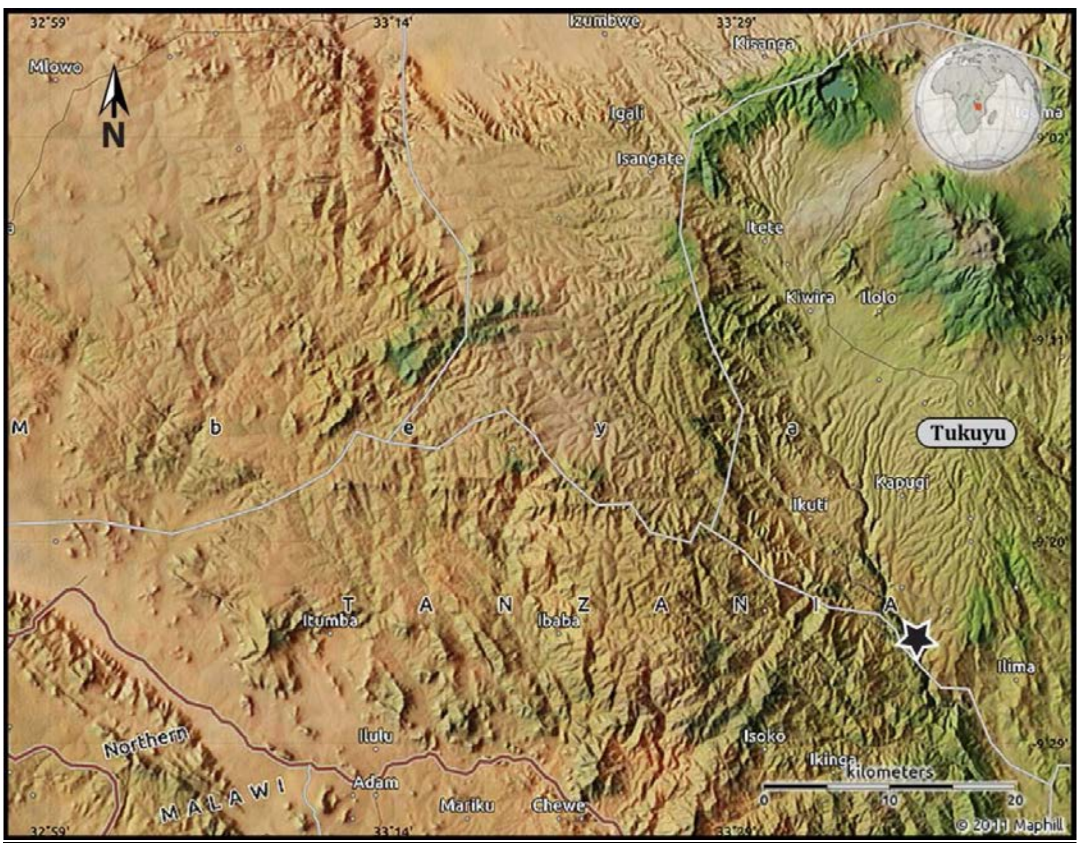

Fig. 3. Satellite map of Tukuyu in the southwestern Tanzania, showing location of the mapped middle Lake Beds unit (insert star) below Kaparogwe Falls, ~80 km southeast Mbalizi (Figs. 1 and 2) and ~14 km south-southwest of Tukuyu town.

.

4. Sedimentology

Sedimentary facies were described along with lithology and sedimentary structures at each of the outcrop sections. A total of 11 lithofacies were identified, and are presented in Table 1 below. The identified lithofacies can be organised into four genetically-related facies associations (FAs), summarized in Table 2. These FAs are described and interpreted here in the context of depositional processes and environments.

Table 1. Sedimentary facies of the middle Lake Beds.

Facies	Texture	Structures and Features	Colour	Interpretations
Gcm: clast-supported conglomerate	Clasts: pebble- to cobble-sized; dominated by vein quartz and meta-granitoids; moderately sorted; sub-round to rounded Matrix: tuffaceous medium- to coarse-grained sandstone	Massive; ungraded to weak normal graded	Yellowish gray (5Y 8/1) to white (N9)	Unidirectional high-energy flow regime deposits
Smvp: volcanic pebbly sandstone	Tuffaceous pebble-sized sandstone; comprised of volcanic (chiefly pumice), and meta-volcanics; moderately sorted; sub-angular to rounded	Massive, crudely fine upward	Very light gray (N8) to medium gray (N5)	Rapid (high-energy) pyrocla-stic flow deposits
Smv: massive sandstone	Medium- to coarse-grained, tuffaceous sand-sized, locally pebbly at base; comprises mainly quartz and feldspars; moderate- to poorly sorted; sub-angular to rounded;	Massive, crudely stratified;crudely fining upward	Pale olive (10Y 6/2) to yellowish gray (5Y 7/2)	Rapid (high energy) sedimentation deposits
Sm: massive sandstone	Fine- to medium- grained sandstone, quartzo-feldspathic in composition; moderate-well-sorted; sub-angular to rounded;	Massive, crudely stratified;crudely fining upward	Pale reddish brown (10R 5/4), moderate red (5R 4/6)	Rapid (low-medium energy) flow regime deposits
Sh: horizontally-stratified sandstone	Fine- to medium-grained sand; well-sorted; sub-round to rounded; quartzo-feldspathic	Horizontally-stratified, fine upward	Pale reddish brown (10R 5/4), moderate red (5R 4/6)	Unidirectional low- to medium-energy deposits
St: trough cross-stratified sandstone	Medium- to coarse-grained sand; composed of dominantly quartz and feldspar; moderate-well-sorted; sub-angular to rounded	Trough cross-stratified; fine upward	Pale olive (10Y 6/2), Pale reddish brown (10R 5/4),	Unidirection high-energy flow regime deposits
Fmv: massive volcanic siltstone	Ash and silt-sized grains	Typically massive; crudely bedded in places	light olive gray (5Y 5/2), medium gray (N5), light	Rapid (low-energy) subaqueous pyroclastic fallout deposits

			brownish gray (5YR 6/1), brownish gray (5YR 4/1),	
Fhv: horizontally stratified volcanic siltstone	Ash and silt-sized grains	Planar stratification	light olive gray (5Y 6/1), pinkish gray (5YR 8/1), medium gray (N5), light brownish gray (5YR 6/1), brownish gray (5YR 4/1),	Subaqueous pyroclastic flow/ fallout deposits
Fb: bentonitic sandy mudstone	Sandy ash, with isolated granules; comprises devitrified ash (bentonized) and pumice	Massive, crudely stratified	Pinkish gray (5YR 8/1), Very light gray (N8)	Rapid, subaqueous low-energy water-lain or airfall pyroclastic deposits
Fcf: massive fines	Silty mud and clay; moderate-well-sorted	Massive, horizontally-stratified	Pale reddish brown (10R 5/4), medium dark gray (N4)	Low-ernegy suspension fallout deposits
Lst: limestone	Crystalline; composed mostly calcium carbonate ($CaCo_3$)	Massive, horizontally-stratified	Very light gray (N8), Pinkish gray (5YR 8/1)	Shallow saline lake precipitation (from solution) deposits

Table 2. Facies associations (FAs), depositional process and environments of the middle Lake Beds.

FA	Facies	Diagnostic Features	Architectural Elements	Depositional Process	Macrofossil	Depositional Environment
FA 1: Fluvial channel deposits:						
FA 1A	Gcm, Sm	Coarse-grained nature; poorsorting; massive or crudely-stratified; ungraded- to weakly normal-gradding; erosive lower bounding surface	SG, CH	Fluvial channel fill, sediment gravity fallout	-	Channel lags
FA 1B	Smvp, Smv, Fb	High degree of sediment rounding; reverse grading; moderately-	CH, SG	Pyroclastic reworking by sheet floods, fluvial channels	-	Fluvial channels.

		poorly-sorted; erosional or sharp basal surfaces.				
FA 1C	Sm, Sh, St	High degree of sediment rounding; upward fining; erosive (lower bounding) surfaces	SG, CH	Fluvial channel-fill, sediment-gravity fallout	Isolated fish bones	Fluvial channels
			FA 2: Lacustrine deposits:			
FA 2A	Fb, Fmv, Fhv, Fcf	Fine-grained sediments; tabular; finely laminated or massive	FF, SH	subaqueous currents, suspension fallouts	Terrestrial plant trace fossils	Lacustrine (small lakes), ponds
FA 2B	Lst	Crystalline $CaCO_3$ composition	-	Precipitation of $CaCO_3$	-	Lacustrine

4.1. FA1: Fluvial Channel deposits

4.1.1. Facies Association1A: Clast-supported Conglomerate:

Facies Association 1A comprises 1-2 m thick tabular to lenticular clast-supported massive conglomerate (Gcm), embedded with thin (<40 cm thick) sandstone beds (Sm, Sh facies) (Table 1, 2). FA 1A is characterized by erosional basal surfaces and gradational or sharp tops. This FA occurs repetitively in the upper portion of the Ikumbi section (Figs. 1, 2 and 4), where it is vertically interbedded and horizontally intercalated with lenticular sandstone deposits of FA 1C. FA 1A also occurs around Tukuyu area, interbedded with volcanic siltstone and ash deposits of Facies 2A (Figs. 3 and 7). Conglomerates are pebble- to cobble-sized, dominated by vein quartz and meta-granitoids clasts or basalts. Lithoclasts are sub-rounded to rounded, moderately sorted, exhibiting weak normal grading. The matrix is tuffaceous medium- to coarse-grained sandstone. Subordinate sandstone facies are massive or horizontally-stratified, fine- to medium-grained. Deposits of FA 1A are yellowish gray (5Y 8/1) to white (N9) coloured.

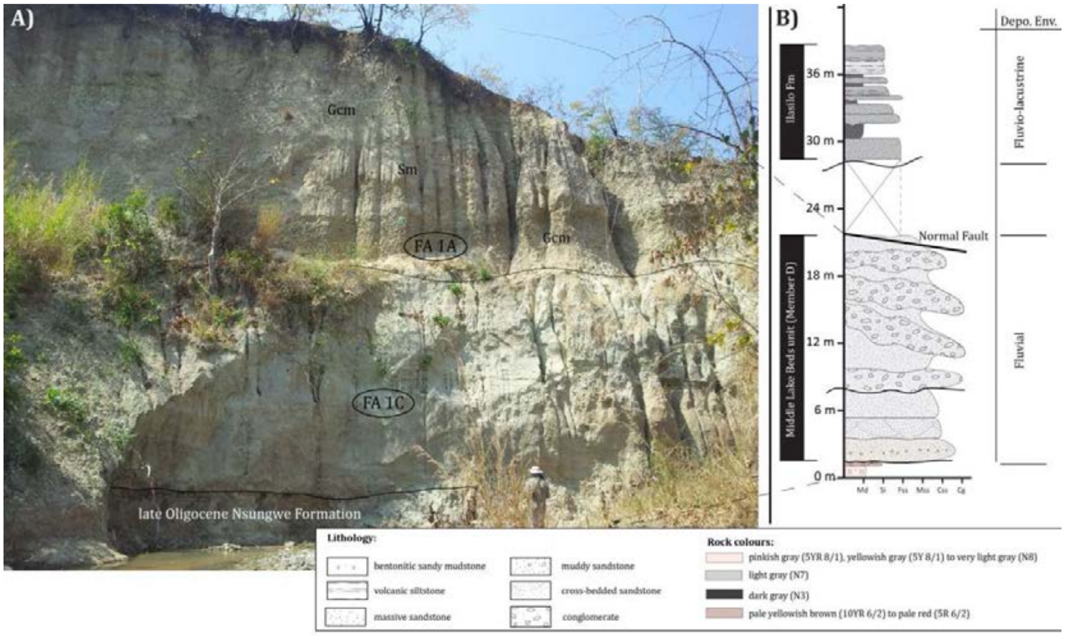

Fig. 4. **A)** Middle Lake Beds exposure along the Ikumbi River, showing lithology and stratigraphic relationship of the late Oligocene Nsungwe Formation, and an informal Member D of middle Lake Beds unit. **B)** Measured stratigraphic section showing constituent facies of the middle Lake Beds informal Member D.

4.1.2. Interpretation: Facies Association 1A

Facies Association 1A is interpreted to represent high-energy fluvial channel lag deposits, based on its coarse-grained sediment character, structureless (massive), and erosive basal surfaces. The typical lenticular bed geometry of FA 1A, their alternation with lenticular sandstone beds of FA 1C suggests deposition by fluvial channels (possibly braided), and associated hydrodynamic changes within braidplain environments (cf. Miall, 1996; Bridge et al., 2000; Mtelela et al., in review). The recurrence of this facies across the stratigraphic section is interpreted to probably indicate repeated channel reactivation.

4.1.3. Facies Association 1B: Volcaniclastic sandstone

Facies Association 1B occurs in the upper portion of the Magogo section (Figs. 1, 2 and 5), and in the Kaparogwe section near Tukuyu (Figs. 3 and 7). Facies 1B consists of 0.4 to 1.5 m thick tuffaceous pebbly sandstone facies (Smvp: Table 1, 2) and minor medium- to coarse-grained tuffaceous sandstone (Smv) and bentonitic mudstone (Fb). The upper and lower contacts of FA 1B are typically erosional or sharp. Tuffaceous pebbly sandstone (lapilli tuff) is typically massive, well-indurated and moderately sorted, exhibiting crudely upward fining. It is composed of sub-angular to rounded pumice particles and mafic volcanic grains that range in size coarse sand to pebbles, and cemented by fine ash. Facies 1B is very light gray (N8) to medium gray (N5).

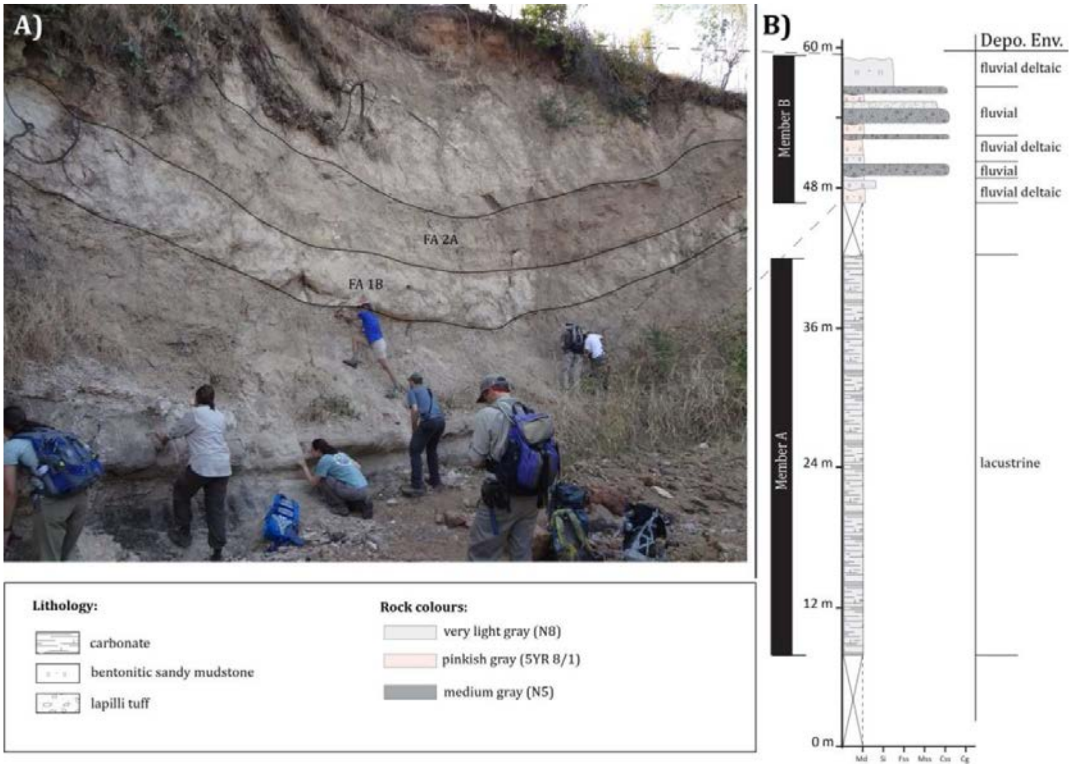

Fig. 5. **A)** Exposed upper portion of the Magogo middle Lake Beds unit showing tuffaceous sandstone facies (Smvp: FA 1B) interbedded with bentonitic mudstone of FA 2A, and **B)** Measured stratigraphic section.

4.1.4. Interpretation: Facies Association 1B

Based on high degree of sediment (clast) rounding, erosive bases, and upward fining, FA 1B is interpreted as high-energy fluvially reworked pyroclastic flow deposits (cf. Bhat et al., 2008). The massive nature of FA 1B is interpreted to indicate rapid deposition by sediment gravity-settling processes during wanning fluvial flows. Alternatively, the massive nature along with ashy matrix of this facies may also reflect the rapid production of volcanic sediment during and immediately after explosive volcanic events most likely from the nearby Rungwe Volcanic Province.

4.1.5. Facies Association 1C: Single and multi-story siliciclastic sandstone bodies

Facies Association 1C occurs in the Ikumbi section, cement quarry section as well as in a small exposure at the waterfalls section east of cement quarry (Figs. 1, 2, 3C, 4). FA 1C comprises single or multiple sandstone bedsets of St, Sh and Sm facies (Table 1, 2). FA 1C reaches up to 6 m thick unit, with individual beds ranging between few tens of cm to 1.5 m thick. The basal surface of this FA is typically erosional, locally containing isolated pebbles. Top contacts are either sharp or gradational. Sandstone beds are tabular or lenticular, locally truncated by conglomerate bodies of FA 1C. They are commonly moderately well-sorted or poorly sorted in places, and comprises sub-rounded to rounded grains. FA 1C are dominantly quartzo-feldspathic in composition, varying in colour from pale reddish brown (10R 5/4), pale olive (10Y 6/2) to yellowish gray (5Y 7/2). In places, Facies IC is fossiliferous, preserving mostly fish remains.

Fig. 6. Exposed section of the middle Lake Beds inside the Songwe cement quarry, showing lithologic composition of an informal Member C (FA 1C), and its relationship with underlying late Oligocene Nsungwe Formation.

4.1.6. Interpretation: Facies Association 1C

Based on erosive basal surfaces, sedimentary structures and textural features such as sediment (grain) rounding and upward-fining, FA IC is interpreted as fluvial channel deposits. Horizontally- and trough cross-stratified intervals of this FA are interpreted to record bedload tractive current sedimentation of a normal fluvial flow, whereas massive intervals are interpreted to have resulted from flood-related gravitational collapse processes (Miall, 1996).

4.2. FA2: Lacustrine deposits

4.2.1. Facies Association 2A: Tabular-lenticular volcanic siltstone and mudstone

Facies Association 2A comprises tabular bentonitic sandy mudstone and minor siliciclastic mudstone (Fcf) (Fb), or in places, volcanic siltstone facies, Fmv and Fhv (Tables 1 ad 2). This FA is well-developed in the Magogo section as well as in Tukuyu lake beds exposure. Mudstone consists of silt to clay-sized sediments, and is massive or crudely-stratified. They are pale reddish brown (10R 5/4), Pale olive (10Y 6/2) coloured. Bentonitic sandy mudstone is also massive, composed of pumice sand-sized grains and isolated granules and devitrified ash. They range in colour from pinkish gray (5YR 8/1) to very light gray (N8). Volcanic siltstone facies of this FA are typically tabular, light olive gray (5Y 5/2) or pinkish gray (5YR 8/1) coloured. They are massive or horizontally stratified. In the Kaparogwe section, Facies 2A is fossiliferous; preserving plant remains and trace fossils (Fig. 7C). Here, FA 2A forms part of a lenticular, concave-up middle Lake Beds strata that pinches out tens or few hundreds of meters laterally, and encased by two basaltic flows.

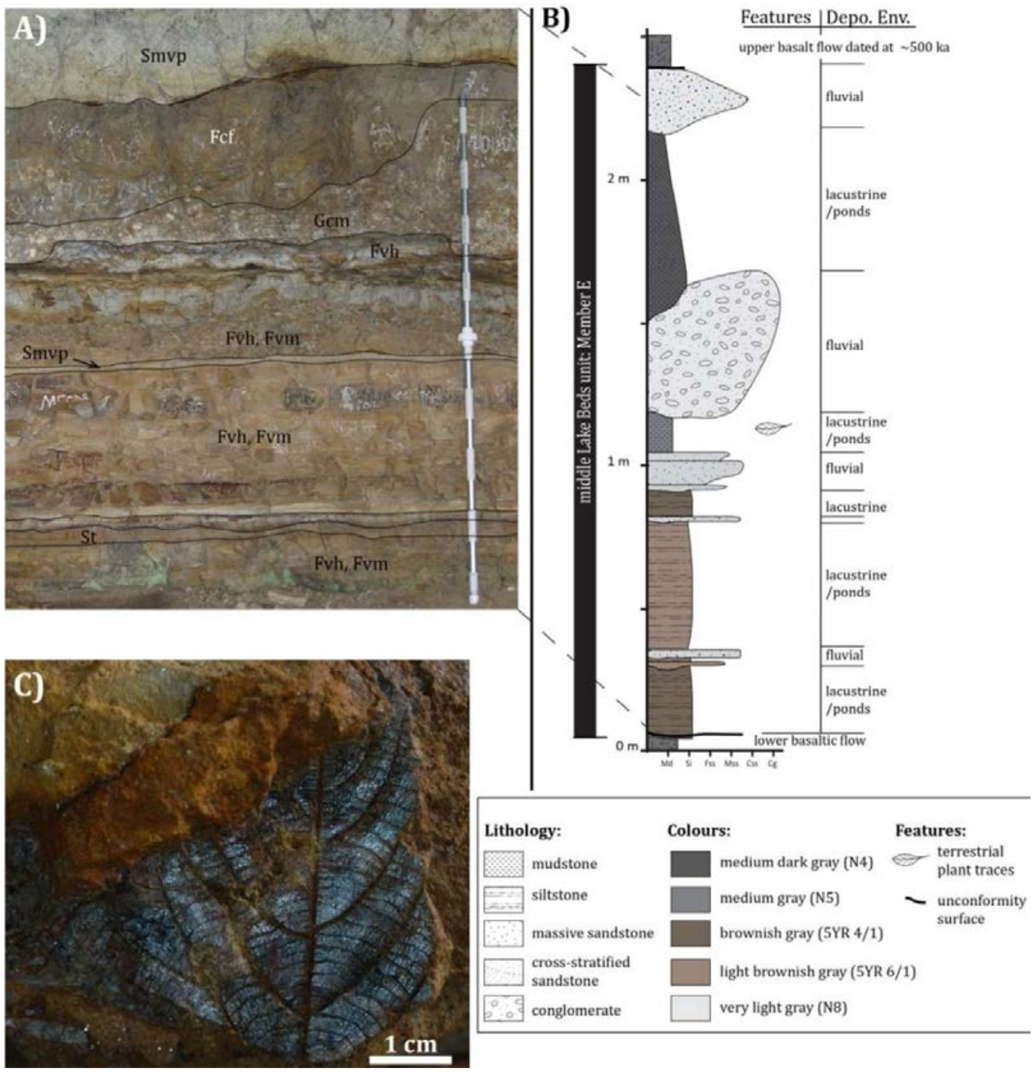

Fig. 7. A) Exposed middle Lake Beds unit along the cliff-face of Kaparogwe Falls ~14 km south of Tukuyu town (See Fig. 3 for location), showing massive and horizontally-stratified volcanic siltstone (Fvm, Fvh) facies of Facies 2A, interbedded with tuffaceous sandstone and conglomerate deposits of FA1. **B)** Measured stratigraphic section. **C)** A close-up photo of a leaf impression observed mid-way (at ~ 1.1 m from the base) across the stratigraphic section in A.

4.2.2. Interpretation: Facies Association 2A

Fine-grained nature of FA 2A is interpreted to indicate low-energy deposition by suspension fallout of very fine (ash and clay-sized) sediments. Typical lenticular nature of this facies in the Kaparogwe section suggests deposition in small lakes or ponds that developed between lavas (basaltic flows). The common alternation of this facies with FA 1B may suggest periodic base-level fluctuations and transition between lacustrine/ponds and fluvial channel systems. Alternatively, interbedded fluvial conglomerate deposits of FA 1B might have resulted from periodic flash flooding events, which deposited these more coarser grained units into small lakes and ponds, from rapidly uplifted and eroded rift flanks. This interpretation is supported by the presence of traces of terrestrial plant macrofossils (Fig. 7C) in FA 2A deposits.

4.2.3. Facies Association 2B: Massive and horizontally stratified Limestone and Travertine

FA 2B is a 50-100 m thick massive and horizontally stratified limestone and travertine (Lst) facies exposed in the lower part of the Magogo section (Table 1, 2). The beds are dipping to the east, however the original horizontal bedding is clear. This locality was visited briefly, and prior to our recognition of the middle Lake Beds stratigraphy, so a complete measured section and detailed stratigraphic log was not completed at the time. However, preliminary description of the site and partial measured section permits a reasonable first-order (overview) description. FA 2B is typically crystalline, composed of mainly calcium carbonate ($CaCO_3$), is very light gray (N8) or pinkish gray (5YR 8/1) coloured. Evidence of horizontal bedding (and bands, for travertine) is present, along with vertical root or burrow traces in some horizons. Although only a limited time was spent investigating for fossils, none were found.

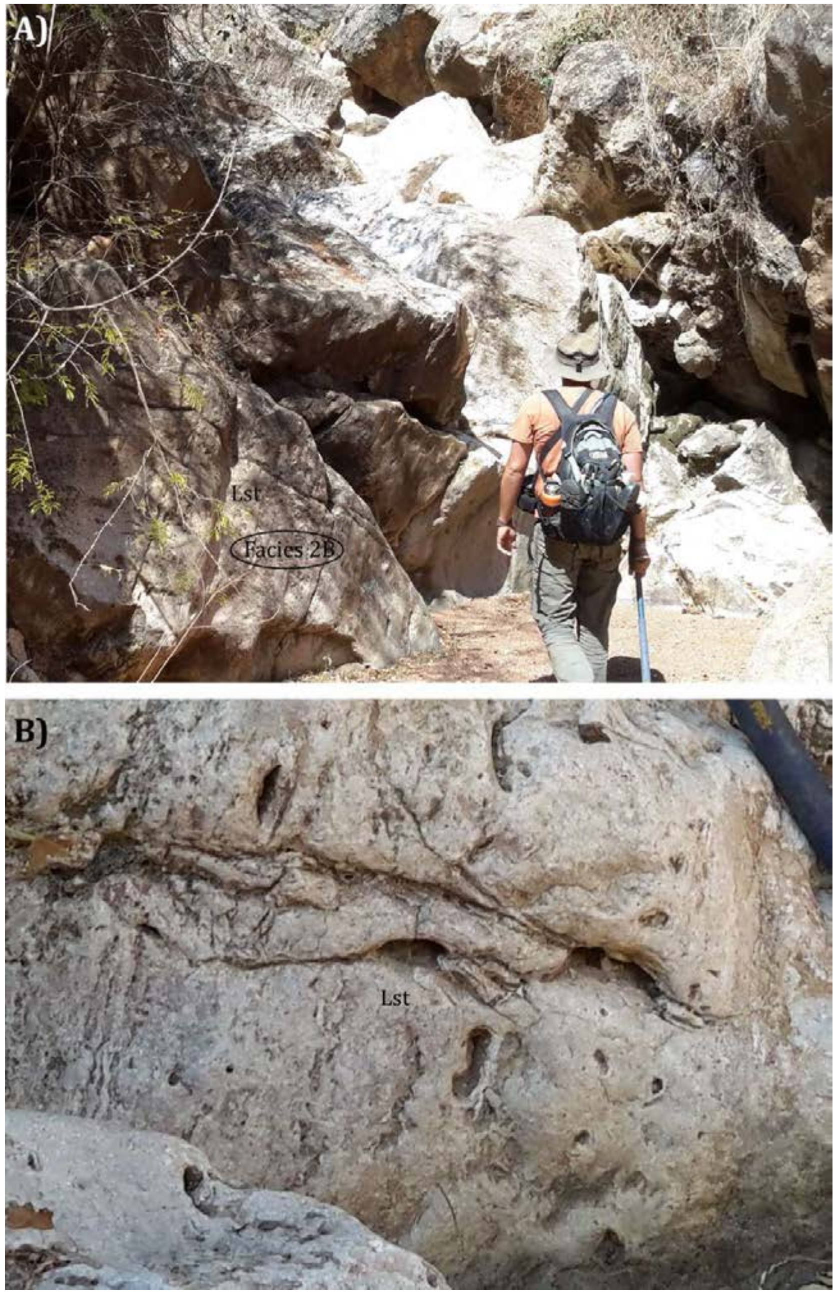

Fig. 8. **A)** Outcrop photo showing a portion of the thick carbonate unit -Limestone (Lst) facies (FA 2B) exposed along the dry tributary river-cuts to the Zira River in the north-eastern portion of the study area, around Magogo Village. **B)** A close-up of the massive, crystalline limestone.

4.2.4. Interpretation: Facies Association 2B

Based on composition, Facies 2B is interpreted to have resulted from precipitation of calcium carbonate from water in lacustrine conditions. The travertine and limestone deposits of FA 2B are similar to the Quaternary Travertine deposits observed in the Songwe Valley, however, it has a much more uniform horizontally bedding and contains burrows/roots in some intervals, suggesting that it was primarily deposited in a lacustrine setting, rather than a hydrothermal setting. However, a hydrothermal origin or perhaps combined hydrothermal-lacustrine origin cannot be completely ruled out (Porta, 2015). FA 2B is overlain by a distinctive succession of volcaniclastic mudstones and sandstones, and both units are tectonically tilted, and have been subsequently overlain by diagnostic deposits of the upper Lake Beds. Hence, this unit appears to be both temporally and stratigraphically distinct from the late Quaternary travertine deposits found in the Songwe Valley. The deposition of FA 2B is envisaged to have probably occurred during relatively dry climatic condition, which could have led to prolonged precipitation of this thick carbonate unit. The greater thickness and massive nature of large portion of FA 2B is interpreted to indicate formation of a local lake basin associated with the deposition of this FA.

5. Lithostratigraphy

Lithostratigraphic relationship between the middle Lake Beds sections is complex and not completely understood. However, sedimentary facies and lithologic variations between and across these middle Lake Beds stratigraphic sections suggest the presence of at least five distinctive lithologic units. These distinctive units are referred to here as informal members (member A-E) of the middle Lake Beds unit, and are described below.

5.1. Member A

Informal member A is defined as the 36 m thick (minimally, but probably much greater) limestone unit (FA 2B) that crops out in the lower part of the Magogo section (Fig. 5B, 8). This thick limestone unit is not observed elsewhere within the Lake Beds succession in the study area, and is distinct from late Quaternary travertines documented in the Songwe Valley. The basal contact of this unit is not exposed, and the upper contact is sharp, and likely unconformable, based on differences in attitude (bedding) of the strata between this unit and the overlying succession of the informal Member B. The unit is gently to steeply inclined towards northeast; exhibiting changes dip angles due to post-depositional tectonic movements (faulting) from 12° near the base, to 36° at the upper portion (Fig. 1B).

5.2. Member B

Overlying member A in the Magogo Lake beds exposure is ~12 m thick succession of volcaniclastic deposits identified here as informal member B of the middle lake beds unit (Fig. 5A-B). Member B is characterized by alternating tuffaceous sandstones, bentonitic mudstone and thin massive volcaniclastic conglomerates (FAs 1A, 1B). Tuffaceous sandstones are coarse-grained sand sized and pebbly, ranging in thickness between 0.4 and 1.5 m, and are typically massive or crudely stratified. They are very light gray (N8) or medium gray (N5) coloured. The tuffaceous pebbly sandstone and conglomerate beds are composed of sub-angular to rounded pumice particles and mafic volcanic grains/pebbles, moderately sorted and cemented by fine ash. The basal surfaces are typically erosive, cutting and filling the bentonitic mudstone beds. The top contacts are either sharp or gradational. Volcanic mudstone is also massive, tabular bedded, and is composed of bentonized ash and isolated sandy pumice grains. These deposits are pinkish gray (5YR 8/1) or very light gray (N8) coloured.

5.3. Member C

Informal member C of the middle lake beds is identified at the cement quarry section, where lake beds crops out as pale reddish brown (10R 5/4) to moderate red (5R 4/6) coloured, medium-coarse grained sandstone and siltstone (FA IC), dipping 15° towards southeast (Fig. 6). Member C is characterized by well-sorted, massive and horizontally stratified siliciclastic sandstones and massive or crudely stratified siltstones and mudstones. Sandstones are composed of sub-round to rounded grains of dominantly quartz and feldspars. Individual beds have erosional basal surfaces, and shows upward fining.

5.4. Member D

Member D occurs along the Ikumbi River, and is informally defined as a ~20 m thick succession of volcanic ash-rich siliciclastic sandstones (FA IC) and conglomerates (FA 1A) unconformably overlying the Oligocene Nsungwe Formation (Fig. 4). Both sandstones and conglomerate deposits of member D are Pale olive (10Y 6/2) to yellowish gray (5Y 7/2) coloured, albeit due to volcanic ash content in the matrix. The basal portion of member D comprises 6° northeast-dipping bedset of massive and trough cross-bedded sandstones. This basal succession is overlain by repetitive tabular and lenticular, massive, pebble-cobble conglomerate beds that are interbedded and intercalated with lenticular sandstones. High-relief erosional scours separates the lower part and upper portion of this unit. The lower sandstone bedset is moderate- to well-sorted, showing generally upward fining trend from pebbly sandstone basal bed to medium-/fine-grained sandstone.

5.5. Member E

Informal member E is identified as a volcaniclastic dominated unit exposed near Tukuyu (Fig.3), unconformably overlying the Cretaceous Galula Formation and capped by a basaltic flow. Member E is dominated by tabular-lenticular volcanic siltstone, mudstone and claystone deposits (FA 2A) that are interbedded with tuffaceous sandstone (lapilli tuff) and conglomerates (Fig. 7). Volcanic siltstone and mudstone/claystone is massive or horizontally stratified, comprised of dominantly silty to clay-sized pumice and ash. They are locally fossiliferous, preserving traces of terrestrial plant macrofossils (Fig. 7C), and varies in colour between brownish gray (5YR 4/1), light brownish gray (5YR 6/1), medium gray (N5) and medium dark gray (N4). The interbedded tuffaceous sandstone and conglomerate are typically massive, with erosion bases, and are very light gray coloured. They are commonly lenticular, and pinch out few meters laterally.

6. Discussion

This study provides insights to a broader understanding of the Lake Beds sedimentology and stratigraphic setting in the Rukwa Rift Basin, providing an overview of a third depositional unit within the strata that was previously unrecognized. This newly identified unit occurs in a suite of isolated, fault bounded sections across the southern Rukwa Rift Basin, unconformably overlying older Red Sandstone Group strata (Roberts et al., 2010), and overlain by the upper Lake Beds succession (Mtelela et al., in press). Based on pilot U-Pb dating (H. Hilbert-Wolf pers. comm.), Ar/Ar dating of basalts (A. Deino, pers. comm.), and cross-cutting relationships, this newly identified series of deposits in the RRB is interpreted to represent an early to middle Pleistocene middle Lake Beds unit, deposited between ~ 2 Ma and 200 ka. However, these radiometric age assignments are considered as preliminary until further dating of the strata can be conducted to improve the geochronology. Due to limited availability of field time, resources, and the expansive and difficult to access nature of the deposits in the rift, full documentation of these deposits lies outside the scope of the this PhD project, but provides a rich target for future research in this part of the East African Rift System.

This sedimentologic investigation reveals remarkable lateral and vertical depositional facies variation across the middle Lake Beds strata, ranging from highly siliciclastics units, volcaniclastics units to carbonates. Similar facies changes between volcaniclastics and siliciclastics units were also observed in the upper Lake Beds succession (see Mtelela et al., in press). However, sedimentologic features such as degree of compaction, textural and compositional variations in addition to stratigraphic positions, suggests that these units may not represent time-equivalent strata. Most of the middle Lake Beds exposures appear to be fault-bounded, which may suggests that deposition occurred during more tectonically active episode. Rift tectonics (faulting) may also be linked to the observed lateral variability in depositional facies and environments, and provenance in a number of possible ways, probably leading to: 1) tectonic subsidence proximal to the paleo-lake Rukwa around Magogo area, where localized lacustrine carbonates were deposited in a small, possibly saline lake; 2) likely simultaneous tectonic uplift of the rift flanks in the hinterland, leading to siliciclastic fluvial deposition around Songwe and Ikumbi areas; and 3) contemporaneously volcanism in the nearby Rungwe Volcanic Province that resulted in primary and fluvially reworked volcaniclastic deposition in the Kaparogwe area (near Tukuyu), and upper part of the Magogo section, as well as volcanic ash-rich siliciclastic deposition in the upper portion of the Ikumbi section.

7. Conclusions

This chapter presents a sedimentologic overview of a yet another previously unrecognized Lake Beds unit in the Rukwa Rift Basin, termed the middle Lake Beds, which was deposited in a series of local depocenteres during the early to mid-Pleistocene. Eleven sedimentary facies are identified across a series of faulted-bounded exposures, which are recognized into five genetically-related facies associations, including: clast-supported conglomerate (FA 1A), volcaniclastic sandstones (FA 1B), and single and multi-story siliciclastic sandstone bodies (FA 1C), which are associated with fluvial channel and fluvially reworked pyroclastic flows; and lacustrine deposits of tabular volcanic siltstone and mudstone (FA 2A), and massive and horizontally stratified limestone (FA 2B).

Lithostratigraphic relationships between the discrete middle Lake Beds units is complex and poorly understood due to complex faulting system associated with these small and isolated exposures, and requires a follow-up mapping. However, lithologic variations between the mapped sections suggest the presence of five distinctive units, herein referred to as informal members (A-E) of the middle Lake Beds succession. The discovery of this new stratigraphic unit in the Rukwa Rift Basin further highlights the need to extend geochronologic investigation into this unit, and to establish a revised, formal stratigraphy of the Lake Beds succession.

Acknowledgements

We thank Tanzania Petroleum Development Corporation (TPDC) and Heritage Oil Rukwa Tanzania Ltd. for providing a PhD bursary to the lead author (CM) and funding to conduct extensive and detailed fieldwork in the rift. We are also grateful to the supported of the US National Science Foundation (EAR_1349825, BCS_1127164), the National Geographic Society (CRE), and the post-graduate research fund from James Cook University.

Chapter 4

Synrift stratigraphy and nomenclature of the late Cenozoic Lake Beds Group in the Rukwa Rift Basin, Tanzania, with comments on source, reservoir and seal rock potential for hydrocarbon prospectivity

Keywords: Stratigraphy; Cenozoic; Lake Beds; Rukwa; Tanzania

ABSTRACT

The aim of this study is to (1) document the sedimentologic and stratigraphic relationships and (2) establish the first formal nomenclature for the late Cenozoic Lake Beds succession in the Rukwa Rift Basin, southwestern Tanzania, and (3) evaluate the hydrocarbon prospectivity of this important synrift depositional succession. This study build upon extensive sedimentologic, geochronologic and paleontologic investigations on Lake Beds succession conducted over the last four years in the Rukwa Rift Basin. The result of these investigations provides the basis for formally establishing a three-fold lithostratigraphic framework for the Lake Beds succession, which is herein raised to Lake Beds Group. Two new formations are recognized and named at this stage within the Lake Beds Group for the lower and upper portions of the stratigraphy. The lower Lake Beds is termed the Malangali Formation, which represents a previously unrecognized 170+ m-thick late Miocene to Plio-Pleistocene unit in the Rukwa Rift Basin, which is internally subdivided into the lower Mpona and upper Hamposia members. A major unconformity and provenance shift marks the transition between the two members of Malangali Formation. The Hamposia Member is particularly significant because it preserves an important new vertebrate fauna in this part of the East Africa. The middle Lake Beds Group remains problematic, and more detailed investigation of the middle Lake Beds Group is required to fully understand the stratigraphic relationships and aerial extent of these deposits. Hence, the middle Lake Beds Group is informally referred to only in terms of informal members (A-E) for the time being. The uppermost late Pleistocene-Holocene Lake Beds succession is termed the Ilasilo Formation. This capping succession in the rift represents a volcanically controlled unit that was deposited in a fluctuating fluvio-deltaic to lacustrine depositional system that records large-scale tectonic, climatic and volcanic shifts in this part of eastern Africa over the last ~50 ka. The Ilasilo Formation records an important continental ichnofauna, as well as abundant disarticulated fish remains, and rare, isolated large vertebrate macrofossils.

The revised stratigraphy, along with detailed sedimentology, petrology and mineralogy presented herein, and in chapters 1 and 2, is critical for evaluating the hydrocarbon prospectivity of the Lake Beds Group in the Rukwa Rift Basin. Lithofacies analysis reveals that regionally extensive profundal lacustrine environments developed several times throughout the late Cenozoic history of the basin, depositing thick organic-rich (diatomaceous) units that could act as potential hydrocarbon source rocks. The Hamposia Member and a large portion of the middle Lake Beds unit have high-quality reservoir characteristics. However, it is the uppermost Ilasilo Formation that has the most intriguing hydrocarobon potential, with high-quality source rocks, whereas the mixed siliciclastics to volcaniclastics-rich sandstones have the potential to provide both high-quality, porous reservoirs and yield good seal rocks, respectively. Sandstone petrography and XRD analysis show that siliciclastic sandstones are typically quartz and

feldspar, with high porosity and permeability, making them effective reservoir possibilities. Similar studies categorize the volcaniclastic units as potential seal rock with typically low porosity (<7%) and thin, impermeable smectite-dominated devitrified ash beds.

Apart from the economic aspects of the Lake Beds Group; it is also important to highlight that prior to the last few years, nothing was known about the vertebrate palaeontology of the Lake Beds Group. However, this project has helped to document a series of entirely new fossiliferous deposits in an otherwise poorly known portion of the East African Rift System. Findings from this study serve as important geologic background for placing this wholly new vertebrate fossil record from this portion of eastern Africa into a more complete evolutionary, palaeoenvironmental and palaeobiogeographic framework.

1. Introduction

Prior to the 1980's virtually nothing was known about the detailed stratigraphy or hydrocarbon potential of rift basins in eastern Africa; in particular the little known Rukwa Rift Basin, in southwestern Tanzania, between lakes Tanganyika and Malawi (Nyasa) (Fig. 1A; Kilembe and Rosenthal, 1989). Although the rift basins of Tanzania, Kenya and Ethiopia have long drawn academic interest as windows for understanding paleoenvironmental changes and floral and faunal evolution in Africa, it was not until regional hydrocarbon surveys across the rift basins of Eastern Africa in the 1980's (Pierce and Lipkov, 1988; Morley et al., 1999), that the Rukwa Rift Basin first attracted notice. Such rift basins have been under scrutiny because they are characterized by high rates of subsidence and sedimentation, multi-phase developmental histories and complex structural patterns; conditions considered favourable for hydrocarbon generation and accumulation (Morley et al., 1990; Mbede, 1991, 1993; Morley, 1995; Tiercelin et al., 2004, 2009, 2012). Furthermore, high geothermal gradients normally associated with rifting events are considered conducive for premature maturation of source rocks even at relatively shallow depths (Morley et al., 1990; Mbede, 1991; Morley et al., 1999). Taken together, these conditions make the eastern Africa rift basins good targets for hydrocarbon exploration.

Recently, the East African Rift basins have been identified as one of the most important new frontiers for hydrocarbon exploration (Cresswell, 2012). The structure and sediment character of these rift basins show strong similarities with rift basins elsewhere in the world (such as the North Sea basins, the Ta Chung basin of China and Sirte basin of Libya), which are proven sources of oil and gas (Frostick and Reid, 1990 and references therein). Despite these important similarities in tectonics and sedimentation patterns, the East African Rift System has remained under-explored for hydrocarbon accumulation and development. However, recent exploration activities within East African Rift basins has resulted in major oil field discoveries in the Neogene strata of the Albertine Graben of Uganda by Tullow Oil and Heritage Oil; as well as in the Turkana Basin of Kenya by Tullow Oil, and large gas fields at Songosongo and Mnazi bay in the Ruvuma and Rufiji Basin of Tanzania (Logan et al., 2009; Thuo, 2009; PEDP, 2011; Tiercelin et al., 2012).

In 2012, Heritage Oil, who was part of the Uganda hydrocarbon discoveries, commenced an exploration program in the Rukwa Rift Basin. However, hydrocarbon exploration of the most prospective Neogene strata of the Rukwa Rift Basin was hampered by the fact that the uppermost Lake Beds deposits in the rift have never been systematically studied from a stratigraphic or sedimentologic perspective. Hence, this thesis project was developed to investigate stratigraphic and sedimentologic context for the late Cenozoic Lake Beds succession in the Rukwa Rift Basin. Chapters 1-3 of this thesis focus on the sedimentology of the three main stratigraphic units in the rift, whereas this chapter synthesises stratigraphic and sedimentologic results from the entire Lake Beds succession to establish a formal stratigraphy nomenclature for these deposits, and to evaluate aspects of hydrocarbon prospectivity in the Lake Beds succession in the Rukwa Rift Basin.

2. Geologic Background

The Rukwa Rift Basin (RRB) in southwestern Tanzania forms part of the Western Branch of the EARS. It is one of the thickest sedimentary successions in East Africa, with up to 11 km of sedimentary fill (Kilembe and Rosendahl, 1992; Morley et al., 1999). The RRB is about 360 km long and 40 km wide, with down-to-northeast half-graben geometry. The basin is bounded by the long-lived Lupa border fault and Tanzania Craton to the northeast, by the Ufipa fault and uplifted Ufipa block to the west, and the Rungwe Volcanic Province and Mbozi block to the south and southwest by (Fig. 1B: Ebinger et al. 1989; Kilembe and Rosendahl 1992). Archean granitoids and uplifted Proterozoic metamorphic rocks of the Ubendian shear belt flank the RRB (Quennell 1956; Daly et al. 1985).

The Rukwa Rift was initiated during the Paleozoic by reactivation of Paleoproterozoic to Neoproterozoic sinistral shear zones in the NW-SE trending Ubendian Belt (Theunissen et al., 1996). Sediment fill in the basin began in the late Carboniferous-Permian, with the deposition of Karoo Supergroup, and continued to the middle/late Holocene (Kilembe and Rosendahl, 1992; Morley et al., 1999; Roberts et al., 2004, 2010; Hilbert-Wolf et al., 2013, 2015; Mtelela et al., 2016). As such, this thick and well-exposed basin provides an extensive sedimentary and palaeontologic record of the East Africa from the least studied Western Branch of the EARS, which is best known for its deep lakes. Analysis of the seismic profiles, coupled with well data and surface geology show that the RRB has undergone at least four episodes of rifting, including: 1) a Permo-Triassic event, which resulted in the deposition of Karoo Supergroup (Kilembe and Rosendahl, 1992; Morley et al., 1999); 2) a Cretaceous rifting event that deposited the fluviatile Galula Formation (lower part of the Red Sandstone Group) (Roberts et al., 2004, 2010, 2012), 3) a late Oligocene event that resulted in short-lived, richly fossiliferous depositional sequence (Nsungwe Formation, upper part of the Red Sandstone Group), which was accompanied by carbonatite volcanism (Roberts et al., 2004, 2010, 2012); and 4) late Miocene to Recent rifting and deposition of Lake Beds succession, which was accompanied by voluminous bimodal volcanism in the Rungwe Volcanic Centre (Grantham et al., 1958; Ebinger et al., 1989; Wescott et al., 1991). The final depositional unit forms the focus of this study.

2.1. Overview of hydrocarbon exploration in the Rukwa Rift Basin

Hydrocarbon exploration history in the RRB goes back to the 1980s. At this time, a gravity survey was conducted by Petro-Canada International Assistance Corporation as part of an assistance program for the Tanzania Petroleum Development Corporation (TPDC) (Pierce and Lipkov, 1988). This reconnaissance gravity survey provided the initial regional view of the geometry of the basin which established the presence of a deep (8-11 km) rift basin (Pierce and Lipkov, 1988; Morley et al., 1999) The RRB was subsequently investigated for hydrocarbons during the widespread southern and central African seismic programs. These programs were driven by hydrocarbon discoveries reported in rift basins such as Muglad, Melut and Blue Nile Basins of southern Sudan by Chevron Oil (Schull, 1984, 1988). As part of these programs, two hydrocarbon exploration wells (Galula-1 and Ivuna-1; Figs. 1A, 2B) were drilled by the Amoco Production Company within the RRB in 1987 (Wescott et al., 1991; Kilembe and Rosendahl, 1992; Wescott, 1993); the results of which were not conclusive. However, preliminary well-log analysis indicated that hot shale and liptinite rich coals of the K2 unit of the Karoo may serve as oil and gas prone and mature source rocks (Wescott et al., 1991; Kilembe and Rosendahl, 1992). The overlying sandstone units in the Karoo Supergroup, Red Sandstone Group and Lake Beds succession were all identified as potential reservoir rocks (TPDC, 2011). These early findings and recent hydrocarbon discoveries in the Turkana Basin and Albertine Graben have led to renewed hydrocarbon exploration in the RRB by Heritage Oil, with special focus on the age-equivalent (i.e. late Cenozoic) Lake Beds succession.

The late Cenozoic Lake Beds strata, which constitute the upper stratigraphic unit in the RRB, are up to 4 km thick based on seismic reflection data and gravity profiles (Fig. 2A; Kilembe and Rosendahl, 1992; Morley et al., 1999). The Lake Beds deposits are the most widespread sedimentary unit throughout the RRB; with thick, cliff-forming exposures observed along the upper and lower Songwe River, and along the Chambua, Hamposia, Namba and Chizi river drainages. In most of their occurrences, the Lake Beds strata unconformably overly the Red Sandstone Group (RSG) across the basin, which has recently been subdivided into the

Cretaceous Galula Formation and the late Oligocene Nsungwe Formation (Roberts et al., 2004, 2010, 2012).

However, due to a lack of detailed sedimentologic, stratigraphic and geochronologic studies focused on the Lake Beds succession, it has long remained the most poorly understood stratigraphic succession in the rift, with little previous information on the stratigraphy of this unit, or on the age, palaeontology, sedimentology or provenance. Understanding these aspects of the Lake Beds succession is important for understanding the basin evolution and is crucial for evaluating potential hydrocarbon source rocks, reservoirs and cap rock characteristics. Thus, this study provides an important, albeit preliminary prospectivity analysis of the late Cenozoic Lake Beds as a possible 'hydrocarbon kitchen' (R. Downey, Heritage Oil, pers comm.). The information documented in this study, and in this thesis more generally will provide important preliminary data that can be used in assessing not only whether to drill a new exploration well in the basin, but also where and what the targets may be.

2.2. Previous studies on chrono- and lithostratigraphy of the Lake Beds succession

In the earlier regional geologic mapping, the Lake Beds are described as conglomerates, sandstones and mudrocks associated with fluvial, floodplain and lacustrine environments (Spence, 1954; Quennell et al., 1956; Grantham et al., 1958). These early studies generally suggest that the Lake Beds are Neogene to Pleistocene in age (e.g. Quennell et al., 1956; van Loenen and Kennerly, 1962). Grantham et al. (1958) proposed an informal two-phase subdivision of the Lake Beds (mostly those found along the Songwe River) into lower and upper units based on structural and lithological features. According to Grantham et al. (1958) the lower (older) unit consists of gently dipping sandstones (to the NE) and overlying volcanic siltstones that occur along the lower Songwe river drainage (around Galula-Ilasilo area), whereas the upper (younger) unit is characterized by flat-lying conglomerate beds, pumice tuffs and limestones that occur in the upper Songwe River Valley, around Songwe and Ifisi areas (see the Mbeya 244 quarter-degree geological map of Grantham et al., 1958).

Most of the subsequent studies on the Lake Beds are based on analysis of the Galula-1 and Ivuna-1 well-cuttings acquired by the Amoco Production Company in the basin (e.g. Wescott et al., 1991), as well as on shallow (less than 25 m) sediment cores drilled through Lake Rukwa (e.g. Haberyan, 1987; Barker et al., 2002; Thevenon et al., 2002; Vincens et al., 2005). Based on pollen and diatom analysis of the well-cuttings from the Red Sandstone Group and Lake Beds Group, Wescott et al. (1991) reported a limited range of depositional ages indicating that the Red Sandstone Group was Miocene to Pliocene in age and the Lake Beds succession was Pliocene to Holocene. They did suggest that the basal portion of the Lake Beds may be as old as Miocene. The age suggestions provided by the biostratigraphy for the Red Sandstone Group have since proven to be inaccurate based on a wealth of recent palaeontological and geochronological work by O'Connor et al. (2006, 2010), Roberts et al. (2010, 2012) and Stevens et al. (2013). Work on the uppermost Lake Beds by Haberyan (1987) involving diatoms analysis and radiocarbon dating on a 23.1 m sediment core recovered from the southern part of the RRB in 1960, suggested ages ranging from 13 ka to 3.3 ka for the top of the Lake Beds. This depositional age set was largely supported by multidisciplinary research conducted on a 12.8 m thick sediment core recovered in 1996 from 13.55 m of water depth near the center of Lake Rukwa, involving sedimentology (Thevenon et al., 2002), diatom investigation (Barker et al., 2002), and pollen analysis (Vincens et al., 2005). These studies focused on paleolimnology, paleohydrology, and chronostratigraphy, and reported radiocarbon ages extending back to ~23 ka.

Recently, Cohen et al. (2013) conducted outcrop based investigation of the ostracodes and mollusks that occur within the upper Lake Beds across the basin. This work reported radiocarbon ages that range from ~11 ka to 6 ka from shallow (less than 2 m thick) Lake Beds exposures north of modern Lake Rukwa. From the south of modern Lake Rukwa, the authors obtained ^{14}C ages ranging between ~23 and 7 ka from the ostracode and mollusk shells collected within the uppermost 20 m of a deep gully exposed along the lower Songwe River. They also summarized a similar range of published and unpublished radiocarbon ages from other nearby locations, including: colluvial deposits on the foot wall of the Lupa Fault scarp along the bank of the Zira River (~23 ka) and a suite of samples from 3-8 km south of Galula town (11-6 ka).

Although the Lake Beds Succession is a widely exposed rock unit in the Rukwa Rift Basin, these early studies only focused on the uppermost 10-50 m of the Lake Beds succession, and none have focused on the sedimentology, or geology of the lower parts of the stratigraphy (>4 km thick). Hence, much of the strata of the Lake Beds remain poorly constrained. In the literature, different nomenclature has been informally adopted for the Lake Beds, such as Lake Beds, Lake Beds Group, Lake Beds Sequence, Lake Beds Succession and Lake Beds Formation (e.g. Kilembe and Rosendahl 1992; Morley et al. 1999; Roberts et al. 2010; Hilbert-Wolf and Roberts 2015).

2.3. Lower, middle and upper Lake Beds Stratigraphy and Sedimentology

This project has helped to document the detailed sedimentology and depositional environments of the Lake Beds strata (Chapters 1-3) in the southern part portion of the Rukwa Rift Basin, recognizing at least three distinct stratigraphic units. These include a basal, richly fossiliferous lower Lake Beds unit (chapter 2: Mtelela et al., in press). Preliminary biostratigraphic and geochronologic data suggest that the Lower Lake Beds was deposited during the late Miocene to early or middle Pleistocene depositional ages (Hilbert-Wolf et al., 2013, 2015; in press; N.

Stevens, pers. comm.). Work by Hilbert-Wolf has focused on the seismicity of these deposits (Hilbert-Wolf and Roberts, 2015). Based on lithologic variation across the strata, the lower Lake Beds was informally subdivided into two distinct members: a poorly fossiliferous, volcanic-rich lacustrine lower member (Member A) deposited during the late Miocene; and a richly fossiliferous, fluvial-floodplain dominated upper member (Member B) deposited between the Pliocene and middle Pleistocene. The middle Lake Beds are characterized by a series of isolated exposures, many fault bounded, throughout the southern end of the rift. The less well-exposed and faulted nature of the middle Lake Beds exposure makes it difficult to fully assess its distribution, age, and lithostratigraphic relationships. However, detailed sedimentology of a series of isolated outcrop exposures, coupled with pilot U-Pb and Ar/Ar age dating, provides a preliminary understanding of these strata, which are most likely early to middle Pleistocene in age (H. Hilbert-Wolf, pers. comm.; A. Deino, pers. Comm.), and were subdivided into five informal stratigraphic units, termed the middle Lake Beds Group members A-E (Chapter 3). As of yet, these deposits have only yielded plant macrofossils and trace fossils. The middle unit is characterized by localized lacustrine (including carbonate), volcaniclastics alluvial fan, and fluvial-floodplain facies. Overlying the middle Lake Beds is a thick succession of late Pleistocene-Holocene volcanic-rich, locally fossiliferous alluvial to deep-water lacustrine strata (Chapter 1: Mtelela et al., 2016). The upper Lake Beds record a spectacular continental ichnofauna, as well as abundant isolated fish remains, and isolated larger vertebrate macrofossils.

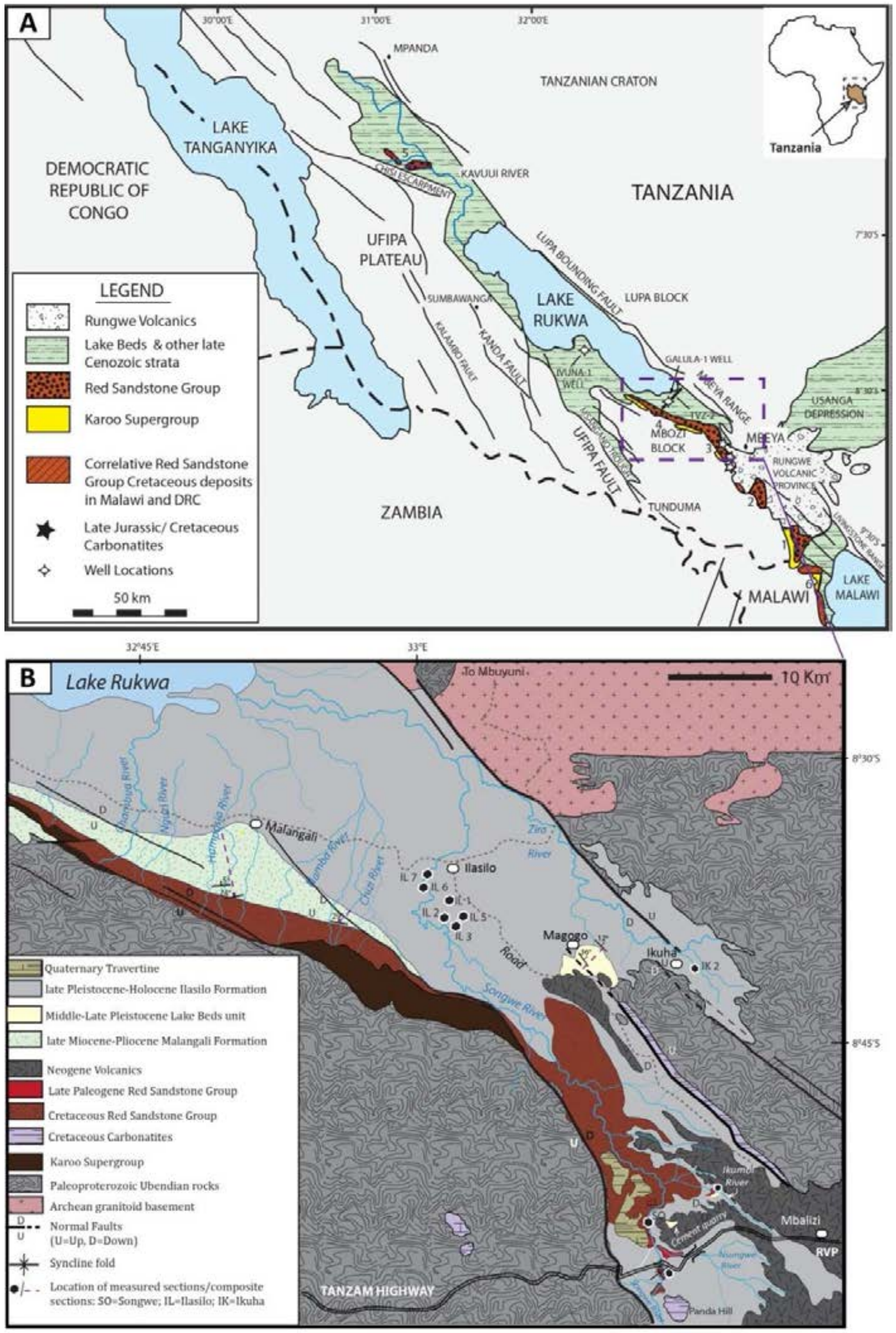

Fig. 1. **A)** Geologic map of the Rukwa Rift Basin showing tectonic elements, distribution of rock units and location of the study area (insert box). **B)** Geologic map of the southern Rukwa Rift Basin (study area), showing the distribution of the middle Lake Beds (at Magogo area and around Songwe Valley), Malangali and Ilasilo formations, as well as location of the measured sections along the upper Songwe River (Songwe area), the lower Songwe River (Ilasilo area), Hamposia, and Chizi river drainages (south and south-eastern Malangali Village) and around Ikuha area. Other lithologies and structures are adopted from Grantham et al. (1958) and Roberts et al. (2010) (Fig. 1A).

3. Methods and data

This study is based on extensive fieldwork conducted by the authors between 2012 and 2015, involving geologic and lithofacies mapping and measurement of numerous stratigraphic sections (Fig. 1). Topographic maps and the Mbeya 244 quarter-degree geologic map of Grantham et al. (1958) were used as base maps. In addition, a GPS set to the Arc 1960, a Jacob's staff, and Brunton compass were used for mapping and measurement of stratigraphic sections. Sedimentologic investigation and stratigraphic analyses of the Lake Beds succession are outlined in Chapters 1-3. The naming of stratigraphic units follows the International Stratigraphic guidelines (Murphy and Salvador, 1999).

In addition, to better understanding the hydrocarbon prospectivity of the basin, a series of representative rock samples from across the Lake Beds stratigraphy were collected for bulk x-ray diffraction (XRD) analysis to supplement sandstone mineralogy data deduced from microscopic (thin-section) petrography (Mtelela et al., 2016, in press). In addition, powdered XRD was performed on a subset of these samples to determine clay mineralogy as a proxy for paleoclimate and reservoir characteristics. The XRD analysis was conducted at Sietronic Laboratory, Australia, involving both qualitative (6 samples) and quantitative (7 samples) mineral phase analyses.

Each sample was air dried then milled in a standard ring mill. The resulting powder was then prepared as an unoriented powder mount of the total sample for XRD analysis. The clay fraction was concentrated from the bulk sample and used to prepare oriented clay mounts. The oriented clay mounts were run as untreated, after glycolation and heat treatments at 350°C and 550°C to aid clay mineral identification. The XRD patterns were produced using a Bruker-AXS D4 XRD with copper radiation at 40 kV and 30 mA. A graphite monochromators was used in the diffracted beam. Powder mounts were run over a range of 3 to 70°2Ø, with a 0.02 degree step and a 2 second per step count time. Clay mounts were run over a range of 1.3 to 22°2Ø, with a 0.015 degree step and a 2 second per step count time. The search/match was carried out using Bruker Diffrac^{plus} Search/Match software and the ICDD PDF-2 database (2006). The quantitative phase analysis was performed using SIROQUANT^{TM} version 4 software.

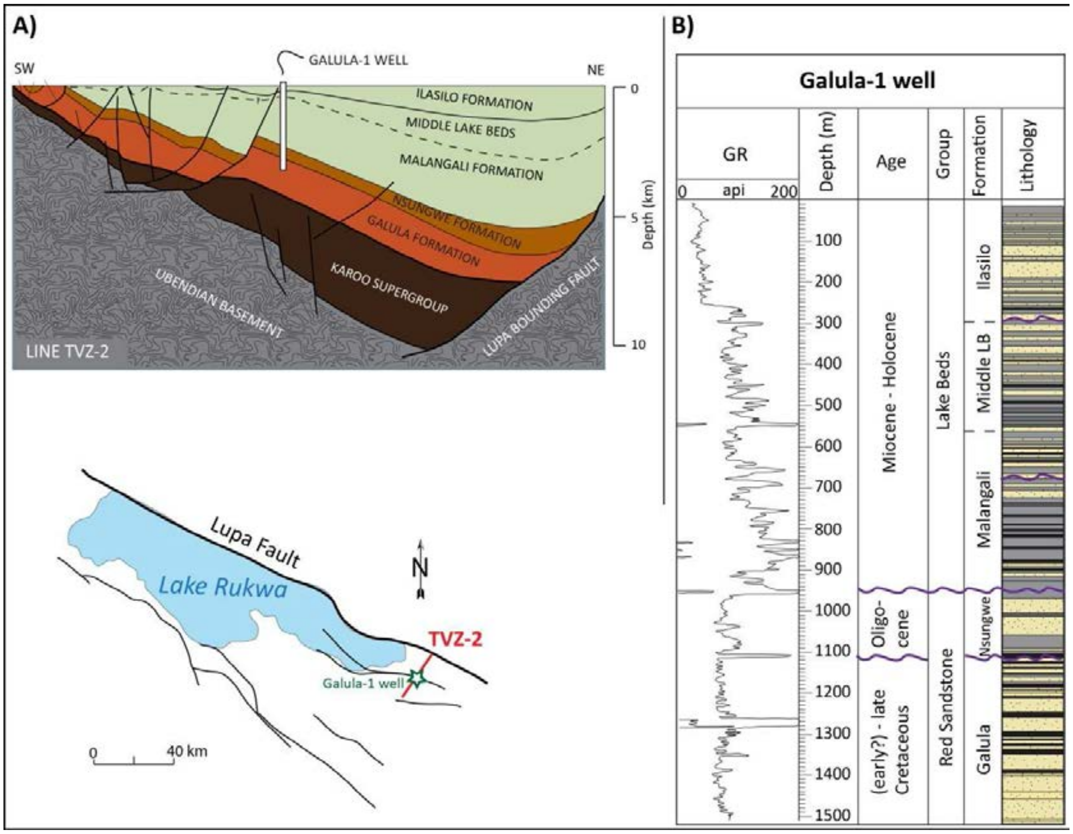

Fig. 2. **A)** Schematic seismic section through the Rukwa Rift Basin in the vicinity of the Galula-1 well (see location in the lower left map, and in Fig. 1), showing the inferred structure and stratigraphy of the basin, including the proposed subdivision of the Lake Beds Group, based on seismic line TVZ-2 (Tanzania Petroleum Development Corporation, Dar es Salaam). **B)** Galula-1 well log, showing lithologic subdivision of the Lake Beds Group and underlying Red Sandstone Group (modified from legacy Galula-1 well log data obtained by Amoco Production Company for Tanzania Petroleum Development Corporation; R. Downie pers. comm.).

4. The proposed subdivision and nomenclature for the Lake Beds Group

4.1. Defining the Lake Beds Group

The term 'Lake Beds' has been consistently used by all previous researchers in the Rukwa Rift Basin, to collectively refer to the uppermost strata in the basin, which has been deposited as a results of late Cenozoic tectonic development of the EARS. In this chapter, we propose to retain the usage of the term 'Lake Beds' for the Miocene - Recent stratigraphic succession in the Rukwa Rift Basin. However, because this package of rocks represents a long-lived heterogeneous suite of deposits, we have elevated the Lake Beds to group status. We propose that the Lake Beds Group (LBG) be formally subdivided into three temporal and lithologically distinctive formations; two formalised herein, with one to remain informal until further work can be completed (Fig. 3). The establishment of this formal stratigraphic subdivision resolves nomenclatural issues for future references, and provides for depositional age control in the Lake Beds strata, and provide an important framework for projecting these units down-dip into seismic and exploration wells for hydrocarbon prospectivity analysis. The proposed formations are defined and described below in stratigraphic order from oldest to youngest.

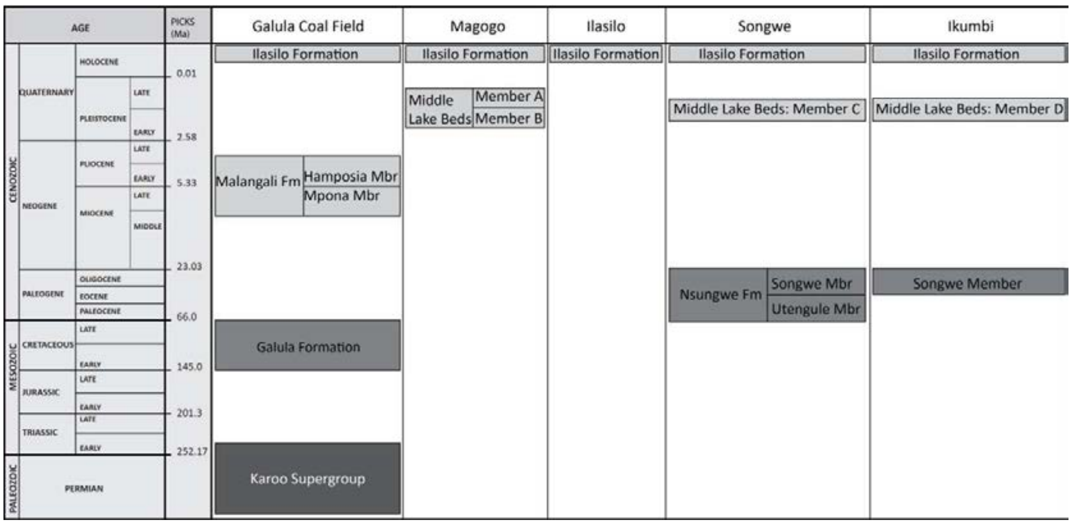

Fig. 3. Stratigraphic summary of the Rukwa Rift Basin, showing the distribution, subdivision and proposed nomenclature of the late Cenozoic Lake Beds Group formations and members.

4.2. Malangali Formation

The name Malangali Formation is proposed for the late Miocene-Pliocene succession of the Lake Beds Group (lower Lake Beds succession of Mtelela et al., in press; Hilbert-Wolf et al., in press). The name 'Malangali' refers to the village located a short distance to the northeast of the proposed type locality in the Galula Coalfields (Figs. 1 and 3). The Malangali Formation is defined here as a succession of siliciclastic-dominated conglomerates, sandstones, mudstones, and paleosols, as well as tuffaceous conglomerate, sandstone and ash (bentonitic) beds of various colours (see Fig. 4), located between the Cretaceous-Oligocene Red Sandstone Group and the middle lake Beds group (in wells) and the late Quaternary upper Lake Beds succession in outcrop.

4.2.1. Faunal record

The Malangali Formation preserves an important new vertebrate and invertebrate fossil record. To date, a total of 44 fossil specimens have been recovered from seven most productive localities across the Malangali Formation (Fig. 4; see also Mtelela et al., in press). Faunal remains identified so far include fishes, turtles and crocodylians, as well as rare, but well-preserved cranial and post-cranial mammals, including hippopotami. A detailed faunal description of the fossil materials from this formation is underway (Stevens et al., in prep.)

4.2.2. Genesis, sedimentology and depositional environments

The Malangali Formation is interpreted as a fluvial-lacustrine depositional system, characterized by proximal to medial reach alluvial setting, long-lived braided fluvial channels and flood-basin ponds and lake environments (Fig. 4). Sedimentology and depositional environments are described in Chapter 2 (Mtelela et al., in press). Paleocurrent indicators suggest that rivers were flowing mainly towards north and northeast directions (see Fig. 3 in Mtelela et al., in press). Climate driven hydrodynamic cyclicity of fluvial systems can be inferred from the alternating nature of fluvial channel-fill complex and calcareous paleosol horizon development, which is consistent with deposition during semi-arid climatic regimes based on sandstone petrology and faunal record. This interpretation is also supported by clay mineralogy data presented in this paper.

4.2.3. Boundaries

The lower boundary of the Malangali Formation is identified as an unconformable (erosional angular unconformity) surface clearly exposed in the cliff-face exposures along the Hamposia River drainage, near the Mpona village, where the basal, gently-dipping vein-quartz conglomerate bed overlie steeply-dipping red sandstones of the Cretaceous Galula Formation. Elsewhere in the study area, including along the Chizi and likely other nearby rivers in the area, a basal angular unconformity of various degrees is also exposed where Lake Beds Group overlies the Cretaceous Galula Formation. The upper boundary of the Malangali Formation is marked by a low-angle unconformity surface that is poorly exposed at the end of the section along the Hamposia River, but clearly mapped out along the middle portion of the section as well as in the Chizi section (Figs. 4 and 5).

4.2.4. Type locality and stratotype section

The type section begins at GPS coordinates (Arc 1960) 8°37′54″S, 32°49′10″E along the Hamposia River drainage near Mpona Village, where the basal conglomerate and sandstone beds dips 18° to the NW, overlying the 24°NW dipping Namba Member of the Galula Formation. Above this angular unconformity, deposits of the Malangali Formation exhibit a gradual decrease in the dip angle to ~5° by several kilometers downstream along a north-northwest transect. At the downstream end of the section, as well as in multiple places upstream, the Malangalali (and in places, the Galula Formation), are overlain with angular unconformity by horizontally-bedded Quaternary-Holocene upper Lake Beds strata, herein termed the Ilasilo Formation. The most complete outcrop section of the Malangali Formation is found the type locality, along the Hamposia River, and is ~170 m thick; however, the top of the unit is covered unconformably by much younger deposits of the Ilasilo Formation. A reference section (lectostratotype section) is identified along the Chizi River (Fig. 5), and other auxiliary sections also crop out along the Chambua, Nguzi and Ikumbi river drainages (Fig. 1). However, the total extent of the Malangali Formation is recorded in seismic logs and two borehole logs of the Galula-1 and Ivuna-1 wells drilled by Amoco and published by Wescott et al. (1991). These borehole logs and well cuttings (Galula-1 and Ivuna-1 wells) from both boreholes are permanently stored in Dar es Salaam at the Tanzania Petroleum Development Corporation office, and were re-examined as part of this study (Fig. 2). Based on lithologic correlation, coupled with outcrop and subsurface (Galula-1 well cuttings) chronostratigraphic correlation reported by Hilbert-Wolf et al. (in press), the 560-950 m interval in the Galula-1 well (representing 390 m thick section) is considered here as a stratotype, and intervals penetrated by Ivuna-1 well as a hypostratotype section.

4.2.5. Mpona and Hamposia Members

The Malangali Formation exhibits clear variations in lithofacies and facies association between the lower and upper portion of the formation, which are separated by a well-developed unconformity surface at the 48 m level. The observed variations in sedimentology indicate clear changes in provenance and depositional environments between the lower and upper portion of the formation. These lithologic variations, described in detail in Mtelela et al. (in press) and summarized below, which clearly permit the subdivision of the Malangali Formation into two formal members. Thus, we propose the lower Mpona Member and the overlying Hamposia Member (Fig. 4). The two end members are well exposed in the type section, and along the Chizi River section (Reference section), and partly along Chambua and Nguzi rivers.

The Mpona Member, which is well-exposed in the type section along the Hamposia River and also at the base of Chizi section (reference section), is 48 m thick and dominated by a volcanic-rich mudstones and sandstone sequence. The basal ~5-23 m of the Mpona Member (Member A of the lower Lake Beds succession: Mtelela et al., in press) is characterized by a distinctive siliciclastic-dominated facies consisting of tabular to lenticular quartz pebble conglomerate and subordinate quartzose sandstones that unconformably overlie Cretaceous Galula Formation. The deposition of this basal interval of Mpona Member is interpreted to have occurred within alluvial setting, proximal to medial alluvial plain. The upper 40-45 m thick comprises volcanic-rich siltstones, ash beds (bentonites), tuffaceous sandstone and conglomerates that interpreted to record deposition in fluvial and floodbasin (lakes and ponds) depositional environments. Individual beds of siliciclastic sandstones vary in colour between very light gray (N8), pale red (5R 6/2) and grayish orange pink (5YR 7/2), whereas primary pyroclastic deposits and re-sedimented (fluvially reworked) volcanic-rich sedimentary deposits are pinkish gray (5YR 8/1), yellowish gray (5Y 8/1) or very light gray (N8) coloured. Mpona Member contains isolated bones of fish and fragments of large mammal bones within muddy/ash-rich fine-grained siliciclastic sandstone beds towards the upper part of this unit.

The Hamposia Member is defined as the siliciclastic dominated interval of the Malangali Formation resting above a calcareous paleosol and unconformity surface at the top of Mpona Member. The Haposia Member (Member B of the lower Lake Beds succession: Mtelela et al., in press) occurs extensively in the type section along the Hamposia River, as well as in the Chizi section and at the base of the Ikumbi section, and is characterized by the basal pebble-boulder clast-supported conglomerates, overlain by medium- to coarse-grained sandstones, pebble-cobble conglomerates, paleosols and minor mudstone and ash beds. Conglomerates are typically massive, tabular-lenticular and polymictic in composition, whereas sandstones are commonly quatzo-feldspathic and range in colour from greenish gray (5GY 6/1) or grayish yellow green (5GY 7/2) to grayish orange pink (5YR 7/2). The Hamposia Member is interpreted to have been deposited by fluctuating discharge, low-accommodation fluvial-flood plain systems that developed in a semi-arid depositional setting in which floodplain deposits and channel-fill fines underwent considerable pedogenesis (Mtelela et al., in press). Deposits of the Hamposia Member are richly fossiliferous, preserving abundant freshwater and terrestrial vertebrate remains including fish, turtles, crocodile and isolated large mammals that occurs within fluvial sandstone bodies and overbank paleosol horizons (Fig. 4).

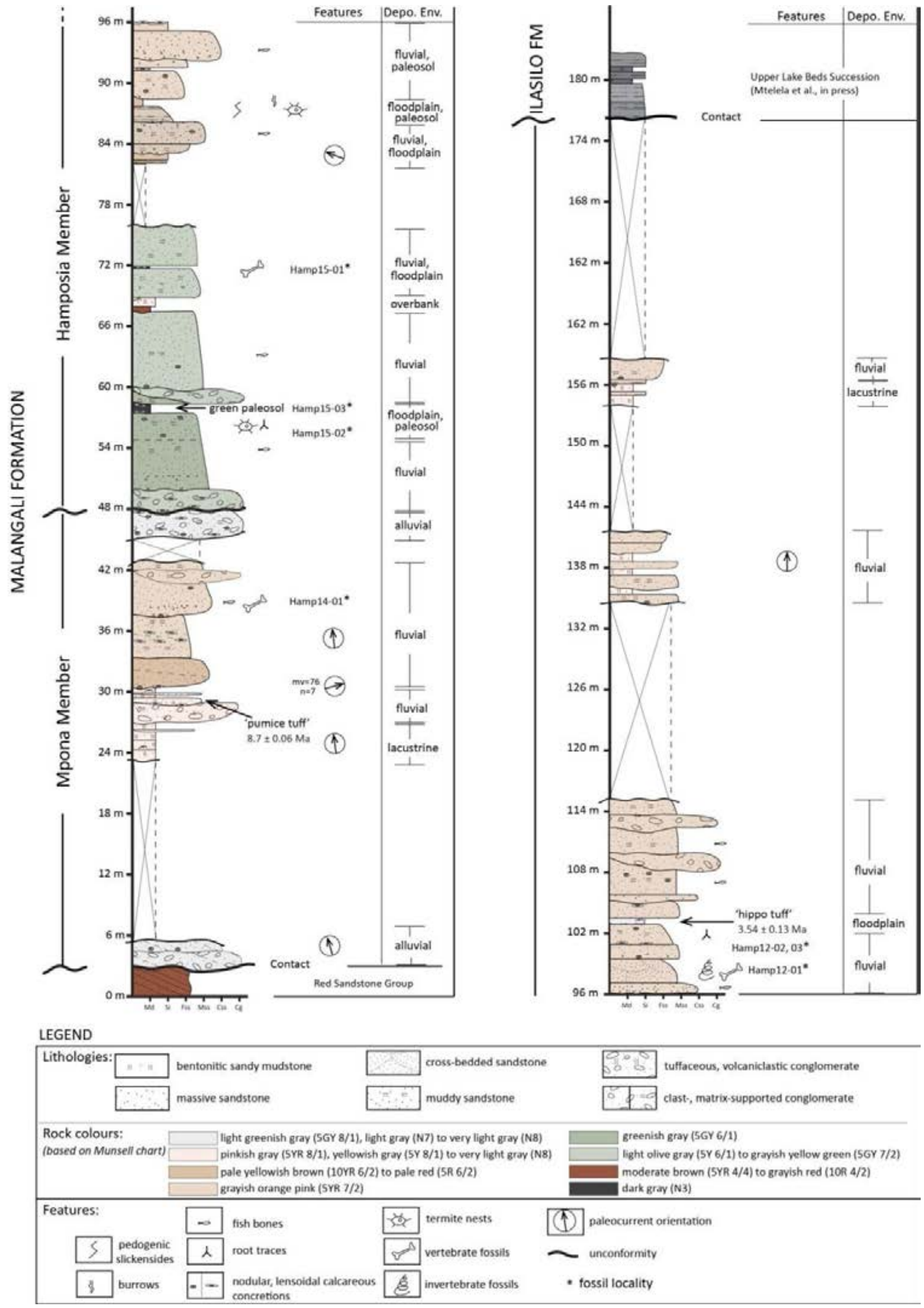

Fig. 4. Type section of the Malangali Formation along the Hamposia river drainage located just south of the Malangali Village (see Fig. 1 for location) (modified from Mtelela et al., in press).

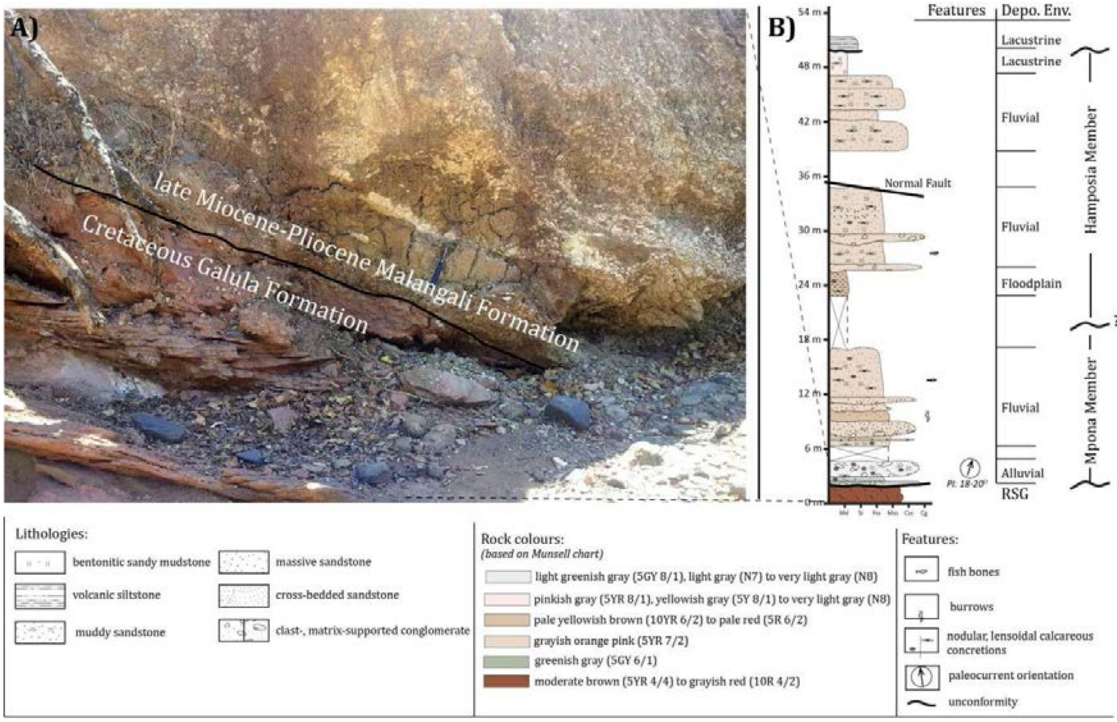

Fig. 5. **A)** The base of the Malangali Formation at the formation's reference section located along the Chizi River, showing an angular unconformity to the underlain Cretaceous Galula Formation. **B)** Chizi Section, Malangali Formation reference section located along the Chizi River.

4.3. The middle Lake Beds Group

The middle Lake Beds are characterized by a series of isolated units, many fault bounded, throughout the southern end of the rift, unconformably overlying the late Oligocene Nsungwe Formation or Cretaceous Galula Formation (Fig. 1, 3; see also Figs. 1 and 2 in Chapter 3). As of yet, these deposits have only yielded isolated fish remains, plant macrofossils and trace fossils. Preliminary Ar/Ar dating of a basalt overlying the middle lake beds near Tukuyu and detrital zircon (U-Pb) dating of two samples obtained from these deposits in the Mbeya Cement Quary indicates early to Mid-Pleistocene depositional ages (Hilbert-Wolf, H., pers. comm.). Sedimentology of the middle Lake Beds units is presented in chapter 3, and reveals that the middle Lake Beds are characterized by lacustrine and fluvial channels deposits.

Lithostratigraphic relationships across the middle Lake Beds Group are less understood, due to poor exposure and lack of continuity due to faulting, and these require follow-up mapping. However, lithologic variations across the mapped sections suggest the presence of at least five distinctive units, referred to as informal members (A-E) of the middle Lake Beds Group (Chapter 3). These include: 50-100 m thick limestone unit (member A), which is overlain by a distinctively different volcaniclastic unit comprising tuffaceous sandstones, siltstones, mudstones and thin conglomerates (member B), both occurs in the Magogo area. Members C and D are identified further to the south, in the Songwe Valley, where a series of faulted well-sorted siliciclastic sandstones (member C) exposed around the vicinity of the Mbeya Cement Company, and tuffaceous/ash-rich siliciclastic sandstone and conglomerate succession (member D) are exposed along the Ikumbi River, A final thin volcaniclastic siltstone unit (member E) crops out in the far south of the basin, near Tukuyu, which is directly overlain by basalt flow dated at ~500 ka.

4.4. Ilasilo Formation

We propose the name Ilasilo Formation for the late Quaternary Upper Lake Beds unit of the Lake Beds Group, deposited between late Pleistocene to Recent (Cohen et al., 2013; Mtelela et al., 2016). The formation is named after Ilasilo Village located where this unit well-exposed (Fig. 1). The Ilasilo Formation occurs everywhere across the study area, resting above the Malangali Formation, and in places directly overlying (with high-angle angular unconformity) the Cretaceous Galula Formation or late Oligocene Nsungwe Formation. The Ilasilo Formation is defined here as a succession of volcaniclastic-dominated (~80% of the succession) unit, comprising volcanic siltstone, ash beds and fluvial reworked volcaniclastic sandstones, interbedded siliciclastic sandstones, mudstone and minor conglomerates.

4.4.1. Faunal record

The Ilasilo Formation records a diverse continental ichnofauna, as well as abundant isolated fish, variety of ostracode and mollusc shell remains, and rare isolated larger vertebrate macrofossils consisting of isolated and heavily abraded bone fragments of limb and vertebral skeletal elements of large ungulates (Cohen et al., 2013; Mtelela et al., 2016). Minimal work has been conducted on the vertebrate fossils from the formation; however, preliminary ichnological investigations are underway.

4.3.2. Genesis, sedimentology and depositional environments

The Ilasilo Formation was deposited by a complex fluvio-lacustrine depositional system. Facies analysis conducted by Mtelela et al. (2016) revealed three major depositional systems, including: (1) the alluvial to fluvial channel system; (2) the delta system; and (3) the profundal lacustrine system. Analysis of paleocurrent indicators reveals basinward-directed fluvial drainage patterns that were strongly influenced by major border fault systems (Figs. 1, 6 and 7; see also Mtelela et al., 2016).

4.4.3. Lower Boundary

The lower stratigraphic boundary is defined as a low-degree (<5°) angular unconformity exposed at the Hamposia section, where the Ilasilo Formation overlie the late Miocene-Pliocene Malangali Formation. This unconformity contact, which is not exposed in most parts of the study area, is also interpreted in the subsurface section in the Galula-1 well logs at the 300 m depth (Fig. 2B; see also Fig. 3 in Hilbert-Wolf et al., in press).

4.4.4. Type locality and stratotype section

The type section is located at GPS coordinates (Arc 1960) 8°38′07″S, 33°00′47″E (Ilasilo section 6: Figs. 1 and 6) along the lower Songwe River, within the Ilasilo Village type area. Here, the Ilasilo Formation begins at ~861 m above sea level, and comprises horizontally-stratified volcaniclastic and siliciclastic conglomerate, sandstone, siltstone, mudstone and ash beds. The basal contact is not exposed at the type locality. Seven reference sections for the Ilasilo Formation have been identified. These reference sections are Ilasilo section 1-5, and Ilasilo section 7 that occurs along the type locality, as well as Ikuha section 2, which occur along the Ikuha Valley (Figs. 1, 6 and 7; see also Mtelela et al., 2016). There are no major lithologic variations across the Ilasilo Formation to warrant lithostratigraphic subdivision of the formation. The exposed section of the Ilasilo Formation is 50-100 m thick. However, the formation may be as thick as 2 km in the subsurface as indicated by overall northeast thickening of the strata in the seismic profiles (Wescott et al., 1991; Morley et al., 1999) and Galula-1 and Ivuna-1 well cuttings. We therefore consider the upper 300 m interval penetrated by the Galula-1 well (Fig. 2B; see also Fig 3 in Hilbert-Wolf et al., in press) as a stratotype.

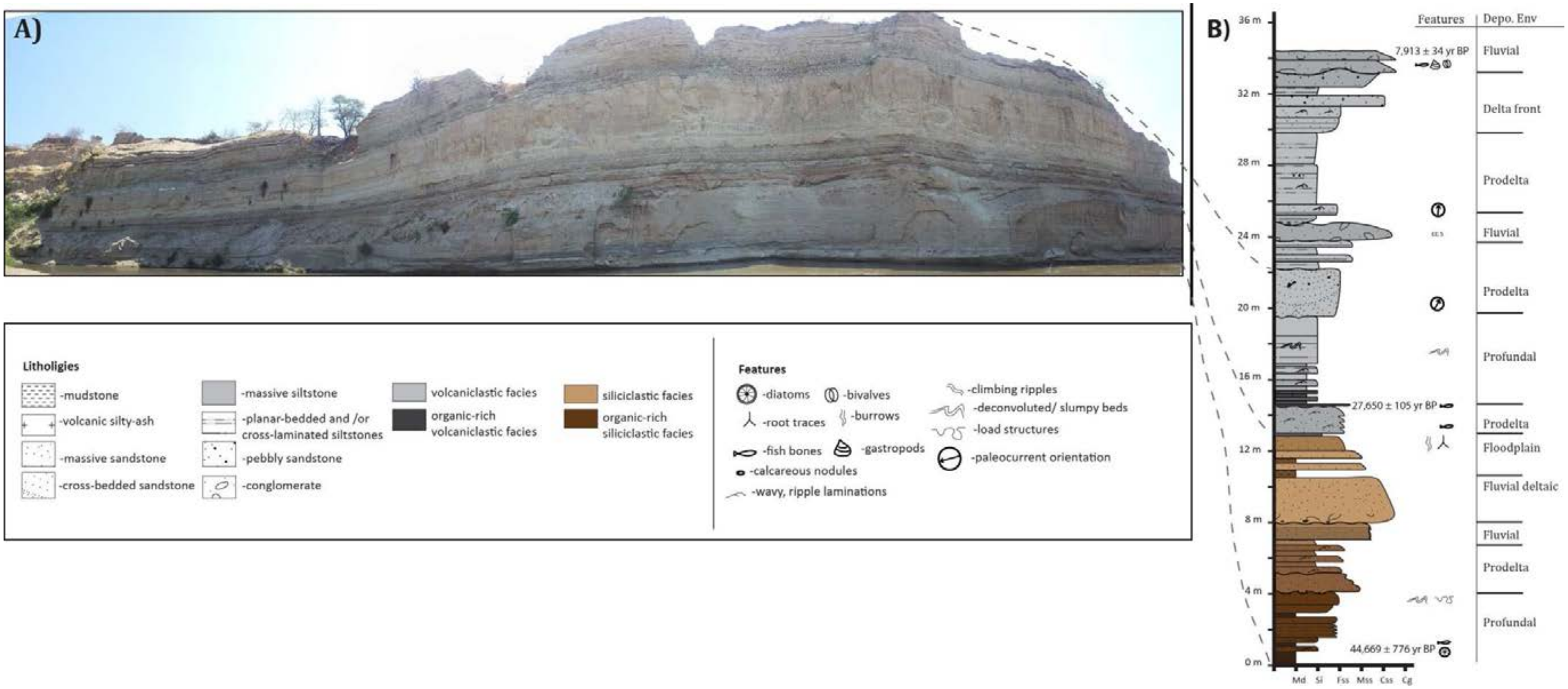

Fig. 6. Type section of the Ilasilo Formation along the lower Songwe River, around Ilasilo area, located at 8°38′07″S, 33°00′47″E (Modified from Mtelela et al., 2016).

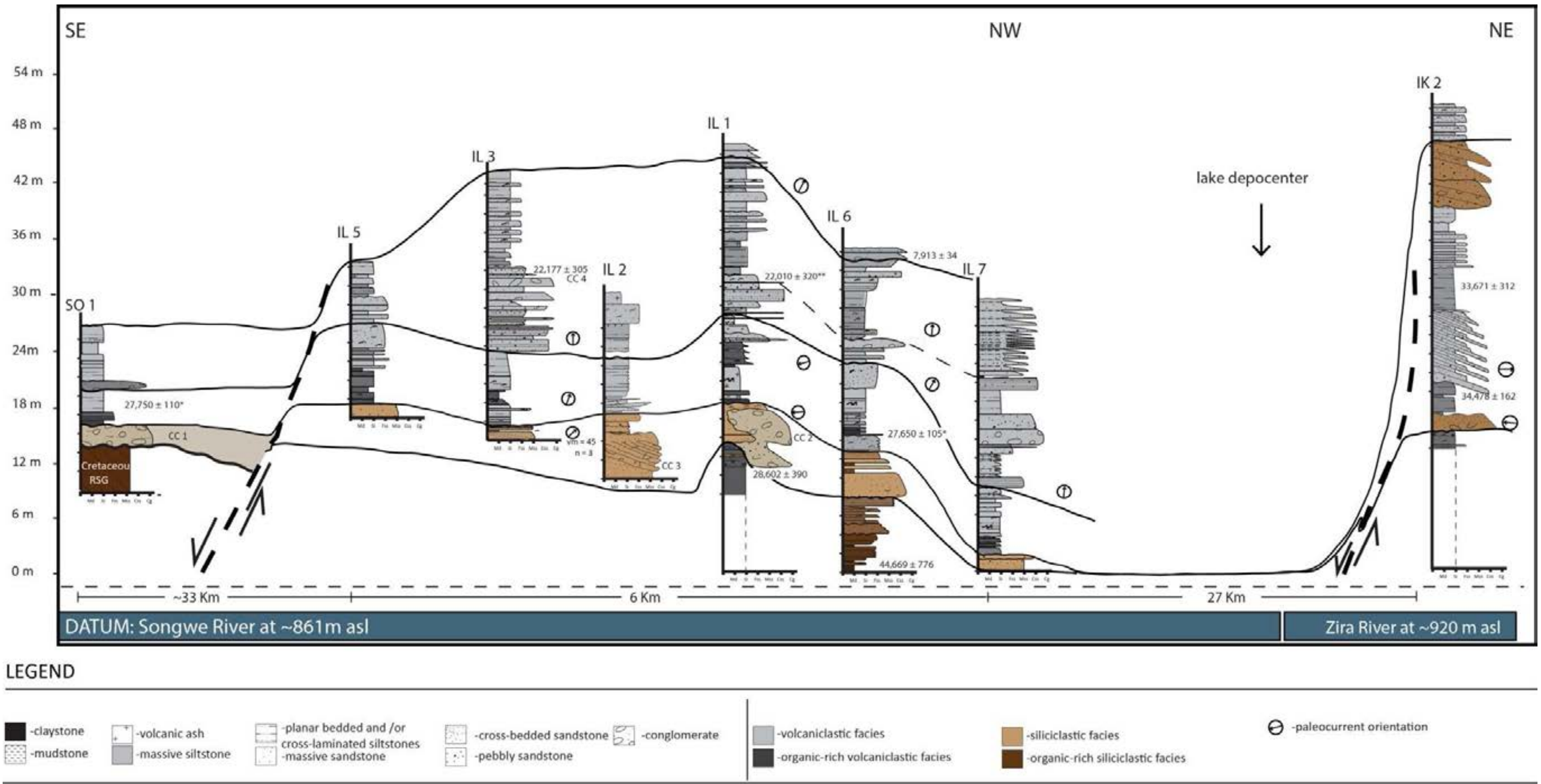

Fig. 7. Litho- and chronostratigraphic correlation of the exposed Ilasilo Formation, type section (IL 6) and reference sections. Radiocarbon age data are from Cohen et al. (2013) -denoted by **, Hilbert-Wolf and Roberts (2015) –denoted as * and from Mtelela et al. (2016).

5. X-ray Diffraction (XRD) Results and Discussions

X-ray Diffraction (XRD) results are presented in Tables 1 and 2, as well as scans (diffraction patterns) (see supplementary material). XRD analysis of oriented clay mounts indicates the presence of smectite, illite and kaolin clay minerals at various proportions across formations and members of the Lake Beds Group (Table 1). The clay mineral XRD data show that the Mpona Member of the Malangali Formation is dominated by smectite. A representative volcanic tuff sample (sample 7713-6) shows pure smectite, which is interpreted to have resulted from devitrification of volcanic ash (cf. Altaner and Grim, 1990; Roberts et al., 2010). Paleosols, and siliciclastic muddy sandstones from the Mpona Member reveals mostly smectite with minor mixed-layer illite/smectite and kaolinite. This composition is interpreted to record tropical semi-arid climatic (e.g., Roberts et al., 2010) conditions during the later stages of deposition of the Mpona Member, and also indicates a volcanic protolith (breakdown of volcanic ash to smectite). From the Hamposia Member, XRD analysis of the clay fractions from the representative siliciclastics lithofacies indicates a relatively smectite-rich composition, with abundant mixed layer illite/smectite clays, suggesting the persistence of the tropical semi-arid climatic conditions during deposition of the Hamposia Member.

On the other hand, the XRD data indicates a complex variation in the proportion of clay mineral content obtained from the representative samples across the Ilasilo Formation (see Table 1), with no specific trends on remarkably smectite-, mixed layer- or kaolinite-dominant phases. However, samples 72323-2, 61513-1, and 715513-1 shows slightly higher values of illite/muscovite (mixed layer), whereas sample 71313-1 reveals relatively higher abundancy of smectite.

Table 1. Mineralogical composition of clay fraction (<4 μm) in the Lake Beds Group

Formation (Member)	Location	Lithology	Sample number	Clay minerals			Interpretations
				Smectite (Montmorillonite)	Illite/muscovite	Kaolin	
Ilasilo Formation	Type section	volcanic siltstone	72323-2	<LOD*	9	3	-
Ilasilo Formation	Ikumbi section	organic rich mudstone	7714-4	Minor	trace	Trace	-
Ilasilo Formation	Type section	siliciclastic sandstone	61513-1	<LOD*	7	<LOD*	-
Ilasilo Formation	Ilasilo section 3	siliciclastic sandstone	71513-1	<LOD*	5	1	-
Ilasilo Formation	Ilasilo section 1	siliciclastic sandstone	61612-3	Trace	trace	Trace	-
Ilasilo Formation	Ilasilo section 1	organic-rich vitric ash	71313-1	14	4	9	-
Ilasilo Formation	Ikuha section	volcanic siltstone	71814-2	Major	trace	Trace	Devitrified volcanic ash; Good seal properties
Malangali Formation	Type section	siliciclastic sandstone	72013-1	minor	trace	Trace	Tropical semi-arid climate;

(Hamposia Member)							Devitrified volcanic ash source
Malangali Formation (Hamposia Member)	Type section	siliciclastic sandstone	71913-6	36	10	2	Tropical, semi-arid climate; Devitrified volcanic ash source
Malangali Formation (Mpona Member)	Chizi section	siliciclastic muddy sandstone	6713-6	43	6	3	Tropical, semi-arid climate
Malangali Formation (Mpona Member)	Chizi section	siliciclastic sandstone	7613-5	major	trace	Trace	Tropical, semi-arid Climate; devitrified volcanic ash source; Good seal properties
Malangali Formation (Mpona Member)	Type section	volcanic tuff	7713-6	84	<LOD*	ND	Tropical, semi-arid Climate; devitrified volcanic ash source; Good seal properties

Qualitative and quantitative analyses data. Qualitative analyses are based on estimation of relative (%) abundance only: major = 100-30, minor = 30-10, trace/possible =10-detection limit. <LOD* = Less than Level of Detection, phase noted in concentrated clay mounts only. ND = Not Detected

5.2. Whole rock Quantitative X-ray Diffraction (XRD) Results

Whole rock quantitative XRD analysis was performed for the seven representative rock samples across the Lake Beds Group to supplement microscopic petrographic investigation reported in Chapers 1 and 2. This mineralogical investigation was carried out to further characterize mineralogy of the volcaniclastic and siliciclastic lithologies of different units of the Lake Beds Group. The results are presented in weight percent in Table 2, and are summarized separately below for volcaniclastic and siliciclastic representative lithologies.

Quantitative XRD data of the three volcaniclastic representative samples indicates that smectite (range 84-14%, avg. ~33%) is the dominant mineral. Quartz proportions range between 1-21% (avg 9%), whereas plagioclase and K-feldspar constitutes 13-18% (avg ~10%) and 15-23% (avg. ~13%), respectively. Other minerals includes mixed-layer illite/muscovite clays (4-9%, avg. ~4%), and kaolin (3-9%, avg. 4%). Amphibole and calcite were revealed from sample 71313-1, constituting 9% and 2%, whereas sample 72313-2 contained 3% Thenardite.

XRD data for the four siliclastic sandstones shows that quartz (25-50%, avg. 37%) is the dominant mineral constituent. Plagioclase and K-feldspar varies from 13-36% (avg. ~21%) and 3-29% (avg. ~14%), respectively. Clay minerals are dominated by smectite (36-43%, avg.

~20%), whereas mixed layer illite/smectite clay ranges between 5 and 10% (avg. 7%) and kaolin constitutes 1-3% (avg. 1.5%). Amphibole and calcite are revealed from one sample (sample 71513-1) obtained from the Ilasilo Formation, constituting 1% of the whole rock composition each.

Table 2. Siroquant quantitative phase analyses of the bulk rock fractions

Formation	**Malangali Formation**			**Ilasilo Formation**			
Lithology	**Silic. Sand-stone**	**Volc. Tuff**	**Silic. Sand-stone**	**Silic. Sand-stone**	**Volc. Silt-stone**	**Silic. Sand-stone**	**Volc. Silt-stone**
Sample ID	**6713-6**	**7713-6**	**71913-6**	**61513-1**	**71313-1**	**71513-1**	**72313-2**
Phase	**Weight %**	**Weight %**	**Weight %**	**Weight %**	**Weight %**	**Weight %**	**Weight %**
Smectile (Montmorillonite)	43	84	36	<LOD*	14	<LOD*	<LOD*
Quartz	25	1	31	43	21	50	5
Plagioclase feldspar (albite)	15	ND	18	36	18	13	13
K-feldspar (sanidine/ microcline/anorthoclase)	8	15	3	14	23	29	ND
Illite/ muscovite	6	<LOD*	10	7	4	5	9
Kaolin	3	ND	2	<LOD*	9	1	3
Amphibole (hornblende)	ND	ND	Possible trace	Trace	9	1	ND
Calcite	ND	ND	ND	ND	2	1	ND
Thenardite	ND	ND	ND	ND	ND	ND	3
Amorphous	ND	ND	ND	ND	ND	ND	67

ND = Not Detected, <LOD* = Less than Level of Detection, phase noted in concentrated clay mounts only.

Margin of error (absolute) in Siroquant analyses should be no greater than ±2% for phases 50-100%, ±5% for phases 10-50% and ±10% for phases 3-10%. Phases of approximately 3% and less are approaching detection limit. Actual accuracy is dependent on crystallinity of component phases, sample matrix, phase overlaps and sample preparation.

6. Discussion

6.1. Depositional history of the Lake Beds Group

6.1.1. Depositional Phase 1

The initiation of the LLB sedimentation (depositional phase 1: Fig. 8A) involved accumulation of super-mature, vein quartz dominated conglomerate and quartz arenites at the base of the Malangali Formation (Mpona Member) from longitudinally oriented (northwest-oriented) fluvial pediment that preceded major tectonic and volcanic reactivation in the basin (Chapter 2: Mtelela et al., in press). Sedimentary textural attributes of the deposits including thick, coarse-grained and massive nature of the conglomerate beds, interpreted as indicators of high-energy gravity-fallout deposits associated with floods or debris flows, suggests deposition during wet climatic conditions. However, the end of this depositional phase was probably marked by seasonal dry climatic conditions as demonstrated by the development of a thick calcareous paleosol horizon towards the upper limit of the quartzose conglomerate in sandstone beds, which is well developed in the Chizi section (Fig. 5).

6.1.2. Depositional Phase 2

The second depositional phase (depositional phase 2: Fig. 8B) records vertical and lateral transition of depositional environments from an initial fluvial pediment and the first appearance of small lakes and ponds (Chapter 2: Mtelela et al., in press) basinward towards the Lupa Fault. The development of depositional phase two is interpreted to have resulted from increased accommodation space associated with a rapid tectonic rifting and subsidence (see Fig. 11 of Mtelela et al., in press). Depositional phase 2 is characterized by massive influxes of volcanic deposits, including both primary ash falls and fluvial-reworked pyroclastic flows, and is associated with the first stage (~9.2-5.4 Ma) of explosive volcanism from the nearby Rungwe Volcanic Province (cf. Ebinger et al., 1989, 1993; Fontijn et al., 2012). This depositional phase and in particular, the occurrence of a lake transpired near the end of a period of putatively wet, stable climatic conditions in the late Miocene (deMenocal, 1995, 2004). A decrease in the rate of generation of accommodation space and rapid filling of available accommodation in the basin is envisaged towards the end of this depositional phase, and is demonstrated by a vertical transition from proximal (conglomerate dominated) braided channels to sandy-dominated channel systems (see Figs. 4 and 6, Chapter 2). A major pause in LLB deposition, which is identified as a sequence boundary, marks the end of this depositional phase. This major break in deposition is interpreted herein to be associated with a period of both volcanic and tectonic quiescence as well as dry climatic conditions, and marks the onset of a depositional phase 3.

6.1.3. Depositional Phase 3

This was the most extensive depositional phase in the Lake Beds sediment-fill history. Depositional phase 3 occurred during the Pliocene-Pleistocene, and is characterized by a combination of longitudinal and transverse fluvial channel flows (Fig. 8C). Based on sequence stratigraphic analysis, sedimentation during this depositional phase is interpreted to record sediment-fill within an underfilled lake-basin setting. The development of this depositional episode is associated with continuous, slow generation of accommodation space in the basin as a result of renewed faulting. Sedimentology, petrology and geochemistry presented in this thesis suggest that deposition was largely controlled by weathering and erosion of the uplifted Archean granitoid basement and Ubendian metamorphic rocks along the rift flanks as well as periodic explosive volcanism in the Rungwe Volcanic Province. Provenance shift in siliciclastic deposits, in particular a higher abundance of feldspars during this depositional phase, is interpreted to be consistent with regional aridification trend during this time. However, the observed fluvial channel depositional cyclicity associated with this depositional phase suggests a seasonal variability of a typical semi-arid regime. This interpretation is also supported by clay mineralogy data presented in this study from the Hamposia Member deposits. The end of deposition phase 3 followed a major in Lake Beds sedimentation, as revealed by an unconformity surface at the top of Late Miocene-Pliocene Malangali Formation to the overlain late Pleisticene-Recent Ilasilo Formation.

6.1.4. Depositional Phase 4

Depositional phase 4 is envisaged to have occurred during the early to mid-Pleistocene. This episode of deposition is interpreted to have developed by cyclic local, and at times basin-wide expanded lacustrine and fluvial channel systems, as indicated by widespread nature of the deposits and alternating nature of fluvial channel and lacustrine deposits (Chapter 3). Depositional units associated with this phase occur in isolated fault-bounded sections, which are interpreted to signal active tectonic movements during this depositional episode. Sedimentation patterns show alternating provenance between volcanic and uplifted rift flanks. Base level fluctuations during this depositional phase were most likely climate-driven, and probably partly influenced by voluminous production of volcanic sediments from explosive volcanic events in the Rungwe Volcanic Province (Fig. 8D) than rift tectonics (subsidence and uplift) related. The latter (tectonic movements in the Rukwa rift) are reported to have been moderate during the Pleistocene to Recent along the major border faults (Delvaux et al., 1998).

6.1.5. Depositional Phase 5

Depositional phase 5, which occurred during the late Pleistocene-Recent, is the last depositional episode of the Lake Beds Group (Figs. 6, 7, and 8D). Similar to depositional phase 4, sedimentation during this phase resulted from a highly dynamic fluvio-lacustrine depositional system that was strongly influenced by local and regional climatic cyclicity during the late Quaternary (Haberyan, 1987; Thevenon et al., 2002). Indeed, sedimentary patterns of this depositional phase are characterized by landward and basin shift of depositional environments, which reflects lake transgression and regression episodes (Fig 8D). Sequence stratigraphic analysis conducted by Mtelela et al. (2016) reveals six discrete depositional sequences that were strongly influenced by availability of water (climate) and sediment supply (explosive volcanism vs. weathering and erosion of the rift flanks). Thus, alternating deposition of siliciclastic vs. volcaniclastic units during this deposition is interpreted to reflect alternating episodes of rapid sedimentation due to pyroclastic fallout and secondary reworking of pyroclastic deposits versus slower sedimentation associated with weathering and erosion of the uplifted metamorphic and granitoid basement rocks along the rift flanks.

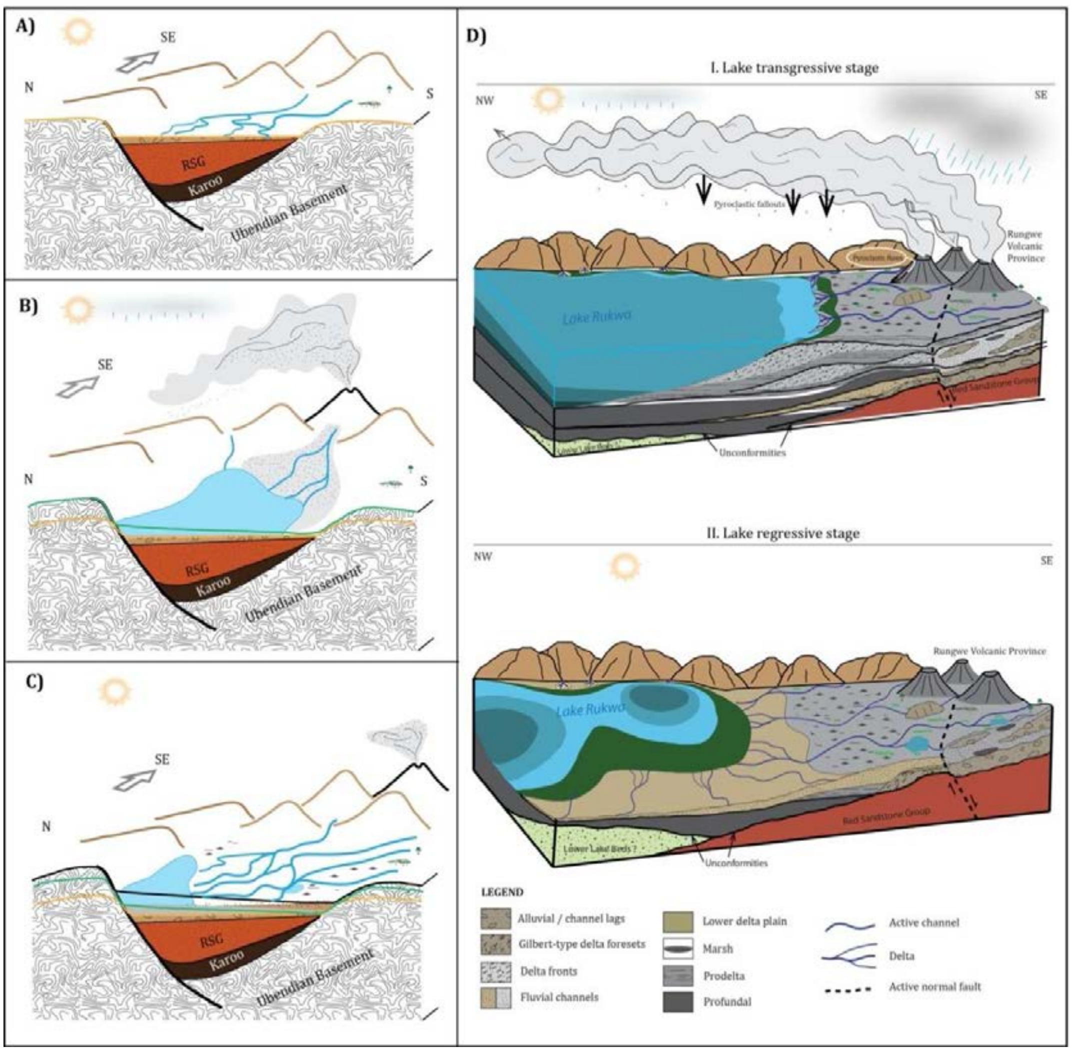

Fig. 8. Depositional history models (A-D) of the late Cenozoic Lake Beds Group.

6.2. Hydrocarbon Prospectivity of the Lake Beds Group

The Rukwa Rift Basin presents an attractive target for hydrocarbon exploration, based on the long history sediment-fill, complex structural patterns and high geothermal gradients, among other factors (cf. Morley et al., 1990, 1999; Mliga, 1994; Mbede, 2000). These factors are considered conducive for hydrocarbon migration and accumulation from lacustrine sources. Karoo sedimentary rocks with the potential to generate oil and/or gas are known from outcrop and could underlie the basin. There are no significant reported hydrocarbon shows from the Galula-1 and Ivuna-1 legacy test wells drilled in the late 1980s.

Here, we synthesize sedimentologic, stratigraphic, petrologic and mineralogic analysis presented in this chapter, to understand hydrocarbon exploration potential of the Lake Beds Group in terms of preliminary evaluation of the possible source, reservoir and seal rocks.

6.2.1. Source Rocks

Existence of regionally extensive and repetitive lacustrine environments in subsiding troughs, characterized by thick (up to 3 m) and possibly more in the depocenter) organic-rich (diatomaceous) mudstone and siltstone in the Lake Beds strata are considered potential source rocks. Sedimentologic and stratigraphic analysis reveals that profundal lacustrine environments occurred different times during the late Cenozoic development of the Lake Beds Group, including during the late Miocene, Pliocene, Pleistocene and Holocene (Figs. 4, 6, 7, and 8; Mtelela et al., 2016; Mtelela et al., in press). The high geothermal gradients in the basin, which is characteristic of the rift basins (Mbede, 1991), should have allowed a rapid maturation of such possible source rocks, and in particular the thicker, deep seated profundal lacustrine units towards the Lupa border fault. The complex structural pattern of the Rukwa Rift Basin, with long lived fault systems that penetrates into the Lake Beds strata (see Morley et al., 1999) might have served as upward-migration path ways for hydrocarbons.

Furthermore, high climatic and partly tectonic driven lake-level fluctuations observed throughout the late Cenozoic history of the Rukwa Rift Basin (Haberyan, 1987; Delvaux et al., 1998; Barker et al., 2002), which led to landward and basinward transition of facies provided for the cyclic development of both low-energy deposits (potential source rocks) and high-energy deposits (potential reservoir rocks) within the Lake Beds Group (Mtelela et al., 2016, in press).

6.2.2. Reservoir Rocks

Potential reservoir rocks in the Lake Beds strata includes thick and lateral extensive siliciclastic sandstone facies in the Late Miocene-Pliocene lower unit, as well as siliciclastic sandstone and carbonate rich middle-late Pleistocene middle Lake Beds units. Petrographic analysis conducted by Mtelela et al. (in press) reveals that these sandstone units are typically coarse- to medium/fine grained and subarkose in composition, dominated by quartz (75-81%) and feldspars (12-23%). Petrographic framework composition analysis is also supported by quantitative X-ray Diffraction (XRD) analysis reported in this study. Although porosity reported between 6% and 10%, most of the analyzed sandstone samples are less well cemented and moderately indurated, which suggests presence of good permeability. The exposed portion of the middle siliciclastics sandstone-dominated strata is ~110 m thick, but much thicker subsurface interval are have been occurs towards the basin depocenter, as revealed by Ivuna-1 and Galula-1 well logs (Fig. 2).

Provenance and sequence stratigraphic analysis (Mtelela et al., in press) suggested that siliciclastic deposition occurred during the volcanic quiescence in the Rungwe Volcanic Province, by weathering and erosion of the uplifted Archean granitoid and Paleoproterozoic Ubendian metamorphic belt. In the late Quaternary upper Lake Beds (in the Pleistocene-Recent Ilasilo Formation) exposures, siliciclastic sandstone are interbedded/overlain by thick volcaniclastic succession that were deposited during and soon after explosive volcanism from the Rungwe Volcanic Province (Figs. 7 and 8; Mtelela et al., 2016).

6.2.3. Seal Rocks

Volcaniclastic deltaic rock sequence (Figs. 1, 6, and 7; see also Mtelela et al., 2016), which are typically less porous (porosity <7%) and impermeable (and susceptible to weathering), occurring mainly at the upper, late Quaternary Ilasilo Formation of the Lake Beds Group provides for good seal rocks. Petrographic analysis of these sequences indicate that they are typified by the crystal-lithic tuffaceous sandstone and glass (shards +pumice) end members (Mtelela et al., 2016). Microscopic analysis of these deposits indicates that some have relatively abundant macropores, although they are patchily distributed, being present mainly within the altered tuffaceous material. These macropores appear mainly secondary in origin, having formed by the pronounced dissolution of the tuffaceous matrix and also variably sized and shaped grains. The macropores range in size from approximately 30-100 µm. Despite the fact that the macropores are abundant, they are either isolated or poorly connected with one another, and therefore impermeable. Bulk fraction quantitative XRD analyses reported here indicate that volcaniclastic deposits are dominated by smectite (up to 84 %; range 84-14%, avg. ~33%). Altogether, these petrographic and mineralogic characteristics of the volcaniclastic deposits make them excellent seal rocks for hydrocarbon accumulation in the Late Cenozoic Lake Beds Group from a lacustrine source.

7. Conclusions

Extensive investigation on Lake Beds succession in the Rukwa Rift Basin conducted between 2012 and 2015, involving geologic and lithofacies mapping, sedimentary petrology and geochronologic studies provide the basis to: subdivide the late Cenozoic Lake Beds into three-fold stratigraphy; and establish the first formal nomenclature for the strata, herein raised to Lake Beds Group, with two new formations defined. The previously unrecognised 170+ m-thick Late Miocene to Plio-Pleistocene lower Lake Beds unit is termed the Malangali Formation. The Malangali Formation is further subdivided into unconformity-bounded two members: the lower volcaniclastic-dominated Mpona Member; and an upper coarse-grained siliciclastic sandstone and conglomerate dominated Hamposia Member that record important new vertebrate fauna for this part of East Africa. The middle Lake Beds Group remains problematic, and more detailed investigation of the middle Lake Beds Group is required to fully understand the stratigraphic relationships and aerial extent of these deposits. Hence, the middle Lake Beds Group is referred to as informal members (A-E) of the middle Lake Beds unit for the time being. The Ilasilo Formation is proposed for uppermost volcanic-dominated late Pleistocene-Holocene Lake Beds succession, deposited in a fluctuating fluvio-deltaic to lacustrine depositional system. The Ilasilo Formation records an important continental ichnofauna, as well as abundant isolated fish remains, and isolated larger vertebrate macrofossils.

A synthesis of facies analysis, sedimentologic lithostratigraphic variations, petrology and mineralogy studies presented herein and in chapters 1, 2, and 3 are used to evaluate hydrocarbon prospectivity of the Lake Beds Group in terms source, reservoir and seal rocks potential. The results reveal that Lake Beds Group have viable source, reservoir and seal rocks for hydrocarbon generation and accumulation. In terms of source rocks, facies analysis indicates extensive lacustrine environments developed several times throughout the late Cenozoic history of the basin, characterized by thick (up to 3 m and possibly more in the depocenter) organic-rich (diatomaceous) mudstone and siltstone. In terms of reservoir rocks, lithologic, petrographic and mineralogic studies strongly suggest that the Hamposia Member and large portion of the middle Lake Beds unit (which comprises dominantly porous, less-indurated coarse-grained quartzo-feldspathic sandstone and conglomerate deposits) have potential reservoir capacity for hydrocarbon accumulation. The typically less porous and impermeable volcanic-dominated upper unit (the Ilasilo Formation) is identified as potential seal rocks.

Acknowledgements

We thank Tanzania Petroleum Development Corporation (TPDC) and Heritage Oil Rukwa Tanzania Ltd. for providing a PhD bursary to the lead author (CM) and funding to conduct extensive and detailed fieldwork in the rift. We are also grateful to the supported of the US National Science Foundation (EAR_1349825, BCS_1127164), the National Geographic Society (CRE), and the post-graduate research fund from James Cook University.

Supplementary material:

Bulk fraction quantitative XRD scans for seven (7) samples analyzed in this study

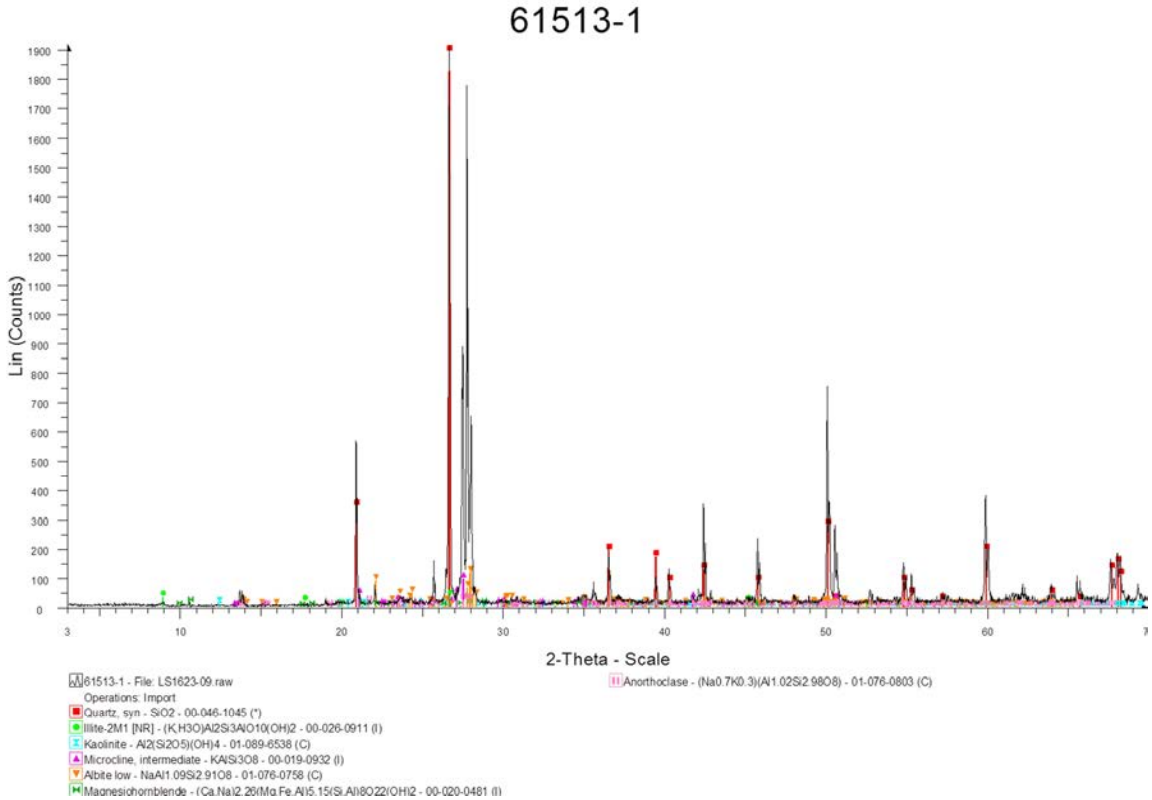

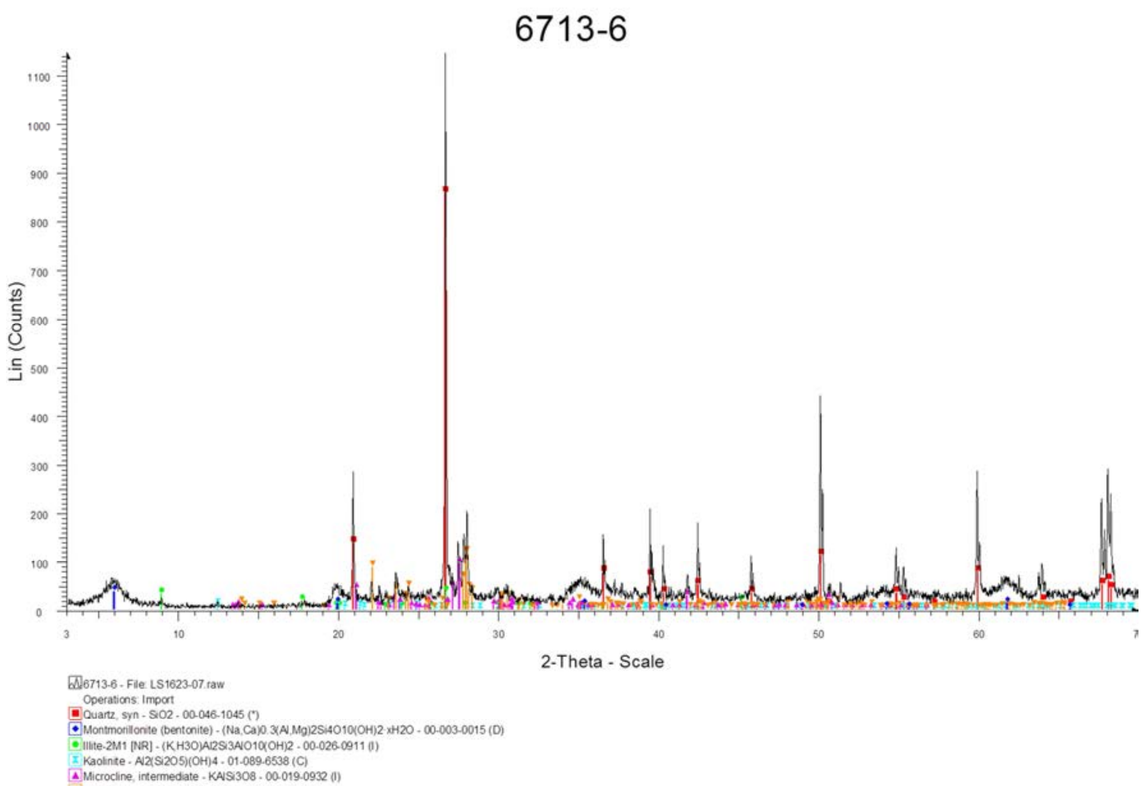

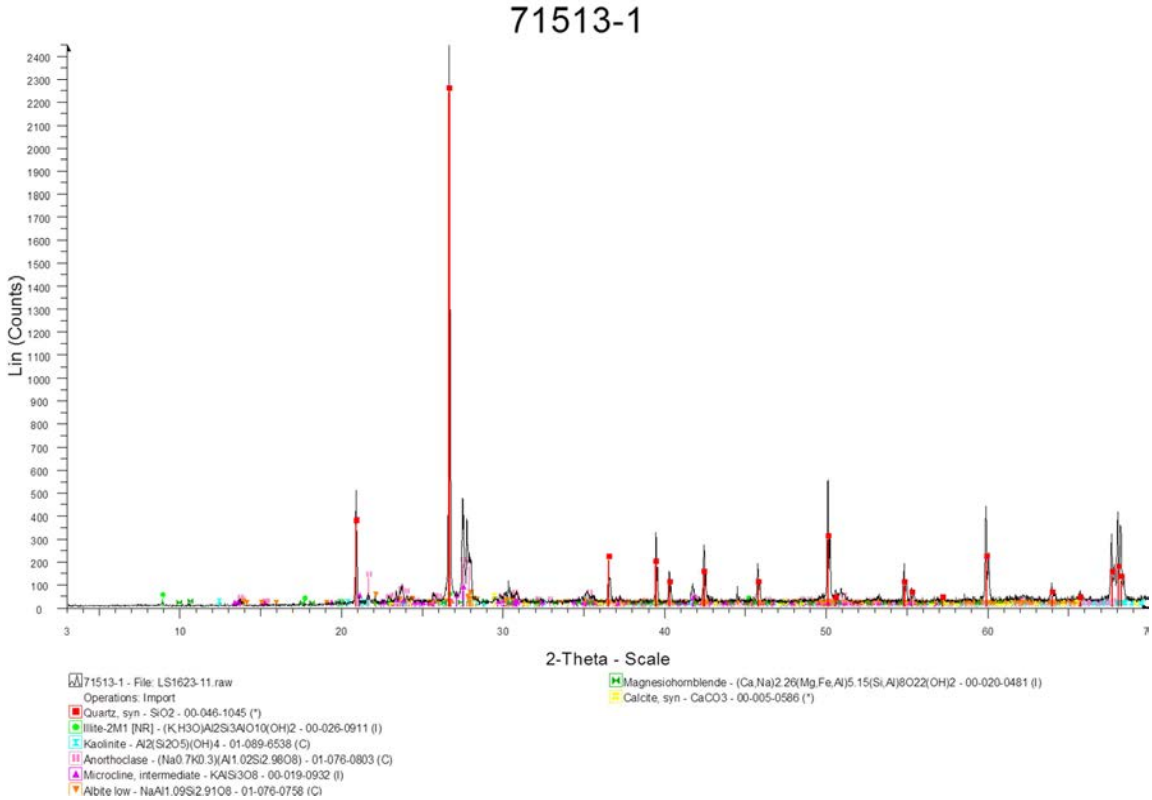
71513-1
Lin (Counts)
2-Theta - Scale
71513-1 - File: LS1623-11.raw
Operations: Import
Quartz, syn - SiO2 - 00-046-1045 (*)
Illite-2M1 [NR] - (K,H3O)Al2Si3AlO10(OH)2 - 00-026-0911 (I)
Kaolinite - Al2(Si2O5)(OH)4 - 01-089-6538 (C)
Anorthoclase - (Na0.7K0.3)(Al1.02Si2.98O8) - 01-076-0803 (C)
Microcline, intermediate - KAlSi3O8 - 00-019-0932 (I)
Albite low - NaAl1.09Si2.91O8 - 01-076-0758 (C)
Magnesiohornblende - (Ca,Na)2.26(Mg,Fe,Al)5.15(Si,Al)8O22(OH)2 - 00-020-0481 (I)
Calcite, syn - CaCO3 - 00-005-0586 (*)

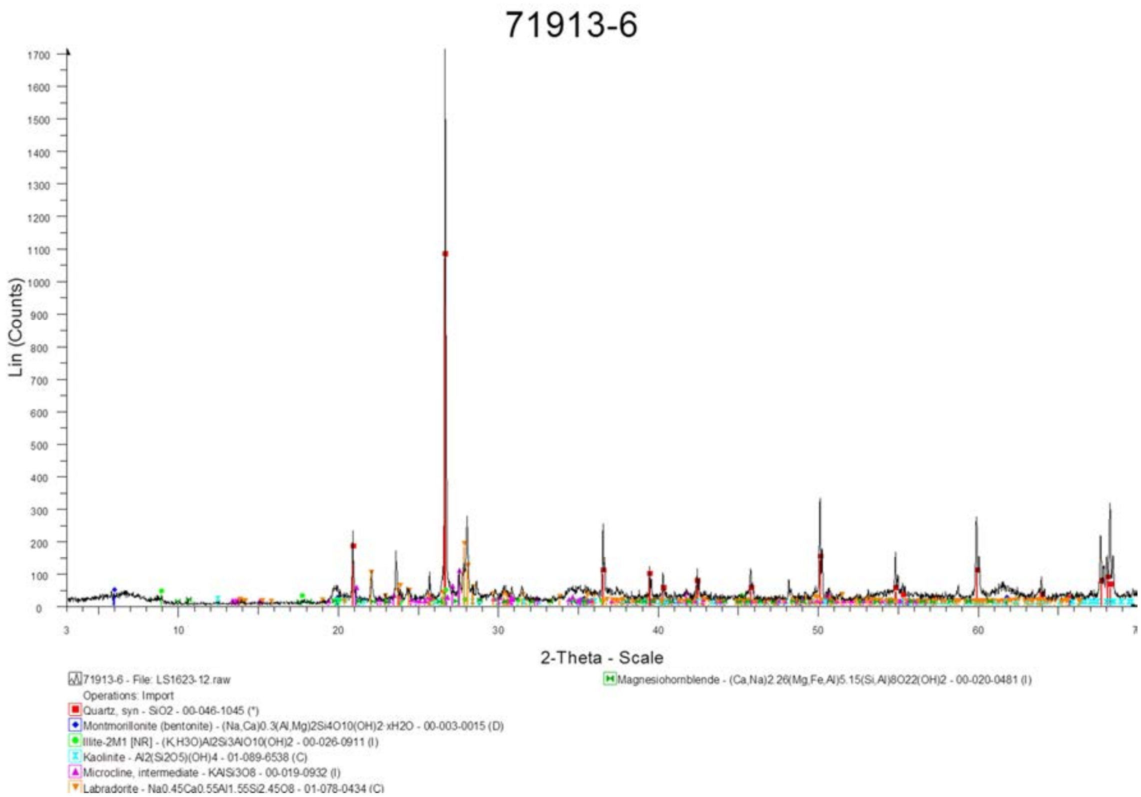
71913-6
Lin (Counts)
2-Theta - Scale
71913-6 - File: LS1623-12.raw
Operations: Import
Quartz, syn - SiO2 - 00-046-1045 (*)
Montmorillonite (bentonite) - (Na,Ca)0.3(Al,Mg)2Si4O10(OH)2·xH2O - 00-003-0015 (D)
Illite-2M1 [NR] - (K,H3O)Al2Si3AlO10(OH)2 - 00-026-0911 (I)
Kaolinite - Al2(Si2O5)(OH)4 - 01-089-6538 (C)
Microcline, intermediate - KAlSi3O8 - 00-019-0932 (I)
Labradorite - Na0.45Ca0.55Al1.55Si2.45O8 - 01-078-0434 (C)
Magnesiohornblende - (Ca,Na)2.26(Mg,Fe,Al)5.15(Si,Al)8O22(OH)2 - 00-020-0481 (I)

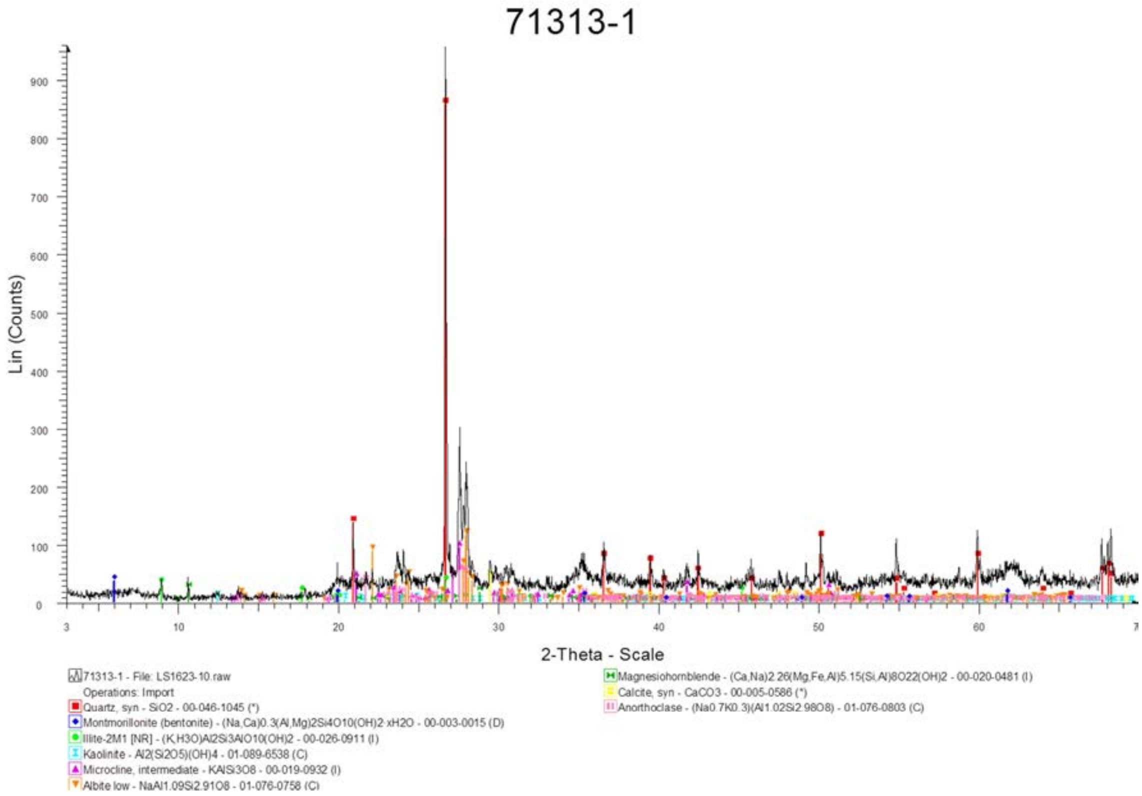
71313-1
Lin (Counts)
2-Theta - Scale
71313-1 - File: LS1623-10.raw
Operations: Import
Quartz, syn - SiO2 - 00-046-1045 (*)
Montmorillonite (bentonite) - (Na,Ca)0.3(Al,Mg)2Si4O10(OH)2·xH2O - 00-003-0015 (D)
Illite-2M1 [NR] - (K,H3O)Al2Si3AlO10(OH)2 - 00-026-0911 (I)
Kaolinite - Al2(Si2O5)(OH)4 - 01-089-6538 (C)
Microcline, intermediate - KAlSi3O8 - 00-019-0932 (I)
Albite low - NaAl1.09Si2.91O8 - 01-076-0758 (C)
Magnesiohornblende - (Ca,Na)2.26(Mg,Fe,Al)5.15(Si,Al)8O22(OH)2 - 00-020-0481 (I)
Calcite, syn - CaCO3 - 00-005-0586 (*)
Anorthoclase - (Na0.7K0.3)(Al1.02Si2.98O8) - 01-076-0803 (C)

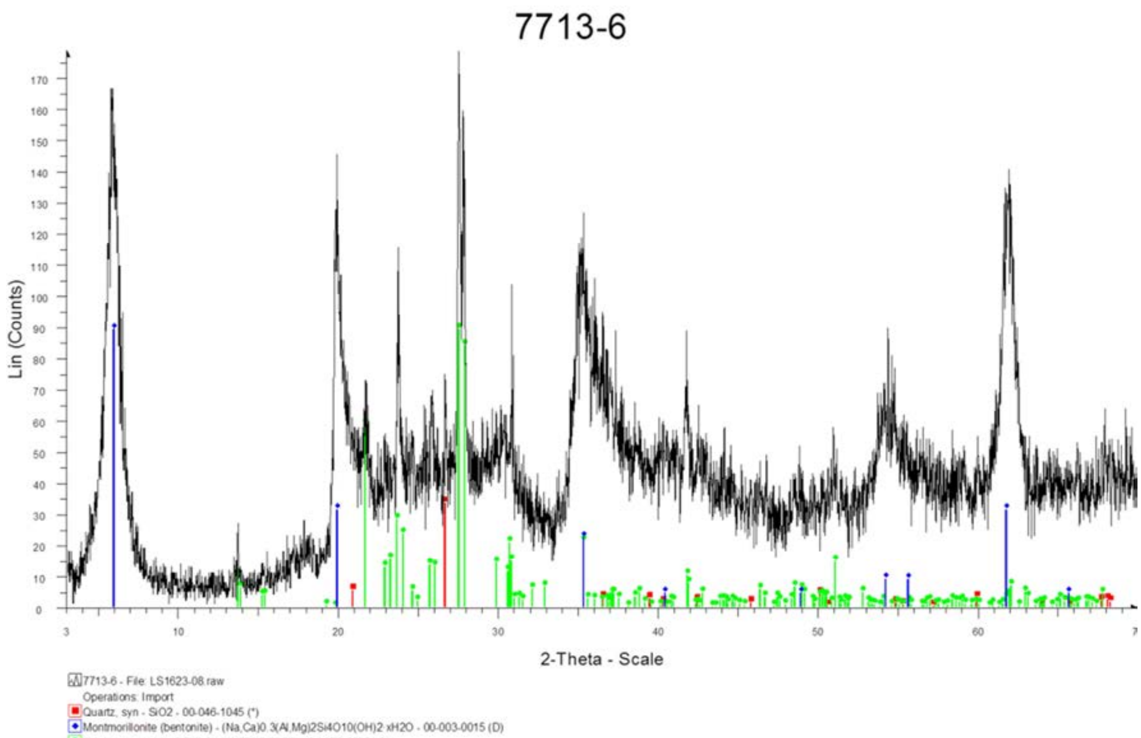
7713-6
Lin (Counts)
2-Theta - Scale
7713-6 - File: LS1623-08.raw
Operations: Import
Quartz, syn - SiO2 - 00-046-1045 (*)
Montmorillonite (bentonite) - (Na,Ca)0.3(Al,Mg)2Si4O10(OH)2·xH2O - 00-003-0015 (D)
Anorthoclase - (Na0.7K0.3)(Al1.02Si2.98O8) - 01-076-0803 (C)

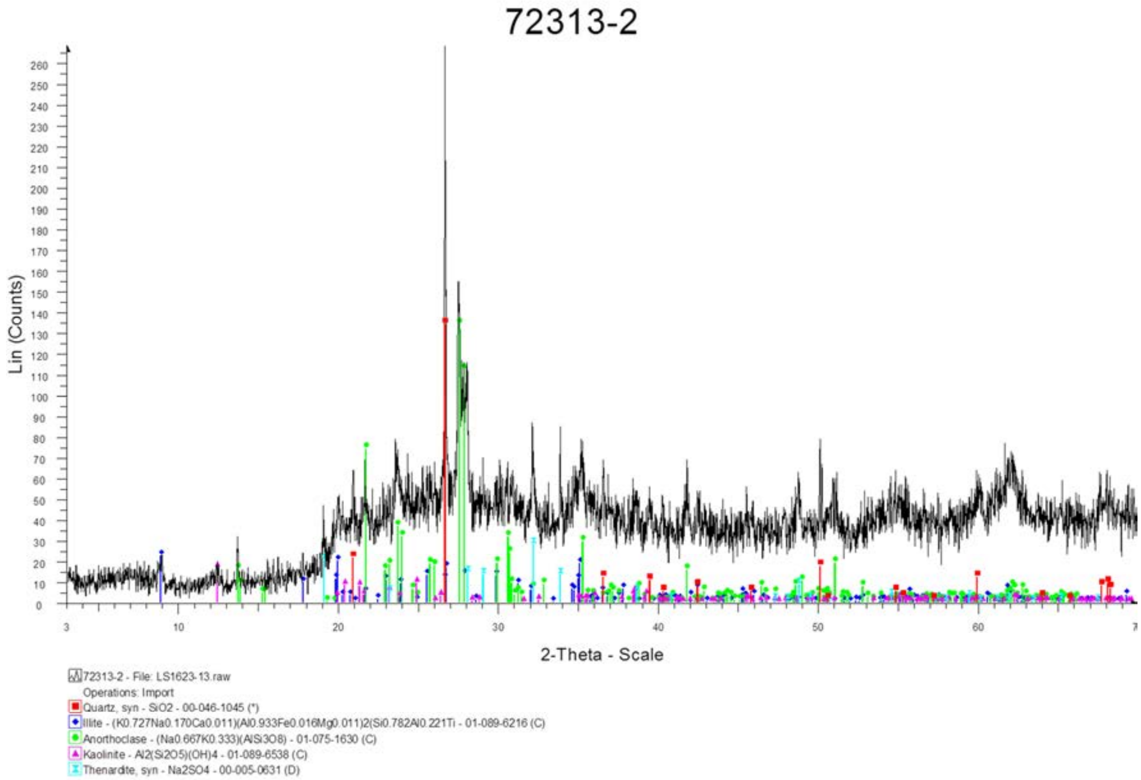
72313-2
Lin (Counts)
2-Theta - Scale
72313-2 - File: LS1623-13.raw
Operations: Import
Quartz, syn - SiO2 - 00-046-1045 (*)
Illite - (K0.727Na0.170Ca0.011)(Al0.933Fe0.016Mg0.011)2(Si0.782Al0.221Ti - 01-089-6216 (C)
Anorthoclase - (Na0.667K0.333)(AlSi3O8) - 01-075-1630 (C)
Kaolinite - Al2(Si2O5)(OH)4 - 01-089-6538 (C)
Thenardite, syn - Na2SO4 - 00-005-0631 (D)

Chapter 5

Conclusions

This research project presents a comprehensive sedimentologic and stratigraphic analysis of the poorly studied late Cenozoic Lake Beds succession in the Rukwa Rift Basin, southwestern Tanzania, and which constitute the main target of a renewed hydrocarbon exploration in the basin by Heritage Oil Company Ltd. Findings of this research contributes to better understanding of the depositional history of the Lake Beds succession, which is more complex than previously suggested during the regional geologic mapping conducted during the late 1950s. Applying a combination of geologic mapping, lithofacies analysis, sedimentary petrology, geochronology, and lithostratigraphic analysis, this study resulted in: (1) identification, description and interpretations of depositional environments of at least three distinctive depositional units associated with the Lake Beds, including the lower (late Miocene to Pliocene), middle (early to middle Pleistocene?), and upper (late Quaternary) units; (2) establishment of a formal nomenclature for this important lithostratigraphic succession, termed here the Lake Beds Group; (3) a refined understanding of the timing and relationships between sedimentation and climate changes, tectonics and volcanism; and (4) discovery of a series of important and previously unknown Miocene-Pleistocene vertebrate fossil localities in the East African Rift System.

Lithologic variations across the three identified stratigraphic units are used to establish a formal stratigraphy of the Lake Beds Group in the Rukwa Rift Basin, along with defining the new formations: the Malangali Formation that constitutes the late Miocene - Pliocene lower Lake Beds; and the Ilasilo Formation, which forms the late Quaternary upper Lake Beds. The middle Lake Beds lithostratigraphy is complex and poorly understood due to complex faulting system associated with the small and typically isolated exposures of this unit, and requires a follow-up mapping. However, sedimentologic analysis of the mapped middle Lake Beds exposures reveals distinctive lithologic characteristics across the strata, which are used to document five informal members (Member A - E) of the middle Lake Beds Group. Due to limited availability of field time, resources, and the expansive and difficult to access nature of the deposits in the rift, full documentation of these deposits lies outside the scope of the this PhD project, but provides a rich target for future research in this part of the East African Rift System.

This sedimentologic and stratigraphic research on the Lake Beds has provided critical data for evaluating the hydrocarbon prospectivity of the Lake Beds succession in the Rukwa Rift Basin. The previous geologic and geophysical surveys conducted on the Rukwa Rift Basin highlighted the potential structural attributes and presence of potential source and reservoir units across the Rukwa Rift Basin stratigraphy. However, these analyses were not conclusive. This study synthesize outcrop-based sedimentologic, stratigraphic, petrologic and mineralogic X-ray Diffraction (XRD) analysis across the Lake Beds strata to highlight hydrocarbon exploration potential of the Lake Beds Group in the Rukwa Rift Basin in terms of preliminary evaluation of possible source, reservoir and seal rocks for hydrocarbon generation and accumulation. The positive results indicated by this alpha-level (overview) evaluation encourage follow up exploration techniques across the basin, as well as sampling and analysis of the subsurface portion of the strata and underlying older units.

Apart from economic significance, this study has led to the discovery of an array of new fossils and trace fossils record that span between 8 Ma and 7 ka portion of the rift stratigraphy. The discovered fossils include fishes, turtles, crocodylians, and well-preserved mammal cranial and post-cranial remains, as well as continental trace fossils. The discovery of this suite of fossils and fossils localities provides a new window into a more complete palaeoenvironmental and palaeobiogeographic evolutionary history of eastern Africa during the late Cenozoic.

Although this research has broadly contributed to understanding of the Lake Beds sedimentology, stratigraphy and hydrocarbon exploration potential of the strata, more work needs to be done to better understand the distribution, litho- and chronostratigraphic relationships between middle Lake Beds units. This will likely take many years to sort out because the middle Lake Beds are exposed in small slices (outcrops), and are hard to identify due to subtle lithologic similarities with the Cretaceous and Oligocene Red Sandstone Group strata. To fully understand sedimentologic and stratigraphy of the middle Lake Beds, the future work will focus on searching and mapping new outcrops around Mbeya and Tukuyu areas, continuing dating new and previously mapped localities. In addition, future work on Lake Beds will also focus on continued investigation of the subsurface Lake Beds via detailed examination and sampling of legacy well-cuttings for hydrocarbon source and reservoir follow-up analyses, and stratigraphic analysis of seismic profiles acquired in the Rukwa Rift Basin.

References

Antia, J., and Fielding, C.R., 2011. Sequence stratigraphy of a condensed low- accommodation succession: Lower Upper Cretaceous Dakota sandstone, Henry Mountains, southeastern Utah. American Association of Petroleum Geologists Bulletin 95, p. 413–447.

Altaner, S.P. and Grim, R.E., 1990. Mineralogy, chemistry and diagenesis of tuffs in the Sucker Creek Formation (Miocene), Eastern Oregon. Clays and Clay Minerals 38, p. 561-572.

Ashley, G. M., 2000. Geologists probe hominid environments. GSA Today, Geological Society of America 10, p. 24–29.

Ashley, G.M., and Hay, R.L., 2012. Sedimentation patterns in a Plio-Pleistocene volcaniclastic rift-platform, basin Olduvai Gorge, Tanzania, in Renaut, R.W., and Ashley, G.M., eds., Sedimentation in Continental Rifts. SEPM (Society for Sedimentary Geology), Special Publication 73, p. 107-122.

Barker, P., Telford, R., Gasse, F., Thevenon, F., 2002. Late Pleistocene and Holocene paleohydrology of Lake Rukwa, Tanzania, inferred from diatom analysis. Palaeogeography, Palaeoclimatology, Palaeoecology 187, p. 295–305.

Barker, P., Williamson, D., Gasse, F., Gibert, E., 2003. Climatic and volcanic forcing revealed in a 50,000-year diatom record from Lake Massoko, Tanzania. Quaternary Research 60, p. 368–376.

Benvenuti, M., 2003. Facies analysis and tectonic significance of lacustrine fan-deltaic successions in the Pliocene–Pleistocene Mugello Basin, Central Italy. Sedimentary Geology 157, p. 197–234.

Berger, L.R., 2012. Australopithecus sediba and the earliest origins of the genus Homo. Journal of Anthropological Sciences 90, p. 1-16.

Berger, L.R., de Ruiter, D.J., Churchill, S.E., Schmid, P., Carlson, K.J., Dirks, P.H., and Kibii, J.M., 2010. Australopithecus sediba: a new species of Homo-like australopith from South Africa. Science 328, p. 195–204.

Berger, L.R., Hawks, J., de Ruiter, D.J., Churchill, S.E., Schmid, P., Delezene, L.K., Kivell, T.L., Garvin, H.M., Williams, S.A., DeSilva, J.M., Skinner, M.M., Musiba, CM, Cameron, N., Holliday, T.W, Harcourt-Smith, W, Ackermann, R.R., Bastir, M., Bogin, B., Bolter, D., Brophy, J., Cofran, Z.D., Congdon, K.A., Deane, A.S, Dembo, M., Drapeau, M., Elliott, M.C., Feuerriegel, E.M., Garcia-Martinez, D., Green, D.J., Gurtov, A., Irish, J.D., Kruger, A., Laird, M.F., Marchi, D., Meyer, M.R., Nalla, S., Negash, E.W., Orr, C.M., Radovcic, D., Schroeder, L., Scott, J.E., Throckmorton, Z., Tocheri, M.W., VanSickle, C., Walker, C.S.,Wei P, and Zipfel, B., 2015. Homo naledi, a new species of the genus Homo from the Dinaledi Chamber, South Africa. eLife 4, e09560.

Bhat, G.M., Kundal, S.N., Pandita, S.K., and Prasad, V.R., 2008. Depositional origin of tuffaceous units in the Pliocene Upper Siwalik Subgroup, Jammu (India), NW Himalaya. Geological Magazine 145 (2), p. 279-294.

Bishop, W.W., 1978. Geological background to fossil man: recent research in the Gregory Rift Valley, East Africa. Geological Society of London, Special Publications 6, p. 1-4.

Bohacs, K.M., Carroll, A.R., Neal, J.E. and Mankiewicz, P.J., 2000. Lake-basin type, source potential, and hydrocarbon character: an integrated sequence-stratigraphic-geochemical framework. In: Gierlowski-Kordesch E, Kelts K (eds) Lake basins through space and time: American Association of Petroleum Geologists Studies in Geology. American Association of Petroleum Geologists, Tulsa 46, p. 3–37.

Bouma, A.H., 1962. Sedimentology of some flysch deposits, a graphic approach to facies interpretation. Elsevier Co., Amsterdam, 168 p.

Bridge, J.S., Jalfin, G.A., Georgieff, S.M., 2000. Geometry, lithofacies, and spatial distribution of Cretaceous fluvial sandstone bodies, San Jorge basin, Argentina: outcrop analog for the hydrocarbon-bearing Chubut Group. Journal of Sedimentary Research 70, p. 341-359.

Bromage, T.G., Schrenk, F., and Kaufulu, Z., 1985. Plio-Pleistocene deposits in Malawi's hominid corridor. National Geographic Society Research Report 21, p. 51–52.

Bromage, T.G., Schrenk, F., and Juwayeyi, Y.M., 1995a. Paleobiogeography of the Malawi Rift: Age and vertebrate paleontology of the Chiwondo Beds, northern Malawi. Journal of Human Evolution 28, p. 37-57.

Bromage, T.G., Schrenk, F., and Zonneveld, F.W., 1995b. Paleoanthropology of the Malawi Rift: An early hominid mandible from the Chiwondo Beds, northern Malawi. Journal of Human Evolution 28, p. 71-108.

Brown, F.H., 1981. Environments in the Lower Omo Basin from one to four million years ago. In G Rapp Jr and CF Vondra (eds.): Hominid Sites: Their Geologic Settings. AAAS Symposium 63. Boulder. Westview, p. 149–164.

Brown, F.H., and Feibel, C.S., 1986. Revision of lithostratigraphic nomenclature in the Koobi Fora region, Kenya. Journal of the Geological Society, London 143, p. 297-310.

Brunet, M., Guy, F., Pilbeam, D., Lieberman, D.E., Likius, A., Mackaye, H.T., Ponce de Leon, M., Zollikofer, C.P.E., and Vignaud, P., 2005. New material of the earliest hominid from the Upper Miocene of Chad. Nature 434, p. 752–755.

Brunet, M., Guy, F., Pilbeam, D., Mackaye, H.T., Likius, A., Ahounta, D., Beauvilain, A., Blondel, C., Bocherens, H., Boisserie, J.R., de Bonis, L., Coppens, Y., Dejax, J., Denys, C., Duringer, P., Eisenmann, V., Fanone, G., Fronty, P., Geraads, D., Lehmann, T., Lihoreau, F., Louchart, A., Mahamat, A., Merceron, G., Mouchelin, G., Otero, O., Pelaez-Campomanes, P., Ponce de Leon, M., Rage, J.C., Sapanet, M., Schuster, M., Sudre, J., Tassy, P., Valentin, X., Vignaud, P., Viriot, L., Zazzo, A., and Zollikofer, C., 2002. A new hominid from the Upper Miocene of Chad, Central Africa. Nature 418, p. 145–151.

Carroll (eds.), Stratigraphy and Paleolimnology of the Green River Formation, Western USA: Syntheses in Limnology 1, DOI 10.1007/978-94-017-9906-5_6.

Carroll, A.R., and Bohacs, K.M., 1999. Stratigraphic classification of ancient lakes: balancing tectonic and climatic controls. Geology 27, p. 99–102.

Cas, R.A.F., Wright, J.V., 1987. Volcanic Successions: Modern and Ancient. Allen and Unwin, London.

Ceramicola, S., Vanhauweart, P., De Batist, M., Kilembe, E., 1997. Structure, seismic stratigraphy and a tentative level change reconstruction of Southern Lake Rukwa (Tanzania). In: European Union of Geosciences 9, Terra Nova, Strasbourg, p. 360.

Chorowicz, J., and Mukonki, M.B., 1980. Linéaments anciens, zones transformantes récentes et géotectonique des fossés dans l'est Africain, d'après la télédétection et la microtectonique. Royal Museum for Central Africa, Department of Geology and Mineralogy Rapp. Ann, Tervuren (Belgium). 1979, p. 143-146.

Clark, J.D., Haynes Jr., C.V., Mawby, J.E., Gautier, A., 1970. Interim report on palaeoanthropological investigations in the Lake Malawi Rift. Quaternaria 13, p. 305–354.

Cohen, A.S., Bocxlaer, B.V., Todd, J.A., McGlue, M., Michel, E., Nkotagu, H.H., Grove, A.T., Delvaux, D., 2013. Quaternary ostracodes and molluscs from the Rukwa Basin (Tanzania) and their evolutionary and paleobiogeographic implications. Palaeogeography, Palaeoclimatology, Palaeoecology 392, p. 79–97.

Cresswell, J., 2012. The remarkable oil and gas bounty of offshore West and East Africa. The Press and Journal Limited: In Ernst and Young –Natural gas in Africa: The frontiers of the Golden Age, p. 10 - 11.

Crevecoeur, I., Skinner, M.M., Bailey, S.E., Gunz, P., Bortoluzzi, S., Brooks, A.S., Burlet,

C., Cornelissen, E., Clerk, N.D., Maureille, B., Semal, P., Vanbrabant, Y., and Wood, B., 2014. First early hominin from Central Africa (Ishango, Democratic Republic of Congo). PLoS ONE 9(1), e84652.

Cuitiño, J.I., Scasso, R.A., 2013. Reworked pyroclastic beds in the early Miocene of Patagonia: Reaction in response to high sediment supply during explosive volcanic events: Sedimentary Geology, v. 289, p. 194–209.Daly, M.C., Klerkx, J., Nanyaro, J.T., 1985, Early Proterozoic terranes and strike-slip accretion in the Ubendian Belt of southwest Tanzania. Terra Cognita 5, p.257.

Cuitiño, J.I., Scasso, R.A., 2013. Reworked pyroclastic beds in the early Miocene of Patagonia. Reaction in response to high sediment supply during explosive volcanic events. Sedimentary Geology 289, p. 194 – 209.

Daly, M.C., 1988. Crustal shear zones in central Africa: A kinematic approach to Proterozoic tectonics. Episodes 11, p. 5–11.

Daly, M.C., Klerkx, J., and Nanyaro, J.T., 1985. Early Proterozoic terranes and strike-slip accretion in the Ubendian Belt of southwest Tanzania. Terra Cognita 5, 257p.

Delvaux, D., Kervyn, F., Macheyeki, A.S., and Temu, E.B., 2012. Geodynamic significance of the TRM segment in the East African Rift (W – Tanzania): Active tectonics and paleostress in the Ufipa plateau and Rukwa Basin. Journal of Structural Geology 37, p. 161-180.

Delvaux, D., Barth, A., 2010. African Stress Pattern from formal inversion of focal mechanism data. Implications for rifting dynamics. Tectonophysics 482, p. 105-128.

Delvaux, D., 2001. Tectonic and paleostress evolution of the Tanganyika-Rukwa-Malawi rift segment, East African Rift System. In: Ziegler, P.A., Cavazza, W., Robertson, A.H.F., Crasquin-Soleau, S. (Eds.), Peri-Tethys Memoir 6: PeriTethyan Rift/Wrench Basins and Passive Margins. Mémoire Musée National Histoire Naturelle, 186, p. 545-567.

Delvaux, D., Kervyn, F., Vittorl, E., Kajara, R.S.A. and Kilembe, E., 1998. Late Quaternary tectonic activity and lake level change in the Rukwa Rift Basin. Journal of African Earth Sciences 26, p. 397-421.

deMenocal, P.B., 1995. Plio-Pleistocene African climate: Science, New Series, 270, p. 53–59.

deMenocal, P., 2004. African climate change and faunal evolution during the Pliocene-Pleistocene. Earth Planet. Sci. Lett. 220, p. 3-24.

Dirks, P.H.G.M., Berger, L.R., Roberts, E.M., Kramers, J.D., Hawks, J., Randolph-Quinney, P.S., Elliott, M., Musiba, C.M., Churchill, S.E., de Ruiter, D.J., Schmid, P., Backwell, L.R., Belyanin, G.A., Boshoff, P., Hunter, K.L., Feuerriegel, E.M., Gurtov, A., du, G., Harrison, J., Hunter, R., Kruger, A., Morris, H., Makhubela, T.V., Peixotto, B. and Tucker, S., 2015. Geological and taphonomic evidence for deliberate body disposal by the primitive hominin species Homo naledi from the Dinaledi Chamber, South Africa. eLife 4:e09651.

Dirks, P.H., Kibii, J.M., Kuhn, B.F., Steininger, C., Churchill, S.E., Kramers, J.D., Pickering, R, Farber, D.L., Me´ riaux, A.S., Herries, A.I., King, G.C., and Berger, L.R., 2010.

Geological setting and age of Australopithecus sediba from Southern Africa. Science 328, p. 205–208.

Duffield, W.A., Bacon, C.R., and Roquemore, G.R., 1979. Origin of reserve-graded bedding in air-fall pumice, Coso Range, California. Journal of Volcanology and Geothermal Research 5, 3 p. 5-48.

Dunham, K., 1961. Black shale, oil, and sulphide ore. Advancement of Science 18, p. 284–299.

Dunkleman, T., 1986. The structural and stratigraphic evolution of Lake Turkana. Thesis, Duke University, Durham, N.C., 64 p.

Ebinger, C., Deino, A., Drake, R. and Tesha, A., 1989. Chronology of volcanism and rift basin propagation: Rungwe Volcanic Province, East Africa. Journal of Geophysical Research 94, p. 15785-15803.

Ebinger, C.J., Deino, A.L., Tesha, A.L., Becker, T., Ring, U., 1993. Tectonic controls on rift basin morphology – evolution of the northern Malawi (Nyasa) Rift. Journal of Geophysical Research 98, p. 17821–17836.

Ebinger, C.J., 1989. Tectonic development of the western branch of East African rift system. Geological Society of America Bulletin 101, p. 885-903.

Feibel, C. S., 2011. A Geological History of the Turkana Basin. Evolutionary Anthropology 20(6), p. 206-216.

Feibel, C.S., Harris, J.M., and Brown, F.H., 1991. Palaeoenvironmental context for the late. Neogene of the Turkana Basin. In JM Harris (ed.): Koobi Fora Research Project,Vol. 3 Oxford. Clarendon, p. 321–370.

Fielding, C.R., 2010. Planform and facies variability in asymmetric deltas: Facies analysis and depositional architecture of the Turonian Ferron Sandstone in the Western Henry Mountains, South-Central Utah, U.S.A. Journal of Sedimentary Research 80, p. 455-479.

Fielding, C.R., 2010. Planform and facies variability in asymmetric deltas: Facies analysis and depositional architecture of the Turonian Ferron Sandstone in the Western Henry Mountains, South-Central Utah, U.S.A. Journal of Sedimentary Research 80, p. 455-479.

Fleagle, J.G., Rasmussen, D.T., Yirga, S., Bown, T.M., and Grine, F.E. 1991. New hominid fossils from Fejej, Southern Ethiopia. Journal of Human Evolution 21, p. 145-152.

Fontijn, K., Ernst, G.G.J., Elburg, M.A., Williamson, D., Abdallah, E., Kwelwa, S., Mbede, E., Jacobs, P., 2010. Holocene explosive eruptions in the Rungwe Volcanic Province, Tanzania. Journal of Volcanology and Geothermal Research 196, p. 91–110.

Fontijn, K., Williamson, D., Mbede, E., Ernst, G.G.J., 2012. The Rungwe Volcanic Province, Tanzania—a volcanological review: Journal of African Earth Sciences 63, p. 12–31.

Fouch, T.D., Dean, W.E., 1982. Lacustrine and associated clastic depositional environments. In: Scholle, P.A., Spearing, D. (Eds.), Sandstone Depositional Environments. American Association of Petroleum Geologists, p. 87–114.

Frostick, L.E. and Reid, I., 1990. Structural control of sedimentation patterns and implication for the economic potential of the East African Rift basins. Journal of African Earth Sciences 10, p. 307-318.

Garcia-Garcia, F., Fernandez, J., Viseras, C., Soria, J.M., 2006. Architecture and sedimentary Facies evolution in a delta slack controlled by fault growth (Betic Cordillera, southern Spain, late Tortonian). Sedimentary Geology 185, p. 79-92.

Gilbert, G.K., 1885. The topographic features of lake shores. U.S. Geological Survey Annual Report 5, p. 75-123.

Gilbert, G.K., 1890. Lake Bonneville.U.S. Geological Survey Monograph 1, p. 438.

Grantham, D.R., Teale, E.O., Spurr, A.M., Harkin, D.A., Brown, P.E., 1958. Quarter Degree Sheet 244 (Mbeya). Geological Survey of Tanganyika, Dodoma.

Haberyan, K.A., 1987. Fossil diatoms and the paleolimnology of Lake Rukwa, Tanzania. Freshwater Biology 17, p. 429–436.

Haile-Selassie, Y., Gibert, L., Melillo, S.M., Ryan, T.M., Alene, M., Deino, A., Levin, N.E., Scott, G., and Saylor, B.Z., 2015. New species from Ethiopia further expands Middle Pliocene hominin diversity. Nature 521, 4p. 83-488.

Hautot, S., Tarits, P., Whaler, K., Le Gall, B., Tiercelin, J.J., and Le Turdu, C., 2000. Deep structure of the Baringo Rift Basin (Central Kenya) from three-dimensional magnetotelluric imaging: Implications for rift evolution. Journal of Geophysical Research 105, p. 23,493-23,518.

Hay, R. L., 1986. Role of tephra in the preservation of fossils in Cenozoic deposits of East Africa, *in* Frostick, L. E., et al., eds., Sedimentation in the African rifts. Geological Society of London Special Publication, no. 25, p. 339–344.

Heller, P.L. and Paola, C., 1992. The large-scale dynamics of grain-size variation in alluvial basins, 2: Application to syntectonic conglomerate. Basin Research 4, p. 91–102.

Herries, A.I.R. and Adams, J.W., 2013. Clarifying the context, dating and age of the Gondolin hominins and paranthropus in South Africa. Journal of Human Evolution 65, p. 676-681.

Hilbert-Wolf, H., Roberts, E., Downie, R., Mtelela, C., Stevens, n. and O'Connor, P., In press. Application of U-Pb detrital zircon geochronology to drill cuttings for age control in hydrocarbon exploration wells: a case study from the Rukwa Rift Basin, Tanzania. American Association of Petroleum Geologists Bulletin.

Hilbert-Wolf, H., Roberts, E.M., Mtelela, C., and Downie, R., 2015. Combining detrital geochronology and sedimentology to assess basin development in the Rukwa Rift of the East African Rift System. European Geosciences Union (EGU) General Assembly, Vienna Austria.

Hilbert-Wolf, H.L., and Roberts, E.M., 2015. Giant seismites and megablock uplift in the East African Rift: Evidence for Late Pleistocene large magnitude earthquakes: PLoS ONE, 10(6): e0129051.doi:101371/journal.pone.0129051.

Hilbert-Wolf, H.L., Roberts, E.M., Mtelela, C., O'connor, P.M., and Stevens, N.J., 2013. Constraining the timing of Cenozoic rifting and basin development in the Rukwa rift basin of the East African Rift System via detrital zircon geochronology. 125th Anniversary of GSA, Annual Meeting in Denver, U.S.A.

Ingersoll, R.V., Bullard, T.F., Ford, R.L., Grimm, J.P., Pickle, J.D., Sares, S.W., 1984. The effect of grain size on detrital modes: a test of the Gazzi-Dickinson point-counting method. Journal of Sedimentary Petrology 54, p. 103-116.

Ivanov, A.V., Rasskazov, S.V., Boven, A., Punzalan, L., Brandt, I.S., Brandt, S.B., Fernandez-Alonso, M., 1999. Timing and Late Cenozoic volcanic activity and rift basin formations in the Rungwe province of Tanzania substantiated by K–Ar and $^{40}Ar/^{39}Ar$ dating. In: Proceedings of Rifting in Intracontinental Setting: Baikal Rift System and other Continental Rifts, 22–30 August 1999, Irkutsk and Lake Baikal, Russia, p. 75–79.

Kataoka, K., 2005. Distal fluvio-lacustrine volcaniclastic resedimentation in response to an explosive silicic eruption: the Pliocene Mushono tephra bed, central Japan. Geological Society of America Bulletin 117, p. 3–17.

Kazmin, V., 1980. Transform faults in the East African rift system. In: Geodynamic Evolution of the Afro-Arabian Rift System, 47. Accademia Nazionale dei Lincey, Roma. Atti dei convegni Lincei, p. 65-73.

Kennerley, J.B., 1962. Itaka: 1:125,000 Map Geol. Surv. Tanzania. Quarter Degree Sheet 243, with brief explanation.

Kilembe, E.A. and Rosendahl, B.R., 1992. Structure and stratigraphy of the Rukwa rift. Tectonophysics 209, p. 143-158.

Kingston, J.D., 2007. Shifting adaptive landscapes: progress and challenges in reconstructing early hominid environments. Am. J. Phys. Anthropol. Suppl. Yearb. Phys. Anthropol. 134 (Issue Suppl. 45), p. 20-58.

Kokelaar, B.P., 1992. Ordovician marine volcanic and sedimentary record of rifting and volcanotectonism: Snowdon, Wales, United Kingdom. Geological Society of America Bulletin 104, p. 1433–1455.

Kullmer, O., Sandrock, O., Kupczik, K., Frost, S.R., Volpato, V., Bromage, T.G., and Schrenk, F., 2011. New primate remains from Mwenirondo, Chiwondo Beds in northern Malawi. Journal of Human Evolution 61, p. 617-623.

Lamb, M.P., Parsons, J.D., Mullenbach, B.L., Finlayson, D.P., Orange, D.L. and Nittrouer, C.A., 2008. Evidence for superelevation, channel incision, and formation of cyclic steps by turbidity currents in Eel Canyon, California. Geological Society of America Bulletin 120, p. 463–475.

Lawley, C.J.M., Selby, D., Condon, D.J., Horstwood, M., Millar, I., Crowley, Q. and Imber, J., 2013. Lithogeochemistry, geochronology and geodynamic setting of the Lupa Terrane, Tanzania: Implications for the extent of the Archean Tanzanian Craton. Precambrian Research 231, p. 174-193.

Leakey, M. G., Feibel, C. S., McDougall, I., and Walker, A., 1995. New four-million-year-old hominid species from Kanapoi and AlliaBay, Kenya. Nature 376, p. 565–571.

Leakey, L.S.B., and Leakey, M.D., 1964. Recent discoveries of fossil hominids in Tanganyika: at Olduvai and near Lake Natron: Nature 202, p. 5-7.

Leleu, S., Hartley, A.J., and Williams, B.P.J., 2009. Large-scale alluvial architecture and correlation in a Triassic pebbly braided river system, Lower Wolfville Formation (Fundy Basin, Nova Scotia, Canada). Journal of Sedimentary Research 79, p. 265-286.

Lockwood, C.A. and Tobias, P.V., 1999. A large hominin cranium from Sterkfontein, South Africa and the status of Australopithecus africanus. Journal of Human Evolution 36, p. 637-685.

Mack, G.H., James, W.C., and Monger, H.C., 1993. Classification of paleosols. Geological Society of America Bulletin 105, p. 129-136.

Manville, V.R., 2001. Sedimentology and history of Lake Reporoa: an ephemeral supra ignimbrite lake, Taupo Volcanic Zone, NewZealand. In:White, J.D.L., Riggs, N.R. (Eds.), Volcanogenic sedimentation in lacustrine settings. International Association of Sedimentologists Special Publication 30: Blackwell Science, Oxford, p. 109–140.

Maslin, M.A., Brierley, C.M., Milner, A.M., Shultz, S., Trauth, M.H., and Wilson, K.E., 2014. East African climate pulses and early human evolution. Quaternary Science Reviews 101, p. 1-17.

Maslin, M.A., Christensen, B., 2007. Tectonics, orbital forcing, global climate change, and human evolution in Africa. Journal of Human Evolution 53, p. 443-464.

Mbede, E.I., 2000. Subsidence history of the Rukwa Rift Basin in south west Tanzania analysed from Ivuna well. Tanzania Journal of Science 26.

Mbede, E.I., 1993. Tectonic development of the Rukwa Rift basin in SW Tanzania. Berliner Geowissenschaftliche Abhandlungen 152, 92 p.

Mbede, E.I., 1991. The sedimentary basins of Tanzania – reviewed. Journal of Africaa Earth Sciences 13, p. 291-297.

Mazzulo, S.J., 1973. Deltaic depositional environments in the Hamilton Group (Middle Devonian), southeastern New York State. Journal of Sedimentary Petrology 43, p. 1061-1071

Menter, C.R., Kuykendall, K.L., Keyser, A.W., and Conroy, G.C., 1999. First record of hominid teeth from the Plio-Pleistocene site of Gondolin, South Africa. Journal of Human Evolution 37, p. 299-307.

Miall, A.D., 1977. A review of the braided river depositional environment. Earth Science Reviews 13, p. 1-62.

Miall, A.D., 1992. Alluvial deposits, in Walker, R.G., and James, N.P., eds., Facies Models - Response to Sea Level Change: Geological Association of Canada, p. 119-142.

Miall, A.D., 1996, The Geology of Fluvial Deposits; Sedimentary Facies, Basin Analysis, and Petroleum Geology: Berlin, Springer-Verlag, (New York), 582 p.

Michaelsen, P., Henderson, R.A., Crosdale, P.J., and Mikkelsen, S.O., 2000. Facies architecture and depositional dynamics of the Upper Permian Rangal Coal Measures, Bowen Basin, Australia. Journal of Sedimentary Research 70, p. 879-895.

Mliga, N.R., 1994. Depositional environments, stratigraphy and hydrocarbon potential of The Rukwa Rift Basin –SW Tanzania. Unpublished Ph.D Dissertation, Duke Universirty, 156 p.

Morley, C. K., Cunningham, S.M., Harper, R.M., and Westcott, W.A., 1999, Geology and geophysics of the Rukwa Rift, East Africa, in Morley, C.K., eds., Geoscience of Rift Systems- Evolution of East Africa. American Association of Petroleum Geologists, Studies in Geology, p. 91-110.

Morley, C.K., Vanhauwaert, P., De Batist, M., 2000. Evidence for high frequency cyclic fault activity from high resolution seismic reflection survey, Rukwa rift, Tanzania. Journal of the Geological Society, London 157, p. 983-994.

Morley, C.K., 2010. Stress re-orientation along zones of weak fabrics in rifts: An explanation for pure extension in 'oblique' rift segments? Earth and Planetary Science Letters 297, p. 667-673.

Morley, C.K., Cunningham, S.M., Harper, R.M., Wescott, W.A., 1992. Geology and geophysics of the Rukwa rift, East Africa. Tectonics 11, p. 68-81.

Morley, C. K., Nelson, R. A., Patton, T. L., and Munn, S. G., 1990. Transfer zones in the East African rift system and their relevance to hydrocarbon exploration in rifts. American Association of Petroleum Geologists Bulletin 74, p. 1234–1253.

Murphy, M.A. and Salvador, A., 1999. International Stratigraphic Guide – An abridged Version. International Commision on Stratigraphy. Episodes 22, p. 255-272.

Mtelela, C., Roberts, E.M., Downie, R., and Hendrix, M.S., 2016. Interplay of structural, climatic and volcanic controls on Quaternary lacustrine-deltaic sedimentation patterns in the Western Branch of the East African Rift System, Rukwa rift, Tanzania. Journal of Sedimentary Research 86, p. 1179-1207.

Mtelela, C., Roberts, E.M., Hilbert-Wolf, H.L., Downie, R., Hendrix, M.S., O'Connor, P.M. and Stevens, N.J., In press. Sedimentology and paleoenvironments of a new fossiliferous late Miocene-Pliocene sedimentary succession in the Rukwa Rift Basin, Tanzania. Journal of African Earth Sciences.

Nemec, W., 1990. Aspects of sediment movement on steep delta slopes. In: Coarse-Grained Deltas (Ed. By A.Colella and D.B. Prior). International Association of Sedimentologists, Special Publication 10, p. 29 – 73.

Nicholson, S.E., 1999. Historical and modern fluctuations of lakes Tanganyika and Rukwa and their relationship to rainfall variability. Climate Change 41, p. 53-71.

Nichols, G.J., Fisher, J.A., 2007. Processes, facies and architecture of fluvial distributary systems deposits. Sedimentary Geology 195, 75-90.

O'Connor, P. M., Gottfried, M.D., Stevens, N.J., Roberts, E.M., Ngasala, S., Kapilima, S. and Chami, R., 2006. Dinosaurs and other vertebrates from the Cretaceous Red Sandstone Group, Rukwa Rift Basin, Southwestern Tanzania. Journal of African Earth Sciences 44, p. 277-288.

O'Connor, P.M., Sertich, J.J.W., Stevens, N.J., Roberts, E.M., Gottfried, M.D., Hieronymus, T.L., Jinnah, Z.A., Ridgely, R., Ngasala, S.E., and Temba, J., 2010. The evolution of mammal-like crocodyliforms in the Cretaceous Period of Gondwana. Nature 466, p. 748 –751.

Olariu, C., Steel, R.J. and Petter, A.L., 2010, Delta-front hyperpycnal bed geometry and implications for reservoir modelling: Cretaceous Panther Tongue delta, Book Cliffs, Utah: American Association of Petroleum Geologists Bulletin 94, no. 6 p. 819–845.

Oyanyan, R. O., Soronnadi-Ononiwu, C. G. and Omoboriowo, A. O., 2012. Depositional environments of sam-bis oil field reservoir sands, Niger Delta, Nigeria. Pelagia Research Library, Advances in Applied Science Research 3, p. 1624-1638.

Palmer, B.A., Shawkey, E.P., 1997. Lacustrine sedimentation processes and patterns during effusive and explosive volcanism, Challis volcanic field, Idaho. Journal of Sedimentary Research 67, p. 154–167.

Pettijohn, F.J., Potter, P.E., Siever, R., 1987. Sand and Sandstone. Springer-Verlag, New York. 553 p.

Pickering, R., Hancox, P.J., Lee-Thorp, J.A., Grun, R., Mortimer, G.E., McCulloch, M. and Berger, L.R., 2007. Stratigraphy, U-series chronology and palaeoenvironments at Gladysvale Cave: insights into the climatic control over South African hominin bearing cave deposits. Journal of Human Evolution 53, p. 602-619.

Pickford, M,, Senut, B. and Hadoto D., 1993. Geology and Palaeobiology of the Albertine Rift Valley, Uganda-Zaire. Volume I: Geology. Orle´ans: C.I.F.E.G. 190 p.

Pierce, J. and Lipkov, L., 1988. Structural interpretation of the Rukwa rift, Tanzania. Geophysics 53, p. 824-836.

Pierson, T.C. and Scott, K.M., 1985. Downstream dilution of a lahar: transition from debris flow to hyperconcentrated stream flow. Water Resources Research 21, p. 1511–1524.

Plink-Björklund, P., Steel, R.J., 2004. Initiation of turbidity currents: outcrop evidence for Eocene hyperpycnal flow turbidites. Sedimentary Geology 165, p. 29–52.

Porta, G.D., 2015. Carbonate build-up in lacustrine, hydrothermal and fluvial settings: comparing depositional geometry, fabric types and geochemical signature. Geological Society, London. Special Publication 418, p. 17-68.

Potts, R., 1998. Environmental hypothesis of hominin evolution. Yearb. Phys.Anthropol. 41, p. 93-136.

Quennell, A.M., 1956, 1:2,000,000 Geological map of Tanzania.

Quennell, A.M., Mcinley, A.C.M. and Aitken, W.G., 1956. Summary of the geology of Tanganyika. Geological Survey of Tanganyika Memoir 1, 264 p.

Renaut, R.W. and Gierlowski-Kordesch, E.H., 2010. Lakes. In: Dalrymple, R. and James, N. (Editors), Facies Models, 4th Edition: Geological Association of Canada, Toronto, p. 541-575.

Roberts, E.M., Stevens, N.J., O'Connor, P.M., Dirks, P.H.G.M., Gottfried, M.D., Clyde, W.C., Armstrong, R.A., Kemp, A.I.S. and Hemming, S., 2012. Initiation of the western branch of the East African Rift coeval with the eastern branch. Nature Geoscience 5, p. 289-294.

Roberts, E.M., O'Connor, P.M., Stevens, N.J., Gottfried, M.D., Jinnah, Z.A., Ngasala, S., Choh, A.M., Amstrong, R.A., 2010. Sedimentology and depositional environments of the Red

Sandstone Group, Rukwa Rift Basin, southwest Tanzania: New insights into Cretaceous and Paleogene terrestrial ecosystems and tectonics in sub-equatorial Africa. Journal of African Earth Sciences 57, p. 179-212.

Roberts, E.M., O'Connor, P.M., Gottfried, M.D., Stevens, N.J., Kapalima, S. and Ngasala, S., 2004. Revised stratigraphy and age of the Red Sandstone Group in the Rukwa Rift Basin, Tanzania: Cretaceous Research 25, p. 749–759.

Roller, S., Hornung, J., Hinderer, M., and Ssemmanda, I., 2010. Middle Miocene to Pleistocene sedimentary record of rift evolution in the southern Albert Rift (Uganda). International Journal of Earth Science 99, p. 1643-1661.

Rosendahl, B. R., and Livingstone, D. A., 1983. Rift lakes of East Africa— New seismic data and implications for future research. Episodes. Quaternary Journal of the International Union of Geological Science, p. 14–19.

Rozzi, F.V.R., Bromage, T., and Schrenk, F., 1997. UR 501, the Plio-Pleistocene hominid from Malawi. Analysis of the microanatomy of the enamel. Earth and Planetary Sciences 325, p. 231-234.

Sandrock, O., Kullmer, O., Schrenk, F., Yuwayeyi, Y. M., and Bromage, T. G. 2007. Fauna, taphonomy and ecology of the Plio-Pleistocene Chiwondo Beds, Northern Malawi. In: Bobe, R., Alemseged, Z., Behrensmeyer, A.K. (Eds.), Hominin Environments in the East African Pliocene: an Assessment of the Faunal Evidence. Springer, Dordrecht, p. 315–332.

Schull, T.J., 1988. Rift basins of interior Sudan: petroleum exploration and discovery, American Association of Petroleum Geologists Bulletin 72, p. 1128-1142.

Schull, T. J., 1984. Oil exploration in the non-marine rift basins of Interior Sudan : Presented to Canadian Society of Petroleum Geology, Calgary.

Scott, J.J., and Smith, M.E., 2015, Trace fossils of the Eocene Green River lake basins, Wyoming, Utah, and Colorado, in Smith, M.E., and Carroll, A.R., eds., Stratigraphy and Paleolimnology of the Green River Formation, Western USA. Syntheses in Limnology 1, 313-350.

Sepulchre, P., Ramstein, G., Fluteau, F., and Schuster, M., 2006. Tectonic uplift and Eastern Africa aridification. Science 313, p. 1419-1423.

Sherwood, R.J., and Kingston, J.D. 2002. Paleoanthropological survey of the Lake Rukwa Basin, Tanzania. American Journal of Physical Anthropology Supplement 34, 141 p.

Smith, G.A., 1987. Sedimentology of volcanism-induced aggradation in fluvial basins: Examples from the Pacific Northwest, U.S.A., *in* Ethridge, F., Flores, R. and Harvey, M., eds., Recent Developments in Fluvial Sedimentology: SEPM, Special Publication 39, p. 217–229.

Smith, G.A., 1991, Facies sequences and geometries in continental volcaniclastic sediments, in Fisher, R.V., and Smith, G.A., eds., Sedimentation in Volcanic Settings. SEPM, Special Publication 45, p. 109–123.

Smith, G.A., Moore, J.D. and McIntosh, W.C., 2002, Assessing roles of volcanism and basin subsidence in causing Oligocene-Lower Miocene sedimentation in the Northern Rio Grande Rift, New Mexico, U.S.A. Journal of Sedimentary Research 72, p. 836-848.

Spandler, C., Hammerli, Sha, P. Hilbert-Wolf, H.L., Roberts, E.M., and Schmitz, M., 2016. MKED1: A new titanite standard for in situ microanalysis of trace elements, Sm-Nd isotopes, and U-Pb geochronology: Chemical Geology 425, p. 110-126.

Sparks, R.S.J. and Wilson, L., 1976. A model for the formation of ignimbrite by gravitational column collapse. Journal of Geological Society of London132, 441-451.

Stanley, S.M., 1995. Climatic forcing and the origin of the human genus, in National Research Council, eds., Effects of Past Global Change in Life: Washington, DC, National Academy Press, Studies in Geophysics, 233-243.

Stevens, N.J., Gottfried, M.D., Roberts, E.M., Ngasala, S., Kapilima, S., and O'Connor, P.M., 2008. Paleontological exploration of Africa: A view from the Rukwa Rift Basin of Tanzania. In: Fleagle, J.G., Gilbert, C.C. (Eds.), Elwyn Simmons: A Search for Origins. Developments in Primatology. Progress and Prospects. Springer, p. 159–180.

Stevens, N.J., Seiffert, E.R., O'connor, P.M., Roberts, E.M., Schmitz, M.D., Krause, C., Gorscak, E., gasala, S., Hieronymus, T.L., and Joseph, T., 2013. Palaeontological evidence for an Oligocene divergence between Old World monkeys and apes. Nature 497, p. 611- 614.

Stewart, K.M., and Murray, A.M., 2013. Earliest fish remains from the Lake Malawi Basin, Malawi, and biogeographical implications. Journal of Vertebrate Paleontology 33, p. 532-539.

Stollhofen, H., Stanistreet, I.G., McHenry, L.J., Mollel, G.F., Blumenschine, R.J., Masao, F.T., 2008. Fingerprinting facies of the Tuff IF marker, with implications for early hominin palaeoecology, Olduvai Gorge, Tanzania. Palaeogeography, Palaeoclimatology, Palaeoecology 259, p. 382–409.

Susman, R.L. and de Ruiter, D.J., 2004. New hominin first metatarsal (SK 1813) from Swartkrans. Journal of Human Evolution 47, p. 171–181.

Syvitski, J.P.M. and Schafer, C.T., 1996. Evidence for an earthquake-triggered basin collapse in Saguenay fjord, Canada: Sedimentary Geology 104, p. 127 – 153.

Talbot, M.R., Livingstone, D.A., 1989. Hydrogen index and carbon isotopes of lacustrine organic matter as lake level indicators: Palaeogeography, Palaeoclimatology, Palaeoecology 70, p. 121–137.

Talbot, M.R., Allen, P.A., 1996. Lakes. In: Reading, H.G. (Ed.), Sedimentary Environments: Processes, Facies and Stratigraphy. Blackwell Science, Cambridge, p. 83-124.

Tanner, L.H., 2003. Pedogenic features of the Chinle Group, Four Corners region: evidence Late Triassic aridification. New Mexico Geological Society Guidebook, 54th Field Conference, Geology of the Zuni Plateau, p. 269-280.

Tanner, W.F., 1967. Ripple mark indexes and their uses. Sedimentology 9, p. 89–104.

Theunissen, K., Klerkx, J., Melnikov, A., and Mruma, A., 1996. Mechanism of inheritance of rift faulting in the western branch of the East African Rift, Tanzania. Tectonics 15 (4), 776-790.

Thevenon, F.,Williamson, D., Taieb, M., 2002. A 22 kyr BP sedimentological record of Lake Rukwa (8°S, SW Tanzania): environmental, chronostratigraphic and climatic implications. Palaeogeography, Palaeoclimatology, Palaeoecology 187, p. 285–294.

Tiercelin, J.J., Potdevin, J.L., Morley, C.K., Talbot, M.R., Bellon, H., Rio, A., Le Gall, B., Vétel, W., 2004. Hydrocarbon potential of the Meso-Cenozoic Turkana Depression, northern Kenya. I. Reservoirs: depositio-nal environments, diagenetic characteristics, and source rock- reservoir relationships. Marine and Petroleum Geology 21, p. 41 – 62.

Tiercelin, J.J., Potdevin, J., Thuo, P.K., Abdelfettah, Y., Schuster, M., Bourquin, S., Bellon, H., Clément, J., Guillou, H., Nalpas, T., Ruffet, G., 2012. Stratigraphy, sedimentology and diagenetic evolution of the Lapur Sandstone in northern Kenya: Implications for oil exploration of the Meso-Cenozoic Turkana depression. Journal of African Earth Sciences 71–72, p 43–79.

Tiercelin, J.J., Chorowicz, J., Bellon, H., Richert, J.P., Mwanbene, J.T., Walgenwitz, F., 1988. East African Rift System: offset, age and tectonic significance of the Tanganyika-Rukwa-Malawi intracontinental transcurrent fault zone. Tectonophysics 148, 241–252.

TPDC. 2011. The Hydrocarbon Potential of the Rukwa Rift Basin. Tanzania Petroleum Development Corporation (TPDC), unpublished internal Report.

Trauth, M.H., Deino, A.L., Bergner, A.G.N., Strecker, M.R., 2003. East African climate change and orbital forcing during the last 175 kyr BP. Earth and Planetary Science Letters 206, p. 297–313.

Trauth, M.H., Maslin, M.A., Deino, A.L., Strecker, M.R., 2005. Late Cenozoic moisture history of East Africa. Science 209, p. 2051–2053.

Trauth, M.H., Maslin, M., Deino, A., Strecker, M.R., Bergner, A.G.N., and Duhnforth, M.,

2007. High- and low-latitude forcing of Plio-Pleistocene East African climate and human evolution. Journal of Human Evolution 53, p. 475-486.

Umazamo, A.M., Bellosi, E.S., Visconti, G., and Melchor, R.N., 2012. Detecting allocyclic signals in volcaniclastic fluvial successions: Facies, architecture and stacking pattern from the Cretaceous of central Patagonia, Argentina. Journal of South American Earth Sciences 40, p. 94-115.

Vrba, E.S., 1988. Late Pliocene climatic events and hominid evolution. In: Grine FE, editor. Evolutionary history of the ‘‘robust’’ australopithecines. New York: Aldine de Gruyter, p. 405–426.

Wescott, W.A., 1993. The diagenesis of continental (Karoo-Tertiary?) siliciclastics from an East African rift valley (Rukwa-Tukuyu area), Tanzania -discussion. Sedimentary Geology 86, p. 121-124.

Wescott, W.A., Krebs, W.N., Engelhardt, D.W., Cunningham, S.W., 1991. New biostratigraphic age dates from the Lake Rukwa rift basin in western Tanzania: American Association of Petroleum Geologists Bulletin 75, p. 1255-1263.

Wheeler, W.H., Karson, J.A., 1994. Extension and subsidence adjacent to a ‘‘Weak’’ continental transform: an example from the Rukwa Rift, East Africa. Geology 22, p. 625–628.

White, T.D., and Suwa, G., 1987. Hominid footprints at Laetoli: Facts and interpretations. American Journal of Physical Anthrolopogy 72, p. 485-514.

WoldeGabriel, G., Heiken, G., White, T. D., Asfaw, B., Hart, W. K. and Renne, P. R., 2000. Volcanism, tectonism, sedimentation, and the paleoanthropological record in the Ethiopian Rift System, in McCoy, F. W., and Heiken, G., eds., Volcanic Hazards and Disasters in Human Antiquity: Boulder, Colorado, Geological Society of America Special Paper 345.

WoldeGabriel, G., Heiken, G., White, T. D., Asfaw, B., Hart, W. K. and Renne, P. R., 2000. Volcanism, tectonism, sedimentation, and the paleoanthropological record in the Ethiopian Rift System, in McCoy, F. W., and Heiken, G., eds., Volcanic Hazards and Disasters in Human Antiquity. Boulder, Colorado, Geological Society of America Special Paper 345, p. 83-99.

Yuretich, R.F., 1982, Possible influences upon lake development in the East African Rift Valleys: Journal of Geology 90, p. 329-337.

Zavala, C., Arcuri, M. and Valiente, L.B., 2012, The importance of plant remains as Diagnostic criteria for the recognition of ancient hyperpycnites: Revue de Paleoobiologie, Geneve, Special Volume 11, p. 457-469.

Zavala, C., J. Ponce, D. Drittanti, M. Arcuri, H. Freije, andM. Asensio, 2006, Ancient lacustrine hyperpycnites: A depositional model from a case study in the Rayoso Formation (Cretaceous) of west-central Argentina: Journal of Sedimentary Research 76, p. 41–59.

Zavala, C., M. Arcuri, M. D., Meglio, H. Gamero Diaz, and C. Contreras, 2011. A genetic facies tract for the analysis of sustained hyperpycnal flow deposits, in R. M. Slatt and C. Zavala, eds., Sediment transfer from shelf to deep water—Revisiting the delivery system. American Association of Petroleum Geologists, Studies in Geology 61, 31–51.

Zingg, T., 1935, Beitrage zur Schotteranalyse: Schweizerische Mineralogische und Petrologische Mitteilungen 15, p. 39-140.

Appendix 1

Eric M. Roberts, Christopher N. Todd, Duur K. Aanen, Tânia Nobre, Hannah L. Hilbert-Wolf, Patrick M. O'Connor, Leif Tapanila, **Cassy Mtelela**, Nancy J. Stevens., 2016. Oligocene Termite Nests with In Situ Fungus Gardens from the Rukwa Rift Basin, Tanzania, Support a Paleogene African Origin for Insect Agriculture. *PLOS ONE.* DOI:10.1371/journal.pone.0156847.

RESEARCH ARTICLE

Oligocene Termite Nests with *In Situ* Fungus Gardens from the Rukwa Rift Basin, Tanzania, Support a Paleogene African Origin for Insect Agriculture

Eric M. Roberts[1]*, Christopher N. Todd[1], Duur K. Aanen[2], Tânia Nobre[3], Hannah L. Hilbert-Wolf[1], Patrick M. O'Connor[4,5], Leif Tapanila[6], Cassy Mtelela[1,7], Nancy J. Stevens[4,5]

1 Department of Earth and Oceans, James Cook University, Townsville, Queensland, 4811 Australia, **2** Laboratory of Genetics, Wageningen University, Droevendaalsesteeg 1, Radix West, Building 107, 6708 PB, Wageningen, The Netherlands, **3** Institute of Mediterranean Agricultural and Environmental Sciences (ICAAM), Universidade de Évora, Núcleo da Mitra, Ap. 94, 7002–554, Évora, Portugal, **4** Department of Biomedical Sciences, Heritage College of Osteopathic Medicine, Ohio University, Athens, Ohio, 45701, United States of America, **5** Center for Ecology and Evolutionary Studies, Ohio University, Athens, Ohio, 45701, United States of America, **6** Department of Geosciences and Idaho Museum of Natural History, Idaho State University, Pocatello, Idaho, 83209, United States of America, **7** Department of Geology, University of Dar es Salaam, P.O. Box 35052, Dar es Salaam, Tanzania

* eric.roberts@jcu.edu.au

CrossMark
click for updates

OPEN ACCESS

Citation: Roberts EM, Todd CN, Aanen DK, Nobre T, Hilbert-Wolf HL, O'Connor PM, et al. (2016) Oligocene Termite Nests with *In Situ* Fungus Gardens from the Rukwa Rift Basin, Tanzania, Support a Paleogene African Origin for Insect Agriculture. PLoS ONE 11(6): e0156847. doi:10.1371/journal.pone.0156847

Editor: Faysal Bibi, Museum für Naturkunde, GERMANY

Received: December 10, 2015

Accepted: May 20, 2016

Published: June 22, 2016

Data Availability Statement: All relevant data are within the paper and its Supporting Information files.

Funding: This research was supported by the US National Science Foundation (NSF EAR_0617561, EAR_0854218, EAR 0933619), National Geographic Society (CRE), and funding from Ohio University and James Cook University. TN was supported by a Marie Curie fellowship (FP7-PEOPLE-2012-CIG Project Reference 321725) and by the Portuguese Foundation for Science and Technology (SFRH/BCC/52187/2013).

Abstract

Based on molecular dating, the origin of insect agriculture is hypothesized to have taken place independently in three clades of fungus-farming insects: the termites, ants or ambrosia beetles during the Paleogene (66–24 Ma). Yet, definitive fossil evidence of fungus-growing behavior has been elusive, with no unequivocal records prior to the late Miocene (7–10 Ma). Here we report fossil evidence of insect agriculture in the form of fossil fungus gardens, preserved within 25 Ma termite nests from southwestern Tanzania. Using these well-dated fossil fungus gardens, we have recalibrated molecular divergence estimates for the origins of termite agriculture to around 31 Ma, lending support to hypotheses suggesting an African Paleogene origin for termite-fungus symbiosis; perhaps coinciding with rift initiation and changes in the African landscape.

Introduction

Termites are among the most diverse and ecologically important groups of insects in modern ecosystems, playing a critical role as natural decomposers of plant tissues. Termites typically rely on gut symbionts to decompose organic matter. However, members of the subfamily Macrotermitinae have turned to agriculture by developing a highly specialized, symbiotic relationship with fungi of the genus *Termitomyces* (Basidiomycotina). The fungus-growing termites cultivate fungi in gardens/chambers inside the colony and then exploit the ability of the fungi to convert recalcitrant, nitrogen-poor, plant material into a more easily digestible,

Competing Interests: The authors have declared that no competing interests exist.

protein-rich food source [1, 2]. After ingestion and brief mastication of woody material, modern Macrotermitinae excrete rounded pellets known as primary faeces or mylospheres, composed of concentrated, undigested plant fragments and *Termitomyces* spores, which germinate and colonize the plant material, thus forming fungal gardens. The critical ecological role of fungus-growing termite colonies as biodiversity and bioproductivity hotspots within African savannah ecosystems has been well documented in recent years [3, 4]. Indeed, much of the decomposition of woody plant material in Africa and Asia takes place as a result of fungus-growing termites [5], with estimates suggesting that more than 90% of dry wood in some semiarid savannahs is reprocessed by members of the Macrotermitinae [6].

A growing body of molecular evidence suggests that termite fungiculture can be traced back to a single origin around 31 Ma (19–49 Ma), when domestication of the ancestor of *Termitomyces* by the ancestor of the Macrotermitinae occurred [2, 7–10]. Once established, this symbiotic relationship is hypothesized to have remained obligate over its entire evolutionary history, with no evidence of Macrotermitinae ever forming a relationship with any other fungi or abandoning fungus farming [2, 7–9]. Until recently, little fossil evidence has been found to document the antiquity of the termite—fungus mutualism. To date only a single unequivocal report of fossilized termite fungus combs has been described, recovered from a succession of Upper Miocene-Pliocene (≤7 Ma) terrestrial deposits in the northern Chad Basin, Africa [11, 12]. Intriguingly, fossilized termite nests that appear similar to those produced by fungus-farming termites have been reported from continental deposits across Afro-Arabia ranging as far back as the early Oligocene or late Eocene [13–15]. However, diagnostic evidence demonstrating the age and presence of *in situ* fungus gardens within these fossil termite nests has not yet been clearly confirmed; and hence, the timing of this important evolutionary coupling between termites and fungus (termite fungiculture) is still uncertain.

Here we report on the discovery of a new occurrence of fossilized termite nests with *in situ* fungus gardens from southwestern Tanzania. The new fossils were discovered in a paleosol horizon in a steeply dipping section of the Oligocene Songwe Member of the Nsungwe Formation in the Rukwa Rift Basin [16–18]. The aim of this study is to investigate the paleontology and geologic context of these new trace fossils, and use our findings to recalibrate the molecular phylogeny for fungus farming termites in order to test existing hypotheses regarding the timing and origin of termite-fungus symbiosis in the fossil record.

Study Area and Fossil Locality

The trace fossil locality is located near the southern end of the Rukwa Rift Basin, a segment of the Western Branch of the East African Rift System in southwestern Tanzania [17, 18] (Fig 1). Excellent exposures of fossiliferous Permian to Plio-Pleistocene strata are exposed within the basin, particularly at the southern end in the Songwe Valley [19–25]. The trace fossils described in this study come from steeply exposed type section of the Paleogene Nsungwe Formation, which represents an overall upward fining succession of alluvial fan (Utengule Member) to volcanic-rich fluvial and lacustrine (Songwe Member) facies [17, 18, 23]. The Songwe Member preserves a particularly important and rare window in the late Paleogene of continental sub-equatorial Africa and has produced a rich new fauna, including the earliest records of Old World monkeys and apes [16, 23], along with a diversity of other mammals, crocodiles, birds, lizards, snakes, crustaceans and mollusks [26–31].

The Songwe Member has been precisely dated as late Oligocene, between 26–24 Ma, using a combination of: (1) single-crystal laser fusion Ar/Ar dating of phlogopite; (2) U-Pb LA-ICPMS dating of titanite; and (3) U-Pb LA-ICPMS, SHRIMP and CA-TIMS dating of zircon from multiple volcanic tuffs [17, 23]. The trace fossils reported in this study come from ~265 m

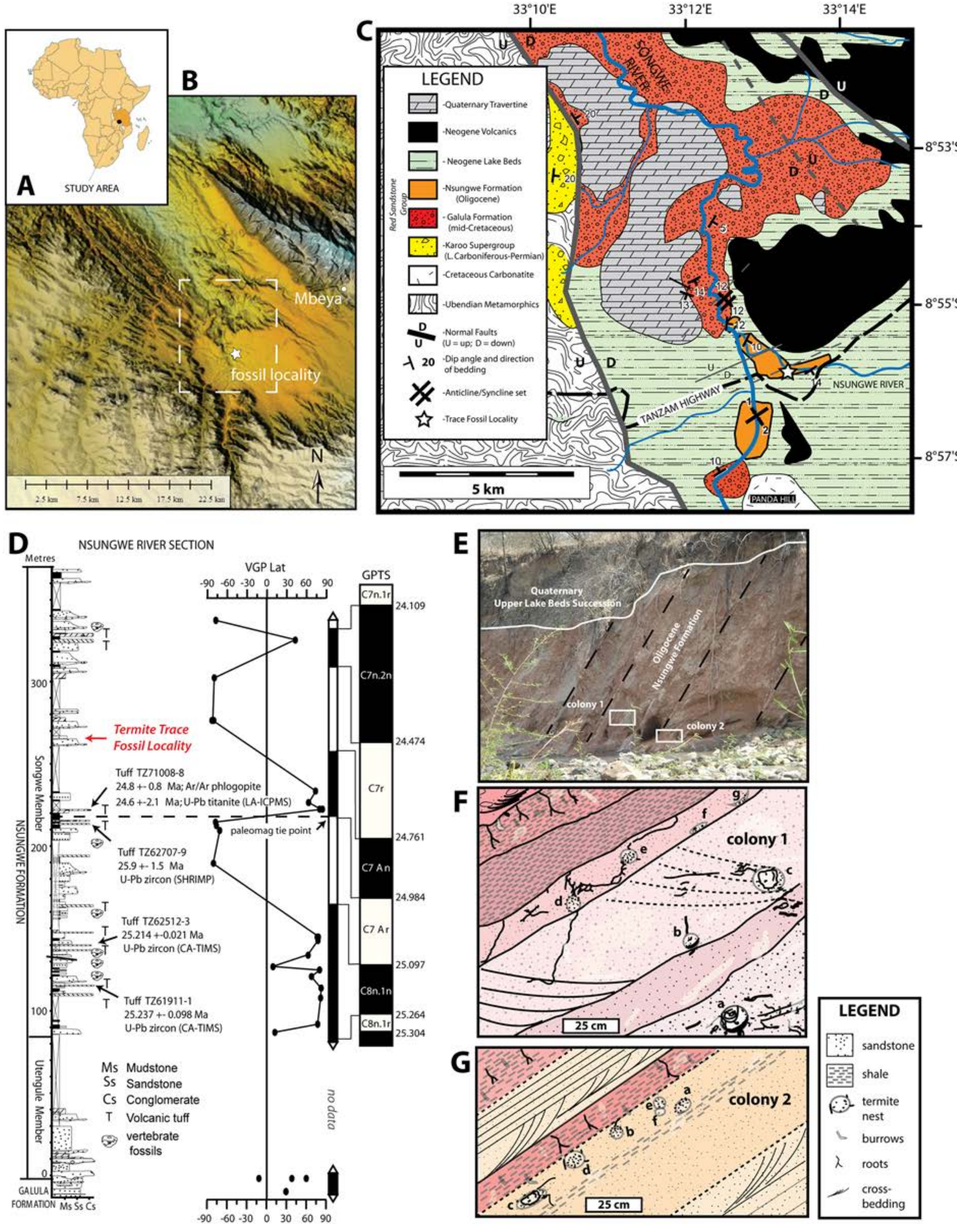

Fig 1. Location and stratigraphy of the trace fossil locality, Tanzania. (A) Location of Tanzania within Africa. (B) Digital elevation model for the study area in the southern end of the Rukwa Rift Basin (white box is shown in C). (C) Geologic map of the Songwe Valley in the southern end of the Rukwa Rift Basin, showing stratigraphy and age of fossil locality. Modified from [18]. (D) Measured section and magnetic stratigraphy through the Nsungwe Formation Type Section, with location of fossil locality shown. Modified from [18]. (E) Photograph of the nest locality in a steeply dipping cliff face along the Nsungwe River. (F, G) Sketch maps of

fossil locality showing the orientation and distribution of the termite colonies 1 (RRBP-08248) and 2 (RRBP-15106), with letters corresponding to the different nest chambers in each colony.

doi:10.1371/journal.pone.0156847.g001

above the basal contact of the Songwe Member, along the Nsungwe River Section. Based on radioisotopic dating and magnetostratigraphy, this part of the section is interpreted to fall within chron C7r of the global polarity timescale, indicating an age between ~24.8–24.5 Ma [17, 23].

The trace fossils, representing two discrete termite colonies, were all collected in the same area, but from beds several meters apart in a steeply dipping section of interbedded fluvial channel sandstones and overlying overbank mudrocks. Colony 1 was found near the top of a fine-grained, muddy sandstone complex and with seven chambers clustered in a small area spanning ~90 cm (vertically) x 150 cm (horizontally) (Fig 1). Colony 2 was found ~3 m below Colony 1 in a single 15 cm thick muddy sandstone horizon with six chambers spread out over 1.2 m (Fig 1). The sandstone beds containing Colony 1 fine upward and the densest concentration of nests were found in the finest-grained strata near the top of the bed. Colony 2 was also found in a fine-grained muddy sandstone unit. In both horizons, poorly preserved trough cross-bedding is cross-cut by the nests, associated galleries and root traces, indicating that the trace fossils formed after termination of fluvial flow and subaerial exposure at the top of the channel. Both colonies are overlain by a thin, pale orange to red color-banded sandy mudstone with abundant root mottling, horizontal and vertical burrows and minor $CaCO_3$ concretions. Considered together, these deposits are interpreted to be the top of an abandoned fluvial channel sequence, which was subjected to several flooding events followed by subaerial exposure and pedogenesis, presumably during the time of nest development and shortly after channel abandonment (see [18] for detailed interpretation of the sedimentology of section).

The site includes two termite colonies (Fig 1), each with six to seven fungus chambers, and three of which preserve fungus gardens (also called fungus combs). The trace fossils are interpreted as having formed synchronously with deposition of the Oligocene Songwe Member, rather than being modern constructions associated with recent termite activity, based on the following evidence: 1) the trace fossils are lithified; 2) some of the nests and fungus combs show compaction features, indicating that they were buried after formation; 3) galleries are infilled with similar sediment to the host rock, rather than more recent volcanic ash which is common in the present soil overlying the Oligocene strata; and 4) the nests and fungal combs are oriented parallel to the steeply dipping beds, rather than parallel to the present-day land surface.

The gross morphology of the trace fossil, its association inside *Vondrichnus*, and its peloidal construction of enclosed cells matches the diagnosis of a laminar-type fungus comb, *Microfavichnus alveolatus* [11]. Upward construction of the comb is evidenced by the concentric form and retention of alveolar form in the upper region. The fossil fungus chamber and fungus comb inside it are comparable to fungus combs produced by extant species of the genera *Macrotermes* and *Odontotermes*. However, no large hypogean chambers (calies) were observed with either colony, possibly due to the limited lateral extent of the outcrop.

Continental Ichnology

Ichnogenus *Vondrichnus* Genise & Bown, 1994

Diagnosis. Diffuse, polychambered, excavated subterranean nest systems. Obovate chambers occur in dense swarms of near 300 in cross section. Burrows simple, branched or unbranched, exiting from one or more points on periphery of chamber and comprising a dense mass of anastomosing burrows that may connect chambers [32].

Description. Thirteen specimens of *Vondrichnus planoglobus* representing two different termite colonies were discovered in the Nsungwe Formation (Fig 1). Three examples represent complete chambers and the remaining are partially eroded chambers. The chamber sizes range between 4 and 13 cm in diameter (width), but are only up to 8 cm in height because they are flattened to concave at their base (Figs 2 and 3). Flattened peloidal material, interpreted as compressed mylospheres are arranged, in part, in concentric lines from the base, as observed in polished cross-sections made from three samples (Figs 2 and 4). Some chamber peripheries consist of a 1–3 mm sediment rind that appears to differ in color and composition to the surrounding sediment, possibly due to differential composition of iron-oxides. Chamber expansion occurred in at least one example with two chambers in apposition oriented horizontally, which display meniscate shapes in cross-section. Chamber infill, subsequent to nest collapse, most often consists of fine sand or muddy sediments, however one example of coarser grained sandstone infill was observed (Figs 2–4). Although nest preservation is incomplete, the semi-spherical shape of the chambers is inferred from the cross-section shapes of the specimens. A number of galleries were observed to emanate from the top of one of the chambers, and in one case, from the bottom of the chamber, otherwise no other galleries were preserved in the next structures. A generally obovate, spaghetti-like mass composed of a meandering network of concave-up tubular shelves composed of small, white, compressed spheres was observed inside three of the nest chambers. These internal structures are interpreted as fungus combs of the ichnogenus *Microfavichnus alveolatus* [11].

Referred specimens. Twelve specimens from two separate colonies, including: (1) one housing an *in situ* fungus comb inside (*Microfavichnus alveolatus*) (RRBP 08248a); (2) one cross-sectioned specimen (RRBP 08248c) with partial fungus comb (isolated mylospheres) preserved inside; (3) one cross-sectioned specimen (RRBP08248g) showing endoecie and single chamber in apposition; (4) seven additional *in situ* specimens that were not collected; and (5) one additional collected specimen (RRBP-15106c) (Figs 2 and 3).

Locality and horizon. Nsungwe River section, late Oligocene Songwe Member (265 and 269 m levels in Fig 1D) of the Nsungwe Formation, Red Sandstone Group, Mbeya Region, southwestern Tanzania (Fig 1). The locality represents a fluvial channel succession with thin, pedogenically modified overbank deposits that host both termite colonies.

Discussion. These ichnofossils are interpreted to be polychambered subterranean termite nests. Nest density is interpreted as being low by comparison to chamber density previously reported for other fossil termite colonies [11, 14], due to the limited outcrop exposure of the Nsungwe Formation. Although the two ichnospecies of *Vondrichnus* are similar to one another, the size and shape of the Rukwa specimens are more consistent with the diagnosis of *V. planoglobus*. The concentric masses of fine-grained sediments within some of the chambers, coupled with the small size of the chambers, supports the interpretation of these nest trace fossils as *Vondrichnus*, rather than such similar ichnotaxa as *Termitichnus* and *Coatonichnus*. These specimens share many similarities with *Termitichnus*, however they can be differentiated based on their small size and morphology. Notably, nest size and the flattening of the chambers indicate that the Nsungwe nests are not *Termitichnus qatranii*, *T. namibiensis* or *T. schneideri* because they are consistently much smaller. Additionally, fungal gardens are currently only associated with the ichnospecies *Vondrichnus planoglobus*.

Ichnogenus *Microfavichnus* Duringer et al., 2007

Diagnosis. Isolated, flattened alveolar masses (~6–9 cm wide x 3–6 cm tall) that resemble a morel. Exhibits an arched-convex upper portion combined with a flattened, sub-concave

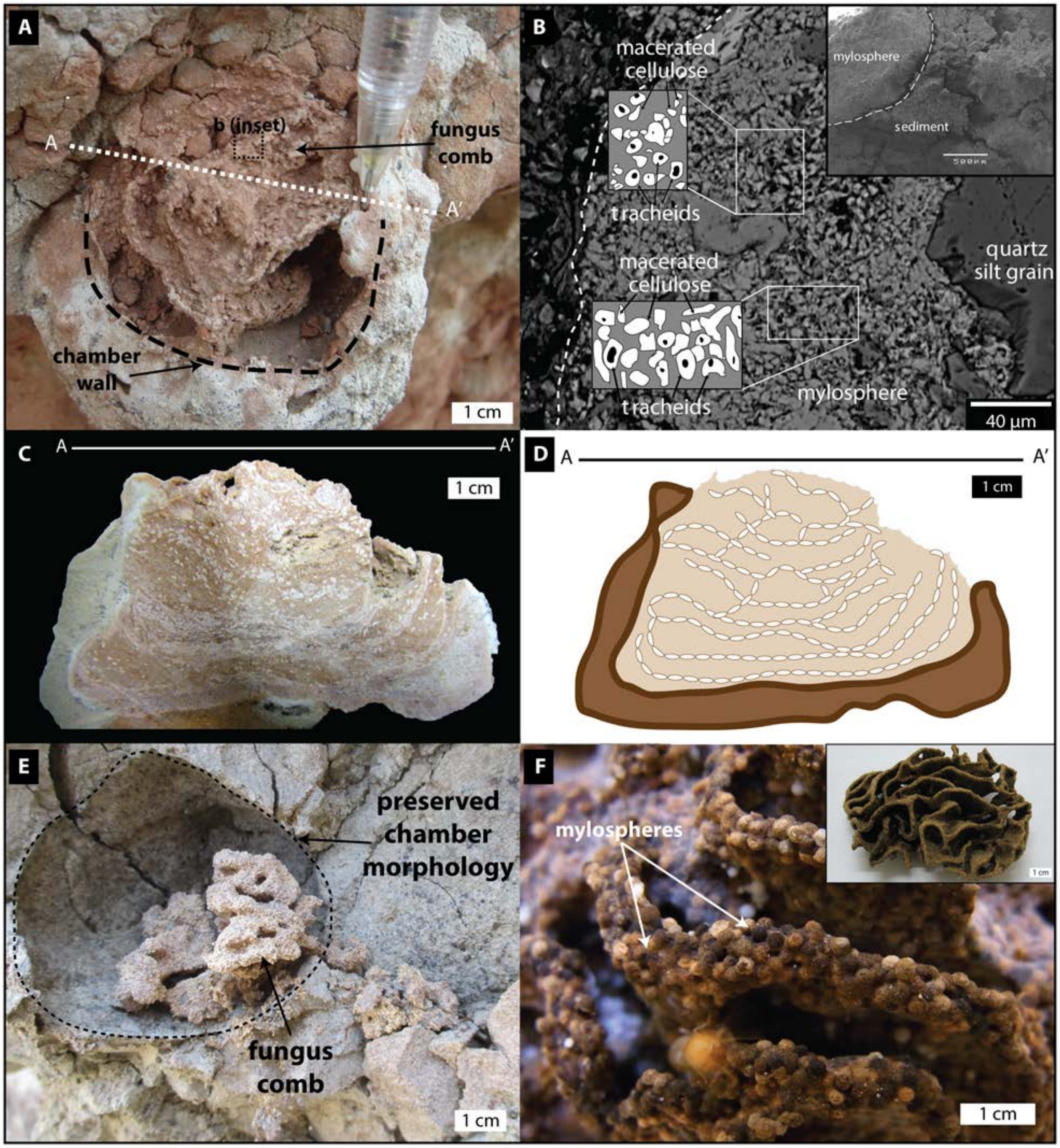

Fig 2. Fossil termite nest and fungus comb with comparative Holocene-Recent examples. (A) *In situ* fossil termite nest (*Vondrichnus planoglobus*; RRBP-08248a) with *Microfavichnus alveolatus* fungus comb trace fossil inside. (B) Backscatter electron (BSE) image of fossilized mylosphere with homogeneous composition of 5–10 μm macerated cellulose and calcified tracheids (elongated cells from the xylem of vascular plants). Inset: Scanning electron microscope (SEM) image of *Microfavichnus* in (A) showing compressed mylospheres and clay infill. (C, D) Photograph (C) and cartoon (D) of cross-section of RRBP-08248a (A). (E) Holocene fungus chamber with fungus comb, near the Galula Village along the Songwe River, Tanzania. (F) Modern *Microtermes* fungus comb, Malaysia (photo: Termite Web). Inset: Modern *Macrotermes* fungus comb.

doi:10.1371/journal.pone.0156847.g002

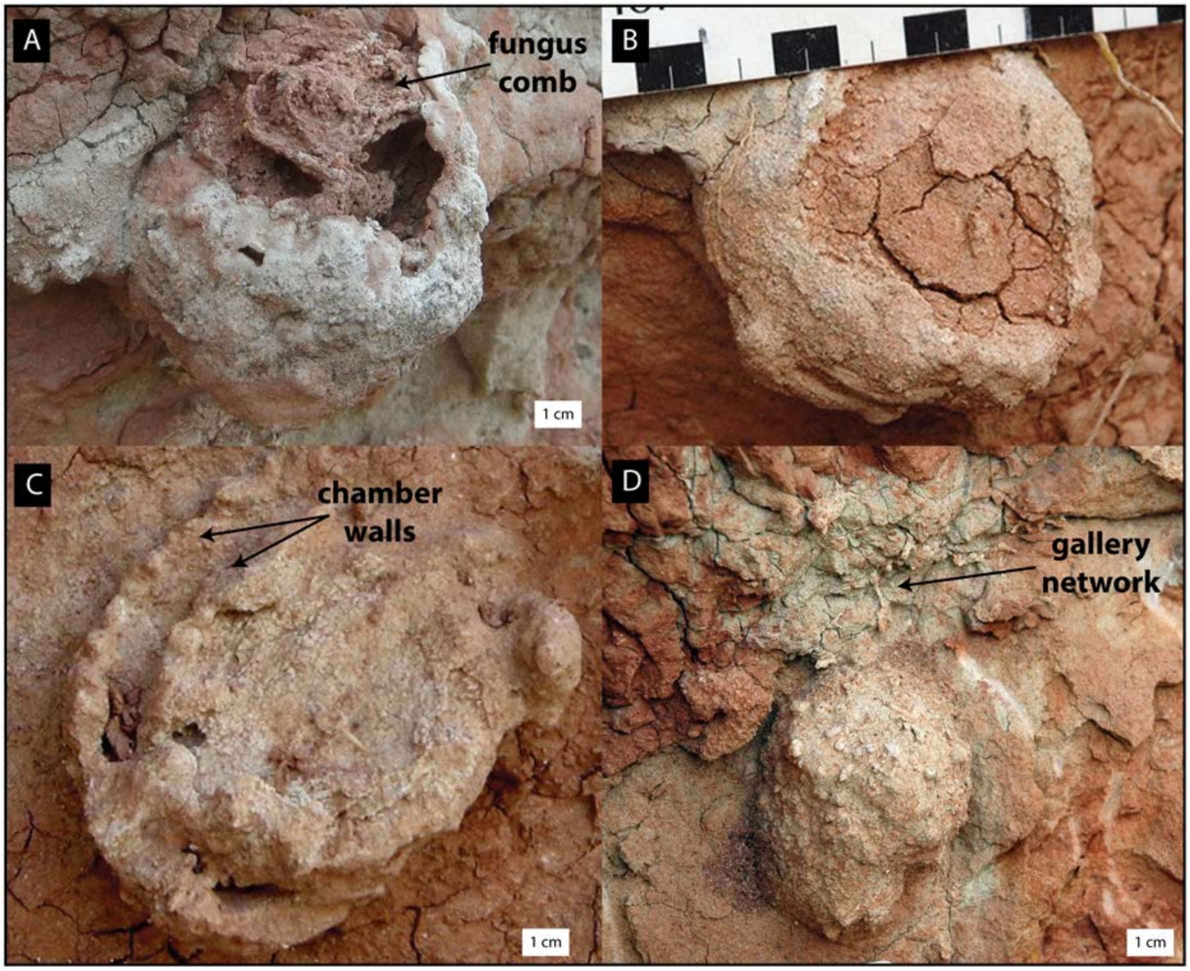

Fig 3. Photographs of specimens *in situ* displaying different morphologies and weathering stages. (A) Sample RRBP 08248a (Colony 1) with preserved fungus comb. (B) Sample RRBP 08248c (Colony 1). (C) Sample RRBP 08248g showing galleries and concentric chambers (Colony 1). (D) Uncollected nest RRBP 08248d (Colony 1) showing an external morphology and gallery network above the main nest.

doi:10.1371/journal.pone.0156847.g003

lower aspect. Specimen lacks an outer wall. The walls of the structure have peloidal texture formed by the juxtaposition and the stacking of mm-sized or smaller peloids.

Description. The outer shape of the trace fossil is hemispherical (radius 4.5 cm), with a flat to slightly concave base and no outer wall (Figs 2C, 2D and 3A). The internal fabric consists of at least eight sub-horizontal laminations or shelves of tan-colored peloids (1 mm, spherical to platelet shape) separated by red-colored, fine-grained sand and rare isolated peloids (Figs 2A–2D and 4A). The laminations (shelves) are concentrically nested from top to bottom, with the lowest levels deflecting upward at the margins of the structure. Compression of laminations and peloids is greatest near the base of the trace fossil (due to passive soil compaction), whereas the uppermost peloidal laminations show subdivision into open cells, 10 mm wide x 4 mm tall. Peloids are dominated by detrital silt grains and finely macerated cellular material, including isolated tracheids that have been replaced by calcium carbonate (Figs 2B, 2C and 4A).

Referred specimens. Three referred specimens, including one *in situ* fungus comb inside a fungus chamber (*Vondrichnus planoglobus*) (RRBP 08248a), an isolated fungus comb (RRBP

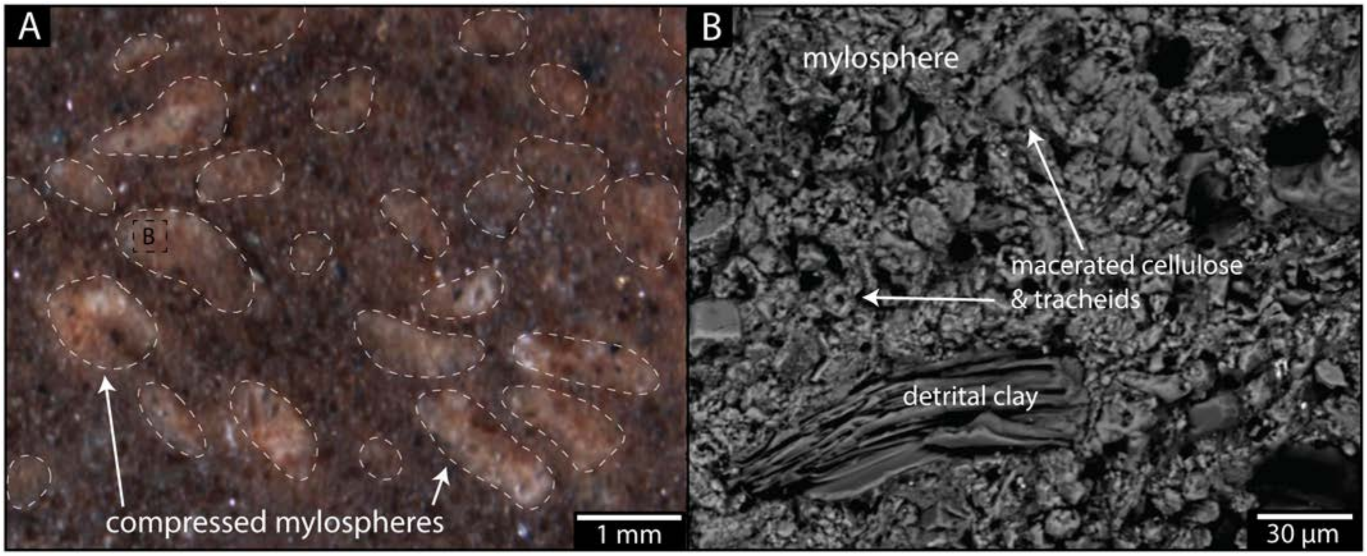

Fig 4. Structure and composition of preserved mylospheres from Macrotermitinae chamber. (A) Image of polished surface from sample RRBP 08248g (Colony 1) exposing compressed mylospheres (white) near the nest wall and detrital sediment (dark red) filling the chamber. Morphologies and chemical compositions were analyzed via energy dispersive spectroscopy (EDS) and backscattered electron imaging (BSE) by electron probe microanalysis. The sediment surrounding the mylospheres is clay-rich and contains occasional detrital quartz and feldspar grains (and accessory minerals such as monazite), deposited as the nest walls were expanded and/or through infilling of the chamber during construction of or later burial of the nest. There is a small presence of diagenetic Fe-, Mn-, and Ti-rich cement. (B) BSE image of a mylosphere from (A) revealing a homogeneous composition. Filled and hollow subcylindrical, 5–10 µm particles with a major Ca component comprise the mylospheres. We interpret the mylospheres to be composed of wood fragments now replaced by calcium carbonate, preserving the remnants of macerated cellulose and tracheids (Fig 2B).

doi:10.1371/journal.pone.0156847.g004

08248f), and one specimen (RRBP 08248c) of a cross-sectioned nest (*Vondrichnus*) with a partial fungus comb (isolated mylospheres) preserved inside (Figs 2–4).

Locality and horizon. Nsungwe River section, late Oligocene Songwe Member (265 and 269 m levels) of the Nsungwe Formation, Red Sandstone Group, Mbeya Region, southwestern Tanzania (Fig 1). Locality represents a fluvial channel succession with thin, pedogenically modified overbank deposits that host the termite colonies.

Discussion. See below.

The Fossil Record of Termites

Trace fossils provide valuable data on the role of poorly-fossilized insects in paleoecosystems through time [11, 13, 14, 33], and they are pivotal in testing the origins and timing of many different insect clades, their behaviors and niche utilization [34, 35]. Although rare, termite trace fossils have been interpreted from the Mesozoic [36–38]. The most abundant examples derive from Cenozoic deposits of Africa, and these are most closely related to nests produced by members of the fungus-growing termites (Macrotermitinae). Trace fossils interpreted as nests used for fungus growth, storage, reproduction and feeding have been assigned to several ichnogenera, including *Termitichnus* and *Vondrichnus*, and reported from the Upper Eocene—Oligocene of Libya and Egypt [13–15], the Neogene of Chad [11], and the Plio-Pleistocene of Namibia [39], Tanzania [40, 41] and South Africa [39] (Fig 5). However, the oldest example of termite nests with *in situ* fungus gardens, providing unequivocal evidence for the antiquity of termite-fungus mutualism, was reported from the late Miocene-early Pliocene in Chad [12]. These workers also reported a spectacular termite ichnofauna [12] with a number of new ichnospecies (e.g., *Termitichnus schneideri*, *Vondrichnus planoglobus*, *Coatonichnus globosus*). In

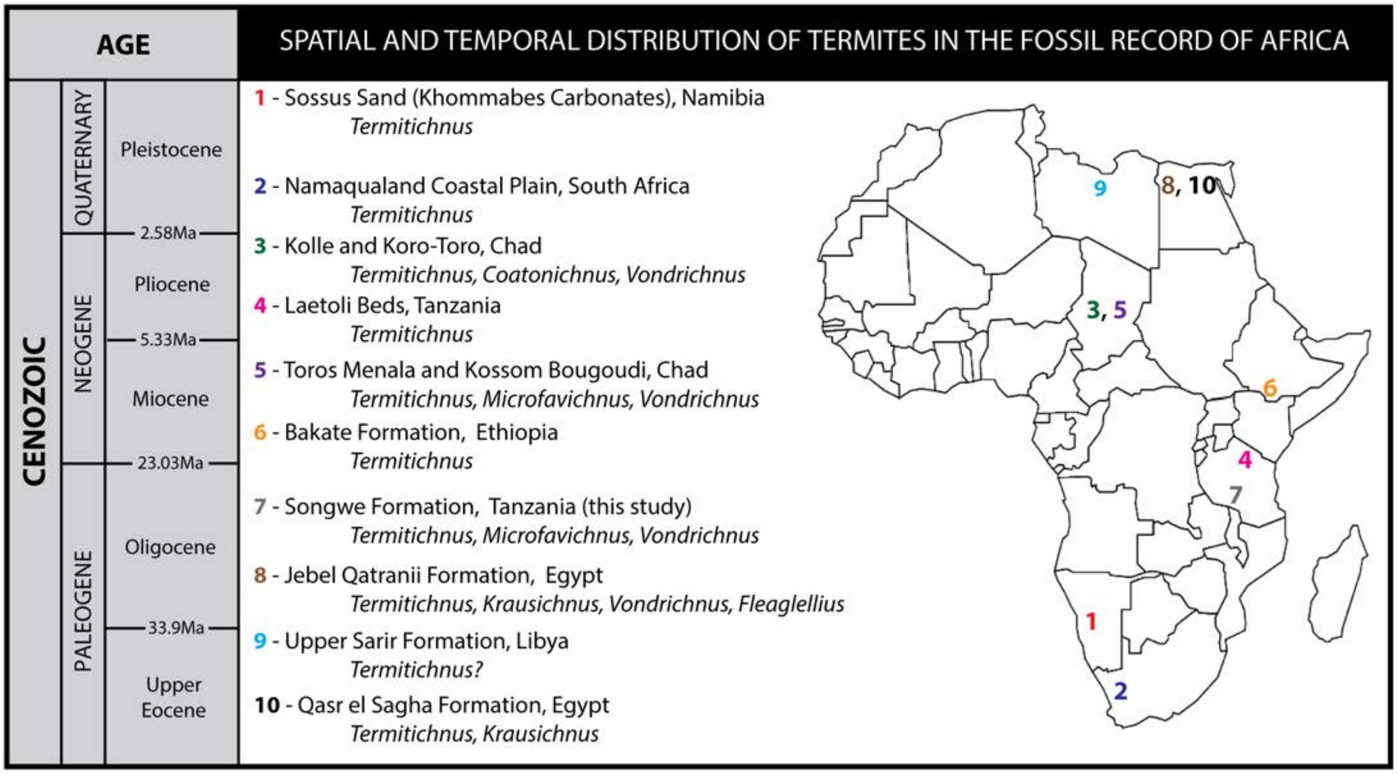

Fig 5. Temporal and spatial distribution of fossil termite nests and fungal gardens in Africa. Colored numbers represent termite trace fossil locations, along with the locality name and taxa present (*represents trace fossil localities with unequivocal fungal gardens associated with termite nests, demonstrating termite agriculture). Numbering refers to stratigraphic position as noted in reference to the Cenozoic time scale (at left). References: 1. Sossus Sand, Namibia [39]; 2. Namaqualand, South Africa [39]; 3. Kolle and Koro-Toro, Chad [11]*; 4. Laetoli, Tanzania [41, 43]; 5. Toros Menala and Kossom Bougoudi, Chad [11]*; 6. Bakate Formation, Ethiopia [44]; 7. Nsungwe Formation, Tanzania (this report)*; 8. Jebel Qatranii Formation, Egypt [14]; 9. Upper Sarir Formation, Libya [15]. 10. Qasr el Sagha Formation, Egypt [14].

doi:10.1371/journal.pone.0156847.g005

their study of this ichnological lagerstaten, these workers [11, 12, 42] documented the clear association between fungus combs, *Microfavichnus alveolatus*, and termite nests, several of which preserve *in situ* fungus combs within the ovoid chambers of the termite nest *Vondrichnus planoglobus*. These trace fossils have served as a critical calibration point in recent molecular studies and ecological modelling aimed at documenting the origins of fungus-growing termites [9]. It has been suggested that even older termite nest from the Paleogene of Egypt [13, 14] and Libya [15] may also be associated with fossil fungus combs, however due to poor preservation, confirmation of this awaits more detailed investigation of these examples.

Implications and Molecular Calibration

We used the well-dated Tanzanian fossil fungus combs reported here to recalibrate molecular divergence dates based on DNA sequences of 19 taxa and two calibration points [9] (S1 Table). First, we plotted representative examples of extant fungus gardens on a genus-level phylogeny [7, 9] (Fig 6). Based on a comparison between the fossil fungus combs and extant fungus combs, we inferred that the fossils most likely belong to the clade composed of all genera except *Pseudacanthotermes* and *Acanthotermes* (node b in Fig 6). Repeating the method used in [9], we applied the most recent common ancestor of this clade as an additional calibration point with a minimum age of 24.65 Ma (Table 1) to estimate the origin of the fungus-growing termites (node a in Fig 6) at 31.41 Ma (25.82, 39.53), which is close to previous estimates [9–10].

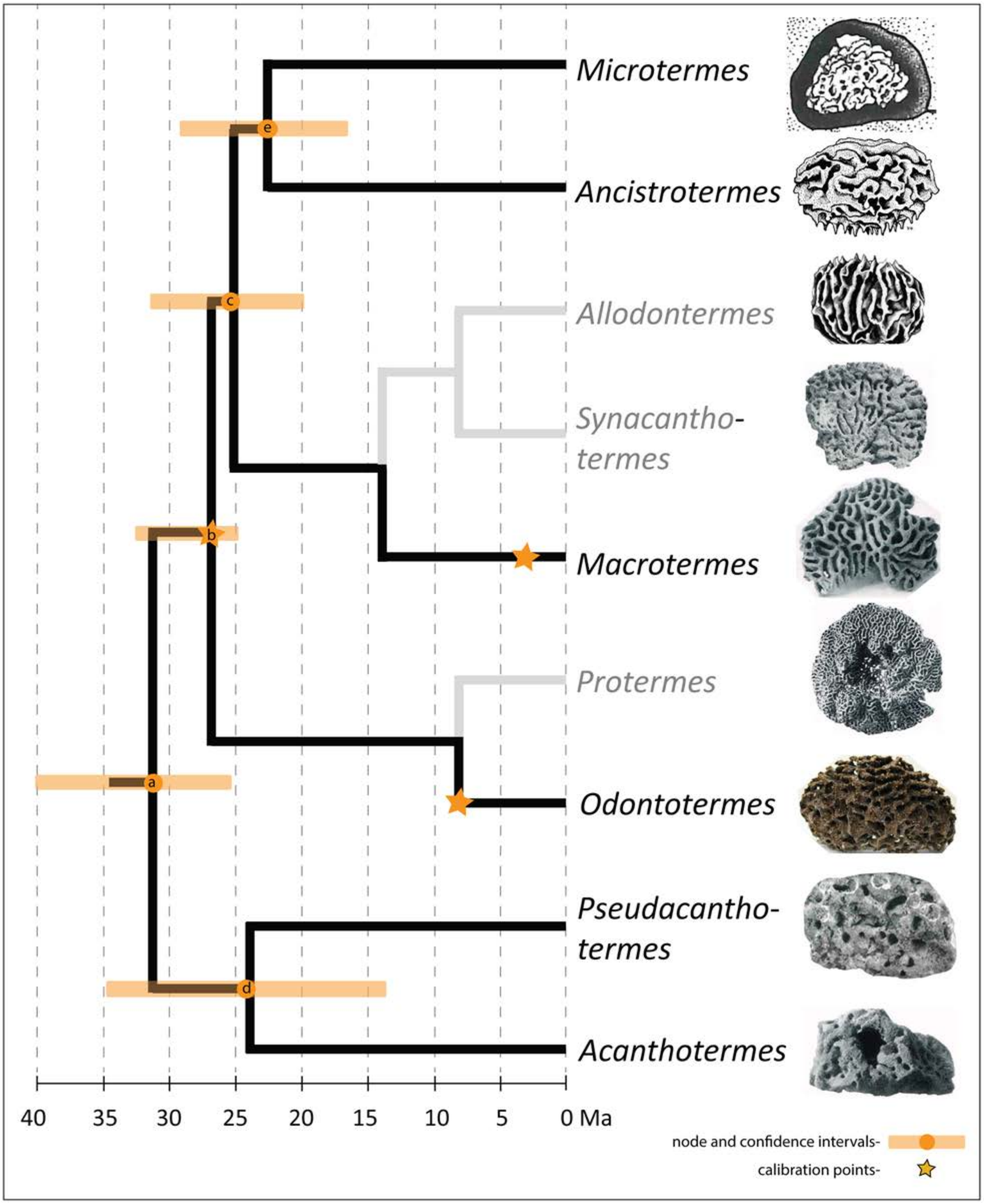

Fig 6. Schematic genus-level phylogeny [7, 9] of fungus-growing termites (Macrotermitinae) with recalibrated molecular divergence dates and confidence intervals from Table 1. This figure is based on simulation 1 and more highly resolved species trees can be found in the S1–S5 Figs. Representatives of the genera *Allodontermes*, *Synacanthotermes* and *Protermes* (faded branches) were not included in the time estimates. Images depict representative fungus combs of the different genera. Sketches of *Microtermes* and *Allodontermes* fungal combs from [45] and *Ancistrotermes* from [46]. Note: the calibration point on the Macrotermes branch corresponds to the age of the ancestor of *Macrotermes jeanneli* [41].

doi:10.1371/journal.pone.0156847.g006

Table 1. Mean estimated divergence dates and associated 95% confidence intervals for the origin of fungus-farming termites.

	(a)	(b)	(c)	(d)	(e)
Simulation 1 (node b)	31.4 Ma [25.8, 39.5]	27.1 Ma [25.0, 32.5]	25.3 Ma [20.1, 31.7]	24.5 Ma [13.7, 34.8]	22.8 Ma [16.8, 29.2]
Simulation 2 (node a)	27.1 Ma [25.0, 32.8]	22.7 Ma [16.9, 28.9]	21.2 Ma [15.4, 27.3]	20.9 Ma [11.7, 28.8]	19.2 Ma [13.3, 25.0]
Simulation 3 (node d)	32.0 Ma [25.8, 41.4]	26.6 Ma [18.7, 36.2]	24.9 Ma [17.2, 34.0]	27.1 Ma [25.0, 32.7]	22.5 Ma [14.7, 30.9]
Simulation 4 (node e)	36.1 Ma [27.8, 47.0]	31.1 Ma [25.8, 38.6]	29.3 Ma [25.2, 35.8]	28.0 Ma [13.8, 41.5]	27.0 Ma [25.0, 32.2]
Simulation 5 (genus *Microtermes*)	50.2 Ma [34.0, 70.4]	43.3 Ma [31.3, 59.1]	37.4 Ma [28.0, 49.6]	39.0 Ma [18.5, 61.0]	29.9 Ma [25.0, 31.7]

In all simulations, the *Odontotermes* node was constrained to a minimum age of 7 Ma, and the ancestor of *Macrotermes jeanneli* was constrained to a minimum age of 3.4 Ma (see Methods). We performed five analyses using alternative calibration points of the newly discovered fossils. Simulation 1 used node b as a calibration point. Alternative calibration points were: node a (Simulation 2), node d (Simulation 3), node e (Simulation 4) and the most recent common ancestor of the genus *Microtermes* (Simulation 5) (see S1 Table; S1–S5 Figs).

doi:10.1371/journal.pone.0156847.t001

Since a comparison between the fossil combs and extant combs is not unambiguous, we also tested various other possible calibration points, resulting in comparable age estimates ranging from 27 to 36 Ma (Table 1; for details see S1 Table, S1–S5 Figs). Dating phylogenies remain an uncertain process, not only depending on the fossil calibration(s) used but also on the DNA regions used and the concomitant accuracy of the recovered phylogeny and calibration methods. As such, the resulting dating should be carefully read as indicators of a time frame and not absolute ages. The proximity of this age estimate, however, is consistent with the hypothesis that the transition to fungus cultivation in the termites was followed closely by the main radiation leading to the extant genera [8, 9].

Antiquity of Insect Agriculture

Only two other insect groups are known to have derived mutualisms with fungi for agriculture: the ambrosia beetles and the leaf-cutter ants. Ants and termites are each considered to have evolved the ability to cultivate fungi for food only once, between 45–65 Ma and 24–34 Ma, respectively [47–49]. However, in ambrosia beetles, this trait may have evolved independently as many as ten different times, probably first around 50 Ma [50, 51]. It is also not clear where fungus gardening developed in ambrosia beetles, although there appears to be a strong evolutionary link to a tropical or sub-tropical forest setting [51]. Unfortunately, no fossil evidence, either in the form of fungal gardens or unequivocal ambrosia beetle borings, exists to validate molecular age estimates for ambrosia beetles or to provide direct geographic evidence on where this symbiosis originated.

The oldest evidence of fungus gardening by leaf-cutter ants dates back to the late Miocene of Argentina, between 5.7 and 10 Ma [52]. However, no fungus gardens are preserved, only fossilized ant (Attini) nests interpreted as fungus chambers based on morphology and the presence of fungal hyphae within them [52]. Together, the late Miocene Argentinian leaf-cutter nests and the macrotermitine fungus combs from Chad [11, 12] represent the oldest previously known definitive fossil evidence for insect domestication of fungi, yet both are considerably younger than the Paleogene molecular estimates for the antiquity of agriculture by insects.

Hence, the newly discovered Tanzanian trace fossils support a Paleogene record for the important evolutionary partnership between insects and fungi, and more specifically, they confirm recent molecular hypotheses for an African origin of symbiosis between the Macrotermitinae and *Termitomyces* fungi [9]. Notably, the features observed in the Tanzanian trace fossils lend support to the idea that similar Paleogene trace fossils documented across Afro-Arabia [13–15] may also represent fungus-farming termites. For instance, termite trace fossils

Vondrichnus and *Termitichnus* from Oligocene-Miocene terrestrial ecosystems in Egypt, Ethiopia, Libya and Arabia [13–15] (Fig 5) may have also been produced by fungus farming termites, however these fossils have not been described in detail and so their position on the tree is not clear (see S1 Text, S2 Table and S6 Fig for details on molecular calibrations using these taxa, which do not greatly alter the ages suggested in Simulation 1). The discoveries of fungus combs within termite nests in Chad [11] and now, in Tanzania, confirm these earlier assertions and suggest that fungus-farming termites radiated across Africa early in their evolutionary history. The diversification of the Macrotermitine termites from an African rainforest origin might have been coeval with expansion of savannahs in Africa [8]. Although the expansion of C4 grasses (and hence savannahs) are not well-documented on continental Africa until ~7–8 Ma, the presence of micromammals with crestiform teeth and active-foraging colubroid snakes from well-dated late Oligocene strata in the Rukwa Rift Basin suggest that isolated mixed forest/grassland ecosystems may have been present in ecosystems by 25 Ma, likely reflecting landscape changes associated with the initiation of the East African Rift System [17].

Methods

Permits

The Tanzanian Commission for Science and Technology (COSTECH) and the Tanzanian Antiquities Unit granted us permission to carry out our field studies and to take samples. Our field studies did not involve endangered or protected species.

Specimens

Portions of two fossilized termite colonies containing 13 individual trace fossil termite nest structures (*Vondrichnus planoglobus*), three of which contained *in situ* fungus combs (*Microfavichnus alveolatus*), were assigned specimen numbers: RRBP 08248a-g and RRBP 15106a-f. Due to the fragile nature of these trace fossils, only five nest structures were collected for further study. These include samples RRBP08248a, c, f, and g and RRBP 15106c. The other trace fossils were too fragile to collect and remain *in situ* or have since weathered out of the outcrop. Specimens included in the contribution are accessioned with RRBP (Rukwa Rift Basin Project) identifiers and are permanently housed through the Antiquities Division of the Republic of Tanzania (Dar es Salaam, Tanzania).

Paleontological approaches

In order to obtain a better understanding of the internal architecture of the trace fossils, three samples were cross-sectioned through a vertical mid-plane passing from the upper to lower surface using a lapidary saw with no water. One side was cross-sectioned through the equator, perpendicular to the first cut. All cut surfaces were polished for higher-resolution observation. Scanning electron microscopy (SEM) was used to image the internal structure of the trace fossils and micro-CT analysis was unsuccessfully employed to observe internal architecture of one of the trace fossils due to a lack of density differences between the different materials. One of the cross-sectioned para-types was also vacuum impregnated with epoxy and polished to observe internal structures in better detail and to construct a microprobe mount. Element concentrations were measured using EDS and BSE images of the sample were taken to examine preservation patterns of the nests and fungus combs (Figs 2 and 4). This work was conducted on an electron probe microanalyser (EPMA; Jeol JXA8200 "superprobe") at the Advanced Analytical Centre (AAC) at James Cook University.

Fungus-growing termite dating

Data and methodology used for the phylogeny calibration were the same as in Nobre et al. [9] (also see S1 and S2 Tables; S1–S7 Figs; S1 Text). Briefly, we used DNA sequences of the mitochondrial genes COI and COII and the nuclear ribosomal gene ITS2 for the 19 species of fungus-growing termites from all genera (except for the genera *Allodontermes*, *Synacanthotermes* and *Protermes*) and three outgroups [9]. Divergence dates were determined using the Bayesian relaxed-clock uncorrelated exponential approach implemented in BEAST 1.54 [53]. In the phylogeny reconstruction, the topology of the resulting tree was constrained to the genus-level phylogeny as estimated previously ([2, 7, 9] drawn schematically in Fig 6), and three Markov chain Monte Carlo searches were run for 10 000 000 generations each. Convergence was assessed using the log likelihood distributions of individual chains, and the burn-in level was assessed graphically in Tracer v1.4. In all simulations, the *Odontotermes* node was constrained to a minimum age of 7 Ma (based on the age of fossilized fungus comb associated with *Odontotermes* nest trace fossils from Chad [7]) following a lognormal distribution going as far back as the new fossil encountered (ca. 25 Ma) [8] [lognormal mean = 1.9, lognormal SD = 2.9, zero offset = 7]; and the ancestor of *Macrotermes jeanneli* was constrained to a minimum age of 3.4 Ma (based on the age of trace fossils reported from Tanzania [41]) [lognormal mean = 1.2, lognormal SD = 3.1, zero offset = 3.4]. We used the new fossils as a third node constraint of 25 Ma [lognormal mean = 3.2, lognormal SD = 2.7, zero offset = 25]. Because we inferred that the new fossils most likely belong to the clade composed of all genera except *Pseudacanthotermes* and *Acanthotermes*, the main approach applied this constraint to node b (simulation 1; the estimates from this analysis were used for the schematic Fig 6). Since the classification of the fossilized combs based on comparison with extant fungus combs is not unambiguous, we did four additional simulations (Table 1; Fig 6), using alternative calibration points of the newly discovered fossils: the most recent common ancestor of fungus-growing termites (node a; simulation 2); the most recent common ancestor of *Pseudacanthotermes* and *Acanthotermes* (node d; simulation 3); the most recent common ancestor of *Microtermes and Ancistotermes* (node e; simulation 4) and the most recent common ancestor of the genus *Microtermes* (simulation 5) (see S1–S6 Figs and S2 Table). Typically, the first 10% of the trees were discarded as burn-in, prior to results being pooled in LogCombiner v1.5.4 and tree visualization (see S1–S7 Figs; S1 Table for details concerning the details on the DNA analysis and files with raw trees produced in BEAST 1.54 [53]).

Supporting Information

S1 Fig. Simulation 1—Phylogenetic relationship of fungus-growing termites. Calibration points are indicated with ●. Each internal node is labelled with age and credibility interval of the corresponding clade; the posterior probabilities are found in italics (please note that not all posterior probability values are meaningful, since part of the topology was constrained). (DOCX)

S2 Fig. Simulation 2—Phylogenetic relationship of fungus-growing termites. Calibration points are indicated with ●. Each internal node is labelled with age and credibility interval of the corresponding clade; the posterior probabilities are found in italics (please note that not all posterior probability values are meaningful, since part of the topology was constrained). (DOCX)

S3 Fig. Simulation 3—Phylogenetic relationship of fungus-growing termites. Calibration points are indicated with ●. Each internal node is labelled with age and credibility interval of the corresponding clade; the posterior probabilities are found in italics (please note that not all

posterior probability values are meaningful, since part of the topology was constrained).
(DOCX)

S4 Fig. Simulation 4—Phylogenetic relationship of fungus-growing termites. Calibration points are indicated with ●. Each internal node is labelled with age and credibility interval of the corresponding clade; the posterior probabilities are found in italics (please note that not all posterior probability values are meaningful, since part of the topology was constrained).
(DOCX)

S5 Fig. Simulation 5—Phylogenetic relationship of fungus-growing termites. Calibration points are indicated with ●. Each internal node is labelled with age and credibility interval of the corresponding clade; the posterior probabilities are found in italics (please note that not all posterior probability values are meaningful, since part of the topology was constrained).
(DOCX)

S6 Fig. Simulation 6—Phylogenetic relationship of fungus-growing termites. Calibration points are indicated with ● including one for the origin of FGT based on Abouessa et al. [15]. Each internal node is labelled with age and credibility interval of the corresponding clade; the posterior probabilities are found in italics (please note that not all posterior probability values are meaningful, since part of the topology was constrained).
(DOCX)

S7 Fig. FASTA file. Original FASTA file for molecular clock calibrations from [9].
(FASTA)

S1 Table. DNA sequences from [9]. For 19 selected termite taxa, we have used 931 bp of the mitochondrial cytochrome oxidase subunit II gene (COI) using the primer pair TL1862 and TH2877 as in Aanen et al. [7], 684 bp of the mitochondrial cytochrome oxidase subunit II gene (COII) using AtLeu and B-tLys and 294 bp of part of the nuclear ribosomal internal transcribe spacer (ITS2) region using the primers ITS2 and ITS2F. Detailed methodology can be found in Nobre et al. [9].
(DOCX)

S2 Table. Alternative Calibration. Mean estimated divergence dates and associated 95% confidence intervals for the origin of fungus-farming termites (as for Table 1 in main text) considering the specimens from Libya [15] for calibration of the mrca of fungus-growing termites.
(DOCX)

S1 Text. Extra simulation for termite-fungus symbiosis excluding Rukwa specimen.
(DOCX)

Acknowledgments

We thank D. Kamamba, F. Ndunguru, and J. Temu (Tanzania Antiquities Unit), P. Msemwa (Tanzania Museum of House of Culture), and N. Boniface (University of Dar es Salaam), and the Tanzania Commission for Science and Technology (COSTECH) for logistical and administrative support; M. Gottfried, M. Hendrix, Z. Jinnah and the RRB excavation teams for field assistance. J. Hammerli, C. Pirard and K. Blake assisted with making polished slabs and microprobe mounts and imaging. We thank Termite Web for giving us permission to use photo shown in Fig 2F. We are grateful to the editor F. Bibi and two reviewers (M. Schuster and J. Scott) for their constructive feedback, which greatly improved the manuscript.

Author Contributions

Conceived and designed the experiments: EMR CNT DKA TN HLHW PMO LT CM NJS. Performed the experiments: EMR CNT DKA TN HLHW. Contributed reagents/materials/analysis tools: EMR CNT DKA TN HLHW PMO NJS. Wrote the paper: EMR CNT DKA TN HLHW PMO LT CM NJS.

References

1. Rouland-Lefèvre C. In: Takuya A, Bignell DE, Higashi M, editors. Symbiosis with Fungi. Termites: Evolution, Sociality, Symbioses, Ecology. Dordrecht: Kluwer Academic Publishers; 2000. pp. 289–306.
2. Poulsen M, Hu H, Li C, Chen Z, Xu L, Otani S, et al. Complementary symbiont contributions to plant decomposition in a fungus-farming termite. Proc. Nat. Acad. Sci. U.S.A. 2014; 111:14500–14505.
3. Pringle RM, Doak DF, Brody AK, Jocqué R, Palmer TM. Spatial pattern enhances ecosystem functioning in an African Savanna. PLoS Biol. 2010; 8:e1000377. doi: 10.1371/journal.pbio.1000377 PMID: 20520846
4. Bonachela JA, Pringle RM, Sheffer E, Coverdale TC, Guyton JA, Caylor KA, et al. Termite mounds can increase the robustness of dryland ecosystems to climate change. Science. 2015; 347:651–655.
5. Collins NM. The role of termites in the decomposition of wood and leaf litter in the southern Guinea savannah of Nigeria. Oecologia. 1981; 51:389–399.
6. Buxton RD. Termites and the turn-over of dead wood in an arid tropical environment. Oecologia. 1981; 51:379–384.
7. Aanen DK, Eggleton P, Rouland-Lefevre C, Guldberg-Froslev T, Rosendahl S, Boomsma JJ. The evolution of fungus-growing termites and their mutualistic fungal symbionts. Proc. Nat. Acad. Sci. U.S.A. 2002; 99:14887–14892.
8. Aanen DK, Eggleton P. Fungus-growing termites originated in African rain forest. Curr. Biol. 2005; 15:851–855. PMID: 15886104
9. Nobre T, Koné NA, Konaté KE, Linsenmair E, Aanen DK. Dating the fungus-growing termites' mutualism shows a mixture between ancient codiversification and recent symbiont dispersal across divergent hosts. Mol. Ecol., 2011; doi: 10.1111/j.1365-294X.2011.05090.x
10. Bourguignon T, Lo N, Cameron SL, Šobotník J, Hayahi Y, Shigenobu S, et al. The evolutionary history of termites as inferred from 66 mitochondrial genomes. Molecular Biology and Evolution. 2015; 32:406–421. doi: 10.1093/molbev/msu308 PMID: 25389205
11. Duringer P, Schuster M, Genise JF, Mackaye HT, Vignaud P, Brunet M. New termite trace fossils: Galleries, nests and fungus combs from the Chad Basin of Africa (Upper Miocene-Lower Pliocene). Palaeogeogr. Palaeoclimatol. Palaeoecol. 2007; 251:323–353.
12. Duringer P, Schuster M, Genise JF, Likius A, Mackaye HT, Vignaud P, et al. The first fossil fungus gardens of Isoptera: oldest evidence of symbiotic termite fungiculture (Miocene, Chad Basin). Naturwissenschaften. 2006; 93:610–615. PMID: 16924476
13. Bown TM. Ichnofossils and rhizoliths of the nearshore fluvial Jebel Qatrani Formation (Oligocene), Fayum Province, Egypt. Palaeogeogr. Palaeoclimatol. Palaeoecol. 1982; 40:255–309.
14. Genise JF, Bown TM. New trace fossils of termites (Insecta: Isoptera) from the late Eocene-early Miocene of Egypt, and the reconstruction of ancient isopteran social behaviour. Ichnos. 1994; 3:155–183.
15. Abouessa A, Pelletier J, Duringer P, Schuster M, Schaeffer P, Metais E, et al. New insight into the sedimentology and stratigraphy of the Dur At Talah tidal-fluvial transition sequence (Eocene—Oligocene, Sirt Basin, Libya. Journal of African Earth Sciences. 2012:72–90.
16. Stevens NJ, Gottfried MD, Roberts EM, Ngasala S, Kapilima S, O'Connor PM. Paleontological Exploration in Africa. In: Fleagle JG, Gilbert CC, editors. Elwyn Simmons: A Search for Origins. Developments in Primatology: Progress and Prospects: Springer; 2008. pp. 159–180.
17. Roberts EM, Stevens NJ, O'Connor PM, Dirks PHGM, Gottfried MD, Clyde WC et al. Initiation of the western branch of the East African rift coeval with the eastern branch. Nature Geoscience. 2012; 5:289–294.
18. Roberts EM, O'Connor PM, Stevens NJ, Gottfried MD, Jinnah ZA, Ngasala S, et al. Sedimentology and depositional environments of the Red Sandstone Group, Rukwa Rift Basin, southwestern Tanzania: New insight into Cretaceous and Paleogene terrestrial ecosystems and tectonics in sub-equatorial Africa. J. African Earth Sci. 2010; 57:179–212.
19. Grantham DR, Teale EO, Spurr AM, Harkin DA, Brown PE. Quarter Degree Sheet 244 (Mbeya). Geological Survey of Tanganyika, Dodoma; 1958.

20. Ebinger CJ. Tectonic development of the western branch of the East African rift system. Geol. Soc. Am. Bull. 1989; 101:885–903.
21. Delvaux D, Kervyn F, Vittori E, Kajara RSA, Kilembe E. Late Quaternary tectonic activity and lake level change in the Rukwa Rift Basin. J. African Earth Sci. 1998; 26:397–421.
22. Roberts EM, O'Connor PM, Gottfried MD, Stevens NJ, Kapilima S, Ngasala S. Revised stratigraphy and age of the Red Sandstone Group in the Rukwa Rift Basin, Tanzania: Cretaceous Research. 2004; 25:749–759.
23. Stevens NJ, Seiffert E, O'Connor PM, Roberts EM, Schmitz M, Krause D, et al. Palaeontological evidence for an Oligocene divergence between Old World monkeys and apes. Nature. 2013; 497:611–614. doi: 10.1038/nature12161 PMID: 23676680
24. O'Connor PM, Gottfried MD, Stevens NJ, Roberts EM, Kapilima S, Ngasala S, et al. Dinosaurs and other vertebrates from the Cretaceous Red Sandstone Group, Rukwa Rift Basin, Southwestern Tanzania. J. African Earth Sci. 2006; 44:277–288.
25. O'Connor PM, Sertich JJ, Stevens NJ, Roberts EM, Gottfried MD, Hieronymous TL, et al. The evolution of mammal-like Crocodyliforms in the Cretaceous Period of Gondwana. Nature. 2010; 466:748–751. doi: 10.1038/nature09061 PMID: 20686573
26. Stevens NJ, O'Connor PM, Gottfried MD, Roberts EM, Ngasala S. An anthropoid primate from the Paleogene of Southwestern Tanzania. J. Vertebr. Paleontol. 2005; 25:986–989.
27. Stevens NJ, Roberts EM, O'Connor PM, Gottfried MD. *Rukwalorax jinokitana* (n.gen., n.sp) (Mammalia: Hyrocoidea) in late Oligocene Rukwa Rift Basin of Tanzania. J. Vertebr. Paleontol. 2009; 29:972–975.
28. Stevens NJ, O'Connor PM, Gottfried MD, Roberts EM, Ngasala S, Dawson M. *Metaphiomys* from the Paleogene of Southwestern Tanzania: J. Paleontol. 2006; 80:407–410.
29. Stevens NJ, Holroyd PA, Roberts EM, O'Connor PM, Gottfried MD. *Kahawamys mbeyaensis* (n. gen., n. sp.) (Rodentia: *Thryonomyoidea*) from the late Oligocene Rukwa Rift Basin, Tanzania. J. Vertebr. Paleontol. 2009; 29:631–634.
30. Feldmann RM, O'Connor PM, Stevens NJ, Gottfried MD, Roberts EM, Ngasala S, et al. A new freshwater crab (Decapoda: Brachyura: Potamonautidae) from the Paleogene of Tanzania, Africa. Neues Jahrbuch fur Geologie und Palaontologie. 2007; 244:71–78.
31. McCartney J, Stevens NJ, O'Connor PM. The earliest Colubroid-dominated snake fauna from Africa: perspectives from the Late Oligocene Nsungwe Formation of southwestern Tanzania. PLOS ONE. 2014; 9(3):e90415. doi: 10.1371/journal.pone.0090415 PMID: 24646522
32. Genise JF. Ichnotaxonomy and ichnostratigraphy of chambered trace fossils in palaeosols attributed to coleopterans, ants and termites. In: McIlroy D, editor. The application of ichnology to palaeoenvironmental and stratigraphic analysis. Geological Society, London, Special Publications; 2004. pp. 419–453.
33. Genise JF, Mangano MG, Buatois LA, Laza JH, Verde M. Insect trace fossil associations in Paleosols: the Coprinisphaera Ichnofacies Palaios. 2000; 15:49–64.
34. Hasiotis ST. Complex Ichnofossils of solitary and social soil organisms: understanding their evolution and roles in terrestrial paleoecosystems. Palaeogeogr. Palaeoclimatol. Palaeoecol. 2003; 192:259–320.
35. Tapanila L, Roberts EM. The Earliest Evidence of Holometabolan Insect Pupation in Conifer Wood. PLoS ONE. 2012; 7:e31668. doi: 10.1371/journal.pone.0031668 PMID: 22355387
36. Hasiotis ST, Dubiel RF. Termite (Insecta: Isoptera) nest ichnofossils from the Triassic Chinle Formation, Petrified Forest National Park, Arizona. Ichnos. 1995; 4:119–130.
37. Bordy EM, Bumby A, Catuneanu O, Eriksson PG. Advanced Early Jurassic termite (Insecta: Isoptera) nests: evidence from the Clarens Formation in the Tuli Basin, southern Africa. Palaios. 2004; 19:68–78.
38. Bordy EM, Bumby A, Catuneanu O, Eriksson PG. Reply to a comment on advanced Early Jurassic termite (Insecta: Isoptera) nests: evidence from the Clarens Formation in the Tuli Basin, southern Africa. (Bordy et al., 2004). Palaios. 2005; 20:307–311.
39. Smith RMH, Mason TR. Sedimentary environments and trace fossils of Tertiary Oasis Deposits in the Central Namib Desert, Namibia. Palaios. 1998; 13:547–559.
40. Sands WA. Ichnocoenoses of probable termite origin from Laetoli. In: Leakey MD, Harris JM, editors. Laetoli, a Pliocene Site in Northern Tanzania. Oxford Science Publications; 1987. pp 409–433.
41. Darlington JPEC. Distinctive fossilised termite nests at Laetoli, Tanzania. Insectes Sociaux. 2005; 52:408–409.

42. Schuster M, Duringer P, Nel A, Brunet M, Vignaud P, Mackaye HT. Découverte de termitières fossiles dans les sites à vertébrés du Pliocène tchadien: description, identification et implications paléoécologiques. C. R. Acad. Sci., Paris. 2000; 331:15–20.
43. Miller WR, Mason TR. Sedimentary environments and trace fossils of Tertiary Oasis Deposits in the Central Namib Desert, Namibia. Ichnos. 2000; 7:195–215.
44. Bown TM, Genise JF. Abstracts with Programs of the Annual Meeting of the Geological Society of America. 1993; 25:58.
45. Uys VM. A Guide to the Termite genera of Southern Africa. Plant Protection Research Institute Handbook No. 15, ARC-Plant Protection Research Institute, Pretoria, South Africa. 2002. 116 pp.
46. Coaton WGH, Sheasby JL. National survey of the isoptera of Southern Africa 9. The genus *Ancistrotermes* silvestri (Termitida: Macrotermitinae). Cimbebasia (A). 1975; 3:95–104.
47. Mueller UG, Herardo NM, Aanen DK, Six DL, Schultz TR. The Evolution of Agriculture in Insects. Annu. Rev. Ecol. Evol. Syst. 2005; 36:563–595.
48. Schultz TR, Brady SG. Major evolutionary transitions in ant agriculture. Proc. Nat. Acad. Sci. U.S.A. 2008; 105:5435–40.
49. Mueller UG, Rehner SA, Schultz TR. The evolution of agriculture in ants. Science. 1998; 281:2034–2038. PMID: 9748164
50. Farrell DB, Sequeira AS, O'Meara BC, Normark BB, Chung JH, Jordal BH. The evolution of agriculture in beetles (Curculionidae: Scolytinae and Platypodinae). Evolution. 2001; 55:2011–2027. PMID: 11761062
51. Jordal BH, Cognato AI. Molecular phylogeny of bark and ambriosa beetles reveals multiple origins of fungus farming during periods of global warming. BMC Evolutionary Biology. 2012; 12:1471-2148/12/133.
52. Genise JF, Melchor RN, Sánchez MV, González MG. A Miocene record of fungus-growing ants. Palaeogeogr. Palaeoclimatol. Palaeoecol. 2013; 386:349–363.
53. Drummond A, Rambaut A. BEAST: Bayesian evolutionary analysis by sampling trees. BMC Evolutionary Biology. 2007; 7:214. PMID: 17996036